Copyright Statement

This copy of the thesis has been supplied on condition that anyone who consults it is understood to recognise that its copyright rests with its author and that no quotation from the thesis and no information derived from it may be published without the author's prior consent.

DIFFUSE MINEWATER POLLUTION: QUANTIFICATION AND RISK ASSESSMENT IN THE TAMAR CATCHMENT

By

ALISON JEAN MAY TURNER

A thesis submitted to the University of Plymouth in partial fulfilment of the degree of

DOCTOR OF PHILOSOPHY

School of Geography, Earth and Environmental Science
Faculty of Science and Technology

In collaboration with Great Western Research, University of Exeter and the Environment Agency

April 2011

DIFFUSE MINEWATER POLLUTION: QUANTIFICATION AND RISK ASSESSMENT IN THE TAMAR CATCHMENT

By

ALISON JEAN MAY TURNER

Abstract

Abandoned metal mines in the Tamar catchment, south west England, represent a significant threat to surface water quality via generation of acid mine waters. Currently the River Tamar fails environmental quality standards (EQS) established under the Water Framework Directive (2000/60/EC) for dissolved Cu ($\bar{x} = 0.19 \pm 0.05$ µmol L^{-1}) and Zn ($\bar{x} = 0.19 \pm 0.06$ µmol L^{-1}, both 1997-2007) downstream of historic mining area of Gunnislake. The aim of this study was to quantify the risk to surface water quality by diffuse drainage generated by mine waste tips.

For the first time, a GIS model was compiled and used to generate a priority list of known areas of mine waste, based on physical and environmental factors. The methodology was consistent with European guidance documentation published to meet the requirements of the Mining Waste Directive (2001/21/EC) and has since been applied, in a modified form, to other catchments in south west England.

Two study sites, with contrasting mineralogy and hydrology, scored highly in the model and were the subject of field investigations from 2007-2009. These were Devon Great Consols (DGC), an abandoned Cu-As mine near Gunnislake and Wheal Betsy (WB), an abandoned Pb-Ag mine, near Mary Tavy. At each site, surface waters

and shallow groundwaters were sampled and analysed for dissolved metals (including Al, Cu, Zn, Mn, Pb, Ni, and Cd), metalloids (As, Sb), major ions and anions. Samples of four selected mine waste tips were also gathered and subjected to a range of laboratory leaching experiments including the novel application of a dynamic upflow percolation test, based on an existing European method (CEN TS 14405).

Leachates generated by the waste tips in the field were highly variable and elevated with respect to EQS for Al (up to 1850 μmol L^{-1}), Cu (570 μmol L^{-1}), Zn (34 μmol L^{-1}), Ni (3.8 μmol L^{-1}), Cd (0.17 μmol L^{-1}), Mn (216 μmol L^{-1}), Fe(537 μmol L^{-1}), As (380 μmol L^{-1}) and Sb (5.4 μmol L^{-1}). Estimated annual fluxes of dissolved metals were predicted using average rainfall data and catchment areas calculated in ArcHydro9 to estimate the annual discharge of waters from the tip. These calculations showed annual contaminant flux from the tips to exceed, or be of the same order of magnitude to, major adit discharges in the catchment (e.g. Cu 50900-66900 mol y^{-1} at DGC and 470 mol y^{-1} Cd at WB) and represented a significant contributor to metal flux in the Tamar catchment. Primary sulphide minerals in the waste were generally highly altered and metals (Pb, Cu, Zn, and Mn) and As were found to be strongly associated with secondary iron minerals, precipitated under oxic conditions. In finer wastes, sorption to clay minerals was also found to be very important for the retention of dissolved metals, particularly Pb.

Concentrations of contaminants in column field leachates were similar for most metals (Cu, Zn, Mn, Ni and Cd) and may provide a useful tool for prediction of leachate composition. However, sorption and release of metals and As to the secondary phases and clays were highly sensitive to pH change and where laboratory experiments did not replicate field pH, discrepancies between in situ and laboratory results were observed up to two orders of magnitude in scale (particularly for As and Pb).

Table of Contents

Chapter 3: Mine Waste Tips as a source of Metals and Arsenic Contamination: Case Study 1: Devon Great Consols

Chapter 4: Mine Waste Tips as a source of Metals and Arsenic Contamination, Case Study 2: Wheal Betsy

Chapter 5: The Geochemistry and Leaching Behaviour of Selected Mine Wastes from the Tamar Catchment

Chapter 6: Final Conclusions and Recommendations

Final Appendix: Conference Papers

Dynamic Up-Flow Percolation Tests - A Model for Mining Waste Leachate Generation, presented at International Mine Water Conference 2009, Pretoria, South Africa

Risk-Based Prioritisation of Closed Mine Waste Facilities Using GIS, presented at the International Mine Water Conference 2011, Aachen, Germany.

Table of Figures

Chapter 1:

Chapter 2:

Figure 2.1: Flowchart showing development of model from input data sets. Abbreviations used: OS - Ordnance Survey; BGS - British Geological Survey;

Chapter 3:

Tables

Chapter 4:

Chapter 5:

Author's Declaration

At no time during the registration of the degree of Doctor of Philosophy has the author been registered for any other University award without prior agreement of the Graduate Committee.

This study was financed with the aid of a studentship from Great Western Research and was carried out in collaboration with Camborne School of Mines, University of Exeter, and the Environment Agency as an industrial partner. An additional grant from the Higher Education Funding Council for England (HEFCE) financed collaboration with the British Geological Survey.

Relevant scientific workshops and conferences were attended at which work was often presented; external institutions were visited for consultation and collaborative purposes.

Publications:

Turner, A., et al. (2009). Dynamic Up-Flow Percolation Tests - a model for mining waste leachate generation. *International Mine Water Association Conference, Pretoria, South Africa, 2009.* Water Institute of Southern Africa's Mine Water Division & International Mine Water Association ISBN/ISSN: 978-0-09802623-5-3. (Appended to this document)

Presentations and Conferences Attended:

International Mine Water Association (IMWA) Conference, Pretoria, South Africa, 19th-23rd October 2009. Co-winner of best technical short paper and platform presentation by a student. Also attendance at 1-day workshop on metalliferous tailings disposal facilities.

IMWA Conference, Karlovy Vary, Czech Republic, 2nd-5th June 2008. Poster presentation entitled: "Unravelling the complex issues of Diffuse Metal Pollution from Abandoned Mine Workings".

Great Western Research (GWR) Conference, Bristol, UK, 18th November 2008. Platform and poster presentation entitled "Sustainable Management of Mine Water Pollution from Headwaters to Estuaries", poster gained 3rd prize in competition across all disciplines of GWR.

SAFEMINEMIN Project Workshop, Vienna, 17-18th January 2008. 'Generation, Prevention and Treatment of Acid Mine Drainage, Old and Abandoned Mining Waste Sites – Environmental Risk and Possible Solutions for Remediation'. Attendee.

Biogeochemistry and Environmental Analytical Chemistry (BEACh) Research Group Annual Conference, University of Plymouth, UK. December 2007, 2008, 2009 and 2010. Platform presenter.

Word count of main body of thesis: 79956

Signed ....

Date ....

Acknowledgements

Glossary of Terms and Abbreviations used in Thesis

Minerals (formulae from Mindat.com):

Albite: $NaAlSi_3O_8$

Alunite: $KAl_3(OH)_6(SO_4)_2$

Anglesite: $PbSO_4$

Arsenian pytite: $Fe(S,As)_2$

Arsenopyrite: $FeAsS$

Basaluminite: $Al_4(SO_4)(OH)_{10.}5H_2O$

Beaverite-(Cu): $(Pb(Fe^{3+},Cu)_3(SO_4)_2(OH)_6)$

Beaverite-(Zn): $(Pb(Fe_2^{3+},Zn)(SO_4)_2(OH)_6)$

Beudantite: $PbFe_3(ASO_4)(SO_4)(OH)_6$

Bornite: Cu_5FeS_4

Calcite: $CaCO_3$

Cassiterite: SnO_2

Chalcopyrite: $CuFeS_2$

Chamosite: $(Fe_3Al)(AlSi_3)O_{10}(OH)_8$

Childrenite: $FeMnAlPO_4(OH)_2.H_2O$

Dolomite: $CaMg(CO)_3$

Dravite: $Na(Mg_3)Al_6(Si_6O_{18})(BO_3)_3(OH)_3(OH)$

Douglasite: $K_2[Fe^{2+}Cl_4(OH_2)_2]$

Enstatite: $MgSiO_3$

Ferrihydrite: $5Fe_2O_3.9H_2O$

Fluorite: CaF_2

Heamatite: Fe_2O_3

Illite: $K_{0.65}Al_{2.0}[Al_{0.65}Si_{3.35}O_{10}](OH)_2$

Galena: PbS

Gibbsite: $Al(OH)_3$

Gismondine: $(Ba\ or\ Ca)_2Al_4Si_4O_{16}.4\text{-}6H_2O$

Goethite: $FeOOH$

Galena: PbS

(*K-*)Jarosite: $KFe_3(SO_4)_2(OH)_6$

Juanitaite: $Bi(Cu,Ca,Fe)_{10}(AsO_4)_4(OH)_{11}.2H_2O$

Jurbanite: $Al_3(SO_4)OH.5H_2O$

Kaolinite: $Al_2Si_2O_5(OH)_5$

Lepidocrocite: $FeOOH$

Löllingite: $FeAS_2$

Orpiment: As_2S_3

Plumbojarosite: $PbFe_6(SO4)_4(OH)_{12}$

Quartz: SiO_2

Maghemite: $Fe^{3+}{}_2O_3$

Marcasite: FeS_2

Melanterite: $FeSO_4.7H_2O$

Molybdenite: MoS_2

Muscovite: $KAl_2(AlSi_3O_{10})(OH)_2$

Pyrite: FeS_2

Pyrrhotite $Fe_{1\text{-}x}S$

Realgar: As_4S_4

Rhodochrosite: $MnCO_3$

Schwertmannite: $Fe_8O_8(OH)_6SO_4$ to $Fe_{16}O_{16}(OH)_{10}(SO_4)_3$

Schorl: $Na(Fe^{2+}{}_3)Al_6(Si_6O_{18})(BO_3)_3(OH)_3(OH)$

Scorodite: $FeAsO_4.2H_2O$

Siderite: $FeCO_3$

Sphalerite: $ZnFeS$

Siderite: $FeCO_3$

Uvite: $Ca(Mg_3)MgAl_5(Si_6O_{18})(BO_3)_3(OH)_3(OH)$

Vivianite: $Fe_3(PO_4)_2.8H_2O$

Wolframite $FeWO_4$ to $MnWO_4$

Chapter 1:

Adit: A passageway into an underground mine, usually near horizontal, through which the mine is accessed, ventilated or drained of water.

Discard (or coarse discard): waste rock resulting from excavation of a mine prior to fine separation processes.

Gangue: Waste rock of no economic value.

Tailings: Waste produced from separation processes used to recover economic minerals from gangue, sometimes referred to as *slimes*, they usually comprise a slurry of fine rock and water.

Variscan Orogeny: Geological mountain-building event caused by Late Palaeozoic continental collision 270-400 MA[1]. The Upper Palaeozoic massif of SW England is situated on the northern margin of the orogen which stretches 1000 km across central and Western Europe[2]

Chapter 2 [3]

3D Analyst (ArcGIS): An extension that provides tools for three-dimensional (3D) visualization, analysis, and surface generation.

Attribute Table (ArcGIS): A database or tabular file containing information about a set of geographic features, usually arranged so that each row represents a feature and each column represents one feature attribute.

Buddle (circular): A device used to gravimetrically separate ore minerals from gangue. A suspension of crushed ore in water was passed over a central cone and spread outwards according to density. Rotating sweep arms fitted with brushes continuously disturbed the suspension allowing for better separation of the fractions.

Batch Watershed Delineation for Polygons Tool (ArcGIS, ArcHydro9): A method for processing the drainage pathway for each mine waste polygon automatically, without user interaction. Results are stored in a watershed (polygon) feature class.

Buffer Tool (ArcGIS): Calculates a zone around a map feature measured in units of distance, useed for proximity analysis.

*Burning in (ArcGIS, ArcHydro9):*See *DEM Reconditioning (AGREE).*

Catchment Polygons (ArcGIS, ArcHydro9): Rainfall catchment area calculated for each area of mine waste, based on the DTM.

---

[1] Reference: Jackson, N. J., Willis-Richards, J., Manning, D. A. C. and Samms, M. (1989). Evolution of the Cornubian Ore Field, southwest England: Part II. Mineral deposits and ore forming processes. *Economic Geology*. **84** pp1101-33.

[2] Reference: E. Leveridge and A.J. Hartley, The Variscan Orogeny: the development and deformation of Devonian/Carboniferous basins in SW England and South Wales. In: P.J. Brenchley and P.F. Rawson, Editors, *The Geology of England and Wales*, Geological Society of London (2006), pp. 225–255

[3] All ArcGIS definitions are taken directly from the ESRI ArcGIS 9.3 Desktop Help and Glossary webpages available online at: http://webhelp.esri.com/arcgisdesktop/9.3 and http://resources.arcgis.com/glossary, respectively. ArcHydro definitions are taken from the help function within ArcHydro9.

Clip Tool (ArcGIS): A command that extracts features from one feature class that reside entirely within a boundary defined by features in another feature class.

Convert: Spatial Analyst tool converts one type of feature class to another

Data Management Toolbar (ArcGIS): *The Data Mana*gement toolbox/toolbar provides a collection of tools that are used to develop, manage, and maintain feature classes, datasets, layers, and raster data structures.

DEM Reconditioning (AGREE) Tool (ArcGIS, ArcHydro9): The DEM Reconditioning function (DEM Manipulation menu) modifies Digital Terrain Models (DTMs) by imposing linear features onto them (burning/fencing). This function is an implementation of the AGREE method developed by Ferdi Hellweger at the University of Texas at Austin in 1997. For a full reference to the procedure refer to the web:

link:http://www.ce.utexas.edu/prof/maidment/GISHYDRO/ferdi/research/agree/agree.html.

Digital Terrain Model (DTM): A model represents the bare ground surface without any objects like plants and buildings. The term Digital Elevation Model (DEM) is often used as a generic term for DTMs, only representing height information without any further definition about the surface.

Dissolve Tool: A geoprocessing command that removes boundaries between adjacent polygons that have the same value for a specified attribute.

Drainage Polygons: Drainage area calculated in ArcHydro9 for each area of mine waste, based on the DTM.

Feature Class (ArcGIS): A collection of geographic features with the same geometry type (such as point, line, or polygon), the same attributes, and the same spatial reference.

Feature Code (ArcGIS): A unique identifier in the attribute table.

Field Calculator (ArcGIS): A tool that computes data from a column in an attribute table from a range of mathematical functions.

Fill Sinks Tool (ArcGIS, ArcHydro9): The Fill Sinks function (DEM Manipulation menu) fills sinks in a grid. If a cell is surrounded by higher elevation cells, the water is trapped in that cell and cannot flow. The Fill Sinks function modifies the elevation value to eliminate these problems. consuming. The status of the processing will be displayed in the ArcMap status bar.

Filling sinks is an operation that needs to be executed with care. The resulting DEM will have no inner depressions, that is, all the runoff from the DEM will reach its edges. In most cases, this is a correct assumption (when depressions are the artefacts of DEM generation), but in some cases that is not correct (e.g. inner lakes).

Flow Direction (ArcGIS, ArcHydro9): The Flow Direction function (Terrain Preprocessing menu) takes a grid ("Hydro DEM" tag) as input, and computes the corresponding flow direction grid ("Flow Direction Grid" tag). The values in the cells of the flow direction grid indicate the direction of the steepest descent from that cell.

Hillshade Tool (ArcGIS): Calculated the hypothetical illumination of a surface according to a specified azimuth and altitude for the sun.

Hydrogrid (ArcGIS, ArcHydro9): A modified Digital Terrain Model (DTM) produced from one of the processing steps in ArcHydro9.

Identity Tool (ArcGIS): A tool that, when applied to a feature (by clicking it), opens a window showing that feature's attributes.

Intersect Tool (ArcGIS): A geometric integration of spatial datasets that preserves features or portions of features that fall within areas common to all input datasets.

Join Tool (ArcGIS): Appending the fields of one table to those of another through an attribute or field common to both tables. A join is usually used to attach more attributes to the attribute table of a geographic layer.

Least cost path (ArcGIS, Spatial Analyst): Cost distance tools calculate for each cell the least accumulative cost to specified source locations over a cost surface. The Cost Path tool produces an output raster that records the least-cost path or paths from selected locations to the closest source cell defined within the accumulative cost surface, in terms of cost distance.

Model Builder Extension: The interface used to build and edit geoprocessing models in ArcGIS.

Multipart to Singlepart Tool (ArcGIS, Data Management): Separates multipart features into separate single part features(opposite function to *Dissolve*). The features in the Output Feature Class will have the same attributes as the Input Features.

Null values (ArcGIS): The absence of a recorded value for a field. A null value differs from a value of zero in that zero may represent the measure of an attribute, while a null value indicates that no measurement has been taken.

Parcel (ArcGIS): A piece or unit of land, defined by a series of measured straight or curved lines that connect to form a polygon.

Personal Geodatabase (ArcGIS): A geodatabase that stores data in Microsoft Access. A personal geodatabase can be read simultaneously by several users, but only one user at a time can edit the same data.

Point Feature (ArcGIS): A digital map feature that represents a place or thing that has neither length nor area at a given scale.

Polygon Feature (ArcGIS): A map feature that bounds an area at a given scale, such as a country on a world map or a district on a city map.

Polyline Feature (ArcGIS): A digital map feature that represents a place or thing that has length but not area at a given scale. A polyline feature may have one or more parts. For example, a stream is typically a polyline feature with one part. A multipart polyline feature is associated with a single record in an attribute table.

Raster (ArcGIS): A spatial data model that defines space as an array of equally sized cells arranged in rows and columns, and composed of single or multiple bands. Each cell contains an

attribute value and location coordinates. Unlike a vector structure, which stores coordinates explicitly, raster coordinates are contained in the ordering of the matrix. Groups of cells that share the same value represent the same type of geographic feature.

Reclassify (ArcGIS): The process of taking input (raster) cell values and replacing them with new output cell values. Reclassification is often used to simplify or change the interpretation of raster data by changing a single value to a new value, or grouping ranges of values into single values—for example, assigning a value of 1 to cells that have values of 1 to 50, 2 to cells that range from 51 to 100, and so on.

Repair Geometry Tool (ArcGIS): Inspects each feature's geometry for problems and fixes the problems that are found. Valid input formats are shapefile and feature classes stored in a personal geodatabase or file geodatabase.

Select by Location (ArcGIS): To choose from a number or group of features or records based on their location relative to other features.

Shapefile (ArcGIS): A vector data storage format for storing the location, shape, and attributes of geographic features. A shapefile is stored in a set of related files and contains one feature class.

Slivers (ArcGIS): A small, narrow, polygon feature that appears along the borders of polygons following the overlay of two or more geographic datasets. Sliver polygons may indicate topology problems with the source polygon features, or they may be a legitimate result of the overlay.

Slope Tool (ArcGIS): Tool used to calculate the incline, or steepness, of a surface. Slope can be measured in degrees from horizontal (0–90), or percent slope (which is the rise divided by the run, multiplied by 100). A slope of 45 degrees equals 100 percent slope. As slope angle approaches vertical (90 degrees), the percent slope approaches infinity. The slope of a TIN face is the steepest downhill slope of a plane defined by the face.

Spatial Analyst Toolbar (ArcGIS): Toolbar containing tools that examine the locations, attributes, and relationships of features in spatial data through overlay and other analytical techniques in order to address a question or gain useful knowledge. Spatial analysis extracts or creates new information from spatial data.

Stream Buffer (ArcGIS, ArcHydro9): Number of cells around the linear feature class for which the smoothing will occur during *DEM Reconditioning (AGREE).*

Table Operations Tool (ArcGIS): A toolset provided by the *Xtools Pro Extension.*

Terrain Preprocessing Toolbar (ArcGIS, ArcHydro9): The purpose of terrain preprocessing is to perform an initial analysis of the terrain and to prepare the dataset for further processing. A Digital Elevation Model (DEM)/Digital Terrain Model (DTM) of the study area is required as input for terrain preprocessing: a DTM is a grid in which each cell is assigned the average elevation on the area represented by the cell. The DTM must be in ESRI GRID format.

Triangulated Irregular Network (TIN, ArcGIS): A vector data structure that partitions geographic space into contiguous, nonoverlapping triangles. The vertices of each triangle are sample data points with x-, y-, and z-values. These sample points are connected by lines to form Delaunay triangles. TINs are used to store and display surface models.

Union Tool (ArcGIS): A topological overlay of two or more polygon spatial datasets that preserves the features that fall within the spatial extent of either input dataset; that is, all features from both datasets are retained and extracted into a new polygon dataset.

Vector (ArcGIS): A coordinate-based data model that represents geographic features as points, lines, and polygons. Each point feature is represented as a single coordinate pair, while line and polygon features are represented as ordered lists of vertices. Attributes are associated with each vector feature, as opposed to a raster data model, which associates attributes with grid cells.

Watershed Processing Toolbar (ArcGIS, ArcHydro9): The Watershed Processing menu provides access to several functions that allow fast watershed delineation and topographic characteristics extraction, e.g. *Batch Watershed Delineation for Polygons.*

Xtools Pro Extension Toolbar: An independent extension used for spatial analysis, shape conversion, and table management tools.

Chapter 3

Hardpan (or Iron Pan): A cemented layer of iron rich material or soil.

Mispickle: Term for arsenopyrite used to describe ore deposits surrounding copper lodes.

Phreatic zone: Saturated soil or rock, lying below the groundwater table. Overlain by the unsaturated zone (*vadose zone*), above the groundwater table.

Chapter 4:

Bryophytes: Bryophytes are the oldest land plants on earth and comprise three main taxonomic groups: mosses (Bryophyta), liverworts (Marchantiophyta) and hornworts (Anthocerotophyta).On bare and disturbed ground they are primary pioneers helping other plants to gain a foothold. Bryophytes show a wealth of adaptive features to all kinds of climates, substrates and habitats. Many are precise indicators: of rock type such as Tortella tortuosa on limestone, Andreaea and Racomitrium on acidic or granitic rocks, of acid bogs, eg. Sphagnum species, of rich fens, eg. Tomentypnum nitens, of metalliferous rocks and soil, eg. Ditrichum plumbicola and Grimmia atrata[4].

Country Rock: Rock native to an area

Hardpan (or Iron Pan): See Chapter 3 entry.

Phreatic zone: See Chapter 3 entry.

Variscan Orogeny: see Chapter 1 entry.

---

[4] Reference: Royal Botanical Garden Edinburgh webpage accessed 03/03/2011, available online at: http://www.rbge.org.uk/science/cryptogamic-plants-and-fungi/bryology

Chapter 5:

EDTA: Ethylenediaminetetraacetic acid, a water- soluble hexadentate ligand and chelating agent.

DTPA: Diethylene triamine pentaacetic acid , a water-soluble ligand capable of forming up to 8 bonds as a chelate.

NTA: Nitrilotriacetic acid, a water-soluble chelating agent, easily biodegraded.

BCR: The Standards, Measurements and Testing Programme (formerly BCR) of the European Commission.

NEN: The Netherlands Standardization Institute (NEN).

CEN: European Committee for Standardization.

Chapter 1

Introduction and Project Aims

1. Introduction

1.1 Mine Water Pollution as an International Problem

The extraction and processing of minerals underpins industry and lifestyles in the modern world, however the cost to the environment, in particularly the negative impact on water quality has become increasingly controversial in recent decades (Younger, 2002). Globally, approximately 80% of modern mining is conducted using vast surface workings whilst older mines, smaller operations and those seeking high value commodities such as gold and diamond are mined by a variety of other methods including deep mining, and hydraulic working of alluvial deposits.

Many metal and coal mines are hosted by sulphide-rich deposits and contain a high proportion of iron sulphide minerals, of which pyrite (FeS_2) is the most common. Mining allows oxygen to penetrate underground deposits that would otherwise be isolated from the atmosphere. The oxidation of pyritic minerals releases acidity, sulphate and constituent metals and metalloids into waters. Reactions are accelerated by acidophilic bacteria (e.g. *Thiobacillus ferrioxidans*), such that concentrations of dissolved metals and metalloids can reach highly toxic levels.

Mine waters may be released following mine-closure as underground workings flood and discharge into surface water bodies through man-made drains *or adits*. One such incident occurred in 1992 at Wheal Jane, Cornwall, when mine waters containing in excess of 3500 mg L^{-1} of dissolved metals discharged into the Carnon River (Younger *et al.*, 2005).

The problem is commonly referred to as acid mine drainage (AMD), although drainage waters can also be alkaline in nature, depending on the host geology. Areas affected by mine pollution have been the subject of numerous water quality (see Table 1.1 for examples), soil quality, environmental impact and human health studies. Recent

examples in the literature span many countries including: Bolivia e.g. Salvarredy-Aranguren *et al.* (2008), Chile e.g. Ramirez *et al.* (2005), China e.g. Fu *et al.* (2010), the Democratic Republic of Conge e.g. Banza *et al.*(2009), France e.g. Casiot *et al.*(2005), South Africa e.g. Winde and Van der Walt (2004), Spain e.g. Olias *et al.*(2004)*,* Conesa *et al.*(2006) , Loredo *et al.* (2006), Nieto *et al.* (2007) and Cánovas *et al.* (2008), the USA e.g. Schmitt *et al.* (2007) and Butler *et al.*(2008), the UK e.g. Palumbo-Roe *et al.* (2007), Hudson-Edwards *et al.* (2008) and Byrne *et al.*(2010) and Zambia e.g. Kribek *et al.*, (2010).

Waste rock at mine sites can contain enough pyritic material to act as sources of pollution in their own right. Such processes are included within the subject area of acid mine drainage (AMD), or sometimes termed acid rock drainage (ARD). AMD from mine waste rock is an internationally recognised threat to water resources capable of producing contaminated drainage for centuries after mining has ceased (INAP, 2009).

The composition of wastes tips varies widely due to variations in ore-deposit mineralogy and differences in the processing techniques and efficiency of metal recovery. The tips contain metal-bearing rock uneconomic to process at the time of operations, and an assortment of other minerals characteristic of the host geology, often referred to as *gangue*. Tips may contain a mixture of wastes from different stages in the extraction process or commonly are divided into coarse *discard,* (resulting from crushing of bulk rock), and finer *tailings* (resulting from gravimetric separation and concentration of valuable minerals). Other materials may also be included in waste deposits including chemicals, machinery and buildings associated with the processing and smelting of ore minerals.

Waste tips resulting from modern open-pit mining can be vast. For example, over three billion metric tons of waste rock have been produced at Bingham Canyon

(USA), covering an area of more than 2000 ha, since open pit mining operations for copper began in 1906 (Borden and Black, 2005).

Table 1.1: Concentrations of dissolved metals reported in selection of other studies of waters impacted by mine drainage metal mines. All values in mg L^{-1}, rounded to 2 s.f.

Authors	Impacted Water / Location	pH	Fe	Cu	Zn	Al	Pb	Cd	As
Salvarredy-Aranguren (2008)	Surface waters in a pyrite mining area, Bolivia.	2.7-9.2	0.01-2900	<0.0001-2.6	0.0168-17	<0.01-14	<0.0001-0.28	<0.0001-1.0	0.0001-2.3
Nieto *et al.*(2007)	River (Rio Odiel) in Iberian Pyrite Belt, Spain.	3.0-5.1	0.31-24	0.5-17	1.3-36	0.58-180	<0.007-0.27	0.005-0.18	<0.003-0.022
Stillings *et al.* (2008)	Stream water in Cu mining area, Alaska.	6.8	0.57	0.038	0.25	0.10	0.0021	-	-
Canovas *et al.* (2008)	River (Rio Tinto) in Pena del Hierro mining area, Spain.	2.3-2.7	10-490	1.6-55	1.7-55	7.0-190	-	-	-
Loredo *et al.*(2006)	Surface waters at an abandoned Hg mine, Spain.	6.7-8.8	<0.01-0.60	<0.002-0.013	<0.005-0.012	-	-	-	<0.030-290

1.2   Current Status of Mine Water Pollution from Abandoned Metal Mines in the UK

There are several historic metal mining regions of the UK (Figure 1.1), hosted in contrasting geological settings. Deposits in Devon and Cornwall occur primarily as sulphide deposits producing acidic drainage waters, while the mines of Northern England are set within carbonates giving rise to circum-neutral or net alkaline drainage waters (Younger, 2000). Soil and water contamination caused by mining in the Tamar catchment, which spans the border between Devon and Cornwall have been the subject of a number of investigations, e.g. (Kavanagh *et al.*, 1997; Price, 2002; Dybowska *et al.*, 2005; Klink *et al.*, 2005; Mighanetara *et al.*, 2009). From the results and regulatory monitoring and survey data from the Environment Agency and British Geological Survey, a clear contamination issue has been identified.

Figure 1.1 Metal Mining Regions of the United Kingdom from Hudson-Edwards *et al.* (2008)

However, whilst contamination issues are widely reported, to date no sustainable, passive or semi-passive method has been established to treat mine drainage waters from non-coal mines in the UK (Johnston *et al.*, 2008). An active treatment system has been successful at Wheal Jane, Cornwall using liming, flocculation and separation procedures to remove metals from solution. However the running costs at inception were estimated to be £ 748 000 per annum (McGuiness, 1999) and overall

expenditure was estimated to be £20 million by 2002 (Younger, 2002). Progress towards remediation of other sites, including those in the Tamar catchment, remains at an early stage.

Directive 2006/21/EC on the Management of Waste from the Extractive Industries, requires that "Member States shall ensure that an inventory of closed waste facilities, including abandoned waste facilities [...] which *cause* serious negative environmental impacts or have the *potential* of becoming in the medium or short term a serious threat to human health or the environment is drawn up and periodically updated"(Stanley *et al.*, 2010). The inventory should be drawn up and made available to the public by 01 May 2012.

Prioritisation of sites with mine water discharges is also necessary for River Basin Management plans driven by the European Water Framework Directive (WFD, 2000/60/EC). Basic requirements of the WFD relevant to mine water discharges include the "aim to achieve good ecological and chemical status for surface and ground waters by 2015" although it goes on to recognise that this may not be possible in some areas. Definition of "good" status is based on existing and updated Environmental Quality Standard (EQS) for controlled substances(UKTAG, 2008).

Measures must also be implemented to "progressively reduce the pollution of surface waters by substances that could prevent achievement of the environmental objectives of the WFD". Such substances are listed by the Dangerous Substances Directive (2006/11/EC) and include cadmium (List I) and zinc, copper, lead and arsenic (List II). The purpose of the Directive is to eliminate pollution from list I substances and to reduce pollution from list II substances (ECE, 2011)

Mayes *et al.* (2009) linked mining areas with EQS quality failures for metals/metalloids associated with metal mine drainage. The results were combined with other impact criteria (e.g. groundwater quality, ecology) to produce a catchment scale

6

risk assessment and prioritisation of water bodies affected by mine waters. The outcome highlighted SW England as having a concentration of priority watercourses, containing 58 impacted water bodies.

South west England also relies heavily on surface water resources for drinking water supplies compared with other regions of the UK. In the absence of significant groundwater aquifers, South West Water abstract 90% of raw waters from reservoirs and rivers (SWW, 2006). Seventeen rivers are abstracted in the Roadford Strategic Supply Area, which encompasses much of the Tamar catchment, including an intake from the River Tamar at Gunnislake, downstream of many abandoned mine sites (SWW, 2009). Elevated metal concentrations in intake waters are reduced with specialist treatment systems and as a result rarely cause regulatory failure. However, the WFD also presses that there must be measures to "safeguard water quality in order to reduce the level of purification treatment for the production of drinking water".

1.3 The Study Area

Geology

The Tamar catchment is an area of approximately 1880 km^2 on the south west coast of England. The northern half of the catchment is hosted by the Milstone Grit and Culm Measures of Carboniferous age. To the south the catchment is underlain by the Upper, Middle and Lower Old Red Sandstones of Devonian age (Webb, 1978). Parts of the catchment are highly mineralised with metal and arsenic deposits, forming part of the Cornubian ore field. The deposits were created during the pre-, syn- and postbatholithic stages of a major geological event, the *Variscan orogeny*, which occurred 270-400 MA (Jackson *et al.*, 1989). During this time, five major and several lesser bosses of granite intruded into host marine mudstone-sandstone sequences across SW England (Figure 1.2).

The heat generated allowed hydrothermal fluids and vapours to concentrate trace elements from the surrounding sedimentary rocks. Cooling and contracting of the granite created fractures into which hydrothermal fluids could deposit metallic ore minerals (Trounson, 1989). The hydrothermal fluids circulated preferentially along existing fractures and other planes of weakness and produced mineral veins with two main orientations. A roughly east-west trending set of lodes containing Sn, Cu, As and W minerals, and later veins, known as "cross-courses" which trend roughly north-south and carry Pb, Zn and Ag ores (Smedley and Allen, 2004). The weathered granite bosses are now recognisable as Dartmoor, Bodmin Moor and Kit Hill which now form the highest parts of the Tamar catchment.

Figure 1.4: Map showing location of five major granite bosses (orange) in south west England and lesser intrusions of Kit Hill, Hingston Down and Gunnislake within the Tamar catchment area (grey outline). Distribution of recorded mines also indicated (EA, black dots). Created in ArcMap. © Crown Copyright and Landmark Information Group Limited (2010). All rights reserved.

As a result of the mineralisation and subsequent mining, some soils within the catchment are highly enriched with respect to the rest of England and Wales for a number of elements, notably As, Cr, Cu, Mo, Ni, Sn,V and Zn (Webb, 1978). Ground waters can also be enriched and are mainly shallow, circulating within thin soils, weathered near-surface bedrock and granite fractures (Smedley and Allen, 2004). The chemistry of the groundwater is strongly controlled by rainfall composition and mineral weathering of the local rock.

Mining History

The mineral deposits associated with the granites have been exploited since the Bronze Age, initially alluvial deposits close to the granite outcrops were worked for tin, then underground mining began to exploit deposits of lead and copper. In the mid 19th century, mines in the Tamar catchment became the world's principle supplier of copper. When arsenic became a prized commodity in the late 19th century, the mines switched to arsenic production, prolonging their life into the 20th Century (Hamilton Jenkin, 2005).

The largest mine in the catchment, Devon Great Consols (DGC), is estimated to have produced around 40 thousand tonnes of copper during its operational life (Burt *et al.*, 1984). This is small compared to the 18.1 million tons of copper produced by the world's largest copper mine, Bingham Canyon (RioTinto, 2010). Nevertheless, at least 500,000 tonnes of good quality ore rock would have been mined at DGC (based on 8% copper content) plus an unrecorded amount of low-grade waste rock. Despite their relatively small size, it is estimated that over 2000 individual mines were once operational across south west England (Dines, 1956). Mined primarily for copper, tin or lead, the mine also produced considerable amounts of zinc, silver, tungsten, and manganese as by-products (Trounson, 1989).

The demise of these mines was due to a combination of factors including falling commodity prices, particularly after the copper crash of 1866 (Hamilton Jenkin, 2005), exhaustion of the copper supply, rising costs of materials and a lack of skilled labour during the first and second world wars (Trounson, 1989). Copper and tin mining moved to more profitable operations around the world taking large numbers of skilled men, often referred to simply as "Cornish Miners", with it (BBC, 2004). A small number of Cornish mines including South Crofty and Wheal Jane continued to mine tin into the late 20th century. However the mines in the Tamar catchment were closed by the mid 20th century.

Some unsuccessful efforts were made to reopen the deep mines but in most cases re-working of waste tips for arsenic, tin, tungsten and uranium were the last activities conducted at the mines before abandonment (Trounson, 1989; Richardson, 1995; CMWHS, 2010). Currently no mines are operational in south west England although South Crofty, which ceased production of tin in 1998, is developing towards a shallow resource and Hemerdon, an open cast tungsten operation 7 miles NW of Plymouth, is expected to commence operations in 2011(Hale, 2008; Moon, 2010).

The relatively low recovery efficiency during the peak period of mining in the mid to late 19th century mining, both in terms of extraction efficiency and because many mines were abandoned for economic reasons, means that a considerable amount of sulphidic material remained in the waste. Furthermore, little environmental consideration was given to the management of mine waste in early mines. As a result wastes were often simply tipped onto large dumps, close to watercourses and left in situ after closure of the mine. Today, over 100 years after closure in most cases, the waste tips pose an unquantified risk to the quality of water courses in south west England.

The abandoned mine sites in the Tamar catchment, and south west England as a whole, have left a two-fold legacy. On the one hand, industrial archaeology of

international importance and ecologically significant areas where rare species are able to thrive (CMWHS, 2010). But mining has also left large areas of contaminated land and discharges of mine waters, which have a negative impact on the health of freshwater and marine ecosystems (Hudson-Edwards *et al.*, 2008). It is the composition of the drainage from mine waste tips, and the impact on surface water quality in the Tamar catchment, which is central to this study. It is hoped that the results will help inform regulators, what measures, if any, should be implemented to minimise the negative environmental impact of mine waste tips on surface water quality.

1.4 Rationale and Project Development

The project set out to provide the Environment Agency, who co-funded the project, with information to improve the management of mine waste tips as a pollutant source, based on sound scientific reasoning. Mine waste tips at two contrasting study sites were investigated in detail to provide an approximation of pollutant loads (Al, As, Cd, Cu, Fe, Mn, Ni, Pb, Zn) from mine waste tips using best available techniques. These estimated loads were compared to the magnitude of contaminant discharges from known point discharges, for which data already exists.

As the project developed it became apparent that with limited resources conducting detailed investigations of many sites in the Tamar catchment was not feasible. Also, for transferability to other sites understanding the geochemical processes controlling the release of eco-toxic elements would be most valuable. Therefore, the development of less expensive alternatives, such as a GIS based risk assessment and rapid laboratory leaching experiments was an appealing avenue for investigation. As a precautionary measure, the laboratory experiments chosen were validated against one another and with data gathered in the field.

1.5   Project Aims and Objectives

The overall aim of this project was to quantify the risk to surface water quality posed by drainage from mine waste tips in the Tamar catchment.

The specific objectives were to:

- Identify and prioritise areas of mine waste in the Tamar catchment based on available data (Chapter 2).

- Develop a GIS-based method of risk assessment that, with limited modification, may be transferable to other catchments in south west England. (Chapter 2)

- Measure dissolved contaminant concentrations in situ (particularly Al, Cu, Zn, Pb, Cd, Ni and As), in waters emerging from mine wastes of different character and representative of others found in the catchment. (Chapter 3 and Chapter 4)

- Measure instantaneous flow of surface drains and where possible estimate contaminant fluxes of dissolved contaminants moving through the study sites. (Chapter 3 and Chapter 4)

- Characterise the mineralogy and physical characteristics of a selection of mine waste samples from sites in the Tamar catchment. (Chapter 5)

- Investigate the use of laboratory-based static and dynamic experiments to generate leachates under controlled conditions and critically assesses their suitability for predicting contaminant concentrations in the field. (Chapter 5)

- Investigate the factors affecting contaminant release and transport from mine waste (e.g. waste composition and site hydrology). (Chapters 3, 4 and 5)

- To assess what measures might be implemented to reduce the contaminant flux emerging from mine waste tips in the Tamar Catchment. (Chapter 6)

1.6   References

Banza, C. L. N., Nawrot, T. S., Haufroid, V., Decrée, S., De Putter, T., Smolders, E., Kabyla, B. I., Luboya, O. N., Ilunga, A. N., Mutombo, A. M. and Nemery, B. (2009). High human exposure to cobalt and other metals in Katanga, a mining area of the Democratic Republic of Congo. *Environmental Research.* **109** (6) pp 745-52.

BBC.(2004). "Immigration and Emigration, I'm Alright Jack." *Legacies, UK History Local to You, Cornwall.* BBC. Accessed 10/05/10. Avaliable on the world wide web at:
http://www.bbc.co.uk/legacies/immig_emig/england/cornwall/article_1.shtml.

Borden, R. K. and Black, R. (2005). Volunteer Revegetation of Waste Rock Surfaces at the Bingham Canyon Mine, Utah. *J. Environ. Qual.* **34** (6) pp 2234-42.

Burt, R., Waite, P. and Burnley, R. (1984). *Devon and Somerset Mines: meterliferous and associated minerals, 1845-1913.* . Exeter, University of Exeter Press. pp

Butler, B. A., Ranville, J. F. and Ross, P. E. (2008). *Observed and modeled seasonal trends in dissolved and particulate Cu, Fe, Mn, and Zn in a mining-impacted stream.*pp 3135-45 pp

Byrne, P., Reid, I. and Wood, P. (2010). Sediment geochemistry of streams draining abandoned lead/zinc mines in central Wales: the Afon Twymyn. *Journal of Soils and Sediments.* **10** (4) pp 683-97.

Cánovas, C. R., Hubbard, C. G., Olías, M., Nieto, J. M., Black, S. and Coleman, M. L. (2008). Hydrochemical variations and contaminant load in the Río Tinto (Spain) during flood events. *Journal of Hydrology.* **350** (1-2) pp 25-40.

Casiot, C., Lebrun, S., Morin, G., Bruneel, O., Personné, J. C. and Elbaz-Poulichet, F. (2005). Sorption and redox processes controlling arsenic fate and transport in a stream impacted by acid mine drainage. *Science of the Total Environment.* **347** (1-3) pp 122-30.

CMWHS.(2010). "Cornish Mining World Heritage Site ". The Cornish World Heritage Site. Accessed 30/04/2010. Avaliable on the world wide web at: http://www.cornish-mining.org.uk/.

Conesa, H. M., Faz, Á. and Arnaldos, R. (2006). Heavy metal accumulation and tolerance in plants from mine tailings of the semiarid Cartagena-La Unión mining district (SE Spain). *Science of the Total Environment.* **366** (1) pp 1-11.

Dines, H. G. (1956). *The metalliferous mining region of south-west England*, HMSO.pp 709 pp

Dybowska, A., Farogo, M., Valsami-Jones, E. and Thornton, L. (2005). Operationally defined associations of arsenic and copper from soil and mine waste in south-west England. *Chemical Speciation and Bioavailability.* **17** (4) pp 147-60.

ECE.(2011). "Directive 76/464/EEC - Water pollution by discharges of certain dangerous substances." *WISE - Water Information System for Europe.* European Comission Environment. Accessed 21/09/2011. Avaliable on the world wide web at:
http://ec.europa.eu/environment/water/water-dangersub/76_464.htm#list2.

Fu, Z., Wu, F., Amarasiriwardena, D., Mo, C., Liu, B., Zhu, J., Deng, Q. and Liao, H. (2010). Antimony, arsenic and mercury in the aquatic environment and fish in a large antimony mining area in Hunan, China. *Science of the Total Environment.* **408** (16) pp 3403-10.

Hale, H.(2008). "Speciality Metals and Development." Wolf Minerals Limited. Accessed 25/08/10. Avaliable on the world wide web at: http://www.asx.com.au/asxpdf/20080331/pdf/3189xxrd3zpr95.pdf.

Hamilton Jenkin, A. K. (2005). *Mines Of Devon*. Trowbridge, Cromwell Press.pp 160 pp

Hudson-Edwards, K. A., Macklin, M. G., Brewer, P. A. and Dennis, I. A. (2008). *Assessment of Metal Mining-Contaminated River Sediments in England and Wales*.SC030136/4   Environment Agency.

INAP.(2009). "Global Acid Rock Drainage Guide (GARD Guide)." International Network for Acid Prevention. Accessed 14/09/10. Avaliable on the world wide web at: http://www.gardguide.com/.

Jackson, N. J., Willis-Richards, J., Manning, D. A. C. and Samms, M. (1989). Evolution of the Cornubian Ore Field, southwest England: Part II. Mineral deposits and ore forming proecesses. *Economic Geology.* **84** pp 1101-33.

Johnston, D., Potter, H., Jones, C., Rolley, S., Watson, I. and Pritchard, J. (2008) *Science Report - Abandoned Mines and the water environment* Environmnet Agency. Report No. SC030136-41

Kavanagh, P. J., Farago, M. E., Thornton, I. and Braman, R. S. (1997). Bioavaliability of arsenic in soils and mine wastes of the Tamar valley, SW England. *Chemical Speciation and Bioavailability.* **9** (3) pp 77-81.

Klink, B. A., Palumbo, B., Cave, M. and Wragg, J. (2005). *Arsenic dispersal and bioccessibility in mine contaminated soils: a case study from an abandoned arsenic mine in Devon, UK*.Research Report RR/04/003   British Geological Survey pp 52.

Kríbek, B., Majer, V., Veselovský, F. and Nyambe, I. (2010). Discrimination of lithogenic and anthropogenic sources of metals and sulphur in soils of the central-northern part of the Zambian Copperbelt Mining District: A topsoil vs. subsurface soil concept. *Journal of Geochemical Exploration.* **104** (3) pp 69-86.

Loredo, J., Ordóñez, A. and Álvarez, R. (2006). Environmental impact of toxic metals and metalloids from the Muñón Cimero mercury-mining area (Asturias, Spain). *Journal of Hazardous Materials.* **136** (3) pp 455-67.

Mayes, W. M., Johnston, D., Potter, H. A. B. and Jarvis, A. P. (2009). A national strategy for identification, prioritisation and management of pollution from abandoned non-coal mine sites in England and Wales. I.: Methodology development and initial results. *Science of the Total Environment.* **407** (21) pp 5435-47.

McGuiness, S. (1999) *Treatment of Acid Mine Drainage* Science and Environment Section, House of Commons Library. Report No. 99/10

Mighanetara, K., Braungardt, C. B., Rieuwerts, J. S. and Azizi, F. (2009). Contaminant fluxes from point and diffuse sources from abandoned mines in the River Tamar catchment, UK. *Journal of Geochemical Exploration.* **100** pp 116-24.

Moon, C. J. (2010). Geochemical exploration in Cornwall and Devon: a review. *Geochemistry: Exploration, Environment, Analysis.* **10** (3) pp 331-51.

Nieto, J. M., Sarmiento, A. M., Olias, M., Canovas, C. R., Riba, I., Kalman, J. and Delvalls, T. A. (2007). Acid mine drainage pollution in the Tinto and Odiel rivers (Iberian Pyrite Belt, SW Spain) and bioavailability of the transported metals to the Huelva Estuary. *Environment International.* **33** (4) pp 445-55.

Olias, M., Nieto, J. M., Sarmiento, A. M., Ceron, J. C. and Canovas, C. R. (2004). Seasonal water quality variations in a river affected by acid mine drainage: the Odiel River (South West Spain). *Science of the Total Environment.* **333** (1-3) pp 267-81.

Palumbo-Roe, B., Klinck, B. and Cave, M. (2007). Arsenic speciation and mobility in mine wastes from a copper-arsenic mine in Devon, UK: a SEM, XAS, sequential chemical extraction study. *Trace Metals and other Contaminants in the Environment*. P. Bhattacharya, A. B. Mukherjee, J. Bundschuh, R. Zevenhoven and H. L. Richard, Elsevier. **9** pp 441-71.

Price, G. D. (2002). The distribution of trace metal pollutants within intertidal sediments of the Tamar Estuary, SW England. *Geoscience in south-west England*. **3** pp 319-22.

Ramirez, M., Massolo, S., Frache, R. and Correa, J. A. (2005). Metal speciation and environmental impact on sandy beaches due to El Salvador copper mine, Chile. *Marine Pollution Bulletin*. **50** (1) pp 62-72.

Richardson, P. H. G. (1995). *Mines of Dartmoor and the Tamar Valley after 1913*. Torquay, Devon Books.pp 160 pp 50-52

RioTinto.(2010). "Kennecott Utah Copper, Facts About Our Operation." Accessed 11/05/2010. Avaliable on the world wide web at: http://www.kennecott.com/our-company/facts-about-our-operation/.

Salvarredy-Aranguren, M. M., Probst, A., Roulet, M. and Isaure, M.-P. (2008). Contamination of surface waters by mining wastes in the Milluni Valley (Cordillera Real, Bolivia): Mineralogical and hydrological influences. *Applied Geochemistry*. **23** (5) pp 1299-324.

Schmitt, C. J., Brumbaugh, W. G. and May, T. W. (2007). Accumulation of metals in fish from lead-zinc mining areas of southeastern Missouri, USA. *Ecotoxicology and Environmental Safety*. **67** (1) pp 14-30.

Smedley, P. L. and Allen, D. (2004). *Baseline Report Series 16: The Granites of South-West England*.Commissioned Report No. CR/04/255 British Geological Society

Stanley, G., Jordan, G., Hamor, T. and Sponar, M. (2010) *Guidance Document for A Risk-Based Pre-Selection Protocol for the Inventory of Closed Waste Facilities (Draft). Inventory of Closed Waste Facilities* Ad-Hoc Group, A Sub-committee of The Technical Adaptatiob Committee for Directive 2006/21/EC. Report No. 02 (Draft)

Stillings, L. L., Foster, A. L., Koski, R. A., Munk, L. and Shanks Iii, W. C. (2008). Temporal variation and the effect of rainfall on metals flux from the historic Beatson mine, Prince William Sound, Alaska, USA. *Applied Geochemistry*. **23** (2) pp 255-78.

SWW (2006). *Quality Matters* South West Water.

SWW (2009). *Water Resources Plan 2010-2035* South West Water pp 120.

Trounson, J. H. (1989). *The Cornish Mineral Industry: Past Performanace and Future Prospect*. Exeter, BPCC Wheatons Ltd.pp 197 pp

UKTAG (2008). *Proposals for Environmental Quality Standards for Annex VIII Substances*.SR1-2007 UK Technical Advisory Group on the Water Framework Directive.

Webb, J. S. (1978). The Wolfson Geochemical Atlas of England and Wales. Oxford, Clarendon Press.

Winde, F. and Jacobus van der Walt, I. (2004). The significance of groundwater-stream interactions and fluctuating stream chemistry on waterborne uranium contamination of streams--a case study from a gold mining site in South Africa. *Journal of Hydrology*. **287** (1-4) pp 178-96.

Younger, P. L. (2000). Nature and practical implications of heterogeneities in the geochemistry of zinc-rich, alkaline mine waters in an underground F-Pb mine in the UK. *Applied Geochemistry*. **15** (9) pp 1383-97.

Younger, P. L. (2002). Mine water pollution from Kernow to Kwazulu-Natal: Geochemical remedial options and their selection in practice. *Geoscience in south-west England.* **10** pp 255-66.

Younger, P. L., Coulton, R. H. and Froggatt, E. C. (2005). The contribution of science to risk-based decision-making: lessons from the development of full-scale treatment measures for acidic mine waters at Wheal Jane, UK. *Science of the Total Environment.* **338** (1-2) pp 137-54.

-End of Chapter 1-

Chapter 2

Environmental Prioritisation of

Mine Waste Tips in the Tamar

Catchment using GIS

2. Environmental Prioritisation of Mine Waste Tips in the Tamar Catchment using ArcGIS

2.1 Abstract

A geographical information system (GIS) was assembled and utilised to analyse the risk to watercourses becoming contaminated by diffuse mine waters in the Tamar Catchment, an area of extensive historical mining in south west England. Environmental factors that influence the generation and transport of mine waters were considered, and included: topography, rainfall, soil type and underlying geology. Data for each input factor were classified and scored from "Low" to "Extreme" risk and combined into a risk model using ArcGIS software (version 9.3). Catchment and drainage areas were identified for individual mine waste tips using ArcHydro extension tools. Relative weightings for each factor were based on expert knowledge and literature information and applied using an analytical hierarchy procedure (AHP).

Whilst the model does not consider the level of contamination of the waste materials, it serves to inform policy makers where best to target resources prior to detailed site investigations. The model also showcases the application of ArcGIS software to processing readily obtainable data to produce useful and flexible environmental risk assessment. The methodology developed here has since been applied in a simplified form to create a priority list for all abandoned mines in the south west of England. Furthermore the methodology on which the model is based already meets most of the requirements of Article 20 of the Mining Waste Directive (2001/21/EC) for pre-selection of potentially harmful abandoned mine sites.

2.2 Introduction

Within the UK, the government through the Environment Agency recognises the need to quantify the number of mine water discharges from metal mines and the contamination levels contained within them:

"A national strategy to deal with the pollution from non-coal mines cannot be developed until we understand the scale of the problem" (Johnston et al., 2008)

However, mine water discharges to watercourses are often diffuse, emerging from complex, interconnected shafts and adits, sub-surface seepages and surface run-off from spoil heaps. This diffuse character makes quantification challenging and future remediation strategies difficult and costly to implement. In recent years, diffuse sources at abandoned mine sites have been recognised as important contributors of mine water pollution (Mayes *et al.*, 2008). A recent survey of mine water inputs from specific point sources (streams and adits) to the River Tamar suggested that an important component, of up to 50% for most dissolved and particulate metals, may result from diffuse sources (Mighanetara *et al.*, 2009). Therefore, research into the location and magnitude of such discharges is a valuable contribution to current understanding.

A component of diffuse mine water pollution into the Tamar catchment originates from mine waste tips (Mighanetara *et al.*, 2009). Mine waste tips in this region, and those found in similar mineral deposits throughout the world, contain sulphide minerals and secondary mineral phases which act as sources of toxic elements including: cadmium, zinc, copper, lead and arsenic (Roussel *et al.*, 2000; Palumbo-Roe *et al.*, 2007; Carmona *et al.*, 2009; Rieuwerts *et al.*, 2009). Leachates from the tips transport high concentrations of dissolved metals to surface watercourses via shallow groundwater movement and surface run-off (Sainz *et al.*, 2002; Turner *et al.*, 2009). The magnitude of pollution is dependent on the extent and situation of tips and the

minerals they contain. Geometry (Kampf *et al.*, 2002), particle size (Smith *et al.*, 1999), compaction (Evans and Loch, 1996) and lack of vegetation (Riley, 1995) affect erosion rates and the exposure of mineral surfaces and therefore influence the level of contamination produced. Once released, migration of dissolved and particulate contaminants depends on the characteristics of the drainage pathway, including slope (IMWR, 2002), precipitation patterns (Sainz *et al.*, 2002), soil type (de Matos *et al.*, 2001) underlying geology (Maskall *et al.*, 1999) and land use (Goulding and Blake, 1998).

Mine waste tips have been investigated throughout the Tamar catchment and SW England as part of this work. Qualitative assessment suggests they are heterogeneous with respect to volume, mineral composition, particle size, stability and degree of vegetation. In addition, ten mining areas in south west England, including Devon Great Consols, are recognised by World Heritage Status (CMWHS, 2010), consequently intrusive investigation and future remediation of these sites requires sensitivity to their archaeological and ecological importance. For complete characterisation and determination of the contamination levels, assessment by qualified individuals on a site-by-site basis would be required. Ideally, comprehensive field investigations at each site, including sampling of waters and soils at high spatial resolution and at depth would be conducted, but these are time-consuming and expensive, particularly as the "polluter pays" principle cannot be applied retrospectively at the abandoned mines (EU directive 2004/35/EC). Directive 2006/21/EC on the Management of Waste from the Extractive Industries, often referred to as the "Mining Waste Directive" − MWD, requires all EC member states to provide an inventory of closed waste facilities by 01 May 2012. It also requires that member states formulate a pre-screening methodology to identify sites that pose a risk to human health or have the

potential to cause negative environmental impacts (Stanley *et al.*, 2010). The methodology applied is at the discretion of the individual member state. For England and Wales, where the total number of mines exceeds 100,000 existing data is currently being gathered and held in a GIS database. Recently published guidance documentation for the development of pre-selection methodology recommends the use of easily available data and a GIS-based system (Stanley *et al.*, 2010).

2.3 Aims and Objectives

The aims of this chapter were to:

- Identify and prioritise areas of mine waste in the Tamar catchment based on available data.
- Develop a GIS-based method of risk assessment that identifies mine waste with the greatest potential to harm watercourses in the Tamar catchment and that may be transferable to other catchments in south west England.

In this chapter a GIS-based methodology is presented which uses existing spatial data to prioritise known areas of mine waste in the Tamar Catchment based on the physical characteristics of their environmental situation. In order to produce the priority list, the following research objectives were set:

1. Review existing soil and water quality data in the Tamar catchment.
2. Compile a list of environmental and physical factors that may increase or attenuate the impact of discharges from mine waste tips on surface watercourses.
3. Review current state of knowledge on the importance of each identified factor.
4. Identify the best sources of data for each input.
5. Compile available data into a GIS compatible format.
6. Apply a suitable method for dividing individual data sets into risk categories.

7. Apply a suitable method of weighting input data sets for relative importance.

8. Combine risk for all input data sets into one GIS-based model.

9. Generate a priority list of mine waste tips in the Tamar catchment.

10. Examine the outcomes of the model and identify major areas of uncertainty, specifically:

   - Compare high priority mine waste tips with existing regulatory failures in surface watercourses.

   - Assess the flexibility and robustness of the model with respect to change of opinion.

   - Asses the usefulness of model as a working tool for regulators.

Objectives 1-4 are presented as a literature review in section 2.4. Objectives 4-8 are presented as methodology in section 2.5. Objectives 9-10 are dealt with in the results and discussion (section 2.6). GIS-related terms are signified by italics and are defined in the glossary at the beginning of the thesis.

2.4 Literature-Informed Method Development

2.4.1 Existing Data in the Tamar Catchment

Academic studies of water, soil or sediment contamination resulting from mining in the Tamar catchment have largely focused on case-study sites, Devon Great Consols being the most widely covered in literature (Kavanagh *et al.*, 1997; Langdon *et al.*, 2001; Piearce *et al.*, 2002; Klink *et al.*, 2005; Palumbo-Roe *et al.*, 2007). Consultancy reports have also been commissioned for some sites including Devon Great Consols, Gunnislake Clitters, Gawton and Bedford United (Wardell-Armstrong, 1990; 1992; Sherrell, 2000; 2001; Buck, 2005; Sherrell, 2005; Buck, 2006) However, such

reports do not extend to detailed quantitative analysis of contaminant levels as they comprise a mixture of ecological, archaeological and geotechnical surveys and preliminary environmental assessments. Government and public organisations have sampled waters and soils across the UK but with generally low spatial resolution. For example, a 1.5 - 2 km^2 sampling grid was used by the British Geological Society's G-BASE project in a comprehensive analysis of physical and chemical parameters in soil, water and sediment (Johnson and Breward, 2004). Monitoring of water quality parameters by the Environment Agency includes routine and targeted surveys and offers the best spatial coverage, being used to identify and prioritise catchments affected by mine water discharges in the UK (Mayes *et al.*, 2009). However, in areas with a high density of mines, current data is insufficient to identify individual contamination sources or resolve diffuse sources, such as mine waste, drainage from point sources, such as adit outflows. Also, the inclusion of data from spot analyses into a prioritisation exercise must be treated with care so as not to skew a spatial assessment model towards areas on which past monitoring efforts have focussed, at the expense of identifying other potential areas of concern.

The Environment Agency has collated information on the location of abandoned metal mine sites throughout the UK, as demanded by the Mining Waste Directive (2006/21/EC), including the spatial extent of contaminated land (e.g. waste heaps, arsenic calciners and mineral processing areas). Data is also available for a range of environmental factors (e.g. rainfall, soil type, geology and topography) which influence the generation and transport of acid mine waters (Evans *et al.*, 2006), especially those resulting from diffuse sources (Xiao and Ji, 2007). This data is available via academic licence or at modest cost and in many cases greater resolution data may be obtained at additional cost. A combination of the environmental data and the mine-specific location

data would produce a valuable tool to prioritise mine sites within catchments, such as the Tamar. The outcomes would supplement existing water quality data and serve to concentrate investigation and remedial efforts to sites of greatest risk, thereby reducing cost.

2.4.2 Geographical Information Systems and Multi-Criteria Decision Analysis

Numerous examples exist in the literature of GIS being used for spatial planning and management. GIS-based multi-criteria decision analysis (GIS-MCDA) combines and transforms geographical data and expert judgements on the relative importance of input data to provide information for decision making (Malczewski, 2006). Examples of GIS application to environmental risk assessment include the study of soil erosion (Nekhay *et al.*, 2009), landslide risk (Barredo *et al.*, 2000) and bushfires (Chen *et al.*, 2003). To date, no one has applied GIS-MCDA to identify high risk areas of mine waste with respect to surface water quality.

In this study, ArcGIS 9.3 software, including the ArcHydro extension, were used to combine the best available geo-referenced data into a GIS catchment prioritisation model for diffuse mine water pollution. Diffuse mine water in this context refers to surface run-off and shallow groundwater movement of leachate emanating mine waste heaps and contaminated land. Although this model covers the Tamar catchment only, the methodology is intended to be flexible and simple such that it may be transferred, with some modification, to other catchments of the UK. This chapter details the procedure used to prioritise mine waste tips in the Tamar catchment and discusses the output from the prioritisation.

The procedure involved the subjective classification of data sets and judgements of the relative importance of input parameters. These decisions are based on literature

information, expert judgement and the understanding of the author gained from site investigations.

2.4.3   Environmental Factors that Influence the Diffuse Pollution Output

Proximity

Migration of mine waters and particulate-associated contaminants are influenced by many environmental factors including proximity to receptors. Waste tips in direct contact with a watercourse are likely to represent greater risk than those at a greater distance to it. In-stream and sub-surface interactions of dissolved and particulate contaminants are complex and care should be taken when generalising elemental behaviour. Interaction with the inorganic and organic content of soils and/or sediments has been shown to reduce the mobility of many dissolved contaminants found in mine waters, including arsenic (Wang and Mulligan, 2006; Asta *et al.*, 2010), copper (Clemente *et al.*, 2006) lead (de Matos *et al.*, 2001) and antimony (Filella *et al.*, 2009). However, attenuation is strongly influenced by soil pH and varies between elements, with zinc and cadmium often remaining the most mobile of the elements commonly associated with mine waters (Harter, 1983; de Matos *et al.*, 2001). Also, some soil components may enhance the release of metals, both Teminghoff *et al.* (1998) and Wu *et al.* (2002) found complexation with dissolved organic matter enhanced copper mobility through soils. Dilution effects, soil cationic exchange capacity and preferential pathways are also important considerations in sub-surface and surface water transport and the effect of natural attenuation. Given the complexity of interactions likely to arise from mine waters in the environment, a reliable measure of contaminant mobility could only be gained from site investigation. However, at the catchment scale it is assumed that extended transport via sub-surface or surface waters (minor streams) would provide

24

greater scope for natural attenuation and dilution than direct input into a major watercourse. This is based on fate and transport studies of metals and arsenic in mine waters, particularly those with similar mineralisation and bedrock geology such as SW Spain (e.g. Asta *et al.* (2010) and Sánchez España *et al.* (2005)). Taking this into account, a simple distance measurement was adopted to incorporate the length of the migration pathway into the model.

Rainfall

Rainfall varies across the catchment; the highest overall rainfall is associated with the upland areas around Dartmoor and Bodmin Moor (Met Office, 2010). The importance of precipitation patterns in this study is two-fold. Firstly in areas of high average rainfall, a larger flux of mobile contaminants from spoil heaps may be generated than in areas of lower average rainfall, assuming other conditions are similar. Secondly, the intensity of rainfall bears great importance to the fate of meteoric waters once they contact land surfaces. During high energy rainfall events, soil infiltration is reduced (e.g. Mamedov *et al,.* (2000), Fan *et al.* (2008)), therefore a greater proportion of meteoric waters will enter watercourses as surface run-off. Surface run-off can transport particulate matter from spoil heaps to watercourses, particularly finer size fractions (Hairsine *et al.*, 1999), thereby enhancing the pollutant flux to watercourses. Extreme rainfall can also trigger slope failures (Cai and Ugai, 2004; Tohari *et al.*, 2007), which may cause an acute pollution incident.

Long-term average rainfall data is available for selected locations from the Met Office for the period 1971-2000. The average annual rainfall for south west England and south Wales (1250 mm) is higher than the national average (1130 mm), and the distribution of the rainfall varies widely from station to station. Published summary statistics for the weather stations closest to the Tamar catchment shows Princetown on

Dartmoor (1970 mm), receives over twice as much as Bude (920 mm) on the north-west coast.

Rainfall intensity is usually categorised based on a depth per unit time and where available, hourly rates are considered most appropriate to capture rainfall events. Dunkerley (2008) recommends the rate classification of Tokay and Short (1996) shown in Table 2.1. Laakso *et al.* (2003) also define rainfall above 5 mm h^{-1} as 'heavy'.

However, hourly rainfall data is often unavailable for large areas over large time-periods. This is the case for the 30 current MIDAS stations (Met Office, 2010) within the Tamar Catchment that log daily rainfall only. Although this data is not suitable for the analysis of heavy rainfall events of short duration, it can be used to differentiate areas receiving periods of heavy rain. Some authors use daily amounts to define 'heavy' rain events in terms of daily depths. For example, Ower *et al.* (2009) use this term for precipitation >10 mm d^{-1}, based on observed aquifer recharge. This approach was adapted for this study and the treatment of MIDAS data to determine heavy rainfall events is detailed in the methodology section.

Table 2.1: Rain rate classification from Tokay and Short (1996).

Classification	Hourly Rainfall mm h^{-1}
Extreme	≥ 20
Very Heavy	$\geq 10 < 20$
Heavy	$\geq 5 > 10$
Moderate	$\geq 2 < 5$
Light	$\geq 1 < 2$
Very Light	<1

Topographical Slope

Alongside hydrology, topographical slope exerts a control on soil erosion rates with greater erosion potential being created by steeper slopes (Gabbard *et al.*, 1998). Topographical slope is a critical factor in soil loss calculations, is an integral part of most soil erosion models and within a GIS (Kim and Miller, 1996; Liu *et al.*, 2000).

Within the context of this study, steep slopes in the tip catchment may increase the risk of waste tip slope failures during or following rainfall events, whilst steep down slopes will maximise the transport of material by gravity or water transport (Dai *et al.*, 2002). Tip geometry is critically important to stability but is unlikely to be adequately described in a catchment scale model due to a lack of resolution and therefore cannot be considered here.

Slope also affects water flow in the saturated zone, as it is governed by hydraulic head which is a function of elevation and pressure (from Darcy's Law). This also applies to water flow in un-saturated zone but drying of soil add complications, due to the development of negative pore pressures and capillary forces (Dominico and Schwarz, 1998). Overall mass transport of dissolved contaminants, through comparable geological and soil media, is likely to occur more quickly for steeper slopes.

Soils, Bedrock and Superficial Geology

The hydraulic conductivity of soils, bedrocks and superficial deposits determines how rapidly aqueous contamination may be transported from source to surface waters, via shallow and deep groundwater movement. Soils and bedrocks have an important impact on hydrological processes influencing the downstream flow observed (Merrington *et al.*, 2006). Well-drained soils can absorb infiltrating surface waters without saturation and reduce direct input into streams. Saturated, finely textured or clay rich soils have a high run-off potential due to low infiltration and water

transmission rates (US-SCS, 1964). The National Soil Map (NATMAP, 1:250 000) is the authoritative digital soil map for England and Wales. Provided by The National Soil Resources Institute (NSRI) at Cranfield University, it offers descriptions for 297 soil types on which catchment scale assessments of hydraulic properties may be made.

Low hydraulic conductivity of the underlying bedrock results in limited infiltration by percolating surface waters. Consequently, soils overlying low permeability strata are more likely to become saturated, resulting in greater surface run off with reduced opportunity for natural attenuation. The Tamar catchment is underlain by rocks of low permeability being predominantly slates and sandstones with no significant aquifers (BGS, 2010). Shallow groundwater movement through soils and superficial deposits is therefore likely to represent the most important migration pathway for leachates leaving mine wastes in the Tamar catchment, but this may not be the case in other areas.

The British Geological Survey holds data on the permeability of bedrock and superficial lithology for the whole of the UK at the regional scale. In the Tamar catchment, bedrock permeability is via fracture flow, whilst superficial permeability is either intergranular or mixed. A limitation of the permeability data is that there is increasing uncertainty with depth. Bedrock units cannot therefore be combined to give an accurate value for transmissivity of the subsurface at a given point. This would require accurate information on thickness of the layers (BGS, 2009). Nevertheless, the permeability index does provide useful regional data from a reliable source which is coded based on expert judgement.

The permeability of superficial geological deposits of quaternary age (generally unconsolidated) is recorded separately to bedrock geology (BGS, 2009; 2010). Within

the Tamar catchment these comprise peat deposits and river terrace/alluvial deposits (mostly sands and gravels) (BGS, 2010).

Soils and superficial deposits both act as pathways for migrating ground waters and as a potential sink for dissolved metals transported with them. Strata with very low hydraulic conductivity, such as those containing clays, offer a barrier to pollutant migration. Many clays minerals also retard metal species via cationic-exchange (van de Lee and De Windt, 2001; Alvarez and Illman, 2006). Natural clay, or derived clay materials, such as bentonite, are therefore often used as a hydraulic barrier or as a retention medium for contaminants in waste leachates (Bellir *et al.*, 2005). Attenuation of pollutant metals via sorption is also well documented for soils with a high humic acid content. Peat, in particular is an effective sorbent of dissolved metal pollutants through a variety of mechanisms, including ion-exchange, complexation, and surface adsorption (Brown *et al.*, 2000; Ringqvist *et al.*, 2002). However, if humic acids are dissolved or suspended in waters, complexation with metals could actually enhance mobility by reducing adsorption on mineral surfaces (Schmitt *et al.*, 2002).

Superficial alluvial deposits (sands and gravels) may also enhance mobility by providing a high permeability pathway for migration of contaminants into rivers. Physical and chemical processes of metal mobility and retention have been investigated in detail for various solid media and different soil types. However, due to the heterogeneous nature of soils and superficial deposits across large areas and with depth, these processes cannot be included in the catchment-scale model developed in this study. The influence of soil, superficial deposits and bedrock geology on metal transport will be taken into account by the inference of hydraulic properties in catchment scale mapping.

Vegetation

The type and degree of vegetation cover has been shown to have a marked impact on the soil erosion rates of catchments worldwide. Soil loss may be greatly reduced in areas of vegetation. For example, Marques *et al.* (2007) showed negligible soil loss for vegetated soils during extreme rainfall (21 mm h^{-1}, classified according to Table 2.1), whereas significant transport of suspended material (74 kg Ha^{-1}) was observed on bare soils. There are a number of ways in which vegetation cover can offset erosion rates under conditions of varying climate, soil type and topography:

1. The vegetation canopy absorbs the energy of rainfall, reducing its capacity to disaggregate the soil surface

2. Vegetation cover reduces the velocity of run-off and therefore its ability to transport suspended matter

3. The physical and biological action of roots result in increased soil strength, granulation and porosity

4. The transpiration of water through vegetation leads to enhanced soil drying

5. Vegetation and derived organic matter can insulate soil against extremes of temperature, reducing cracking and freeze-thaw processes.

6. Vegetation results in the compaction of underlying soils

Adapted from Lai et al. (2003)

All the above factors are applicable when assessing the erosion of mine waste tips and the attenuation potential of the drainage pathway. Vegetated tips are more stable with respect to erosion and the maintenance of a stable water balance through evapo-transpiration (Gatzweiler *et al.*, 2001). This reduces the turnover of fresh surface and its exposure to the atmosphere, thereby reducing the production of acidic leachates and suspended material. Furthermore, vegetation provides dissolved organic matter

(DOM) to the soil layer which quickly consumes the dissolved oxygen in percolating waters via aerobic respiration. This reduces the amount available to drive sulphide oxidation reactions in the underlying mine waste (Peppas *et al.*, 2000). Therefore, it can be concluded that dissolved and particulate contaminants entering watercourses from vegetated tips is likely to be lower than from un-vegetated tips.

In some cases, the action of plant roots penetrating through artificially applied covers (including soils), has also been cited as a cause of failure, allowing oxygen and water ingress (Koener and Daniel, 1997). However, root growth is observed to be poor in most cases for shrubs and trees growing in soils overlying spoil heaps. Laboratory and field studies under various conditions and soil types have indicated that grass roots penetrate to <0.4 m and most trees and shrubs <1.0 m, where sufficient water exists (Kohler and Sanger (1998), in Gatzweiler, *et al.* (2001)). Furthermore, vegetated soils show reduced crusting and higher infiltration rates, resulting in reduced run-off (Boix-Fayos *et al.*, 1998). Therefore migration of mine waters through vegetated soils is likely to be slower and may enhance attenuation of pollutants, whether dissolved or particulate.

The available data set for land cover has a resolution of 25 m x 25 m (LCM, 2001). Therefore, the presence and type of vegetation cover for some mine waste heaps may be hard to distinguish from the surrounding area. Areas of land cover < 0.5 ha are also generalised according to the dominant classification (vegetation type, water body or bare soil). This is a limitation, but may be accepted at the catchment scale because land cover categories identified as high risk for the tips are also high risk for the drainage pathway. Also, in terms of spatial extent the drainage pathway incorporates drainage through the area occupied by mine waste tip.

Wind Speed and Exposure to Sunlight

When exposed to wind, fine material from mine waste tips, typically < 2 mm, may be transported and re-deposited downwind either as wind-blown dust or via saltation (Roberts and Johnson, 1978; Davies and White, 1981). Wind and exposure to sunlight increase evaporation from bare soils or mine wastes, this can dry out surface layers in periods of low rainfall making the surface of the tips more susceptible to erosion (Poesen *et al.*, 1999). Evaporation also encourages the formation of efflorescent salts (e.g. copper sulphates) at the surface. Dissolution of these salts is an important mechanism for increasing flux of dissolved metals leaving a mine waste tip (Nordstrom and Alpers, 1999).

Based on the literature information gathered, twelve input factors were incorporated into the model. These were divided into three categories, factors affecting primarily the waste tips themselves, factors most important within the tip catchment area and factors influencing the migration of contaminants through the drainage pathway to the nearest watercourse (Table 2.2).

Table 2.2: Environmental factors considered in diffuse mine water model. Factors attributed to either the extent of the mine waste tips, the tip catchment areas or the drainage pathway.

Mine Waste Tip	Catchment	Drainage Pathway
Area	Rainfall Average	Slope
Proximity To Watercourse	Rainfall Intensity	Soil Type
Wind Speed		Bedrock Geology
Sun Exposure (Aspect or Hill Shade)		Superficial Geology
Sun Exposure (Vegetation Cover)		Vegetation Cover

Other Considerations

Mine waste tips in the Tamar Catchment are frequented by walkers, dog-walkers, mountain bikers, off road motorcyclists and in some cases are blighted by fly-tipping. The extent to which these activities take place is a measure of their accessibility to the public and vehicles. In some cases the use of these sites is managed in partnership between the site owner and the users, and the use of designated tracks is actively encouraged. The best example of this may be seen at two of the largest sites within the Tamar catchment; Devon Great Consols and Gawton mine, where managed mountain biking tracks were located during the duration of this study. Unfortunately this does not prevent the unauthorised use of these and other mine sites. Apart from the risk to public health from uncapped mine shafts and exposure to contaminated wastes there is also an implication for erosion of the sites. Destruction of vegetation covers and physical action of activities disaggregates the surfaces of mine spoil. The effect is to increase the transport potential of particulate contaminants and enhance the exposure of fresh mineral surface to infiltrating waters. Gawton mine was historically used by motorcycle riders, but this has now been reduced by the actions of Tamar Valley AONB via the installation of fences. Woodland Riders (*http://www.woodlandriders.com)* and Tavistock Woodlands Estate both police Blanchdown woods at Devon Great Consols to actively discourage motorbikes and un-sanctioned building of mountain bike tracks outside their designated area. Since its formation in 2005, Woodland Riders believe they have been successful in greatly reducing unauthorised usage, but a small number of mountain bike tracks may exist in the Kitt Hill area, shown in Figure 2.7 (section 2.6.4) (Cleaver, 2010 *pers. comm.*). Assessment of the negative effect of human activity on the abandoned mine sites is not feasible at the catchment scale, and is therefore not included

in the model. This is because information is largely anecdotal or reliant on site inspection to provide evidence of post-mining activities.

2.5 Methodology:

2.5.1 Summary

Construction of the model involved several key phases, as summarised here and in Figure 2.1. The procedure applied to each data set and combination into the model is described in detail in the sub-sections 2.5.2 to 2.5.15.

Relevant data for each parameter was obtained and transformed into a suitable format for display within ArcGIS (ESRI), the chosen GIS software. ArcHydro9 (ESRI) was used to model a catchment and drainage area for each identified mine waste tip in the catchment. The catchment and drainage areas were utilised as a template to isolate areas of interest from other data sets. This reduced the time required by the computer to process commands.

The data sets were divided into six risk categories from 'Low Risk', scoring 1, to 'Extreme Risk', scoring 6. The division of data was based either on literature information and expert judgement (e.g. soil classification, permeability) or statistical division of the data (e.g. rainfall, wind speeds). Each data set was then *reclassified* within ArcGIS to include the risk score.

Each data set was judged on its relative importance to the overall risk posed by diffuse drainage from waste heaps. An importance weighting was assigned, following the analytical hierarchy process (AHP), described by Saaty (1980).

The risk scores for input data sets were multiplied by their importance weighting and the products were summed. The summed data sets formed small areas or *packets* of risk. The combined risk score for each tip, its corresponding catchment and drainage

34

area were calculated as the average of the packets within each boundary (tip, catchment or drainage).

The combined risk scores for corresponding tip, catchment and drainage areas were then summed to produce a total risk score for each tip. Tips were ranked by their total risk score and classified into 6 categories, from "Low" to "Extreme". A sensitivity analysis was performed by re-running the model with AHP weightings shifted toward climatic, geological or physical bias.

Finally, the results of the model, including those from the alternative AHP weightings were examined and compared with known data from water analysis and site reconnaissance surveys.

Figure 2.1: Flowchart showing development of model from input data sets. Abbreviations used: OS - Ordnance Survey; BGS - British Geological Survey; BADC – British Atmospheric Data Centre; EA – Environment Agency; NATMAP – National Soil Map; DTM – Digital Terrain Model; AHP – Analytical Hierarchy Process.

2.5.2   Location of mines, mining wastes and areas of associated contaminated land

Geo-referenced data collated and supplied by the Environment Agency (EA) was used as the primary resource to identify mine sites and associated areas of contaminated land (e.g. mineral processing areas and arsenic calciners). The data set contained information on the location of mine shafts, adits, mineral railways, streamed workings and areas of associated contaminated land (mine wastes) from literature and surveys, stored as a *polyline feature class*. Areas of mine waste (including streamed workings) were selected out from other line features. The data set was edited to correct errors such as overlapping or incomplete lines, and then converted to a *polygon* feature class (see Appendix 2A for method description).

2.5.3   Areas of Mine Waste

The area of each mine waste polygon in the polygon feature class was calculated using the *geometry* tool, equating to 806 features. Six area categories were classified based on quantile division of the data set. Risk scores from 1 (Low) to 6 (Extreme) were assigned. Summary statistics and classifications are listed in Table 2.3. A histogram of the areas showed that they were not normally distributed; this was due to the assignment of a default radius of 25 m to 352 shafts in the original data set. The equivalent area (1963 m^2) accounts for the high population of features falling into the 'Moderate-Low' category. It is assumed that these areas contain waste materials and have been included in the model.

Table 2.3: Classification and summary statistics of spatial extent of spoil and associated contaminated land. * Number in parenthesis denotes count of stream workings.

Area (m^2)	Risk Classification	Class Frequency	Risk Score
> 98700	Extreme	7 (5)	6
> 49100, < 98700	Very High	12 (2)	5
> 23800, < 49100	High	36 (14)	4
> 8750, < 23800	Moderate	62 (10)	3
> 1910, < 8750	Moderate -Low	575 (6)	2
< 1910	Low	114 (1)	1
Total Area	6107065 m^2	(30% stream workings by area)	
Mean	7577 m^2		
Range	126 – 276231 m^2		

2.5.4   Proximity to Nearest Known Watercourse

The distance between each mine waste polygon and nearest stream was determined using the *Select by Location* tool in ArcMap. Two stream layers were used, a stream layer digitised from OS 1:10000 mapping, (OS, 2009a) (digitised at a minimum zoom of 1: 5 000 with estimated error +/- 2m); and a drainage line generated from ArcHydro9 and a digital terrain model (see Appendix 2B). The latter layer contained errors in predicted watercourses in areas of low relief and errors caused by poor characterisation of man-made streams. Distances were measured from the closest perimeter of the mine waste polygon to the centreline of the watercourse and classified according to Table 2.4.

Table 2.4: Classification of risk to watercourse from mine waste tips, based on distance from watercourse.

Distance to Stream/River	Risk Classification	Class Frequency	Weighting
Direct contact	Extreme	38	6
0 - 50 m	Very High	77	5
50 - 100 m	High	51	4
100 - 250 m	Moderate	119	3
250- 500 m	Moderate -Low	140	2
> 500 m	Low	381	1

2.5.5 Average Rainfall

Rainfall data for the Tamar catchment was obtained from the Met Office Tamar catchment, comprising a 1 km *raster* grid with long-term monthly average data for the period 1971-2000. A monthly average was calculated using the raster calculator tool by summing the monthly data and dividing by 12. The data was divided into the categories derived from natural breaks in the data set, as calculated by ArcMap and shown in Table 2.5. The resulting input layer is displayed in Figure 2.22, Appendix 2G.

Table 2.5: Classification of average rainfall data for Tamar Catchment

Category	Rainfall (mm per month)	Weighting
Extreme	> 161	6
Very Heavy	> 138, < 161	5
Heavy	> 121, < 138	4
Moderately Heavy	> 107, < 121	3
Moderate	> 95 < 107	2
Low	< 95	1
Range	74.4 – 210	

2.5.6 Rainfall Intensity

Daily rainfall data (WADRAIN, DLY3208) from the British Atmospheric Data Centre (BADC) (MetOffice, 2010) was used as the source of rainfall intensity data. MIDAS stations were identified within the Tamar Catchment (+ 5 km) using the Google Earth locations supplied by the BADC. All stations providing continuous daily rainfall data for the period 01 Dec 1999- 31 Oct 2009 (~10 years) were selected, numbering 30. In addition, 35 stations surrounding the catchment with data for the same period were identified to help improve interpolation of the data around the edges of the catchment. Data for each of the selected stations was downloaded from the BADC using the data extractor service provided. The obtained data file was converted to an excel spreadsheet and the data was sorted by station identification number and date of measurement. The data was reviewed and duplicate readings (superseded or unverified) or readings taken over multiple days were removed. The average daily rainfall for stations within the Tamar catchment was determined as 4 mm d^{-1} for the reviewed period. The count and magnitude of all days with rainfall ≥ 4 mm d^{-1} were logged and classified; a summary is shown in Table 2.6.

Table 2.6: Classification of Daily Rainfall Intensity based on MIDAS daily rainfall data (1999-2009) for stations within the Tamar Catchment (+ 5 km).

Category of Rain Event, *C*	Daily Rainfall , *P* (mm d^{-1})	Percentage of Days in Category
Extreme	≥ 50	0.1
Very Heavy (II)	≥ 40	0.3
Very Heavy (I)	≥ 30	1.1
Heavy	≥ 20	3.7
Moderately Heavy	≥ 10	12.5
Moderate (above average)	≥ 4	26.9
Range	0 - 220	

For each station, the return period (*R*) was calculated for each category of rain event (C) via Equation 1:

$$\frac{\textbf{\textit{Total Number of Observations}}}{\textbf{\textit{Number of Days where }} P<C_1, C_2, C_3 ..etc.} = \textbf{\textit{Return Period of Event }} (R_1, R_2, R_3.. etc.)$$

A plot of log *R* verses *C*, yielded a straight line plot ($R^2 \geq 0.99$). From the gradient of the plot a return time for any value of C could be determined. The return time for a heavy event (≥ 20 mm d^{-1}) was determined from the log *R* versus *C* plot for each station. The return times were reclassified into the six categories based on natural breaks in the data set (Table 2.7).

Table 2.7: Categories used to define the return time of a heavy rain events (> 20mm d^{-1}) within the Tamar Catchment.

Category	Return Time of 20 mm d^{-1} event (days)	Risk Score
Extreme	< 20.7	6
Very High	> 20.7, < 24.6	5
High	> 24.6, < 29.0	4
Moderately Heavy	> 29.0, < 34.3	3
Moderate	> 34.3 < 39.4	2
Low	> 39.4	1
Range	17.2 – 50.6 days	

The data was introduced to ArcMap as a *point feature class*. An inverse distance weighted interpolation of the data points was selected from the *Spatial Analyst* toolbar to produce a map of estimated return time of a heavy rain event across the Tamar catchment. The resulting *raster* was reclassified to include the risk score 1-6. The raster served as input data set for rain intensity and is shown in Figure 2.23, Appendix G.

2.5.7 Topography

Ordnance Survey Land-form PROFILE (10m) contour tiles and spot heights (OS, 2009b) were used to create a *triangulated irregular network* (TIN) from which drainage pathways and topographical slope were derived. Input heights were verified against the Ordnance Survey 1 :10 000 mapping (OS, 2009a).

The TIN was converted to raster grids using the *3D Analyst* toolbar in ArcMap 9.3. A cell size of 5 m was defined, as this was found to be the highest resolution that could subsequently be processed with ArcHydro9. A full description of the method used to derive the *digital terrain model* (DTM) is provided in Appendix 2B.

Slope

Slope angles were calculated for the catchment in ArcMap using a DTM grid of 5m cell size and the *Slope* tool in the Spatial Analyst toolbar. Hodgson (1997) devised a standard classification system to describe slopes in categories from level to precipitous. The calculated slopes in the Tamar catchment were reclassified as a raster ("grid5slope") with six categories, resulting from a modification of Hodgson's scheme as shown in Table 2.8. The raster was then converted to a *vector* file using the *Convert* option in the Spatial Analyst Toolbar.

The slope vector file was one of the most complicated input files for the model comprising many small polygons. To aid subsequent processing steps, artefacts in the geometry were removed using the *multipart to singlepart*, and *repair geometry* tools. An example of the output from this process is shown in Figure 2.24, Appendix G.

Table 2.8: Slope Classification according to Hodgson (1997) and the revised classification used for the model.

Class (Hodgson)	Angle (°)	Model Classification	Angle (°)	Risk Score
Precipitous	36+	Extreme	≥ 25	6
Very steeply sloping	26-35			
Steeply sloping	16-25	Very Steep	$\geq 15, < 25$	5
Moderately steeply sloping	12-15	Steep	$\geq 7, < 15$	4
Strongly sloping	8-11			
Moderately sloping	4-7	Moderate	$\geq 4, < 7$	3
Gently sloping	2-3	Gentle	$\geq 1, < 4$	2
Level	0-1	Level	< 1	1

2.5.8 Soils

The National Soil Map (NATMAP, 2008) was used as the base data set for risk assessment of surface run-off due to soil type. Soil types were ranked according to the permeability of the dominant soil type and its capacity to absorb inflowing drainage, i.e. perennially wet soils were scored highest and free-draining soils scored lowest (Table 2.9). Permeability descriptions were defined by the data set but assignment of risk was based on the judgement of the author. Any favourable retardation or attenuation of migrating pollution resulting from the presence of significant peat or clay deposits are included in the model via the superficial deposit layer, described later. The Tamar catchment does not feature significant aquifers and therefore, the risk to groundwater bodies and their input to stream base flow has not been considered.

A sample of the reclassified NATMAP data set is given in Figure 2.25, Appendix 2G

Table 2.9: Risk classification applied to NATMAP soil types.

Dominant Soils Description	Risk Score
Thick very acid (amorphous) raw peat soils. Perennially Wet.	6
Slowly permeable seasonally waterlogged loamy upland soils with a peaty (or humose) surface horizon/ Gritty loamy very acid soils with a wet peaty surface horizon, thin ironpan often present / Slowly permeable seasonally waterlogged fine loamy (and/or clayey and/or silty)	5
Deep stoneless fine silty and clayey soils variably affected by groundwater / China clay spoil workings.	4
Fine loamy permeable soils variably affected by groundwater/ Loamy permeable upland soils over rock with a wet peaty surface horizon and bleached subsurface horizon, often with thin ironpan/ Permeable gritty coarse loamy upland soils with a wet humose or peaty surface horizon affected by groundwater/ Reddish very acid permeable loamy upland soils over sandstone.	3
Deep stoneless permeable silty soils/ Shallow well drained loamy soils over rock.	2
Lake or water body/ Sea/ No soil (miscellaneous coastal feature)/ Well drained fine loamy and/or fine silty soils over rock. Well drained fine loamy soils over deeply weathered rock locally/ Well drained fine loamy soils over slate or slate rubble/ Well drained fine silty over clayey soils stoneless or with chert stones, often deep/ Well drained gritty loamy soils with a humose surface horizon in places/ Well drained humose gritty loamy soils. Occasionally with thin ironpan/ Well drained loamy soils over rock with a humose or peaty surface horizon/ Well drained very stony loamy soils on moderate to steep bouldery slopes.	1

2.5.9   Bedrock and Superficial Geology

The maximum and minimum permeability values for bedrock and superficial lithology in the Tamar catchment were taken from the Permeability Indices (version 5) data set (BGS, 2009).

Bedrock

The bedrock data set indicates qualitatively the maximum and minimum permeability encountered in the unsaturated zone for each rock unit and lithology combination. Five classes are used: "very high"," high", "moderate low" and "very low" as determined at the outcrop of the deposit. Six classes were of risk applied to the bedrock geology data set, based on the minimum and maximum permeability combinations. Risk scores were assigned on the basis that lower permeability bedrock will promote greater surface run-off and shallow groundwater movement (Table 2.10).

Table 2.10: Classification of bedrock geology based on permeability data and rock classification scheme (RCS, BGS 2010).

Maximum Permeability	Minimum Permeability	Rock Classifications included in class (RCS)	Risk Score
Low	Low	e.g. Slate / Mudstone	6
Moderate	Low	e.g. Interbedded Slate and Sandstone / Granite / Basaltic rock	5
Moderate	Moderate	Breccia / Sandstone	4
High	Low	e.g. Slate and Limestone/ Sand, Silt and Clay	3
High	High	Limestone	2
Very High	High	Limestone	1

The rock classification scheme (RCS) was joined to the permeability data set using 1: 50000 geology data in vector format (BGS, 2010). This allowed identification of the characteristics of the lithology attached to the permeability index. The output risk layer for bedrock permeability is shown in Figure 2.26, Appendix 2G.

Superficial

Superficial deposits in the Tamar catchment comprise mainly peat deposits associated with Dartmoor and Bodmin Moor, and alluvial deposits close to watercourses. Thickness of the recorded superficial deposits was between 1m (minimum mapped depth) and 5 m. Division of the data set based on thickness was not feasible because interpolation modelling used to produce thickness of the data creates false thicknesses in river valley and hill environments.

The highest permeability deposits (e.g. alluvial gravels and sands) were ranked with the highest risk score, assuming that they could provide a preferential migration pathway to streams. Peat and clay deposits were assumed to be beneficial for natural attenuation of metals in migrating waters. Since superficial deposits are at least 1 m in depth, this was deemed significant enough to assign a negative risk score to these deposits (Table 2.11). This addresses the conflict between the hydraulic properties of soils rich in clay and peat soils which were ranked high risk of surface run off, with the chemical properties which may be favourable for attenuation of dissolved metals.

As superficial deposits are not continuous through the catchment, it was necessary to assign a default score of 1 to all other areas in the catchment. The output risk layer for superficial deposits is shown in Figure 2.27, Appendix 2G.

Table 2.11: Classification of superficial geological deposits in the Tamar catchment based on permeability data and rock classification (BGS, 2009; 2010).

Maximum Permeability	Minimum Permeability	Rock Classifications included in category (RCS)	Risk Score
Very High	Very High	Gravel /Granite Boulders*	+ 6
Very High	High	Sand and Gravel	+ 6
Very High	Moderate	Gravel, Sand and Silt	+ 6
High	High	Sand	+ 3
High	Very Low	Clay, Silt, Sand and Gravel	+ 2
Moderate	Low	Silt	+ 1
Low	Very Low	Peat / Clay and Silt	- 3
		All other areas	+ 1

*'Granite boulders' refer to areas of weathered regolith, on high ground, usually above of other superficial deposits. Although not directly relevant, the category was retained to prevent no data areas appearing in model.

2.5.10 Vegetation Cover

The data set used to estimate vegetation cover in the Tamar catchment was the Land Cover Map 2000 (LCM, 2001), which provides 26 broad habitats (Table 2.12), based on a 25m pixel grid. Further information on LCM2000, may be found on the LCM website (CEH, 2010). The 26 broad habitats were classed according to their potential for contaminant transmission or retardation (scores 1 to 6 representing low to high transport potential). Judgement was based on the effect of vegetation in terms of stabilising mine wastes and soils, reducing the impact of high intensity rainfall and reducing surface run-off and transport of metal contaminants. Sunlight exposure risk is also shown in Table 2.12, see explanation in section 2.5.12.

Table 2.12: Classification of risk for vegetation cover in the Tamar catchment based on contaminant transport and sunlight exposure factors. Derived from LCM2000 data set (CEH, 2010).

LCM2000 Subclass, Broad Habitat	Class No.	Contaminant Transport Risk Score	Sunlight Exposure Risk Score
Sea/Estuary	221	6	1
Water (inland)	131	6	1
Littoral Sediment	211	5	5
Continuous Urban	172	5	3
Inland Bare Ground	161	5	6
Saltmarsh	212	4	5
Suburban/rural developed	171	4	3
Bog	121	3	5
Dwarf shrub heath	101	3	3
Open dwarf shrub heath	102	3	4
Arable cereals	41	3	3
Arable horticulture	42	3	3
Acid grass	81	3	2
Bracken	91	3	2
Coniferous woodland	21	2	1
Improved grassland	51	2	2
Neutral grass	61	2	2
Fen, marsh, swamp	111	2	4
Broad-leaved woodland	11	1	1
Calcareous grass	71	1	2

The LCM2000 data set was calibrated by the creators with 569 1 km squares from field surveys. The estimated pixel to pixel correspondence between field survey and LCM2000 was only 60%. This includes errors due to the more detailed recording parcels of the field surveys (> 0.04 ha) compared with the minimum mapped unit of LCM2000 (> 0.5 ha) (CEH, 2010). Since 631 out of the 806 mapped areas of mine

waste in this study are less than 0.5 ha, waste tip scale analysis of vegetation cover with this data set is not permissible. Vegetation cover is clearly very important at the site-specific scale for the reasons described in section 2.4.3. The low accuracy of remotely gathered data and its age mean that it must be applied with caution, but it is still useful to a catchment-wide prioritisation model. The low weighting applied to this data set in the final model is a reflection of its confidence rather than it's importance. A revised data set, LCM2007 is expected for release in 2011(CEH, 2011).

2.5.11 Wind Speed

Average annual wind speed at 10m from ground level was obtained from the Department of Trade and Industry's database (DTI, 2010) as a raster data set. This database is the result of an air flow model that estimates the effect of topography on wind speed and no allowance is made for the effect of local thermally driven winds. The data used comprised a raster data set of average wind speeds at 10m from ground level with a resolution of 1km. The data was reclassified into six risk score categories (Table 2.13), based on quantile division.

Table 2.13: Wind speed classification for the Tamar catchment based on 10m high wind speed estimates (DTI, 2010).

Wind speed (km h^{-1})	Classification	Risk Score
≥ 6.2	Extreme	6
$\geq 5.7, < 6.2$	Very High	5
$\geq 5.3, < 5.7$	High	4
$\geq 4.9, < 5.3$	Moderately High	3
$\geq 4.4, < 4.9$	Moderate	2
$\geq 0, < 4.4$	Low	1

2.5.12 Exposure to Sunlight

The ArcGIS *Hillshade* tool was used to determine the degree of shading experienced by the terrain model of the catchment. The Azimuth and altitude of the sun were set to 170.3° and 62.5° respectively, equivalent to the mid-summer position on the 25th June 2009 with respect to a point in the centre of the catchment (50' 36' °N, 4' 12' ° W) (USNO, 2010). After conversion of raster to polygon format, the results were classified into six categories based on quantile division of the data set. Areas with lowest shadow were assigned a value of 6 for exposure potential. This model makes no correction for land cover (LCM2000 data set section 2.5.10).

2.5.13 Hydrology

Using the ArcHydro9 application (ESRI), the catchment DTM was transformed in to a series of *hydrogrids* which allowed streams, drainage paths and catchments to be modelled. The following processes were applied to the available DTM (resolution 10m) in order to create hydrological features for the model.

Creating the Hydrogrid from the Catchment DTM

Erroneous low points in the catchment DTM were filled using the *fill sinks* tool in the *Terrain Preprocessing* (TP) menu.   The flow direction was then established in the filled DTM by running the *Flow Direction* function in the TP menu.

The results were reviewed according to guidance documentation (Djokic, 2008) and verified with existing knowledge of drainage features by consultation of maps and site visits. In some areas of low relief (< 1 m above sea level) minor discrepancies were observed between the known flow direction of primary rivers, such as the River Tamar or River Ottery, and streams and the drainage pattern generated by the DTM. To improve the model the flow paths of the major rivers and streams were imposed

manually, using the method of *burning in*. The imposed stream layer was created from OS 1: 10 000 OS mapping (OS, 2009a), and consisted of a continuous and non-braided line network. "Burning in" was only undertaken in circumstances where there was reliable information on the flow direction at a suitable scale. In all other cases the drainage channels were not altered as the process may introduce untraceable errors to the DTM. With higher resolution elevation data to produce the DTM, the burning in process may not be necessary.

Modelling of Catchment and Drainage Areas for Mine Waste Tips

Catchment areas for each mine waste polygon were determined using the *Batch Watershed Delineation for Polygons* tool in the *Watershed Processing* toolbar of ArcHydro9. The data input consisted of a flow direction grid and the mine waste polygon layer (described in section 2.5.2) containing the spatial extent of the mine spoil. Figure 2.2 displays the necessary processing steps required to generate the drainage areas.

Figure 2.2: Sequence used to create drainage pathway polygons for each area of mine waste using ArcHydro9 tools.

The process used to generate the drainage and catchment areas were identical, with the exception that the step required to invert the DTM was omitted in the latter.

2.5.14 Assignment of weighting for all input parameters (GIS layers)

The relative significance of each input data set with respect to other data sets were determined using the analytical hierarchy process described by Saaty (1980). Each data set was assigned a score based on its relative importance to the generation of diffuse mine waters. The numerical scores with a short description of their meaning are listed in Table 2.14 and the resulting scores are given in Table 2.15, as a pairwise comparison matrix.

Table 2.14: Scoring in AHP via pairwise comparison (adapted from Saaty 1980).

Numerical Importance	Verbal Judgement of Importance
1	Equal Importance
3	Moderate Importance
5	Strong Importance
7	Extreme Importance
9	Most Important
2,4,6,8 and decimals	*Intermediate Values*

The weight of each layer (*w*) was calculated using Equation 2.

$$w = M_i / \sum_{i=1}^{n} M_i$$

Equation 2 **(Wang *et al.*, 2010)**

For the PCM in Table 2.15, the summation of the components for each layer, M_i, i.e. 57.0 for proximity and 51.5 for slope, were divided by the denominator of the matrix, ΣM_i (355). The weights calculated by this method for all input data sets and are shown in Table 2.16. For ease of input into ArcGIS each weighting was multiplied by

1000 to give parts per thousand (ppth) without decimal places. The PCM matrix shown in Table 2.15   places the greatest importance on the physical input parameters of proximity, size and slope angle. Although the author considers this the most suitable weightings for the model, the effect of different approaches on the outcome of the model were tested. Each placed a greater emphasis on the role of a group of factors described as climatic (rainfall intensity, average rainfall, wind speed and sun exposure), geological (soils, bedrock and superficial geology) and biological (vegetation cover). The weightings derived from each alternative PCM are also shown in Table 2.16.

To check for the consistency of judgement within the PCMs, the principle eigenvector method (PEM) was employed. PEM is the most widely applied process used to ensure that consistency of judgement is maintained (Bana e Costa and Vansnick, 2008). Eigenvectors ($x_{i,j}$) were manually calculated using Equation 3. Each component of the PCM matrix ($a_{i,j}$) was divided by the total for its layer column (C_i) (Teknomo, 2006). For the PCM in Table 2.15, the left first component (top, left) was calculated as:

$$x_{i,j} = \frac{a_{i,j}}{C_i} = \frac{1}{3.76} = 0.266$$

Equation 3

All components of the PCM in Table 2.15 were transformed by this method resulting in the normalised matrix shown in Table 2.18. The principle eigenvector (W) was calculated for each input data set as the average of the eigenvectors for that row (2nd to right column, Table 2.18). Eigenvalues for each input data set were then calculated by multiplying the principle eigenvector (W) by the total of the data set column in the PCM ($C_{i,}$ Table 2.15). The principle eigenvalue (λ_{max}) was calculated as the sum of the eigenvalues for the matrix (see right most column, Table 2.18).

Table 2.15: Pairwise comparison matrix (PCM) constructed for input parameters in environmental model.

	Proximity	Slope Angle	Area	Soil	Rainfall Intensity	Superficial Deposits	Rainfall Average	Vegetation Cover	Bedrock Geology	Wind Speed	Sun (HIlshade)	Sun (Vegetation)	Total Score for Row
Proximity	1	2	2	3	4	4	5	5	6	8	8	9	**57.0**
Slope Angle	1/2	1	1	2	3	4	5	5	6	7	8	9	**51.5**
Area	1/2	1	1	2	3	4	5	5	6	7	8	9	**51.5**
Soil	1/3	1/2	1/2	1	2	3	4	4	5	6	7	9	**42.3**
Rainfall Intensity	1/4	1/3	1/3	1/2	1	2	3	4	5	5	6	8	**35.4**
Superficial Deposits	1/4	1/4	1/4	1/3	1/4	1	2	3	4	5	6	8	**30.6**
Rainfall Average	1/5	1/5	1/5	1/4	1/3	1/2	1	2	3	5	6	8	**26.7**
Vegetation Cover	1/5	1/5	1/5	1/4	1/4	1/3	1/2	1	2	3	5	7	**20.9**
Bedrock Geology	1/6	1/6	1/6	1/5	1/5	1/4	1/3	1/2	1	3	5	8	**19.0**
Wind Speed	1/8	1/7	1/7	1/6	1/5	1/5	1/5	1/3	1/3	1	3	5	**10.8**
Sun (Hillshade)	1/8	1/8	1/8	1/7	1/6	1/6	1/6	1/5	1/5	1/3	1	4	**6.8**
Sun (Vegetation)	1/9	1/9	1/9	1/9	1/8	1/8	1/8	1/8	1/8	1/5	1/4	1	**2.5**
Sum of Column (C_i)	**3.76**	**5.99**	**5.99**	**10.0**	**14.8**	**19.6**	**26.3**	**30.2**	**38.7**	**50.5**	**63.3**	**86.0**	**355**

Table 2.16: Weightings (parts per thousand) applied to input data sets as determined by pairwise comparison for each of four scenarios; Physical, Climatic, Geological and Biological.

Input Data set	Scenario 1: Physical	Scenario 2: Climatic	Scenario 3: Geological	Scenario 4: Biological
Proximity	161	177	160	160
Slope	145	135	140	137
Area	145	135	140	137
Soil	119	119	117	118
Rainfall Intensity	100	105	96	100
Superficial Deposits	86	85	99	80
Rainfall Average	75	81	73	67
Vegetation Cover	59	45	56	97
Bedrock Geology	53	39	59	53
Wind Speed	31	44	32	28
Sun Exposure (Hillshade)	19	26	20	17
Sun Exposure (Vegetation)	7	10	7	7

The Consistent Index (*CI*) was then calculated for the example PCM as:

$$CI_{physical} = \frac{\lambda_{max} - n}{n - 1} = \frac{13.81 - 12}{11} = 0.165$$

Equation 4

(Aguarón and Moreno-Jiménez, 2003; Teknomo, 2006)

Where *n* is equal to the number of input data sets in the matrix.

The Consistency Ratio (*CR*) is defined as:

$$CR = \frac{CI}{RI(n)}$$

Equation 5

(Aguarón and Moreno-Jiménez, 2003; Teknomo, 2006)

Where *RI* is the Random Index for a matrix of order *n*, equal to 1.535 when *n* = 12. The *CR* gives a measurement of the consistency of the judgements in the PCM, lying between totally consistent and totally random , according to *Aguarón and Moreno-Jiménez* (2003). A *CR* value is < 0.1, it indicates that the consistency of the judgements is acceptable using a 'within 10%' rule set by Saaty (1980). The *CR* values were calculated for each of the four PCM scenarios and are displayed in Table 2.17. The *CR* values calculated for the four PCM are below or close to this acceptance limit. It has been shown that *CR* < 0.1 is much harder to achieve for large matrices, even if consistency, proven by another means is upheld (Vargas, 2008). As the order of the PCM matrices generated in this study is large by comparison to most literature examples (*n* = 12), consistency was judged to be fit for purpose.

Table 2.17: Calculated Consistency Ratios for all weighting scenarios applied to the model.

Weighting Scenario	Consistency Index (*CI)*	Consistency Ratio (*CR)*
Physical	0.165	0.107
Climatic	0.148	0.097
Geological	0.115	0.075
Biological	0.186	0.121

Table 2.18: Transformed pairwise comparison matrix (physical weightings) showing calculated eigenvectors for each component and principle eigenvector for each input data set.

	Proximity	Slope Angle	Area	Soil	Rainfall Intensity	Superf. Deposits	Rainfall Average	Veg. Cover	Bedrock Geology	Wind Speed	Sun (Hillshade)	Sun (Veg.)	Row Average (Principle Eigenvector)	Principle Eigenvector multiplied by sum of each column in PCM
Proximity	0.266	0.332	0.332	0.301	0.271	0.0204	0.190	0.166	0.155	0.158	0.126	0.105	0.217	**0.817**
Slope Angle	0.133	0.166	0.166	0.201	0.203	0.0204	0.190	0.166	0.155	0.139	0.126	0.105	0.163	**0.982**
Area	0.133	0.166	0.166	0.201	0.203	0.0204	0.190	0.166	0.155	0.139	0.126	0.105	0.163	**0.982**
Soil	0.089	0.083	0.083	0.100	0.135	0.153	0.152	0.133	0.129	0.119	0.111	0.105	0.116	**1.154**
Rainfall Intensity	0.066	0.055	0.055	0.050	0.068	0.102	0.114	0.133	0.129	0.099	0.095	0.093	0.088	**1.305**
Superficial Deposits	0.066	0.041	0.041	0.033	0.034	0.051	0.076	0.099	0.103	0.099	0.095	0.093	0.069	**1.360**
Rainfall Average	0.053	0.033	0.033	0.025	0.023	0.026	0.038	0.066	0.078	0.099	0.095	0.093	0.055	**1.451**
Vegetation Cover	0.053	0.033	0.033	0.025	0.017	0.017	0.019	0.033	0.052	0.059	0.079	0.093	0.043	**1.292**
Bedrock Geology	0.044	0.028	0.028	0.020	0.014	0.013	0.013	0.017	0.026	0.059	0.079	0.093	0.036	**1.393**
Wind Speed	0.033	0.024	0.024	0.017	0.014	0.010	0.008	0.011	0.009	0.020	0.047	0.058	0.023	**1.153**
Sun (Hillshade)	0.033	0.021	0.021	0.014	0.011	0.009	0.006	0.007	0.005	0.007	0.016	0.047	0.016	**1.033**
Sun (Vegetation)	0.030	0.018	0.018	0.011	0.008	0.006	0.005	0.004	0.003	0.004	0.004	0.012	0.010	**0.889**
Sum of Columns	**1.000**	**1.000**	**1.000**	**1.000**	**1.000**	**1.000**	**1.000**	**1.000**	**1.000**	**1.000**	**1.000**	**1.000**	**1.000**	**13.81**

2.5.15 Combination into Final (Vector) Risk Model

For clarity, the first part of the combination process is displayed in Figure 2.3. Input data sets in raster format (slope, rainfall intensity, rainfall average, vegetation cover, wind speed and hillshade) were converted to polygon features using the Raster to Features tool in the Spatial Analyst toolbar.

Figure 2.3: Summary flow chart of method used to create vector model from input data sets.

The rainfall intensity and rainfall average data sets were reduced to the spatial extent of the *catchment polygons*, as generated by ArcHydo9 (section 2.5.13), using the *clip* tool. The *union* tool was then used to combine the rainfall intensity and rainfall average layers. The output layer represented attributes of the catchments for each mine waste polygon (hereafter abbreviated to "tip").

The soil, superficial permeability, bedrock permeability and vegetation cover data sets were clipped to the spatial extent of the *drainage polygons*, as generated by ArcHydro9 (section 2.5.13). Again the *union* tool was used to combine the resulting polygons and produce an output layer representing the attributes of the drainage pathway for each tip.

The wind speed and sun exposure data sets were clipped to the spatial extent of the tip polygon file and unioned to give the attributes of the tips. Proximity and area

inputs were already contained within the tip polygon layer and were combined with the unioned attributes of the tips in the final model.

During the union process a number of very small polygons or *slivers* were created around the fringes of the catchment. This was caused by an imperfect match in the catchment boundaries of unioned layers. The slivers were identifiable as *null values* in the *attribute table* and removed from the unioned data set as their inclusion might cause erroneous low values in the final risk calculation.

To each of the three unioned data sets; catchment (*c*), drainage pathway (*d*) and tip extent (*t*), and also the mine waste polygon data set (*p*), two fields were added to the attribute table to hold the weighting (w_i) applied to each input data set and the result of the combined risk score for that data set ($R_{C,D,T,P}$), respectively. The fields were populated using the *field calculator* tool with weightings according to the outcome of the PCM (shown in Table 2.16) and the combined risk score according to Equation 6:

$$Combined\ Risk_{C,D,T,P} = \sum^{n} w_i . R_i$$

<div align="right">***Equation 6***</div>

Where R_i represents the risk score (1-6) assigned to each polygon in the layer. The combined risk was therefore calculated for every discrete polygon or *parcel* within the model. However, this meant that in most instances each catchment, drainage or tip polygon contained more than one score. In order to provide a useful output to rank individual tips, these scores were statistically averaged to give a single mean score for each tip. In this study, the mean score was deemed the most suitable statistical output, but maximum, minimum and weighted scores may also be calculated at this stage.

To achieve this, the *intersect* and *dissolve* tools were used (see Appendix 2D for full method). The combined risk calculated for the catchment (R_C) and drainage areas

(R_D) were joined to the tip (mine waste polygon) layer (See Appendix 2E for full method).

A "Total Risk" column was added as a new field to the tip layer and populated with the sum of the combined risk scores for the tip, catchment and drainage pathway. This was achieved using the field calculator tool, as shown in Figure 2.21 (Appendix 2F).

The results for total risk (R_{Total}) were categorised into 6 classes from "Low" to "Extreme" based on quantile division of the data set. The list was sorted to provide the ten sites with the highest score. These were used to compare the results obtained by using the four categories of input weightings (Physical, Climatic, Geological and Biological). An example of the output is shown in Figure 2.28, Appendix 2G.

2.6 Results and Discussion

2.6.1 Priority List of Mine Sites from the Final Risk Model

Comparison of the total risk scores (T_R) calculated by the vector model from the physical, climatic, geological and biological weightings demonstrated positively skewed normal distributions (Figure 2.4). Several sites consistently score very highly in the model, regardless of the weighting applied. The identities of the highest scoring sites are displayed in Table 2.19 (actual scores are also provided in Table 2.22, Appendix 2H).

Notable was the prevalence of streamed workings at the top of the priority list, producing nine of the highest ten scores. Forty sites from a total of 806 were designated as "streamed workings", of which 37 were classified as posing an "Extreme" or "Very High" risk to watercourses. Their location on high moorland areas exposes them to high average and intense rainfall and high wind speed and they are also by definition in

direct contact with a drainage channel or stream and can extend for a distance of several hundred metres along stream banks. All these attributes incur high risk classification within the model.

Figure 2.4: Data distribution for each of the four weighting schemes applied to risk model

The results emphasise that the model considers only environmental and physical attributes of the waste location. It does not in any way consider the level of contamination associated with the waste materials found at each site. Inclusion of contamination levels into the model which would require a wide and expensive program of site sampling, would defeat the purpose of the model (see section 2.3). The burgeoning technology of hyperspectral remote sensing may offer a way of identifying 'hotspots' of contaminated land over large areas in the future. This method uses visible or near-IR spectral data to map indicators of metal pollution either mineral signatures e.g. Choe *et al.* (2008), or plant stress Malenovsky *et al.* (2009). Such technologies were

not available at time of writing but may be integrated with this environmental model if
the data were to become available.

**Table 2.19: Areas of contaminated land scoring highest in vector model and comparison of result
from weighting scheme applied, physical (P), climate (C), geological (G) or biological (B).**

Mine ID	Description	Rank (P,C,G,B)	Receiving Watercourse
787	Stream Workings at Foxhole, Dartmoor	1,1,1,1	Doetor Brook (*River Lyd*)
794	Stream Workings at Great Nodden, Dartmoor	2,2,2,2	River Lyd
57	Stream Workings east of Brisworthy, Dartmoor	3,3,3,3	River Plym
710	Waste Tips at Wheal Betsy, Mary Tavy	4,4,4,4	Cholwell Brook (*River Tavy*)
765	Stream Workings 400 m S of Doe Tor, Dartmoor	5,5,5,5	Walla Brook (*River Lyd*)
202	Stream Workings 500 m NE of Down Tor, Dartmoor	6,7,6,6	Newleycombe Lake (*River Meavy u/s Burrator Reservoir*)
134	Stream Workings 3 km SW of Down Tor, Dartmoor	7,8,7,8	River Plym
551	Stream Workings 500 m NE of Kings Tor, Dartmoor	8,10,8,7	River Walkham
494	Stream Workings at Meavy Head, 500 m SW of Princetown	9,6,9,10	River Meavy
247	Stream Workings at Wheal Chance, 1.5 km NE of Down Tor, Dartmoor	10,9,10,9	Newleycombe Lake (*River.Meavy u/s Burrator Reservoir*)

2.6.2 High Priority Site: Streamed Workings at Foxhole

The workings at Foxhole, known also as Wheal Frederick, scored highest in the
model with 4400 out of a maximum possible score of 6000. The location and extent of
these workings are shown in Figure 2.5.

Available spatial data was reviewed in order to investigate the reasons for the high score at Foxhole and results are summarised in the paragraph below. Extracting such information from the GIS model was easily achievable for all of the 806 sites. The formative layers of the model (e.g. LCM 2000, BGS 1:50 000 geology data) were displayed in the same window as the model results and information retrieved from selected layers using the *identity* tool in ArcMap.

Figure 2.5: OS 1: 25 000 Map showing location, topography and model outcome for "Foxhole" stream workings produced in ArcMap. OS Map © Crown Copyright/database right 2009. An Ordnance Survey/EDINA supplied service.

The workings at Foxhole extend along approximately 3km of stream banks at an altitude of 450 – 500 m on Dartmoor, 12.5 km NNE of Tavistock. The mine waste occupies an area of approximately 204500 m^2 (score 6) that is in direct contact (score 6) with Doetor (also "Doe Tor") Brook, a tributary of the River Lyd. The slope gradient is mainly gentle (score 2) to steep (score 4), very steep (score 5) in places and tends from E to W. The mine waste and drainage area are underlain by seasonally wet peat soils

which have been assigned as high risk (score 5) due to the high run-off potential. The bedrock geology in the area is the Dartmoor granite intrusion of Permian to Carboniferous age. This was classed as being of low to moderate permeability (via fracture flow) and therefore scores highly for run-off risk (score 5). The mine waste is classified as an alluvial deposit and incurs a high score (+6) as a high permeability superficial deposit. The uppermost extent of the workings lay in superficial peat deposits which have been assigned a negative score (-3) due to their potential for attenuation of metal pollutants. Average monthly rainfall was between 161-210 mm giving a maximum score of 6. The estimated return time of a high intensity rain event was 20.8-24.6 days equating to a score of 5. Vegetation cover comprised predominantly acid and neutral grasses with some pockets of broad-leaved woodland and dwarf shrub heath and the associated risk ranged from "Low" (score 1) to "Moderate" (score 3). Overall the environmental model ranked the risk to watercourses from diffuse pollution emanating from the mine waste as "Extreme".

The level of contamination within mine waste is not considered by the model and in reality the level of risk posed by waste rock at historical streamed workings may be low. The streamed workings of Dartmoor were principally concerned with the early extraction of tin ore (cassiterite) from alluvium by gravimetric separation. By the 13th century the richest alluvial deposits of Dartmoor were exhausted and although it continued, predominantly in Cornwall, by the 16th century streaming had largely given way to underground mining (Hamilton Jenkin, 2005). Tin streaming wastes are likely to be among the oldest and therefore most weathered in the catchment. Furthermore, tin (and tungsten) deposits commonly occur closest to the granite intrusion, the Cornubian Batholith, whose emplacement caused the mineralisation of the surrounding country rocks approximately 270-300 Ma (Jackson *et al.*, 1989). Surface workings on Dartmoor

exploit the exposure of these mineralised deposits of tin close to where the granite outcrops, whereas deposits formed further from the granites follow a well-developed zonal distribution with copper minerals followed by tin, lead and zinc and finally a zone of iron minerals (Webb, 1995). The low solubility, low bioavailability and low toxicity of inorganic tin (Rüdel, 2003) mean that the pollution risk from waste rock containing exclusively tin ore minerals and associated gangue, typically quartz and tourmaline (Chesley *et al.*, 1993; Dominy *et al.*, 1995), is probably low. However, contamination of streamed workings waste with waste rock from underground workings containing other minerals cannot be ruled out, as ore was often transported for processing to locations with suitable facilities. At Foxhole (Wheal Frederick), there is evidence of on-site mineral processing, including a ruined counthouse (SX545853), and the remains of waterwheel pits, *buddles* and evidence of former track ways (Popham, 2007). The mine is also in close proximity to underground workings at Wheal Mary Emma (SX532832) which were worked for tin but also contained the lead ore galena (Dines, 1956). Further investigation of the site and examination of water quality for the receiving watercourse would be the recommended next step.

2.6.3   High Priority Sites: Non-Streamed Workings

To identify the highest risk areas of waste associated with underground or pit mining, the stream workings were selected from the attribute table (ArcMap) and removed from the model output. The revised list of non-streamed workings (Table 2.2) with the ten highest scores shows similar ranking between the weighting schemes, resulting in the same classification in most cases. The actual scores are shown in Table 2.23, (Appendix 2H). Of the 766 sites that were not classified as streamed workings, 103 were classified as "Extreme" based on quantile division of the model outcome data set.

Table 2.20: Areas of contaminated land scoring highest in vector model when streamed workings are excluded. Also comparison of results obtained by the weighting scheme s: physical (P), climate (C), geological (G) or biota (B).

Mine ID	Description	Rank (P,C,G,B)	Receiving Watercourse
710	Waste tips at Wheal Betsy, 1.5 km NNE of Mary Tavy	1,1,1,1	Cholwell Brook (*River Tavy*)
651	Waste tips/shafts at Tegune Mine, 300m S of Trenilk.	2,2,2,2	River Lyhner
281	Waste Tip at summit of Caradon Hill	3,7,4,12	Unnamed stream (*River Lyhner*)
141	Waste tips at Gawton Mine, 1.3 km NE of Tuckermarsh.	4,8,5,3	River Tamar
514	Waste tips and shafts at Wheal Lucky, SW Princetown	5,5,7,4	River Meavy
806	Surface workings at Foxhole Mine, Dartmoor	6,6,8,5	Doetor Brook (*River Lyd*)
14	Pits and shafts at Hemerdon Mine, 1.5 km NE of Hemerdon.	7,10,10,6	Smallhanger Brook (*River Plym*)
639	ACL associated with Treburland Manganese Deposits, Treburland	8,9,9,10	River Lyhner
627	Waste tips at Wheal Friendship, Mary Tavy	9,11,11,9	Cholwell Brook (*River Tavy*)
239	Waste tips and shafts at East Caradon Mine, 600 m NW of Middlehill	10,4,6,11	Unnamed Stream (*River Lyhner*)
137	Pit workings (and stream works) at Crane Lake Mine, Dartmoor	11,2,3,7	River Plym
529	Waste tips at New Great Consols Mine, Luckett	12,15,12,8	Luckett Stream (*R.Tamar*)

Wheal Betsy, Former Lead-Silver Mine, Mary Tavy

The waste tips at Wheal Betsy (Figure 2.6) scored very highly, (4251/6000) being ranked first amongst non-streamed workings and fourth overall.

Figure 2.6: OS 1: 25 000 Map showing location, topography and model outcome for waste tips at "Wheal Betsy", produced in ArcMap. OS Map © Crown Copyright/database right 2009. An Ordnance Survey/EDINA supplied service.

The Wheal Betsy site is located on the NW edge of Dartmoor, approximately 8.5 km NNE of Tavistock. The tips at Wheal Betsy extend for approximately 1 km alongside Cholwell Brook, a tributary of the River Tavy. There is direct contact with the watercourse in the southern part of the site (score 6) and the area of designated spoil is approximately 59300 m^2 (score 5). The slope gradient ranges from gentle (score 2) to extreme (score 6) being situated in a N-S orientated V-shaped valley. The tips and drainage areas are mainly underlain by "loamy permeable upland soils over rock with a wet peaty surface horizon and bleached subsurface horizon, often with iron pan"(NATMAP, 2008), scoring 3 for run-off potential. The bedrock geology comprises the interbedded sandstones and argillaceous rocks of the Bealsmill Formation with moderate to low permeability from fracture flow (BGS 2010, score 5). The southernmost part of the site is underlain by slates of the Brendon Formation with low permeability, again from fracture flow (BGS, 2010, score 6). The tip and catchment area

67

spans two classifications of average monthly rainfall, 121-137 mm (score 4) to the NE and S and 138-160 mm (score 5) in the central area. The estimated return time of a high intensity rainfall event is 11.5-20.7 days (score 6). Vegetation cover comprised mainly calcareous grass (score 1) with some improved grass (score 2) and acid grass (score 3). An area of bare ground (score 5) at the centre of the site is coincident with the spoil material itself. Overall the risk to watercourses from diffuse pollution at this site was determined as "Extreme". The site is the subject of further investigation in Chapter 4.

2.6.4 Model Ranking of Known Areas of Contamination

The largest concentration of mine waste in the catchment occurs close to Kit Hill and Gunnislake (Figure 2.7). The model results for each site in this grouping (Table 2.21) according to the four weighing schemes showed more variability than for the first ten sites. The frequency of sites increases as the risk score approaches the mean value for the data set (Figure 2.4), therefore a change in score is likely to produce a greater change in rank.

Table 2.21: Model outcomes for known sites in the Tamar catchment. Rank shown for physical (P), climate (C), geology (G) and biota (B) weightings in model with stream works included.

ID	Description	Classification (P)	Rank (P,C,G,B)	Receiving Watercourse
539	Waste tips at Wheal Fanny, Devon Great Consols Mine	"Extreme"	92,109,88,85	River Tamar
534	Waste tips at Wheal Anna Maria, Devon Great Consols Mine, 1.2 km N of Gunnislake	"Extreme"	50,90,64,63	River Tamar
479	Precipitation Launders at Devon Great Consols Mine, 900 m N of Gunnislake	"Extreme"	19,42,39,40	River Tamar
456	'White Tips' at Gunnislake Clitters Mine, 1 km NW of Gunnislake	"Extreme"	35,64,58,54	River Tamar
411	'Red Tips' at Gunnislake Clitters Mine, 900 m W of Gunnislake	"Very High"	188,213,198,193	River Tamar

Some of the sites, particularly Devon Great Consols, have been the subject of investigations of soil, sediment and water quality. The model outcomes for selected sites in this area (Table 2.21) were examined for consistency with existing knowledge of the tip area and contamination. Two sites were selected for discussion, Devon Great Consols and Gunnislake Clitters.

Figure 2.7: Map displaying the location and model outcomes for known sites in the centre of the catchment. * Devon Great Consols include (E to W): Wheal Fanny tips, Wheal Anna Maria tips and arsenic works , Wheal Emma tips , precipitation launders to S. **Gunnislake Clitters include (N to S) "White Tips", "Red Tips" and Greenhill Arsenic Works. OS Map © Crown Copyright/database right 2010. An Ordnance Survey/EDINA supplied service.

Devon Great Consols

Devon Great Consols is an abandoned copper-arsenic mine that hosts the largest and most visible spoil deposits in the catchment (See Chapter 3 for site investigation). The spoil and soils are heavily contaminated with arsenic and copper (Kavanagh *et al.*,

1997; Langdon *et al.*, 2001) and the site discharges mine waters from adits and surface drainage directly into the River Tamar (Minghanetara, 2009). There is therefore an established risk at this site. The areas of waste at Devon Great Consols were sub-divided in the data set provided by the Environment Agency, giving rise to individual scores in the model. The model outcome assigned an "Extreme" risk category for the three main areas of spoil comprising the tips at Wheal Fanny, tips and arsenic works at Wheal Anna Maria/Wheal Josiah and the precipitation launders at the south of the site (Figure 2.8). The precipitation launders were ranked highest, being in direct contact with the River Tamar and underlain by alluvial deposits.

Figure 2.8: Individual waste tips designated within Devon Great Consols. OS Map © Crown Copyright/database right 2010. An Ordnance Survey/EDINA supplied service. Legends as for Figure 2.7.

Gunnislake Clitters

Gunnislake Clitters lies to the south of Devon Great Consols, on the Cornish side of the River Tamar. The site consists of three main spoil deposits: "White" and

"Red" tips and the contaminated land associated with Greenhill Arsenic Works, which was part of the mine operation on site, closing circa 1925 (DeNull, 2007). The white tips are skirted by the River Tamar. At the Greenhill Arsenic Works, there is visible arsenic contamination, including brightly coloured deposits of realgar (AsS) and orpiment (As_2S_3) on the mine buildings and soils. Large quantities of arsenic were processed here and some barrels of refined arsenic are reported to be buried at the site (De Null, 2007). The outcome from the environmental model for the White Tips was "Extreme" risk, and highest of the three main areas (rank 35). Variability in area extent, proximity, slope and soils across the sites resulted in the Greenhill Arsenic Works and Red Tips being classified as being "Very High" and "High Risk" (ranked 178 and 188 respectively).

Figure 2.9: Waste tips and topography at Gunnislake Clitters. OS Map © Crown Copyright/database right 2010. An Ordnance Survey/EDINA supplied service. Legends as for Figure 2.7.

2.6.5   Uncertainty and Transferability

Uncertainty

The accuracy of drainage pathways calculated using ArcHydro9 is determined by the accuracy of DTM data. Inaccuracies result in errors in the spatial extent of catchment and drainage areas, slope angles and the identification and direction of streams. This in turn affects the risk classification of wastes with respect the streams. Since proximity and slope were weighted highly in the model, the most improvement would be gained by including higher resolution elevation data. Improvements in the accuracy of all input data sets would be desirable, particularly the resolution of the vegetation cover. A new version of Landcover Map (LCM2007), is due for release, but was not available at the time of model construction (LCM, 2010).

Averaging parcels of risk to arrive at risk scores for the attributes of the tip, catchments and drainage areas (see section 2.5.15) is an oversimplification that could mask high risk preferential paths to watercourses. A more accurate measure of risk could be calculated if the actual drainage path through the site could be determined. One potential method worthy of future investigation would be the application of cost distance modelling. Functions are available within ArcGIS (Spatial Analyst) software for the determination of *least cost paths,* based on the summed scores of grid squares from overlaid data sets (ESRI, 2007). There are a number of literature examples from other subject disciplines where such methods have been used in planning and management studies e.g. in the determination of transport routes (Choi *et al.*, 2009) and animal migration pathways (Wang *et al.*, 2009). The data sets created in this project may be adapted for a cost-distance model of mine water migration pathways.

Transferability

The statistical division of data sets based on the distribution of values within the Tamar catchment only means that the risk scores and risk classifications for mine wastes are only relevant for intra-catchment comparison. The Water Framework Directive (2000/60/EC), dictates that water resources are managed on a River Basin scale. For a regional prioritisation to cover the south west river basin, it would be necessary to reclassify the input data sets based on the regional spread of data or fixed guideline values. The method used depends on the requirements of the end-user and could be modified if necessary, but establishment of the assessment criteria at an early stage in the modelling process is imperative.

2.7 Conclusions

A model for ranking abandoned mine sites within the Tamar Catchment according to their risk of contaminating water courses from diffuse sources was developed. The model was based on physical and biological characteristics of the mine sites' locations. The model responded robustly to changes in the weighting of physical, geological, climatic and biological factors, showing that a change in emphasis – within reason – would make little difference to the model outcome.

The model identified some of the streamed workings as posing extreme risk to water courses. The contributing factors to this risk assessment were their direct contact with watercourses, impermeable geology and exposure to higher rainfall and stronger winds than other areas in the Tamar catchment. The model is not designed to take the composition of the mine waste material into account, but it would be expected that the high scores of the streamed workings may be used as a trigger to investigate further. As streamed workings within the Tamar Catchment generally relate to the extraction of cassiterite and associated wastes are among the longest abandoned, a mineralogical

analysis of the waste materials (or desk-top study of existing information) may enable the investigating body to downgrade the risk associated with these wastes.

The model included in the "Extreme" risk category a number of non-streamed abandoned mine sites within the Gunnislake and Mary Tavy region, for which published information confirms high levels of contamination with metals and arsenic. Furthermore, the locations of these sites concur with existing water quality data and EQS failures in the River Tamar and/or its tributaries.

The application of the model developed here to the whole of the Tamar catchment confirmed that it is a useful screening tool that allows investigating bodies, such as the Environment Agency, to prioritise sites worthy of further investigation. The GIS built in conjunction with the model also aids the access of site-specific data (e.g. rainfall, soil and geology) and more importantly, predicts the catchment and drainage areas relevant to each waste tip. This improves the efficiency of any field investigations by aiding the design of site sampling regimes so that migrating contamination through surface and sub-surface waters may be captured and analysed. Detailed site investigations of two mine sites posing "Extreme" risk are presented in the following chapters.

The GIS and model developed here provide a flexible tool that may be adapted to meet with the requirements of regulatory authorities in other catchments and countries, assuming that sufficient geo-spatial information is available. The approach taken in this model is transferable to other catchments and regions with similar mineralogy, whereby some of the catchment-specific risk category classifications (e.g. quantile division of rainfall data or topographical information) will have to be adapted to take into account the range encountered in climatic or geographic regions, rather than individual catchments. The work completed here demonstrates a principal, rather

than an absolute approach. However, in areas with significant groundwater reservoirs, such as the mining areas hosted in the limestone of Northern England, further consideration to groundwater transport processes would be required.

The work carried out here has been included in the Environment Agency's South West River Basin Management Plan (EA, 2009; 2011) as an 'Investigation' that forms part of the 'Programme of Measures' that will be applied to identify what 'Actions' are needed to improve water bodies to 'good status' in order to meet the objectives of the Water Framework Directive (2000/60/EC).

A modified version of the model, based on proximity, area and slope has since been adapted and applied to the five catchments in south west England with the highest frequency of abandoned mines. These were North Cornwall, West Cornwall, Tamar, North Devon and South Devon which collectively contained 1897 areas of mine waste (> 1263 m^2). This work was carried out at the request of the Environment Agency in order to meet their obligations for the Water Framework and Mining Waste Directives. It also demonstrated the flexibility of the methodology and GIS approach to meet the needs of regulators.

Furthermore the methodology on which the model is based already meets most of the requirements of Article 20 of the Mining Waste Directive (2001/21/EC) for pre-selection of potentially harmful abandoned mine sites. Recently published guidance documentation for member states encourages the use of a GIS system to aid in the application of Article 20, for example in the establishment of proximity to watercourses and slope angles of terrain in drainage pathways. The methodology presented here can prioritise mine waste tips based on existing data and high priority sites were consistent with known pollution sources in the test catchment. The model may be tailored to the needs of other areas in the UK, or EC member countries to aid

achievement of water quality and mine waste management targets under European

legislation.

2.8 References

Aguarón, J. and Moreno-Jiménez, J. M. (2003). The geometric consistency index: Approximated thresholds. *European Journal of Operational Research.* **147** (1) pp 137-45.

Alvarez, P. J. J. and Illman, W. A. (2006). *Bioremediation and natural attenuation: process fundemetals and mathematical models.* New Jersey, John Wiley & Sons pp

Asta, M. P., Ayora, C., Román-Ross, G., Cama, J., Acero, P., Gault, A. G., Charnock, J. M. and Bardelli, F. (2010). Natural attenuation of arsenic in the Tinto Santa Rosa acid stream (Iberian Pyritic Belt, SW Spain): The role of iron precipitates. *Chemical Geology.* **271** (1-2) pp 1-12.

Bana e Costa, C. A. and Vansnick, J.-C. (2008). A critical analysis of the eigenvalue method used to derive priorities in AHP. *European Journal of Operational Research.* **187** (3) pp 1422-8.

Barredo, J., Benavides, A., Hervás, J. and van Westen, C. J. (2000). Comparing heuristic landslide hazard assessment techniques using GIS in the Tirajana basin, Gran Canaria Island, Spain. *International Journal of Applied Earth Observation and Geoinformation.* **2** (1) pp 9-23.

Bellir, K., Bencheikh-Lehocine, M., Meniai, A. H. and Gherbi, N. (2005). Study of the retention of heavy metals by natural material used as liners in landfills. *Desalination.* **185** (1-3) pp 111-9.

BGS (2009). DigMap, Permeability Indices (Version 5), British Geological Survey. NERC.

BGS (2010). DigMap GB-50 (Geology), British Geological Survey. NERC.

Boix-Fayos, C., Calvo-Cases, A., Imeson, A. C., Soriano-Soto, M. D. and Tiemessen, I. R. (1998). Spatial and short-term temporal variations in runoff, soil aggregation and other soil properties along a mediterranean climatological gradient. *CATENA.* **33** (2) pp 123-38.

Brown, P. A., Gill, S. A. and Allen, S. J. (2000). Metal removal from wastewater using peat. *Water Research.* **34** (16) pp 3907-16.

Buck, C. (2005). *Wheal Russell MIne, Devon. Archaeological Assessment* Historic Environment Service, Environment and Heritage, Cornwall County Council.

Buck, C. (2006). *Gawton Mine, Devon. Archaeological Assessment* Historic Environment Service, Environment and Heritage, Cornwall County Council. Truro.

Cai, F. and Ugai, K. (2004). Numerical Analysis of Rainfall Effects on Slope Stability. *International Journal of Geomechanics.* **4** (2) pp 69-78.

Carmona, D. M., Faz Cano, Á. and Arocena, J. M. (2009). Cadmium, copper, lead, and zinc in secondary sulfate minerals in soils of mined areas in Southeast Spain. *Geoderma.* **150** (1-2) pp 150-7.

CEH.(2010). "Land Cover Map 2000." Centre for Ecology and Hyrology, NERC. Accessed 20/08/08. Avaliable on the world wide web at: http://www.ceh.ac.uk/sci_programmes/BioGeoChem/LandCoverMap2000.html.

CEH.(2011). "Land Cover Map 2000." Centre for Ecology and Hyrology, NERC. Accessed 03/03/11. Avaliable on the world wide web at: http://www.ceh.ac.uk/sci_programmes/BioGeoChem/LandCoverMap2000.html.

Chen, K., Blong, R. and Jacobson, C. (2003). Towards an Integrated Approach to Natural Hazards Risk Assessment Using GIS: With Reference to Bushfires. *Environmental Management.* **31** (4) pp 0546-60.

Chesley, J. T., Halliday, A. N., Snee, L. W., Mezger, K., Shepherd, T. J. and Scrivener, R. C. (1993). Thermochronology of the Cornubian batholith in southwest England: Implications for pluton emplacement and protracted hydrothermal mineralization. *Geochimica Et Cosmochimica Acta.* **57** (8) pp 1817-35.

Choe, E., van der Meer, F., van Ruitenbeek, F., van der Werff, H., de Smeth, B. and Kim, K.-W. (2008). Mapping of heavy metal pollution in stream sediments using combined geochemistry, field spectroscopy, and hyperspectral remote sensing: A case study of the Rodalquilar mining area, SE Spain. *Remote Sensing of Environment.* **112** (7) pp 3222-33.

Choi, Y., Park, H.-D., Sunwoo, C. and Clarke, K. C. (2009). Multi-criteria evaluation and least-cost path analysis for optimal haulage routing of dump trucks in large scale open-pit mines. *International Journal of Geographical Information Science.* **23** (12) pp 1541 - 67.

Cleaver, N. (2010). Email corresondance. A. Turner, Woodland Riders.

Clemente, R., Almela, C. and Bernal, M. P. (2006). A remediation strategy based on active phytoremediation followed by natural attenuation in a soil contaminated by pyrite waste. *Environmental Pollution.* **143** (3) pp 397-406.

CMWHS.(2010). "Cornish Mining World Heritage Site ". The Cornish World Heritage Site. Accessed 30/04/2010. Avaliable on the world wide web at: http://www.cornish-mining.org.uk/.

Dai, F. C., Lee, C. F. and Ngai, Y. Y. (2002). Landslide risk assessment and management: an overview. *Engineering Geology.* **64** (1) pp 65-87.

Davies, B. E. and White, H. M. (1981). Environmental pollution by wind blown lead mine waste: A case study in wales, U.K. *Science of the Total Environment.* **20** (1) pp 57-74.

de Matos, A. T., Fontes, M. P. F., da Costa, L. M. and Martinez, M. A. (2001). Mobility of heavy metals as related to soil chemical and mineralogical characteristics of Brazilian soils. *Environmental Pollution.* **111** (3) pp 429-35.

DeNull, R. (2007). The Greenhill Arsenic Works.

Dines, H. G. (1956). *The metalliferous mining region of south-west England*, HMSO.pp 709 pp

Djokic, D.(2008). "Comprehensive terrain preprocessing using Arc Hydro tools." ESRI. Accessed 01/02/2009. Avaliable on the world wide web at: http://www.hydrosys.net/myplus/bbs/table/hydrosys_doc/upload/Comprehensive%20terrain%20preprocessing%20using%20Arc%20Hydro%20tools.pdf.

Dominico, P. A. and Schwarz, F. W. (1998). *Physical and Chemical Hydrogeology.* New York, John Wiley & Sons. pp 51-52

Dominy, S. C., Camm, G. S., Bussell, M. A., Scrivener, R. C. and Halls, C. (1995). A review of the tin stockwork mineralisation in the south-west England orefield. *Proceedings of the Ussher Society.* **8** pp 368-73.

DTI (2010) UK Wind Speed Database (10m above ground level). Department of Trade and Indusrty. Accessed.10/01/2010. Avaliable online at http://www.bwea.com/noabl/index.html.

Dunkerley, D. (2008). Rain event properties in nature and in rainfall simulation experiments: a comparative review with recommendations for increasingly systematic study and reporteing. *Hydrological Processes.* **22** pp 4415-35.

EA (2009). *Water for Life and Livelihoods, River Basin Management Plan South West River Basin District* The Environment Agency. Exeter.

EA.(2011). "Water for life and livelihoods: River Basin Management Plans." *Water Framework Directive.* The Environment Agency. Accessed 21/03/11. Avaliable on the world wide web at: http://www.environment-agency.gov.uk/research/planning/33106.aspx.

ESRI.(2007). "Understanding cost distance analysis." ESRI. Accessed 03/03/2011. Avaliable on the world wide web at: http://webhelp.esri.com/arcgisdesktop/9.2/index.cfm?TopicName=Understanding_cost_distance_analysis.

Evans, C. D., Cooper, D. M., Juggins, S., Jenkins, A. and Norris, D. (2006). A linked spatial and temporal model of the chemical and biological status of a large, acid-sensitive river network. *Science of the Total Environment.* **365** (1-3) pp 167-85.

Evans, K. G. and Loch, R. J. (1996). Using the RUSLE to identify factors controlling erosion rates of mine soils. *Land Degradation & Development.* **7** (3) pp 267-77.

Fan, Y., Lei, T., Shainberg, I. and Cai, Q. (2008). Wetting Rate and Rain Depth Effects on Crust Strength and Micromorphology. *Soil Sci Soc Am J.* **72** (6) pp 1604-10.

Filella, M., Philippo, S., Belzile, N., Chen, Y. and Quentel, F. (2009). Natural attenuation processes applying to antimony: A study in the abandoned antimony mine in Goesdorf, Luxembourg. *Science of the Total Environment.* **407** (24) pp 6205-16.

Gabbard, D. S., Huang, C., Norton, L. D. and Steinhardt, G. C. (1998). Landscape position, surface hydraulic gradients and erosion processes. *Earth Surface Processes and Landforms.* **23** (1) pp 83-93.

Gatzweiler, R., Jahn, S., Neubert, G. and Paul, M. (2001). Cover design for radioactive and AMD-producing mine waste in the Ronneburg area, Eastern Thuringia. *Waste Management.* **21** (2) pp 175-84.

Goulding, K. W. T. and Blake, L. (1998). Land use, liming and the mobilization of potentially toxic metals. *Agriculture, Ecosystems & Environment.* **67** (2-3) pp 135-44.

Hairsine, P. B., Sander, G. C., Rose, C. W., Parlange, J. Y., Hogarth, W. L., Lisle, I. and Rouhipour, H. (1999). Unsteady soil erosion due to rainfall impact: a model of sediment sorting on the hillslope. *Journal of Hydrology.* **220** (3-4) pp 115-28.

Hamilton Jenkin, A. K. (2005). *Mines Of Devon.* Trowbridge, Cromwell Press.pp 160 pp

Harter, R. D. (1983). Effect of soil pH on adsorption of lead, copper, zinc, and nickel. *American Journal of the Soil Science Society.* **47** (1) pp 47-51.

Hodgson(ed.), J. M. (1997). *Soil Survey Field Handbook,* Silsoe. pp

IMWR.(2002). "RUSLE On-Line Soil Erosion Assessment Tool." Institute of Water Research, Michigan State University. Accessed 02/03/10. Avaliable on the world wide web at: http://www.iwr.msu.edu/rusle/factors.htm.

Jackson, N. J., Willis-Richards, J., Manning, D. A. C. and Samms, M. (1989). Evolution of the Cornubian Ore Field, southwest England: Part II. Mineral deposits and ore forming proecesses. *Economic Geology.* **84** pp 1101-33.

Johnson, C. C. and Breward, N. (2004). *G-BASE Geochemical Baseline Survey of the Environment.*Commisioned Report CR/04/016N British Geological Survey. Keyworth.

Johnston, D., Potter, H., Jones, C., Rolley, S., Watson, I. and Pritchard, J. (2008) *Science Report - Abandoned Mines and the water environment* Environmnet Agency. Report No. SC030136-41

Kampf, S. K., Salazar, M. and Tyler, S. W. (2002). Preliminary Investigations of Effluent Drainage from Mining Heap Leach Facilities. *Vadose Zone J.* **1** (1) pp 186-96.

Kavanagh, P. J., Farago, M. E., Thornton, I. and Braman, R. S. (1997). Bioavaliability of arsenic in soils and mine wastes of the Tamar valley, SW England. *Chemical Speciation and Bioavailability.* **9** (3) pp 77-81.

Kim, K. H. and Miller, W. P. (1996). Effect of rainfall electrolyte concentration and slope on infiltration and erosion. *Soil Technology.* **9** (3) pp 173-85.

Klink, B. A., Palumbo, B., Cave, M. and Wragg, J. (2005). *Arsenic dispersal and bioccessibility in mine contaminated soils: a case study from an abandoned arsenic mine in Devon, UK.*Research Report RR/04/003 British Geological Survey pp 52.

Koener, R. M. and Daniel, D. E. (1997). *Final covers for soild waste landfills and abandoned dumps.* London, Thomas Telford Publications (co-published in UK). pp 58-59

Köhler, M. and Sänger, H. (1998). *Biotic and abiotic factors influencing the long-term stability of covers on waste rock piles in the uranium mining districts of Saxony and Thuringia.* Proceedings of the Uranium Mining and Hydrology II, Verlag Sven von Loga, Köln.

Laakso, L., Gronhölm, T., Kosmale, U., Fiedler, M., Vehkamäki, V. and Kulmala, H. (2003). Ultrafine particle scavanging coefficients calculated from 6 years field measurements *Atmospheric Environment.* **37** pp 3605-13.

Lai, L., Niu, D. and Wang, H.(2003). "Soil Erosion and Conservation." College of Agriculture, University of Saskatchewan, China. Accessed 16/02/2010. Avaliable on the world wide web at: http://159.226.205.16/curriculum/3w/01/index.html.

Langdon, C. J., Piearce, T. G., Meharg, A. A. and Semple, K. T. (2001). Survival and behaviour of the earthworms Lumbricus rubellus and Dendrodrilus rubidus from arsenate-contaminated and non-contaminated sites. *Soil Biology and Biochemistry.* **33** (9) pp 1239-44.

LCM (2001). Land Cover Map 2000, Centre for Ecology and Hydrology. NERC.

LCM.(2010). "Land Cover Map." Countryside Survey. Accessed 17/05/2010. Avaliable on the world wide web at: http://www.countrysidesurvey.org.uk/land_cover_map.html.

Liu, B. Y., Nearing, M. A., Shi, P. J. and Jia, Z. W. (2000). Slope Length Effects on Soil Loss for Steep Slopes. *Soil Sci Soc Am J.* **64** (5) pp 1759-63.

Malczewski, J. (2006). GIS-based multicriteria decision analysis: a survey of the literature. *International Journal of Geographic Information Science.* **20** (7) pp 703-26.

Malenovsky, Z., Mishra, K. B., Zemek, F., Rascher, U. and Nedbal, L. (2009). Scientific and technical challenges in remote sensing of plant canopy reflectance and fluorescence. *J. Exp. Bot.* **60** (11) pp 2987-3004.

Mamedov, A. I., Shainberg, I. and Levy, G. J. (2000). Irrigation with Effluent Water: Effects of Rainfall Energy on Soil Infiltration. *Soil Sci Soc Am J.* **64** (2) pp 732-7.

Marques, M. J., Bienes, R., Jiménez, L. and Pérez-Rodríguez, R. (2007). Effect of vegetal cover on runoff and soil erosion under light intensity events. Rainfall

simulation over USLE plots. *Science of the Total Environment.* **378** (1-2) pp 161-5.

Maskall, J., Whitehead, K., Gee, C. and Thornton, I. (1999). Long-term migration of metals at historical smelting sites. *Applied Geochemistry.* **11** (1-2) pp 43-51.

Mayes, W. M., Gozzard, E., Potter, H. A. B. and Jarvis, A. P. (2008). Quantifying the importance of diffuse minewater pollution in a historically heavily coal mined catchment. *Environmental Pollution.* **151** (1) pp 165-75.

Mayes, W. M., Johnston, D., Potter, H. A. B. and Jarvis, A. P. (2009). A national strategy for identification, prioritisation and management of pollution from abandoned non-coal mine sites in England and Wales. I.: Methodology development and initial results. *Science of the Total Environment.* **407** (21) pp 5435-47.

Merrington, G., Fishwick, S., Barraclough, D. and Morris, J. (2006). *The development and use of soil quality indicators for assessing the role of soil in environmental interations*.SC030265 Environment Agency. Bristol.

MetOffice (2009) MIDAS Land Surface Observations Data British Atmospheric Data Centre. Accessed: Avaliable online at http://badc.nerc.ac.uk/data/ukmo-midas/.

MetOffice (2010) MIDAS Land Surface Observations Data British Atmospheric Data Centre. Accessed: Avaliable online at http://badc.nerc.ac.uk/data/ukmo-midas/.

Mighanetara, K., Braungardt, C. B., Rieuwerts, J. S. and Azizi, F. (2009). Contaminant fluxes from point and diffuse sources from abandoned mines in the River Tamar catchment, UK. *Journal of Geochemical Exploration.* **100** pp 116-24.

Minghanetara, K. (2009) *Impact of Metal Mining on the Water Quality of the Tamar Catchment* PhD Thesis.University of Plymouth.

NATMAP (2008). National Soil Map (NATMAP vector) 1:250000, National Soil Resources Institute (NSRI), Cranfield University.

Nekhay, O., Arriaza, M. and Boerboom, L. (2009). Evaluation of soil erosion risk using Analytic Network Process and GIS: A case study from Spanish mountain olive plantations. *Journal of Environmental Management.* **90** (10) pp 3091-104.

Nordstrom, D. K. and Alpers, C. N. (1999). Negative pH, efflorescent mineralogy, and consequences for environmental restoration at the Iron Mountain Superfund site, California. *Proceedings of the National Academy of Sciences of the United States of America.* **96** (7) pp 3455-62.

OS (2009a) OS 1: 10000 Scale Raster. Ordnance Survey, an EDINA supplied service. Accessed.02/03/2009.   Avaliable   online   at http://digimap.edina.ac.uk/main/download.jsp.

OS (2009b) OS Land-form PROFILE 1: 10000. Ordnance Survey, an EDINA supplied service.   Accessed.02/11/09.   Avaliable   online   at http://digimap.edina.ac.uk/main/download.jsp.

Ower, M., Taylor, R. G., Tindimugaya, C. and Mwesigwa, D. (2009). Rainfall Intensity and Groundwater recharge: empirical evidence from the Upper Nile Basin. *Environmental Research Letters.* **4** pp.

Palumbo-Roe, B., Klinck, B. and Cave, M. (2007). Arsenic speciation and mobility in mine wastes from a copper-arsenic mine in Devon, UK: a SEM, XAS, sequential chemical extraction study. *Trace Metals and other Contaminants in the Environment*. P. Bhattacharya, A. B. Mukherjee, J. Bundschuh, R. Zevenhoven and H. L. Richard, Elsevier. **9** pp 441-71.

Peppas, A., Komnitsas, K. and Halikia, I. (2000). Use of organic covers for acid mine drainage control. *Minerals Engineering.* **13** (5) pp 563-74.

Piearce, T. G., Langdon, C. J., Meharg, A. A. and Semple, K. T. (2002). Yellow earthworms: distinctive pigmentation associated with arsenic- and copper-tolerance in Lumbricus rubellus. *Soil Biology and Biochemistry*. **34** (12) pp 1833-8.

Poesen, J., De Luna, E., Franca, A., Nachtergaele, J. and Govers, G. (1999). Concentrated flow erosion rates as affected by rock fragment cover and initial soil moisture content. *CATENA*. **36** (4) pp 315-29.

Popham, C.(2007). "A Walk Around North Dartmoor Consols." Mindat.org. Accessed 28th March 2010. Avaliable on the world wide web at: http://www.mindat.org/article.php/80/A+Walk+Around+North+Dartmoor+Consols.

Rieuwerts, J., Austin, S. and Harris, E. (2009). Contamination from historic metal mines and the need for non-invasive remediation techniques: a case study from Southwest England. *Environmental Monitoring and Assessment*. **148** (1) pp 149-58.

Riley, S. J. (1995). Aspects of the differences in the erodibility of the waste rock dump and natural surfaces, Ranger Uranium Mine, Northern Territory, Australia. *Applied Geography*. **15** (4) pp 309-23.

Ringqvist, L., Holmgren, A. and Öborn, I. (2002). Poorly humified peat as an adsorbent for metals in wastewater. *Water Research*. **36** (9) pp 2394-404.

Roberts, R. D. and Johnson, M. S. (1978). Dispersal of heavy metals from abandoned mine workings and their transference through terrestrial food chains. *Environmental Pollution (1970)*. **16** (4) pp 293-310.

Roussel, C., Neel, C. and Bril, H. (2000). Minerals controlling arsenic and lead solubility in an abandoned gold mine tailings. *The Science of The Total Environment*. **263** (1-3) pp 209-19.

Rüdel, H. (2003). Case study: bioavailability of tin and tin compounds. *Ecotoxicology and Environmental Safety*. **56** (1) pp 180-9.

Saaty, T. L. (1980). *The Analytic Hierarchy Process*
New York, McGraw-Hill. pp

Sainz, A., Grande, J. A., de la Torre, M. L. and Sanchez-Rodas, D. (2002). Characterisation of sequential leachate discharges of mining waste rock dumps in the Tinto and Odiel rivers. *Journal of Environmental Management*. **64** (4) pp 345-53.

Sánchez España, J., López Pamo, E., Santofimia, E., Aduvire, O., Reyes, J. and Barettino, D. (2005). Acid mine drainage in the Iberian Pyrite Belt (Odiel river watershed, Huelva, SW Spain): Geochemistry, mineralogy and environmental implications. *Applied Geochemistry*. **20** (7) pp 1320-56.

Schmitt, D., Taylor, H. E., Aiken, G. R., Roth, D. A. and Frimmel, F. H. (2002). Influence of Natural Organic Matter on the Adsorption of Metal Ions onto Clay Minerals. *Environmental Science & Technology*. **36** (13) pp 2932-8.

Sherrell (2000). *Devon Great Consols and Bedford United Mines Report on the Results of a Desk Study and Surface Reconnaissance Inspection in Relation to Past Metalliferous MIning Activity* Frederick Sherrell Limited. Tavistock.

Sherrell (2001). *Gunnislake Clitters Mine, Tamar Valley. East Cornwall. Risk Assessmsnt in Relation to Public Access within the Site* Frederick Sherrell Limited Tavistock.

Sherrell (2005). *Gawton Mine, Tamar Valley. West Devon. A Report on the Results of a Desk Study and a Surface Reconnnaissance Inspection in Relation to Past Metalliferous MIning Activity* Federick Sherrells Ltd.

Smith, C. C., Cripps, J. C. and Wymer, M. J. (1999). Permeability of compacted colliery spoil -- a parametric study. *Engineering Geology.* **53** (2) pp 187-93.

Stanley, G., Jordan, G., Hamor, T. and Sponar, M. (2010) *Guidance Document for A Risk-Based Pre-Selection Protocol for the Inventory of Closed Waste Facilities (Draft). Inventory of Closed Waste Facilities* Ad-Hoc Group, A Sub-committee of The Technical Adaptatiob Committee for Directive 2006/21/EC. Report No. 02 (Draft)

Teknomo, K.(2006). "Analytical Hierarchy Process (AHP) Tutorial." Accessed 25/03/2010. Avaliable on the world wide web at: http://people.revoledu.com/kardi/tutorial/ahp/.

Teminghoff, E. J. M., Zee, S. E. A. T. M. and Haan, F. A. M. (1998). Effects of dissolved organic matter on the mobility of copper in a contaminated sandy soil. *European Journal of Soil Science.* **49** (4) pp 617-28.

Tohari, A., Nishigaki, M. and Komatsu, M. (2007). Laboratory Rainfall-Induced Slope Failure with Moisture Content Measurement. *Journal of Geotechnical & Geoenvironmental Engineering.* **133** (5) pp 575-87.

Tokay, A. and Short, D. A. (1996). Evidence from tropical raindrop spectra of the origin and fate of rain from stratiform versus convestive clouds. *Journal of Applied Meterology.* **35** pp 355-71.

Turner, A., Braungardt, C., Worsfold, P., Rieuwerts, J., Williamson, B. and Potter, H. (2009). *Dynamic Up-Flow Percolation Tests - A Model for Mining Waste Leachate Generation*. Proceedings of the International Mine Water Association Conference, Pretoria, South Africa.

US-SCS (1964). Hydrology. Section 4. *National Engineering Handbook.* Washington D.C, U.S. Soil Conservation Service.

USNO.(2010). "Sun or Moon Altitude/Azimuth Table." US Naval Observatory. Accessed 12/1/2010. Avaliable on the world wide web at: http://aa.usno.navy.mil/data/docs/AltAz.php.

van der Lee, J. and De Windt, L. (2001). Present state and future directions of modeling of geochemistry in hydrogeological systems. *Journal of Contaminant Hydrology.* **47** (2-4) pp 265-82.

Vargas, L. G. (2008). The consistency index in reciprocal matrices: Comparison of deterministic and statistical approaches. *European Journal of Operational Research.* **191** (2) pp 454-63.

Wang, I. J., Savage, W. K. and Bradley Shaffer, H. (2009). Landscape genetics and least-cost path analysis reveal unexpected dispersal routes in the California tiger salamander (Ambystoma californiense). *Molecular Ecology.* **18** (7) pp 1365-74.

Wang, J., Chen, J., Ju, W. and Li, M. (2010). IA-SDSS: A GIS-based land use decision support system with consideration of carbon sequestration. *Environmental Modelling & Software.* **25** (4) pp 539-53.

Wang, S. and Mulligan, C. N. (2006). Natural attenuation processes for remediation of arsenic contaminated soils and groundwater. *Journal of Hazardous Materials.* **138** (3) pp 459-70.

Wardell-Armstrong (1990). *Preliminary Report on the Pollution Risk from Mine Waste Tips in the Gunnislake Area, Cornwall for South West Water Services Ltd* Wardell Armstrong. Cardiff.

Wardell-Armstrong (1992). *Gunnislake Intake Pumping Station River Tamar, Pollution Riak Study Phase II - Stability Assessment of Selected Tips for the National Rivers Authority, South West Region* Wardell Armstrong Cardiff.

Webb, P. (1995). Ore Deposits formed by hydrothermal processes. *S268 Physical Resurses and Environment*. T. O. University. Milton Keynes, The Open University. pp 127-8.

Wu, J., West, L. J. and Stewart, D. I. (2002). Effect of humic substances on Cu(II) solubility in kaolin-sand soil. *Journal of Hazardous Materials*. **94** (3) pp 223-38.

Xiao, H. and Ji, W. (2007). Relating landscape characteristics to non-point source pollution in mine waste-located watersheds using geospatial techniques. *Journal of Environmental Management*. **82** (1) pp 111-9.

2.9 Chapter 2 Appendices

2A. Conversion of Polyline features to polygon features and removal of errors.

Features labelled as 'Areas of Mine Associated Land' and 'Streamed Workings' were selected in the attribute table of the original mine *polyline* file supplied by the EA. Selected features were saved to a new polyline file. Using the *features to polygon* tool in the *Data Management Toolbar,* the new layer was converted to a polygon feature file. The polygon file was cleaned of errors: broken polygons were repaired and spurious line features removed. In a small number of cases, there was overlap of polygons (See Figure 2.10), a problem caused by the conversion process. These were corrected by merging polygons and reassigning attributes as appropriate.

Figure 2.10: Example of error caused in polygon layer by overlapping polylines in the original file, and the correction applied.

2B. DTM Generation, full method

The quality of the *digital terrain model* (DTM) underpins the accuracy of the

prediction of all factors that are derived from it e.g. drainage pathways and

topographical slope. The DTM was derived from Ordnance Survey Land-form

PROFILE (10m) contour tiles selected and downloaded from the EDINA database to

cover the Tamar catchment. Tiles include spot heights (air and ground data) and contour

data, incorporation of spot heights improves the DTM based on contours alone.

MapManager9 was employed to convert the extracted files (NTF format), to *shapefiles*.

The resulting contour and spot height shapefiles, were output to a *personal geodatabase*

("dtm") as a data set ("L_F_PROFILE_CON"), from where they could be loaded into

ArcMap (Figure 2.11).

Figure 2.11: Layer files in geodatabase as output from MapManager9 NTF Converter.

The shapefile "LFPCOSpoints_Init", resulting from conversion with MapManager9

had no Z data. In the attribute table, this was added using the *Table Operations Tool*

"Add X,Y,Z Coordinates" in the *Xtools Pro extension toolbar* (Figure 2.12).

Figure 2.12: Adding Z data to point (spot height) layer file

The contour layer file output from MapManager9 contained <NULL> values for high and low water marks. To improve the final DTM, the low water mark features were selected (by *feature code*) and arbitrarily assigned a height of 0 m, high water mark features were assigned a height of 1 m. High water mark features were excluded from the data set and exported to a separate file in the geodatabase ("dtm") to allow them to be easily added or removed from the *Triangulated Irregular Network* (TIN).

The final contours and spot heights to be used in the construction of a TIN were checked against the Ordnance Survey 10 km layer. The layers were *clipped* to the spatial extent of the Tamar Catchment polygon file supplied by the EA (+500 m *buffer*), to reduce the amount of memory required to process the TIN. The "TamarTIN" was created using the *3D Analyst toolbar* from the spot height (LFPCOSpoints_ClipTamar) and contour (LFPCOSlines_ClipTamar) layer files, contours were encoded as soft lines (Figure 2.13).

85

Figure 2.13: Construction of TIN from spot heights (brown points) and contour heights (green lines).

Occasional artefacts in the TIN occurred where there were incomplete contour lines, as seen in the example (Figure 2.14) where contours are intersected by a railway embankment. Although it is possible to manually join the contour lines, this was not undertaken for the entire catchment. Instead the TIN at sites of interest was inspected to highlight missing contour lines as a potential source of error to calculations of slope and drainage pathways. The problem may be avoided by using improved resolution elevation data, such as NEXTMap® Britain. However this would incur additional cost.

The TIN was converted to raster (grids) using the "3D analyst" toolbar (Figure 2.15). Cell sizes of 5m, 4m and 3m were defined to create grids of differing resolution. Greater resolution is desirable but requires greater processing power in ArcHydro9. The resolution used is limited by the computing power of ArcGIS host. The DTM created with a 5m grid was the highest resolution that could be successfully processed by ArcHydro9.

Figure 2.14: Example of incomplete contour lines in OS mapping (circled above) creating artefacts in the TIN (circled below).

Figure 2.15: Conversion of TIN to Raster with cell size 5m

2C. Modelling of Drainage Channels and Catchment Boundaries using ArcHydro9, full method.

Catchment boundaries, rivers, streams, and drainage channels were modelled using ArcHyro9 (ESRI). Before hydrological analysis can be conducted the DTM (Appendix 2B) must be pre-prepared in order to establish the correct drainage pattern (Djokic, 2008). Firstly, in the *DEM Manipulation* tab of the *Terrain Preprocessing* menu, the *fill sinks* tool was used to fill any artificial lows in the DTM. The catchment DTM with the smallest computable cell size (5 m) was used in this first step, which requires the most processing capability. The flow direction was then established in the filled DTM ("FilSinkgrid5") by running the *Flow Direction* function in the Terrain Preprocessing menu.

The results were reviewed according to Djorkic (2008), and verified with existing knowledge of drainage features from mapping and site visits. In particular, areas of low relief, the known flow direction of primary rivers and major streams (e.g. River Tamar, River Ottery, River Claw, Luckett Stream etc.) showed minor discrepancies to the drainage pattern generated by the DEM. To improve the model the flow paths were imposed manually where necessary, using the method of *burning in*. The imposed stream layer was created from OS 1:10,000 OS Mapping "indicative_mainrivers_flood_TamarClip" (Figure 2.16); and was carefully inspected and cleaned of errors and braided channels. This process can only be undertaken in circumstances where reliable information on the flow channel at a suitable scale (here latest 1:10,000 OS mapping) is available. In all other cases the drainage channels were not altered at the regional scale as the process may introduce unknown errors to the DTM.

Figure 2.16: Burning in the stream layer to the (filled) DTM

At the site-specific scale, man-made drainage ditches, such as mine and mill leats pose a particular problem to the flow direction model. This is because they are often not identified in the DTM and do not always follow a dentric flow pattern. It is therefore recommended that known leats are "burned in" only if the flow direction is certain. The *DEM Reconditioning (AGREE)* tool (found in the *DEM Manipulation* menu in *Terrain Preprocessing*) was used to perform this task and produce a modified DEM ('agreeDEM_grd5'). The input DEM was "FilSinkgrid5", input parameters for the smooth drop/rise and sharp drop/rise (DEM Z unit) were optimised and iterated to give the best results. The final parameters were 10 m and 100 m respectively. The *stream buffer* was set to 2 cells, increasing this number reduced the accuracy of the drainage path. Again it is important to stress that the accuracy of the drainage pattern generated by the model may also be improved with higher resolution or alternative data used to create the input DTM. After *burning in,* the *fill sink*s step in the procedure was repeated to eliminate potential depressions caused and generate a new HydroDEM ("FSnk210100"). The output hydro-grid is only suitable for drainage analysis as the

burning in process creates artificial slopes next to the rivers and streams. A *flow direction grid* was then calculated in ArcHydro from the Hydro DEM (Figure 2.17).

Figure 2.17: Flow Direction Grid as displayed in ArcMap. Flow direction grid should have only eight distinct values (1, 2, 4, 4, 16, 32, 64 and 128), each represented by a different colour on the map.

2D. Intersection and Dissolving of Risk Polygons to Provide Mean Value output for Mine Waste Polygons.

The *intersect* and *dissolve* tools were combined using the *model builder extension* (see example, Figure 2.18). The catchment, drainage pathway or tip extent polygons were used as the intersect layers as appropriate.

Figure 2.18: Geoprocessing model used to average risk scores for catchment attributes. Constructed in Model Builder extension of ArcMap.

The intersect function added the Mine_ID index code to each of the component polygons. This allowed dissolution based on their association with the mine waste polygons field. Statistical outputs were set within the 'Dissolve' toolbox (See Figure 2.19). In this study, the mean score was deemed the most suitable statistical output, but maximum, minimum and weighted scores may also be calculated in this stage.

Figure 2.19: Statistical fields applied to unioned model data sets using "Dissolve" toolbox in order to calculate total risk.

2E. Joining Tip, Drainage and Catchment Attributes to Mine Waste Polygon File, Full Method.

The output layers from the dissolve process were combined using the *Join* tool. The mine polygon layer, which contained scores for area and proximity risk, was used as the base attribute table. The three data sets containing the combined risk for catchment, drainage path and tip were joined to this data set based on the unique "MineID" field (shown in Figure 2.20). The joined data was permanently added by and copying in the desired data to a new field using the *Field Calculator* tool.

Figure 2.20: Joining attribute data to base attribute table based on the "MineID" field.

2F. Final Summation of Risk for Tip, Drainage Areas and Catchments, Full Method.

A "Total Risk" column was added as a new field to the mine polygon layer. The new field was populated with the sum of the combined risk for: proximity and area (from the base attribute table), tip, catchment and drainage pathway. This was achieved using the *field calculator* tool, as shown in Figure 2.21.

Figure 2.21: Final summation of combined risk scores for attributes of tip, catchment and drainage path

2G. **Selected Maps Referenced in Text**

Figure 2.22: Map of the Tamar catchment showing risk classification of long term average rainfall. Created in ArcMap using Met Office Data (1971 - 2000).

Figure 2.23: Map of the Tamar catchment area showing risk classification of rain intensity, determined as the return time (in days) of a ≥ 20 mm. Produced in ArcMap using MIDAS daily rainfall (MetOffice, 2009).

Figure 2.24: Slope Risk Map for part of the Tamar catchment around Gunnislake, created in ArcMap using OS Landform PROFILE data. © Crown Copyright/database right 2009 An Ordnance Survey/EDINA supplied service.

Figure 2.25: Example map of part of the Tamar catchment showing risk classification for soils. Created in ArcMap using National Soil Map data (NATMAP, 2008).

Figure 2.26: Map of the Tamar catchment showing risk classification for surface run off with respect to bedrock permeability. Created in ArcMap and based upon 1: 50 000 scale permeability and bedrock data, with the permission of the British Geological Survey.

Transport Risk from Superficial Deposits
Risk Score, Min. perm, Max Perm

- -3, Very Low, Low
- 1, Unclassified Areas
- 1, Low, Moderate
- 2, Very Low, High
- 3, High, High
- 6, Moderate, Very High
- 6, Very High, Very High
- 6, High, Very High

Figure 2.27: Map of the Tamar catchment showing risk classification for contaminant transport with respect to superficial deposit type and permeability. Created in ArcMap and based upon 1: 50 000 scale permeability and superficial deposit data, with the permission of the British Geological Survey.

Figure 2.28: Example output from vector model using climatic weightings. Created using ArcMap.

99

2H.   Results Tables

Table 2.22: Ten highest scoring areas of mine associated contaminated land, according to four weighting schemes applied.

Weighting Scheme Applied:	Physical (P)		Climatic (C)		Geological (G)		Biota (B)	
Position	ID	Score	ID	Score	ID	Score	ID	Score
1	787	4400	787	4525	787	4411	787	4389
2	794	4317	794	4427	794	4339	794	4332
3	57	4298	57	4418	57	4315	57	4262
4	710	4251	710	4366	710	4259	710	4234
5	765	4236	765	4357	765	4258	765	4231
6	202	4222	494	4326	202	4240	202	4212
7	134	4180	202	4324	134	4185	551	4194
8	551	4177	134	4301	551	4184	134	4183
9	494	4176	247	4288	494	4182	247	4170
10	247	4171	551	4270	247	4173	494	4135

Table 2.23: Ten highest scoring areas of mine associated contaminated land, according to four weighting schemes applied. Streamed workings excluded.

Weighting Scheme Applied:	Physical (P)		Climatic (C)		Geological (G)		Biota (B)	
Position	ID	Score	ID	Score	ID	Score	ID	Score
1	710	4251	710	4366	710	4259	710	4234
2	651	3841	137	3975	651	3899	651	3773
3	281	3827	651	3951	137	3891	141	3735
4	141	3733	239	3807	281	3870	514	3717
5	514	3711	514	3799	141	3757	806	3680
6	806	3671	806	3785	239	3737	14	3634
7	14	3635	281	3754	514	3709	137	3573
8	639	3618	141	3747	806	3685	529	3570
9	627	3597	639	3727	639	3674	627	3562
10	239	3581	14	3706	14	3663	639	3561

-Chapter 2 End-

Chapter 3

Mine Waste Tips as a source of

Metals and Arsenic Contamination,

Case Study 1: Devon Great Consols

3. Mine Waste Tips as a source of Metals and Arsenic Contamination: Case Study 1: Devon Great Consols

3.1 Abstract

Waste tips at abandoned mines are a threat to water quality in SW England via surface run off and shallow groundwater movement. The concentrations of eco-toxic metals (Al, Cu, Zn, Al, Ni, Cd, Mn and Fe) and As in tip drainage from three waste tips at Devon Great Consols mine, were highly elevated with respect to Environmental Quality Standards (EQS). Concentrations of dissolved Al and Cu, in the final drain discharges were high enough to cause the known EQS failure in the River Tamar, based on conservative mixing of the waters. Dissolved concentrations of Zn and Cd are also likely to be significantly contributor to EQS failures recorded downstream of the mine.

Annual fluxes emanating from the tips were calculated using catchment modelling and determined dissolved concentrations. Cinders waste generated the largest flux of As (32000 mol y^{-1}) and waste from the Wheal Anna Maria Upper tip the largest flux of Cu and Cd (38900 mol y^{-1} and 376 mol y^{-1} respectively). Closer to the River Tamar, abandoned precipitation launders generated the highest fluxes of Zn and Ni (2240 mol y^{-1} and 398 mol y^{-1} respectively). The predicted annual fluxes from the three tips investigated at Devon Great Consols were the same order of magnitude as previously predicted for the main adit discharge at the mine (Blanchdown Adit, Mighanetara (2009)) for Mn, Zn, Ni and Cd.

Preferential sorption of some elements, particularly As, to mineral surfaces, particularly freshly precipitated Fe(OH)$_3$(s), appear to inhibit their migration into the River Tamar. This effect may be exploited in future management strategies. Dissolved Fe was low in tip drainage waters, which remain largely oxic through the site, migrating

in surface drains and shallow groundwater. High concentrations of dissolved Fe in the discharges from Blanchdown Adit offer the possibility of precipitating fresh $Fe(OH)_3(s)$ surface. This could help remediate the high metal concentrations in the final collection drain, particularly for dissolved Cu, in future management schemes.

3.2 Introduction

The south west region of England hosts a large proportion of the UK's surface water bodies with reduced water quality due to receipt of mine waters (Mayes *et al.*, 2009). The Tamar catchment, which contains more than 300 recorded abandoned mines, has elevated levels of metals and arsenic in its surface waters due to the discharge of mine waters and the dispersion of mine wastes into stream systems e.g. Price (2002), Mighanetara *et al.* (2009) and Rieuwerts *et al.* (2009). The Environment Agency (EA), through regular monitoring of watercourses, has recorded dissolved concentrations for some metals in the catchment. Table 3.1 lists the proposed EQS values for metals most commonly associated with mine drainage waters and compares them with the maximum values recorded in the River Tamar, main tributaries and targeted surveys of mine water discharges by the EA. The contaminant concentrations occurring in mine waters in the Tamar catchment at times exceed the EQS values for Cd, Cu, Ni, Pb, Zn and As and therefore pose a water quality issue to the River Tamar.

Many of the likely sources of mine waters, such as adit discharges and deposits of mine waste, are known locally and are currently subject to regulatory review (Mayes *et al.*, 2010). However, the contribution of mine water contamination arising from diffuse inputs remains largely unresolved. Such inputs can include run-off from mine waste tips, diffuse seepages close to point discharges, contaminant remobilisation from resuspended river sediments and direct groundwater inputs (Mayes *et al.*, 2008). Their contribution to the overall contaminant input have been suggested to be high (Mayes *et*

al., 2008), representing 46% to 90% of the total metal flux arriving in the River Tamar (Mighanetara, 2009).

Table 3.1: Environment Quality Standards for selected metals named as priority substances (Cd, Ni and Pb) or named in Annex VIII of the Water Framework Directive (UKTAG, 2008), and range of filtered concentrations recorded for the River Tamar and major tributaries by the Environment Agency (1974-2008). Results for River Tamar and main tributaries exclude direct discharges from mines, water treatment works, and industrial sites/dockyards. EQS, where stated as ranges, are dependent on water hardness. Environment Agency data supplied under licence. *No data for filtered Fe, unfiltered data shown.

Contaminant	EQS Annual Average or Long-term Limit ($\mu g\ L^{-1}$)	River Tamar Range ($\mu g\ L^{-1}$)	Major Tributary Range ($\mu g\ L^{-1}$)	Targeted Surveys of Mine Discharges Range ($\mu g\ L^{-1}$)
Al	0.05	10-1200	10-7940	10-7500
As	50	0.2-10.0	0.2-28.5	0.2-315
Cd	≤ 0.08-0.25	0.01-1.0	0.01-5.0	0.2-10.0
Cu	1-28	0.5-63	0.4-75	13-4400
Fe	0.016	2-15500*	1-26300*	Limited data
Mn	7	5-590	2-460	10-2400
Ni	20	0.05-50	1.0-10	3.0-280
Pb	7.2	0.1-20	0.1-15	0.1-20
Zn	8-125	2.0-210	2-216	28-2800

The results of the catchment prioritisation exercise in Chapter 2 indicated mine waste tips that might pose an extreme risk to watercourses based on their location and associated environmental characteristics. Among these, Devon Great Consols (DGC), an abandoned copper and arsenic mine near Gunnislake, and tips at Wheal Betsy, an abandoned lead-zinc mine on the margins of Dartmoor National Park (examined in

Chapter 4), ranked highly in risk. Both are situated upstream of public water supply abstraction points from the River Tamar and River Tavy respectively (South West Water, 2009). At DGC the abstraction point is very close to a number of surface and adit discharges.

Highest levels of contamination are recorded for adit and surface drains from mine sites, and their confluences with larger watercourses, including Blanchdown surface drain at DGC, Gunnislake Clitters adit and the confluence of the River Tamar with South Wheal Fanny drain (DGC). Several studies have investigated the levels of contamination in the waste tips material at Devon Great Consols (Kavanagh *et al.*, 1997; Langdon *et al.*, 2001; Sparrow and Wilkins, 2001; Dybowska *et al.*, 2005; Palumbo-Roe *et al.*, 2007; van Herwijnen *et al.*, 2007), and Wheal Betsy (WB) 53,848 mg kg^{-1}, Pb and 3,135 mg kg^{-1} Zn (Rieuwerts et al., 2009). A selection of comparable studies is shown in Table 3.2. All reported highly elevated metal and metalloid concentrations in soils, sediments and efflorescent salts. Maximum As content in Devon Great Consols waste material were 52600 μg g^{-1} by Kavanagh *et al*. (1997), and up to 204478 mg kg^{-1} (including As-rich salts on flue gas chambers of arsenic calciners) by Klink *et al*. (2005).

Mighanetara (2009) determined metal concentrations in mine wastes from a number of sites in the Tamar Catchment. The results showed that waste tips varied in metal content between mines, but that those at Devon Great Consols, particularly cinders from As processing, yielded some of the highest totals of the tips surveyed for As, Cu, Mn, Ni and Cd. Total metal and As concentrations previously determined for tip waste are highly elevated in relation to mine sites in other areas of the world such as Spain, France and South America (Table 3.2). They also exceed UK and Dutch regulatory guidelines for assessment of contaminated land with respect to As, Cu, Cd, Pb and Zn (Table 3.3).

Table 3.2: Total metal concentrations (mg kg^{-1}) reported in other studies of mine spoil and mine contaminated soils from Devon Great Consols and around the world.

Author	Location	As	Cu	Cd	Mn	Ni	Pb	Zn
Mighanetara (2009)	Cinders tips at Devon Great Consols, (SW England)	30400-37500	5400-6500	<LOD	1600-2000	49 ±5.9	91 ±7.6	500 ±80
	Wheal Anna Maria tip at Devon Great Consols	21300-27200	2100-3300	<LOD	420-840	23 ±1.2	34 ±6.7	100 ±60
Klink *et al.*(2005)	Waste tips at Devon Great Consols, including As-salts from flue chambers of As calciners.	249-204478	-	-	-	-	-	-
Dybowska *et al.*(2005)	Cinders tips at Devon Great Consols	57381	3362	-	-	-	-	-
	Waste Tips at Devon Great Consols	13643-15893	987-1524	-	-	-	-	-
Kavanagh *et al.*(1997)	Waste Tips at Devon Great Consols	173-52600	-	-	-	-	-	-
Rieuwerts *et al.*(2009)	Waste Tips at Wheal Betsy (SW England)	-	-	-	-	-	1028-53848	43-3135
Roussel *et al.*(2000)	Waste Tailings at former gold mine (France)	41150-78150	-	-	-	-	14600-14910	-
Alvarez *et al.* (2003)	Tips at an abandoned mine in Galicia (NW Spain).	-	273-5421	<LOD	294-2105	<LOD	<LOD	73-894
Moreno-Jiménez et al.(2009)	Soils around Monica pyrite mine, NW Madrid (Spain).		17-605	1.8-35	185-658			92-2244
Bech *et al.*(1997)	Soils around a copper mine, Piura (Northern Peru).	143-7670	69-5270	8.9-499	213-965	-	87-341	56-772

Table 3.3: UK Soil Guideline Values (SGVs) for residential, allotment and commercial land use determined and published by the Environment Agency (2010). Dutch SGV from the Dutch National Institute for Public Health & the Environment (Soil Remediation Circular 2009). Values based on current published exposure and toxicological assumptions. All values in mg kg^{-1}, dry weight.

Contaminant	UK SGV			Dutch SGV
	Residential	Allotment	Commercial	Intervention values
As	32	43	640	76
Cu	-	-	-	190
Cd	0	1.8	230	13
Ni	130	230	1800	100
Pb	-	-	-	530
Zn	-	-	-	720

There is a recognised risk to local and regional water quality from leachates emanating from Devon Great Consols and Wheal Betsy which may be indicative of other metal mine sites in the Tamar catchment. To date, there is little knowledge of the mobility of the dissolved metals in the spoil leachates as they move through their respective sites in surface drains and ground waters toward regulated watercourses. There is a need to quantify the contaminant flux that is entering receiving watercourses via diffuse pathways in order to elucidate their relative contribution from direct inputs and in-stream re-mobilisation.

3.3 Aims and Objectives

The aim of this chapter (and Chapter 4) was to:

- Measure dissolved contaminant concentrations in situ emerging from mine wastes of different character and representative of others found in the catchment.

- Measure instantaneous flow of surface drains and where possible estimate contaminant fluxes of dissolved contaminants moving through the site.

- Investigate the factors affecting contaminant release and transport from mine waste (e.g. waste composition and site hydrology)

The contaminant metals of interest were Cd, Cu, Zn, Ni, Pb, Mn, and Fe, together with metalloids As and Sb. These elements are of particular concern due to their high eco-toxicity and/or inclusion in environmental regulations as part of the Water Framework Directive (2000/60/EC). Devon Great Consols, on the Devon side of the River Tamar near Gunnislake, Cornwall, and Wheal Betsy near Mary Tavy, Devon, were selected as examples of mining in the two major mineral deposit types, found in the Tamar catchment. Their selection was based on literature information, research and local knowledge (from the Plymouth Mining and Mineral Club) of the mining history and extent of contamination found at these sites. Devon Great Consols exploited copper and arsenic deposits in E-W trending lodes whilst Wheal Betsy is an example of an older Pb/Ag mine exploiting N-S trending mineral "cross-courses" (Dines, 1956). The sites also have some of the largest waste tips in the catchment, as shown in Chapter 2, making them worthy of investigation as major contaminant sources to their respective receiving watercourses, the River Tamar and Cholwell Brook, a tributary of the River Tavy.

The objectives of the study at each site were:

1. To quantify the concentrations of metals in mine waste leachates, surface drains and shallow ground waters entering the receiving watercourse. (To act as a robust survey for regulators and other interested parties, and to validate laboratory methods introduced in Chapter 5).

2. To investigate the dominant geochemical controls influencing the composition of the mine waters at two contrasting sites.

3. To estimate the fluxes that may arise from areas of mine waste.

4. To investigate the effect of seasonality on the concentrations and fluxes of contaminant metals and metalloids.

A sampling scheme was adopted to monitor the quality of discharges emanating mine waste tips on repeated visits between June 2007 and July 2009. Initial site walkover surveys and where available, existing reports (e.g.Wardell-Armstrong, 1992; Sherrell, 2000; Buck, 2002) and local expertise were used to design a suitable sampling strategy. Annual contaminant flux was estimated via a combination of measured flows and determined concentrations, daily rainfall data and GIS-modelled tip catchment areas. No attempt was made to determine the speciation of contaminants directly. However, the geochemical modelling code PHREEQC (version 2) was employed to aid in the interpretation of the results with respect to the solubility of mineral phases and element speciation.

3.4   Literature Review: The Geochemistry of Mine Waste Leachate

3.4.1   Acid Generation and Metal Release

The mineral deposits in south west England are predominantly hosted in sulphide mineral veins, leading to the presence of sulphide minerals in the waste rock tips found at abandoned mines. Iron sulphides, such as pyrite (FeS) and pyrrhotite ($Fe_{1-x}S$), and other metal sulphide minerals, such as sphalerite ((Zn,Fe)S), galena (PbS), chalcopyrite ($CuFeS_2$) and arsenopyrite (FeAsS), are largely stable under in-situ geological conditions but oxidise when exposed to the atmosphere. The oxidation reactions, which are accelerated by microbiological activity, produce acidic mine waters that are commonly high in dissolved sulphate, metals and metalloids, such as Al, Cd, Co, Cu, Fe, Mn, Ni, Pb, Zn and As (Lee *et al.*, 2002; Hulshof *et al.*, 2006; Mohan and Chander, 2006; Navarro Flores and Martínez Sola, 2010). The principal generator of acidity is the oxidation of iron sulphide minerals, predominantly pyrite (FeS_2) and pyrrhotite ($Fe_{1-x}S$). Generation of acidic waters can involve chemical, biological and electrochemical reactions and may take place in oxygenated or anoxic systems, depending on the prevailing conditions and the oxidant involved (Lollar, 2005).There is an extensive body of literature on the topic and detailed reviews of pyrite oxidation and the generation of acid mine/rock drainage (AMD/ARD) may be found on the world wide web e.g. INAP (2009), and in the literature (Evangelou and Zhang, 1995, Nordstrom and Southam, 1997, Younger *et al*., 2002 ,and Lollar, 2005). For consistency, reaction equations 1-4 have been taken from Younger *et al.* (2002) and references therein. Initially, pyrite is oxidised by atmospheric oxygen with the transfer of electrons to dissolved oxygen from sulphur via Equation 1.

$$FeS_2(s) + 7/2\ O_2 + H_2O \rightarrow Fe^{2+} + 2\ SO_4^{2-} + 2\ H^+$$

Equation 1
(Stumm and Morgan, 1996a)

The reaction releases ferrous iron (Fe^{2+}) and acidity into solution resulting in decreased pH. In the presence of sufficient dissolved oxygen, oxidation continues with Fe^{2+} oxidised to ferric iron (Fe^{3+}) via Equation 2.

$$Fe^{2+} + \tfrac{1}{4} O_2 + H^+ \rightarrow Fe^{3+} + \tfrac{1}{2} H_2O \qquad\qquad \textbf{\textit{Equation 2}}$$

At pH > 3.5, the ferric ion reacts with oxygen to form an insoluble precipitate releasing more acidity into solution via a reaction commonly represented by Equation 3:

$$Fe^{3+} + H_2O \leftrightarrow Fe(OH)_3(s) + 3H^+ \qquad\qquad \textbf{\textit{Equation 3}}$$

Where $Fe(OH)_3$ represents a Fe(III) oxyhydroxide precipitate, which may be ferrihydrite ($5Fe_2O_3.9H_2O$,) schwertmannite (between $Fe_8O_8(OH)_6SO_4$ and $Fe_{16}O_{16}(OH)_{10}(SO_4)_3$), goethite ($FeO(OH)$) or jarosite ($KFe_3(SO_4)_2(OH)_6$), depending on pH-Eh conditions (Dold, 2005). Equation 3 is a simplification of a series of complex reactions which occur to reach the end product, but the overall result of reactions 1-3 is to release 4 moles of acidity into solution for every mole of pyrite. If the pH of the system falls to $\leq$ pH 3.5, $Fe(OH)_3(s)$ is no longer stable with respect to ferric iron, and the Fe^{3+} generated by Equation 2 remains in solution (Evangelou, 1995). In these circumstances the ferric iron may react with pyrite via Equation 4, yielding 16 moles of acidity per mole of pyrite (Younger *et al.*, 2002). Without significant buffering capacity, the pH of the system can plummet to pH values as low as -4 in extreme cases (Nordstrom *et al.*, 1999).

$$FeS_2(s) + 14\ Fe^{3+} + 8\ H_2O \rightarrow 15Fe^{2+} + 2\ SO_4^{2-} + 16\ H^+ \qquad \textbf{\textit{Equation 4}}$$

The ferrous iron produced by Equation 4 can be re-oxidised by oxygen (Equation 2) and the cycle of reactions will proceed until oxygen is depleted, at which point Equation 4 will continue to completion, leaving predominantly ferrous iron in solution.

The conversion of ferrous to ferric iron (Equation 2) is the rate-limiting step in the overall pyrite reaction sequence (Singer and Strumm, 1970). Bacteria such as *Acidithiobacillus ferrooxidans* obtain energy by oxidising Fe^{2+} to Fe^{3+} and as part of complex microbial consortia are able to catalyse this reaction. The increased rate of reaction is estimated to be up to a factor of 10^5 higher than abiotic oxidation (Singer and Strumm, 1970).

Pyrrhotite oxidation has received much less study than pyrite oxidation but results suggest it can react 20-100 times faster than pyrite under standard conditions (Lollar, 2005). The amount of acid produced by the oxidation of pyrrhotite is linked to its stoichiometry with the iron deficient form ($x = 0.125$) producing acidity via Equation 5, while the end-member troilite ($x = 0$) produces none. However, the ferrous ions produced from both pyrrhotite and troilite oxidation in Equation 5 (Lollar, 2005) go on to produce acidity via Equations 3 and 4 resulting in net acid generation in both cases.

Pyrrhotite: $Fe_{1-x} S\ (s) + (2 - 1/2\ x)O_2 + xH_2O \rightarrow (1-x)Fe^{2+} + 2\ SO_4^{2-} + 2x\ H^+$

Equation 5

Other sulphide minerals with metal/sulphur ratios = 1 (e.g., sphalerite, galena, chalcopyrite) tend not to produce acidity when oxygen is the oxidant (INAP, 2009), but are dissolved under acidic conditions, releasing metals into solution, for example via Equations 6-8 (Younger *et al.*, 2002, and references therein):

Galena: $PbS(s) + 2\ O_2(aq) \rightarrow Pb^{2+} + SO_4^{2-}$ *Equation 6*

Sphalerite: $ZnS(s) + 2\ O_2(aq) \rightarrow Zn^{2+} + SO_4^{2-}$ *Equation 7*

Chalcopyrite: $CuFeS_2(s) + 4\ O_2(aq) \rightarrow Cu^{2+} + Fe^{2+} + 2\ SO_4^{2-}$ *Equation 8*

Other contaminant metals are found in solution by means of being trace elements in common sulphide minerals. For example, Mn, Ni and Co are found in Fe-sulphides, whilst sphalerite is the principal source of Cd in mine tailings (Moncur *et al.*, 2009).

The oxidation of galena, sphalerite and chalcopyrite can be enhanced by a number of factors including pH, temperature, mineral surface area and the concentration of oxidants in solution (Dutrizac, 1981; Kang and Sproull, 1991). As for pyrite and pyrrhotite, these minerals may be oxidised by either oxygen or ferric iron, releasing metals into solution (Equations 9-11):

Galena: $PbS(s) + 2\ Fe^{3+} + 1.5\ O_2(aq) + H_2O \rightarrow PbSO_4 + 2\ H^+ + 2\ Fe^{2+}$ ***Equation 9***
(da Silva, 2004)

Chalcopyrite: $CuFeS_2(s) + 4\ Fe^{3+} \rightarrow 5\ Fe^{2+} + Cu^{2+} + 2\ S^0$ ***Equation 10***
(Hiroyoshi et al., 1997)

Chalcopyrite: $CuFeS_2(s) + 4\ H^+ + O_2(aq) \rightarrow Cu^{2+} + \ Fe^{2+} + 2S^0 + 2\ H_2O$

Equation 11
(Hiroyoshi et al., 1997)

Hiroyoshi *et al.* (1997) reported that the ferrous ions produced via Equation 10 catalysed the leaching of copper from chalcopyrite by Equation 11, and the latter reaction is favoured at low pH, as protons are consumed in the reaction.

Mine wastes arising from sulphide ores are generally complex mixtures and the dissolution rate of a particular metal sulphide mineral can be dependent on the other minerals around it. For example, the dissolution of chalcopyrite may be accelerated in the presence of pyrite and molybdenite (Dutrizac and MacDonald, 1973), whereas the oxidation of galena was shown to be diminished in the presence of sulphide minerals containing Zn and Cd (Urbano *et al.*, 2007). Many of the observed differences in reactivity relate to galvanic effects, where physical contact between two different metal-

disulphide minerals in an acid/ferric solution creates a galvanic cell (Evangelou, 1995). The mineral with the lowest resting potential, acting as the anode, will be dissolved, while the mineral with the higher resting potential (cathode), will be galvanically protected (Mehta and Murr, 1983).

Galvanic effects have been shown to increase the dissolution of galena, sphalerite and chalcopyrite in a two phase system with pyrite (Abraitis *et al.*, 2004) and have also been established for Cu-Ni sulphides by Tong *et al.* (2009). Dissolution rates of galena were observed to be very similar in a pyritic sludge as compared to the raw mineral, whereas rates of sphalerite and chalcopyrite dissolution were observed to be accelerated in the sludge (Cama and Acero, 2005). Mineral structure can also alter observed oxidation and dissolution rates. For example, in the structure of sphalerite in which Fe partially substitutes for Zn, higher rates have been observed to increase with increasing Fe content in the mineral (Moncur *et al.*, 2009). Also, the framboidal form of pyrite is generally accepted as the most reactive form of the mineral, having a very large surface area compared with other polymorphs (Evangelou, 1995).

The formation of an armouring layer around sulphide mineral grains is often observed in mine wastes and can inhibit oxidation. Such an effect has been shown for galena, forming Pb-sulphide (metal deficient) coatings under conditions of low pH and high sulphate, (Buckley and Woods, 1984; Lin, 1997). Similarly the development of a surface layer of metal deficient sulphide has been observed in natural sphalerites within which an accumulation of copper, thought to originate from the bulk mineral, was also observed (Buckley *et al.*, 1989). Again, bacteria can be involved and increase the rates of reaction. Torma (1988) stated that the role of bacteria in the galvanic cell was to continuously oxidise elemental sulphur (produced from the anodic reaction) to sulphate, thus preventing the formation of a sulphur barrier on the surface of the anode mineral (chalcopyrite in this instance), hence increasing dissolution rates.

In addition to variations observed within the sample environment, literature evidence also suggests that prediction of the relative rates of sulphide mineral dissolution, based on empirical measurements, can vary with sample preparation, surface area to volume ratios and the presence of impurities (Lollar, 2005).

Cathodic protection of an acid-generating sulphide can reduce the leaching potential, while microbial mediation may enhance the weathering of sulphides with a high electrode potential. The galvanic processes can compete with microbial activity in effecting the oxidation of sulphides with a low electrode potential in a mixed sulphide assemblage (Kwong *et al.*, 2003). It is considered likely that in these systems different mechanisms of oxidative/dissolution, electrochemical oxidation and oxidation by Fe^{3+}, O_2 and bacteria occur concurrently (Evangelou, 1995), but there is a lack of literature to resolve the relative contribution of each to overall mineral dissolution in mixed sulphide systems.

3.4.2 Sorption and Precipitation Reactions

Interactions between dissolved metals and the waste material, soils, rocks, water and the atmosphere determine the mobility of elements once released. Depending on conditions, metal ions released from sulphide weathering can precipitate as sulphate-, carbonate- and in some cases silicate- mineral phases. This is generally a favourable process as it immobilises some metals and metalloids, for example ferric iron in jarosite $(KFe_3(OH)_6(SO_4)_2)$, ferrous iron in malanterite $(FeSO_4.7H_2O)$, aluminium in alunite $(KAl_3(OH)_6(SO_4)_2)$ and lead in anglesite $(PbSO_4$ (Younger *et al.*, 2002). Precipitates can also lead to a discolouration of waters, sediments and rocks: most often this is dominated by iron hydroxides giving a characteristic ochre colour.

A relatively small change in pH or Eh can shift the balance between dissolution or precipitation for many of the identified secondary iron precipitate species, e.g.

heamatite (Fe_2O_3), goethite (FeOOH) schwertmannite ($Fe_8O_8(OH)_{8-2x}(SO_4)_x$), K-jarosite ($KFe_3(OH)_6(SO_4)_2$), lepidocrocite (FeOOH) and ferrihydrite ($FeO_3.1.8H_2O$) (O'Neill, 1998; Lee *et al.*, 2002; Romero *et al.*, 2007). It is common to see clear discharges from mine adits, which subsequently become ocherous downstream as the pH rises in response to dilution or buffering processes and waters become more oxic.

When precipitated, the fresh surface of the secondary iron phases have a large surface area with many sorption sites and acts as an effective scavenger for other dissolved metals (Kairies *et al.*, 2005). However, as mine waste matures under acidic conditions, secondary Fe-oxyhydroxides become more crystalline, resulting in decreased sorptive capacity (Moncur *et al.*, 2009). The sorption properties of these phases are complex and a number of studies (e.g. Lee *et al.*, 2002; Kairies *et al.*, 2005; Romero *et al.*, 2007; Moncur *et al.*, 2009) have shown sorption of dissolved metals (Pb, Zn, Cr, Cu and Cd) to be dependent on pH as well as the relative affinity of dissolved metals for specific sorption sites.

Manganese, though less abundant than iron, shows similar geochemical behaviour, being redox sensitive and controlled by pH-Eh conditions. In contrast to Fe, Mn remains in solution under mildly oxidising conditions. In strongly oxidising conditions it precipitates on mineral surfaces as manganese oxides. Furthermore, manganese oxides are effective scavengers of trace metals, and may be enriched in Co, Fe and Ni and As, Ba, Cu, Pb and Zn (Shand *et al.*, 2007).

The formation of secondary sulphate minerals (commonly known as efflorescent salts) can occur where iron-oxyhydroxides are not precipitated and dissolved metal concentrations remain high. Such a scenario may occur under conditions of low pH and high dissolved sulphate. Soluble salts, such as chalcanthite ($CuSO_4.5H_2O$) and goslarite ($ZnSO_4.7H_2O$) can act as a short-term sink for metals, forming in the pore waters of

hydraulically-unsaturated mine wastes which may be re-mobilised by hydraulic flushing (Younger *et al.*, 2002; Lollar, 2005).

If present, the dissolution of carbonate minerals such as dolomite ($CaMg(CO_3)_2$) will help buffer acidity in mine wastes and can lead to the precipitation of secondary siderite ($FeCO_3$), and simple salts such as gypsum ($CaSO_4.2H_2O$). Several secondary carbonate and hydroxide minerals of copper and zinc have been reported in mine wastes and stream sediments in receipt of mine drainage, including smithsonite ($ZnCO_3$) and azurite ($Cu_3(CO_3)_2(OH)_2$ (Hudson-Edwards, 2003, and references therin). Also, in lead-rich mine wastes, secondary Pb-carbonate and Pb-sulphate phases have been reported including cerussite ($PbCO_3$), hydrocerussite ($Pb_3(CO_3)_2(OH)_2$) and beudantite $PbFe_3(AsO_4)(SO_4)(OH)_6$ (Roussel *et al.*, 2000; Lollar, 2005).

3.4.3 Mineral Weathering Reactions and Acid Buffering

The acid buffering capacity of soils is largely determined by their content of carbonate and weatherable silicate minerals, cation exchange capacity and base saturation (Edwards *et al.*, 1990). Carbonate buffering is often used as a remedial treatment for acid mine water and is based on the dissolution of limestone, containing a solid carbonate phase such as calcite ($CaCO_3$). The carbonate system is able to buffer acidity via the reaction sequence shown in Equations 12-14 (Stumm and Morgan, 1996):

$$CaCO_3(s) \leftrightarrow Ca^{2+} + CO_3{}^{2-}$$ *Equation 12*

$$CO_3{}^{2-} + H^+ \leftrightarrow HCO_3{}^-$$ *Equation 13*

$$HCO_3{}^- + H^+ \leftrightarrow H_2CO_3$$ *Equation 14*

The reaction sequence consumes protons and can cause a rapid rise in pH depending on the amount of dissolved carbonate already in solution. A further increase in pH can also be achieved via further dissolution from the solid phase (Stumm and

Morgan, 1996b), but it has been observed in many systems that this is inhibited by the armouring of the carbonate surface by ferric hydroxide precipitates (Evangelou, 1995). The aluminium silicate minerals provide considerably more resistance toward pH changes than carbonates (Stumm and Morgan, 1996b). Silicate minerals include feldspars, micas, chlorites, amphiboles, olivines, pyroxenes and clay minerals (aluminosilicates); these are abundant in most geological settings including many parts of the south-west of England where kaolinite (China Clay) is mined for the paper and ceramics industries (Kraukopf and Bird, 1995). Weathering of aluminium silicate minerals may proceed via congruent dissolution into simple dissolved ions (e.g. Equations 15 and 16) and such reactions consume protons and release Al ions into solution (Krauskopf and Bird, 1995):

$$KAlSi_3O_8(s) + 4H^+ \leftrightarrow K^+ + Al^{3+} + 3\ SiO_2 + 2H_2O \qquad \textbf{\textit{Equation 15}}$$
K-feldspar   *Silica*

$$KAl_3Si_3O_{10}(OH)_2(s) + 10\ H^+ \leftrightarrow 3Al^{3+} + 3H_4SiO_4 + 6\ H_2O + K^+$$
Muscovite   *Silica*   **_Equation 16_**

In addition, an array of incongruent dissolution reactions are possible depending on prevailing geochemical conditions (pH, temperature, solution chemistry). Incongruent dissolution reactions release base cations and salicic acid into solution producing a secondary weathering mineral with a higher Al:Si ratio, Three examples of possible equilibrium reactions are given in Equations 17, 18 and 19:

$$3\ KAlSi_3O_8 + 12H_2O + 2\ H^+ \leftrightarrow KAl_3Si_3O_{10}(OH)_2 + H_4SiO_4 + 2\ K^+$$

Microcline (K-feldspar)   *Muscovite*   *Silica*   **_Equation 17_**

$$2\ KAl_3Si_3O_{10}(OH)_2 + 3H_2O + 2\ H^+ \leftrightarrow 3Al_2Si_2O_5(OH)_4(s) + 2\ K^+ \quad \textbf{\textit{Equation 18}}$$

Muscovite   *Kaolinite*

$$CaAl_2Si_2O_8 + H_2O + 2\,H^+ \leftrightarrow Al_2Si_2O_5(OH)_4(s) + \ Ca^{2+}$$

Anorthite (Ca-feldspar)   *Kaolinite*   ***Equation 19***

The equilibrium system represented by equation 19, at pH 8 has a buffer intensity 10^3 times higher than that of a 10^{-3} mol L $^{-1}$ carbonate solution and equilibrium systems containing a number of co-existing phases are in principal able to offer infinite buffering capacity (Stumm and Morgan, 1996b).

Overall the buffering reactions of various minerals operate in different pH regions and there are discrepancies in the literature about the exact pH ranges of these zones (Lottermoser, 2007). Broadly, the pH of mine waters emanating from mine waste indicates whether carbonates (pH 6.5 -7.5), aluminium silicates and iron carbonates (pH 5-6), exchange reactions with clay minerals (pH 4-5), aluminium hydroxides (pH 4.5-5.0) or iron hydroxides (pH 3) are the dominant buffering system. However, in practice the actual buffering capacity of a system is dependent on the reaction kinetics of the acid producing reactions versus those consuming protons and reaction rates of ion exchange and mineral dissolution. It is rare that step changes from one buffering system to the next are observed because different minerals undergo weathering simultaneously (Lottermoser, 2007).

3.4.4 Complexation, Speciation and Toxicity

Once released, metal ions in solution do not necessarily exist as free hydrated ions but can be present as complexed inorganic and organic species and colloidal material, commonly 20-200 nm (Slowey *et al.*, 2007). In practice, the distinction between dissolved and particulate material is operationally defined by the filtration technique employed (typically with a pore size of 0.45 or 0.20 μm). The speciation of

trace metals in natural freshwaters is important as it affects the mobility, bioavaliability and toxicity of many elements (Sigg *et al.*, 2006).

Iron and Aluminium

The availability of dissolved Fe in natural waters is dependent on the redox condition. The highly soluble ferrous (Fe^{2+}) cation is prevalent under anoxic conditions. Ferric (Fe^{3+}) iron dominates in aerobic waters and is sparingly soluble in the pH range 5-8, being found as $Fe(OH)_3(s)$, Fe_2O_3 and suspended colloidal iron oxyhydroxide particles (Harley, 2010). Iron precipitates negatively impact upon aquatic life by reducing oxygen availability and coating benthic habitats and the body surfaces and respiratory systems of marine organisms (Earle and Callaghan, 1988; Harley, 2010). Dissolved iron is frequently associated with dissolved organic matter (e.g. humic or fulvic acids), and brown colouration of waters often indicates a high organic and Fe content (Perdue *et al.*, 1976). Because Fe precipitates rapidly in oxic waters at relatively low pH (≥ 3.5), it is difficult to separate the effect of dissolved iron on aquatic life from that caused by low pH associated with mine waters (Earle and Callaghan, 1988).

However, a number of toxicity studies have been conducted on aquatic organisms, for example Milam and Farris (1998) recommended a no-effect level of 0.4 mg L^{-1} (as Fe^{2+}) based on studies of species of freshwater clam. Also a recent review of available data concluded that a dissolved iron concentration of 1 mg L^{-1} was an appropriate level to protect aquatic life in Colorado. The same level has been adopted in the UK and a number of states in the USA (Harley, 2010).

Dissolved Al can exist as the free trivalent cation (Al^{3+}), or as a range of soluble organic (humic and fulvic acids) and inorganic complexes (e.g. fluoride, chloride and sulphate). It can also form monomeric and polymeric hydroxyl species, colloidal polymeric solutions and gels and precipitates (Fawell, 2010). Depending on size

distribution, a portion of the latter forms may be included in the "dissolved" fraction passing through 0.45 and 0.2 μm pore size filters. Dissolved aluminium displays conservative and non-conservative behaviour in acidic stream waters with a transition from one to the other in the pH range 4.6 to 5.0, consistent with precipitation of the first hydroxyl product (Nordstrom and Ball, 1986). Lee *et al* (2002) also reported decreased dissolved Al activity at pH >5 consistent with the formation of $Al(OH)_3$ solid, and that the formation of $Al-SO_4$ compounds may influence Al activities at pH < 5.

Dissolved Al has been shown to be toxic to a range of aquatic organisms via osmoregulatory failure, including daphnids, mayflies, crayfish, and in a range of fish species, where sensitivity is species-dependent (Herrmann, 1987; Klöppel *et al.*, 1997, and references therein ; Poléo *et al.*, 1997). Monomeric Al hydroxyl species have been found to be primarily responsible for Al toxicity in the aquatic environment (Wauer *et al.*, 2004). Recent research has also highlighted the toxicity of Al nanoparticles to aquatic organisms (e.g. Strigul *et al.*, 2009) and plants (e.g. Ma *et al.*, 2010), but as a man-made species are not universally encountered.

Ionic Al toxicity is well documented for acidic waters, but in mixing zones with high pH waters conversion of dissolved Al to high molecular weight polymeric species can also bring about fish mortality, via clogging of the gills (Rosseland *et al.*, 1992; Klöppel *et al.*, 1997). The free ion Al^{3+} is also phytotoxic, interfering with root growth and respiration and the uptake and use of water and nutrients (Rout *et al.*, 2001). Aluminium phytotoxicity is dependent upon soil conditions, but can occur at nanomolar concentrations (Costantini *et al.*, 1992; Poschenrieder *et al.*, 2008). Kinraide (1997) found the toxicity of Al species to wheat followed the order Al_{13} (a hydroxyl precipitate) $> Al^{3+} > AlF^{2+} > AlF_2^+$ with no proven phytotoxicity for sulphate species or mono-hydroxyls. Phytotoxicity is an important consideration in remediation of abandoned mine sites where re-vegetation of tips is desirable.

122

Copper, Zinc, Cadmium, Nickel Lead and Manganese,

Dissolved Cu, Zn, Cd, Ni, Pb and Mn may exist in one of three forms: as the divalent free cation, as a range of inorganic complexes or associated with organic matter (Kozelka and Bruland, 1998). Mobility of all of these metals is dependent on pH, with sorption reactions to Fe and Mn oxyhydroxides, clays and solid organic material being an important mediator of contaminant transport. Complexation with dissolved organic matter has also been shown using a variety of laboratory techniques, to be the dominant form of these metals in natural waters (Buffle *et al.*, 1988; BGS, 2003). The highest affinity for organic matter (dissolved or solid) is reported for Cu and Pb (Weng *et al.*, 2002; Shand *et al.*, 2007), but is also important for Zn, Ni and Cd speciation and mobility (Chakraborty and Chakrabarti, 2006). Lead usually exhibits the lowest mobility in mine waters, due to the low solubility of secondary precipitates such as anglesite ($PbSO_4$) and plumbojarosite ($PbFe_6(SO4)_4(OH)_{12}$, Harris *et al.* (2003)).

The availability and toxicity of trace metals to aquatic life (e.g. phytoplankton, zooplankton, ciliates, copepods, and crab-larvae) is generally correlated to the free metal ion concentration, rather than the total concentration (Kozelka and Bruland, 1998, and references therein). Typical lethal concentrations of Cu^{2+} (LC_{50}) for freshwater fish range from $0.16 – 47.2$ µmol L^{-1}. Effect concentrations (EC_{50}), are also sometimes used to determine levels where a detrimental effect is observed on freshwater invertebrates or microorganisms: typical EC_{50} concentrations of Cu^{2+} being $0.16 – 47$ and $0.01 – 5.4$ µmol L^{-1}, respectively (Rodgers *et al.*, 2005). Toxicity (LC_{50}) for "dissolved" Zn and Cd have been found to be of the order of 1000 and 10-100 µmol L^{-1}, respectively for fathead minnows and 100 and 1-10 µmol L^{-1}, respectively for daphnia in freshwaters impacted by acid mine drainage, depending on conditions and distance downstream from the mine (Balistrieri *et al.*, 2007). In general, Cd displays similar geochemical behaviour to Zn and the two are often found together in mine affected waters. Cadmium

differs slightly in that it forms anionic complexes with organic matter more readily than

Zn (Pettersson *et al.*, 1993). Cadmium, though much less abundant than Zn, is more

toxic to aquatic life and this is reflected in the low Environmental Quality Standard

(EQS) values applied to UK freshwaters in Table 3.15 (Appendix 3F).

Nickel toxicity varies considerably between waters with different physico-

chemical parameters such as pH, alkalinity and dissolved organic carbon (DOC)

(Schlekat *et al.*, 2010). Nickel is bioavailable and most toxic as the hydrated divalent

ion. Griffitt *et al.* (2008) examined the effect on zebrafish, daphnia and algal species

from exposure to nanoparticles including silver, copper, aluminium, and nickel. Their

results indicated that nanocopper and nanosilver caused toxicity directly to all tested

species, but that dissolution to soluble species accounted for the toxicity of nickel.

Reported Ni LC_{50} values for freshwater fish are 0.29-1.6 µmol L^{-1}(Kumar and Nath,

1987). Manganese is a toxic element frequently overlooked when assessing toxicity of

effluents, sediments, and pore waters (Lasier *et al.*, 2000). Manganese is redox sensitive

and mobilised under reducing conditions when insoluble Mn^{4+} species are reduced to

Mn^{2+} (Crane *et al.*, 2007), the latter can remain at toxic levels in oxic waters due to slow

precipitation kinetics. Reported LC_{50} concentrations for acute toxicity to daphnia and

crustaceans (*Hyalella azteca*), which are reported to be the most sensitive species to

dissolved Mn, were 0.11-0.27 µmol L^{-1} and 0.055-0.25 µmol L^{-1}, respectively (Lasier *et

al.*, 2000). As for other elements, toxicity varies with pH, temperature and alkalinity.

Arsenic and Antimony

Arsenic exists in sulphide mineral tailings most commonly as arsenopyrite

(FeAsS) and arsenian pyrite (Fe(S,As)$_2$), and is released during oxidative dissolution of

these phases. As a metalloid and redox sensitive element, As does not form single

cations but reacts readily to from oxyanions and corresponding salts. Arsenite (As(III)),

dominates in reducing conditions and arsenate (As(V)) dominates in oxidising conditions but the exact species is also dependent on pH. Arsenate ($H_2As(V)O_4^-$) and arsenite ($H_3As(III)O_3$) are the most commonly found arsenic species in AMD and groundwater and inter conversion between the two in changing Eh and pH conditions can affect mobility; however disequilibrium is often observed due to the slow kinetics of As redox reactions (Shand *et al.*, 2007). Arsenates are mobile (as dissolved H_3AsO_4 and $H_2AsO_4^-$) only at pH < 3.5 in a narrow range of Eh (Cheng *et al.*, 2009). The capacity for iron oxides to adsorb As(V) is well documented in circum-neutral and acidic waters (Shand *et al.*, 2007) and adsorption reactions are generally considered the most important control on the concentration of dissolved arsenic in groundwater environments. Arsenic species can adsorb on many soil colloids and particles, particularly oxyhydroxide surfaces in the natural environment (Carrillo and Drever, 1998). Arsenic is toxic to plants and animals, including humans where it is a proven carcinogen (EA, 2009). To date few studies have been conducted on the toxicity and biotransformation of As in aquatic organisms (Ventura-Lima *et al.*, 2011). Toxicity is highly dependent on its chemical form and generally inorganic arsenic species are more toxic to living organisms than organic forms (Sharma and Sohn, 2009). Arsenite (AsIII) is about 60 times more toxic than arsenate (AsV) which is about 70 times more toxic than methylated species, although biotransformation of arsenic within organisms can also produce toxic metabolites (Ventura-Lima *et al.*, 2011).

Antimony exhibits similar geochemical behaviour to arsenic, existing in a range of oxidation states (-3, 0, +3, +5) but is mainly found in the Sb(III) and Sb(V) states in environmental samples (Shand *et al.*, 2007). Antimony is typically present at low concentrations (< 1 ugL^{-1}) in unpolluted waters (Filella *et al.*, 2002), but high concentrations may be associated with sulphide mineral deposits where antimony is found as stibnite (Sb_2S_3), or incorporated into other sulphide minerals (Shand *et al.*,

2007). Zhu *et al.*(2009, in Fu *et al.* (2010)) reported Sb concentrations in mine waters as high as 7502 μg L^{-1}. Antimony is a toxic trace element and suspected carcinogen but the bioavailability and behaviour of Sb in aquatic ecosystems and the environment as a whole remains unclear and worthy of further study (Fu *et al.*, 2010; Wilson *et al.*, 2010). Increased Sb concentrations in the growth media led to significant suppression of leaf and root growth in wheat seedlings (Shtangeeva *et al.*, 2011). However, a recent comparative study by Duester *et al* (2011) reported inorganic and organic As (III) and As(V) species to be more toxic to aquatic plants than the corresponding Sb species.

Analytical Challenge

The mineral assemblage, electrochemical and oxidation reaction kinetics, bacterial mediation, and hydrology affect which reactions proceed, and how quickly. Combination of these factors determines the geochemistry of the mine waters emerging from waste material. Given the complexities of reactions likely to arise in sulphide wastes, empirical studies of dissolved metals are the most reliable method of determining mine water chemistry. In the UK, current EQS values are based on laboratory toxicity data and expressed as total dissolved concentrations, and accordingly this work reports total dissolved metal and metalloid concentrations.

However in a recent report, the Environment Agency acknowledged that this may lead to underprotection or overprotection of aquatic environments and recommended a move toward bioavailability and chemical speciation in the future (Bass *et al.*, 2008). Sigg *et al.*(2006) also highlighted the need for robust methods to routinely measure parameters that give information on the potential ecotoxicological risk of metals based on their speciation, rather than total or "dissolved" concentrations which are usually reported. The same authors did however acknowledge that this was a "considerable challenge", requiring a range of analytical methods.

3.5 Background Information: Devon Great Consols

3.5.1 Location and Ownership

Devon Great Consols is situated on the Devon side of the River Tamar close to the Cornish mining town of Gunnislake (Figure 3.1). The site was designated within the Tamar Valley Area of Outstanding Natural Beauty (AONB) in 1995, and was inscribed as part of the Cornish Mining UNESCO World Heritage Site in July 2006 (CMWH, 2010). It is currently managed by the Tamar Valley Mining Heritage Project, initially led by West Devon Borough Council in conjunction with a number of other stakeholders (WDBC, 2006). One of the stakeholders is the Tamar Valley AONB partnership, through which permission for site access was granted. The site is bounded to the SE by Blanchdown Farm which is privately owned.

Figure 3.1: Devon Great Consols site located in and around Blanchdown Wood on north bank of River Tamar. Mineral veins superimposed as red lines. Created in ArcMap using BGS 1 : 50 000 geology data and current OS 1 : 25000 scale map. © Crown Copyright and Landmark Information Group Limited (2010). All rights reserved.

3.5.2 History

Devon Great Consols began working following the discovery of a copper mineral lode in 1844 and for twenty years was the richest copper mine in Europe (Booker, 1967). The existence of mineral deposits in the area had been suspected since Elizabethan times but the site remained undeveloped until the reluctant land owner, the 6th Duke of Bedford, finally granted permission to Josiah Hitchins to develop a mine (Hamilton Jenkin, 1974). By 1845, the workings comprised a number of individual mines which exploited four main E-W tending mineral lodes (Figure 3.1). The original discovery was at Wheal Maria on the western part of the site with the workings of Wheal Fanny, Wheal Anna Maria (WAM), Wheal Josiah and Wheal Emma tracking the lodes from W-E. Other subsidiary workings to the south, including South Wheal Fanny (800m SSW of WAM), Wheal Frementor (a tungsten and tin mine,1 km SSW of WAM) and Watson's Mine (1 km SE of WAM) were also included in the site which together became known as Devonshire Great Consolidated Copper Mining Company (Devon Great Consols). By 1865, the surface area of the mine covered more than 140 acres and at Wheal Josiah, 15 shafts granted access to 40 miles of levels, the deepest shaft extending to a depth of 420 m (Hamilton Jenkin, 1974).

By the late 1860s, the copper lode had become deeper and harder to work and global copper prices had fallen considerably such that mining copper at DGC became unprofitable. From this point on until its eventual closure in 1903, the mine principally worked the rich arsenic deposits. Commonly referred to as *mispickle*, this ore comprised arsenopyrite deposits which remained in situ on the walls of the worked copper lode when the chalcopyrite was mined out. By 1870, half the world's supply of arsenic came from the site (Booker, 1967), and by 1889 the mine was producing three times more arsenic than copper (Buck, 2002). The layout of the mine during this period can be seen in the maps dated 1882-1884 and 1889-1891 (Figure 3.25 and Figure 3.24, Appendix

3A). Rising costs and reduced revenue from the sale of arsenic in the following years led to the abandonment of the mine in 1903 (Buck, 2002). After closure, much of the infrastructure and the materials of the mine were sold off (Hamilton Jenkin, 1974), the remaining features can be seen in the maps dated 1906 and 1907 (Figure 3.27 and Figure 3.26, Appendix 3A).

The mine lay dormant until about 1915, when underground mining was recommenced at Wheal Fanny for arsenic and at Wheal Frementor for tin and tungsten (Richardson, 1995). Arsenic ore (arsenopyrite) was crushed and roasted on site in Brunton and Oxland calciners and the resulting fumes were drawn through a series of brick chambers, known as a labyrinth, toward a tall chimney stack. Condensing fumes resulted in a crude grey precipitate that was subsequently recovered and roasted for a second time in a refining furnace, the fumes being drawn through another tiled labyrinth to produce pure white arsenic oxide (As_2O_3) (Richardson, 1995). This activity continued into the 1920s with the construction of new furnaces, a new chimney stack and new labyrinths, the remains of which can still be seen on site along with the extensive waste tips. The arsenic works are believed to have been abandoned around 1925, with limited re-working of the waste tips for arsenic continuing until about 1930, (Richardson, 1995), with work focussing mainly around Wheal Frementor (Buck, 2002).

At the same time, toward the south of the site and the River Tamar, metallic copper was recovered from the copper-rich streams draining the large waste tips at Wheal Anna Maria. The waters were directed through narrow wooden launders and precipitated onto scrap iron. This activity probably started before the 1903 closure and continued on a small scale after closure of the mine (Booker, 1967; Richardson, 1995; Buck, 2002), with the latest reported activity in 1979 (Sherrell, 2000). Around the time of the Second World War, an unknown quantity of material was removed from the site

and processed in mills at other local mines including Harrowbarrow and Luckett (Buck, 2002). In 1965 a small modern plant was constructed, including a ball mill, concentrating tables and a magnetic separator – used in the recovery of tungsten and tin (Richardson, 1995). This operation to recover valuable metals from the "White Sands" waste tips (likely to be those from Wheal Frementor) continued into the early 1970s and is the last recorded mining activity at the site (Buck, 2002).

In the 1990s the site was used for car rallying and testing of off-road vehicles; however this ceased in 1994 due to concerns over the production of dust clouds from the waste (Sharples *et al.*, 2008). The site has recently been redeveloped and re-opened to the public through the Tamar Valley Mining Heritage Project. A number of designated heritage trails and a purpose-built downhill mountain bike track have been installed, designed to stop the unlawful use of the waste tips by stewarding usage away from the archaeologically and ecologically important areas of the site ("Tamar Valley Area of Outstanding Natural Beauty," 2010). The site remains a popular recreational centre for walkers, cyclists, geologists and mining enthusiasts.

3.5.3 Site Topography, Hydrology, and Geology

The largest waste tips at the Devon Great Consols site are located near to the abandoned arsenic works at Wheal Anna Maria (WAM) (Figure 3.2, and photograph 1, all photographs in Appendix 3C) and comprise wastes from the arsenic processing, including furnace cinders (referred to as cinders tip) and coarse grained crushed waste, and from the post-WW2 re-working of the tips (referred to as the Wheal Anna Maria upper tip, photographs 2-4). These tips are the subject of this chapter together with the waste found down gradient at South Wheal Fanny precipitation launders (Figure 3.2 and photographs 11 and 12). There are other waste deposits within the Devon Great Consols

notably the lower tailings tip at wheal Anna Maria and other deposits at Wheal Josiah, Wheal Emma, Wheal Fanny. These are outlined shown in Figure 14, Chapter 2.

The site mineralisation is hosted by Devonian Hornfelsed Slates of the Tavy Formation which exhibit low permeability (BGS 2009,2010). The overall site topography slopes steeply (average slope of 7-8°) and fairly evenly to the SE, before levelling over alluvial deposits close to the River Tamar (Figure 3.3). The gradient transects marked in Figure 3.2 and Figure 3.3, are shown in Figure 3.4. Surface drainage from the central area flows similarly SE, passing over the remains of the precipitation launders before discharging via a drainage ditch at the bottom of the slope. Shallow groundwater is expected to move in a similar direction, whilst deeper groundwater is likely to preferentially drain through the extensive underground workings. The main discharge from the workings is via Blanchdown Adit (SX 435733), approximately 1 km east of the WAM tips shown in Figure 3.2.

The sloping area between the main DGC tips and the precipitation launders is largely covered by mixed woodland. The low lying area at the bottom of the site, between the final drain and the River Tamar, belongs to Blanchdown Farm and is mainly pasture with some woodland.

Figure 3.2: Schematic diagram of main waste tips at Devon Great Consols including: Upper Wheal Anna Maria waste tip (dark orange), finer tailings (light brown), western tips including cinders waste from arsenic furnaces (grey) and remains of precipitation works at South Wheal Fanny (red).

Devon Great Consols (DGC) is a complex array of underground workings, adits, leats, mine wastes, tracks, dense woodland and abandoned ore processing buildings, including the remains of two arsenic calciners. Buck (2002) conducted a detailed investigation of the archaeology of the site, including the tracks and gulleys, the location of which may be viewed in Figure 3.28 (Appendix 3A). In addition, the recent work carried out for the UNESCO Mining Heritage project has included installation of drainage pipes and ditches around the site, one of which is shown in photograph 7. All of these features re-direct and store migrating waters and suspended solids during transport to the River and complicate the hydrology of the site.

Figure 3.3: Map showing superficial deposits underlying Devon Great Consols. Approximate outlines of cinders, precipitation launders and WAM upper and lower waste tips outlined in red Gradient transects shown as purple lines. Created in ArcMap using BGS 1 : 50 000 geology data and current OS 1 : 25000 scale map. © Crown Copyright and Landmark Information Group Limited (2010). All rights reserved.

Figure 3.4: Cross sections through Devon Great Consols site as marked on Figure 3.2 and Figure 3.3. Note plateau at top of C-D transect, this is due to the lack of contour data for the areas underlying the main mine waste heaps. The gradient transects do not show the man-made leats, tracks, and historic rail embankments that are orientated across the slope between the tips and the River Tamar.

133

3.5.4 Mine Waste Mineralogy

The mineralogy of the waste produced at each of the individual mines within DGC depended on the composition of the particular branch of the mineral lode worked. The original mineralogy of the worked lode at WAM may be found in the coarser waste tips, which lie to the north of the WAM upper tip, and these are recognised as a regionally important geological site, representing the original and varied mineralogy of the Main Lode (Page, 2004). Re-working of the tips for arsenic, and latterly tin and tungsten, has served to homogenise and re-distribute much of the waste material, such that tips can contain a wide array of mineral phases. Minerals identified at the site include the principal sulphide ore-bearing minerals of chalcopyrite ($CuFeS_2$), and arsenopyrite (FeAsS), also pyrite (FeS_2), sphalerite (ZnFeS), galena (PbS), wolframite ($FeMnWO_4$) and cassiterite (SnO_2) and gangue minerals including quartz (SiO_2), chlorites (e.g. chamosite $(Fe_3Al)(AlSi_3)O_{10}(OH)_8$), fluorite ($CaF_2$), siderite ($FeCO_3$), dolomite ($CaMg(CO)_3$), childrenite ($FeMnAlPO_4(OH)_2.H_2O$) and secondary phases including scorodite ($FeAsO_4.2H_2O$) and efflorescent salts (Photograph 3, Appendix 3C) (Page, 2004 and *pers.comm*).

3.6 Methods

3.6.1 Reagents

All aqueous solutions were prepared with Milli-Q water (Millipore, R $\geq$ 18.2 MΩ cm^{-1}, reverse osmosis followed by ion exchange). Standard solutions and reagents were prepared in a Class 5 (BS EN 150 14644) laminar flow hood (model BassAir 06VB), according to trace metal clean techniques to minimize contamination. Multi-element calibration standards were prepared as serial dilutions from standard solutions (1000 or 10000 ug L^{-1}, Romil Pure Chemistry, Fisher and BDH) and acidified to < pH 2

with Q-HNO$_3$ (Q denotes purified by sub-boiling distillation, Romil SPA). Analytical reagent grade acids were used for washing of equipment unless stated otherwise.

3.6.2 Cleaning Protocol

High density polyethylene bottles (250 mL, Nalgene®) were used for sample collection and polyethylene centrifuge tubes (15mL and 50 mL, Sterilin®) for standard and sample preparation. These were cleaned by immersion in a series of cleaning solutions (Decon 90, 2% v/v, > 24 h; HCl, 6 mol L^{-1}, ≥7 days, HNO$_3$, 2 mol L^{-1}, ≥3days). Filtration units (polycarbonate, Nalgene), and all coloured components (centrifuge tube lids, silicone rubber 'O' rings) were rinsed with detergent (Decon 90, 2%) and immersed in HCl, 2 mol L^{-1}, ≥3 days. All items were rinsed with deionised water prior to the Decon 90 step and rinsed with MQ water after each acid-washing step. Polycarbonate filters (Whatmann Nuclepore) were acid washed with 2 % HNO$_3$ (Romil SpA), rinsed with MQ, dried in vented petri dishes. Items were dried in a Class 5 laminar flow hood and stored in two plastic zip-lock bags prior to use. Filters were pre-weighed on a 5-place analytical balance.

3.6.3 Sampling Strategy and Sample Treatment

Sampling Strategy

The sampling strategy was designed to capture seepages, surface drainage and shallow groundwater migrating from the largest areas of mine waste (shown in Figure 3.2) to the River Tamar, assuming that shallow groundwater movement followed the site gradient, sloping from north-west to south-east. Surface water and shallow ground water was sampled at the locations displayed in Figure 3.5, for the whole study site, and in Figure 3.6 with more detail for the area surrounding South Wheal Fanny near the

River Tamar. Detailed information on sample locations is provided in Appendix 3B and all photographs are shown in Appendix 3C.

Surface water was collected from a number of preferential drainage channels. Ephemeral streams collecting seepages from the cinders tips (sample 1, photograph 4) only flow in wet conditions initially eastwards (samples 2-3, photograph 5), then south-eastwards, along the E extent of the tailings tip (sample 9, photograph 6). This stream then passes underneath a pathway via a plastic pipe (sample 10, photograph 7) and continues towards the western extent of the precipitation launders. Seepages emerge from the base of the WAM tip (samples 3-4, 6-7, photograph 8) and also flow from an inspection hole (sample 5, photograph 9). These are collected by an ephemeral stream, which directs some drainage toward the centre of the lower tailings tip (Photograph 10) and some into a drain to the east (sample 8). This ephemeral stream rarely flows but crosses the track via another engineered channel then continues through thick vegetation before reaching the precipitation launders (Figure 3.5).

Figure 3.5: Schematic overview of Devon Great Consols next to the River Tamar, showing location of major waste tips, surface water (red) and borehole (blue) samples, ephemeral streams and drainage channels.

Down gradient from the tips are two large areas of embankment, which appear to be constructed largely from mine waste and wooden slats and comprise the remains of the South Wheal Fanny precipitation launders (photographs 11 and 12). The eastern section is the larger and less vegetated than the western section. Two drainage ditches connect the eastern launders and a collection pond (locations 12 and 13). However water levels in the ditches are often low with little or no flow and it is unclear whether drainage collected in these ditches regularly reaches the pond. Above these ditches is a terraced bank/mine leat which was water-logged on all visits. A presumed drainage adit from South Wheal Fanny is framed by a brick portal (location 16, Photograph 13) and was sampled where it drains into the leat.

Figure 3.6: Schematic map of South Wheal Fanny and precipitation launders at DGC. Showing surface sample and borehole locations.

There are two drainage ditches in front of the eastern launders (Figure 3.6), within which water flows are variable in magnitude and direction. These were captured at locations 17 and 18. A final collection drain (locations 19-23, photograph 14) flows east and discharges to the River Tamar. Two surface drains, which flow in a south easterly-direction, enter the final drain at locations 14 and 15. A deep ditch runs alongside the final drain, but appeared dry during all visits.

Boreholes were installed in the low-lying area close to the River Tamar, at the locations shown in Figure 3.6. BH1 and BH3 were intended to capture shallow groundwater moving toward the final collection drain. BH2 and BH4 were intended to capture drainage moving beyond the final drain. BH5 targeted waters within the precipitation launders and BH6 was intended to sample ground waters below surface clay found in the south west part of the site (Table 3.4).

Table 3.4: Borehole depth data and observations. FCD = Final collection Drain. Core logs are presented in Appendix 3D.

Borehole	Depth (at installation)/Location	Additional Comments
1	0.53 m below N water's edge of FCD	Waters cloudy orange/brown. Fast recharge.
2	1.22 m below S water's edge of FCD	Waters clear. Fast recharge.
3	1.54 m below ground surface next to surface drain (sample 14).	Light brown suspended fine particles. Fast recharge.
4	1.21 m below bottom of dry ditch (~0.5m deep)	Waters clear to start, becoming orange/brown and opaque after purging. Fast recharge.
5	0.58 cm below terrace of precipitation launders	Waters clear. Area prone to water-logging. Fast recharge.
6	1.67m below clay-rich ground surface.	Waters clear. Area prone to water-logging. Slow recharge.

Rainfall and Temperature

The sampling campaign set out to encompass a range of flow conditions and seasons in order to capture seasonal variation. Rainfall data was obtained for the nearest MIDAS land surface data station, located at Millhill (SX 455745), approximately 2.5 km NE of the site (Met Office, 2009). Rainfall data and sample temperatures for each survey are summarised in Table 3.5.

The ten year average rainfall (1999-2009) recorded at Millhill was 3.8 mm d^{-1}, slightly less than the catchment average of 4.0 mm d^{-1}. Heavy rainfall (> 20 mm d^{-1}) falls on average every 24 days which is more frequent than the estimated catchment average return time of 30 days, placing it in the "high risk" category for rain intensity in the Tamar catchment area (Chapter 2).

Table 3.5: Surface water sample temperatures and rainfall data for Devon Great Consols preceding each site visit. Rainfall data obtained from nearest MIDAS land surface station at Millhill (SX 455745), located 2.5 km NE of site. Ten year (1999-2009) average for station = 3.8 mm d^{-1} and Tamar catchment = 4.0 mm d^{-1}. *Indicates visits where seepages from WAM and cinders waste tips were observed. [1]Borehole samples in parentheses.

Sampling Date	Sample Temp (°C)[1]	Rainfall in 7 days before sampling (mm)							Rainfall on day (mm)	7 Day Total (mm)	14 Day Total (mm)
		Day: 7	6	5	4	3	2	1	0		
28/06/2007*	11.5-12.5	9.3	8.7	21.2	14.2	13.7	0.9	3.0	8.0	71	127
07/02/2008*	8.1-11.2	10.1	2.6	5.0	15.1	17.6	1.7	0.8	1.2	53	57
13/09/2008*	12.3-16.9	3.3	0.0	24.6	2.2	12.2	2.2	1.7	0.0	46	136
14/01/2009	4.4-10.3 (6.4- 9.4)	0.0	0.0	0.0	0.0	21.4	11	3.6	3.8	36	37
28/02/2009	8.9-10.5 (7.9 -10.6)	0.0	0.8	0.1	0.0	0.0	0.0	0.0	0.0	0.9	6.6
16/05/2009	10.7- 23.0 (11.0-13.0)	0.0	0.0	0.0	0.9	0.0	8.2	6.9	20.4	16	20
20/07/2009*	10.8-20.2 (14. 5-15.5)	0.2	1.9	7.8	0.2	32.9	12.8	3.0	3.5	59	124

Sampling on 28/02/09 took place in dry conditions following low rainfall in the 14 days prior to sampling. The surveys conducted on 14/01/09 and 16/05/09 were conducted in wet conditions after a few days rainfall in an otherwise dry period. On 28/06/07, 07/02/08, 13/09/08 and 20/07/09 surveys followed prolonged periods of rainfall. In addition, four samples of seepages from the WAM tip were captured on the 13/09/08. Surface water temperatures varied with location and season between 4.4-20.3 °C, shallow ground waters showed less variability (6.4-15.5 °C).

Sampling and in-situ determination

In the Tamar River valley in the southern part of Devon Great Consols, boreholes were drilled using a hand-augering rig. Double-layer tubes were installed into boreholes (50 mm diameter) in order to intercept shallow ground waters in the mine waste and soil zone (Figure 3.7). Borehole and water depths were recorded at installation and prior to sampling. Measured depths were converted to height above an ordnance datum (mAOD), set at 2m. Boreholes were sampled using a Wattera™ bailer and purged to at least three borehole volumes prior to sample collection. Bailed water samples were transferred to HDPE bottles after three rinses with sample water, sealed in labelled zip-lock polythene bags and stored cool. Stream and tip drainage waters were similarly treated but captured directly into HDPE bottles. Conductivity, pH, dissolved oxygen and redox potential (Eh) were determined where possible in situ, using portable instruments (Hanna HI9635, MeterLab PHM201, YSI 85 and Hanna H9025 respectively).

Figure 3.7: Cross-section schematic of borehole installation. On the right, the double-layer construction of the installed tubes is shown.

When boreholes were too deep for in situ determination, ~ 200 mL of sample were decanted with minimum disturbance from the bailer to a plastic beaker and readings were quickly taken, dissolved oxygen first, followed by Eh, temperature, pH and conductivity.

The velocity of water flow in surface streams was determined using a flow meter with a small impellor (Valeport Braystoke BFM002). The measurements were taken at the centre of the stream at a depth of approximately one third from the bottom of the streambed (all studied streams were less than 1.0 m deep), and at a point of minimal turbulence. Streams wider than 0.5 m were divided into (2-4) subsections and a discrete set of measurements was taken for each section. Measured revolutions per second were converted into velocity (m s^{-1}) using the calibration equation provided by the instrument manufacturer. Stream discharge was then calculated by multiplying the flow velocity(s) and stream cross-sectional area(s) for each section of the stream. For small drainages unsuitable for flow meter, the discharge time into a graduated vessel was recorded. This was repeated at least 3 times and an average result calculated.

Twenty-five determinations (five measurements each at five adjacent locations) of flow in a test stream were calculated by this method. The variation in the measured revolutions per second was < 6% for each location. The final result for flow from all 25 measurements of the test steam was 96.9 +/-7.2 L s^{-1}, which represents an RSD of 7.5%.

Sample Treatment

Samples were returned to the laboratory within 12 hours of collection and stored in a refrigerator. Water samples were vacuum filtered (0.4 μm followed by 0.2 μm pore size, Whatmann Nuclepore polycarbonate filters, acid washed, dried and pre-weighed) within hours of collection in a class 5 laminar flow hood (Bassaire). During the filtration the original sample bottle was thoroughly rinsed with MQ followed by a portion of the filtrate. Samples were then returned to their original sample-conditioned bottles. An aliquot was transferred to a 2 ml glass vial and returned to the refrigerator pending anion analysis by ion chromatography (< 3 days). The remaining sample was

acidified (Q-HNO_3, < pH 2), pending analysis by ICP-MS and ICP-OES. Filters were retained, dried and weighed to determine total suspended solids (TSS).

3.6.4   Instrumentation and Analysis

pH, Eh and DO Meters

The pH meter was calibrated daily before use and checked after use using standard solutions (pH 4 and 7, BDH). The maximum recorded daily drift in calibration was 0.3 pH units. The Eh meter was checked daily before use by measuring against ZoBell's solution, using the following relationship (Nordstrom and Wilde, 2005):

$$Eh = emf + E_{ref} \qquad\qquad \textit{Equation 18}$$

Where: Eh is the potential (mV) of the sample solution relative to the standard hydrogen electrode, *emf* is the potential (mV) of the water determined at the sample temperature and E_{ref} is the reference electrode (saturated KCl) potential of the ZoBell's solution corrected for the sample temperature. The dissolved oxygen meter was corrected for altitude and calibrated in air, prior to site measurements being taken.

Elemental Analysis

Metal analysis was undertaken using a Varian 725-ES Inductively Coupled Plasma Optical Emission Spectrometer (ICP-OES) and a Thermo Fisher X Series 2 ICP-MS instrument (ICP-MS) in an ISO9001:2000 accredited analytical research facility. Yttrium and indium (100 μg L^{-1}) were used as internal standards.

Dissolved anions were determined by ion chromatography (Dionex DX-500 system, Dionex Ionpac AS9-HC column). Na and K analysis were performed by flame photometery (Corning 400). Analyses were verified against a certified reference material for trace elements (TMDA-64, National Water Research Institute, Canada). Total suspended solids were determined gravimetrically from filter residues using a five decimal place balance.

3.6.5 Principal Component Analysis

Master variables (pH, Eh, dissolved O_2 and conductivity) and dissolved metal, metalloid and anion concentrations were used as input variables for a principal component analysis (PCA) (XLSTAT version 2010.4.01). Observations where one or more variable data points were missing were excluded from the dataset and pH values were converted to hydrogen ion activities, as the PCA assumes linear relationships between variables. All variables were normalised by dividing each observation by the mean of the observations for each variable. Observations were organized into groups according to sample type, based on sample location and preliminary examination of trends in the geochemical datasets (Table 3.6). Boreholes were treated individually by location.

Table 3.6: Sample Type Groupings for Devon Great Consols Dataset.

Sample Location	Sample Type Grouping (PCA label)
1	Cinders Drain (CD)
2-4	Cinders Mixing Zone (CMZ)
5-8	Wheal Anna Maria Tip Drainage (WAMD)
9-10	Path Mixing Zone (PMZ)
11	South Wheal Fanny Shaft (SWFS)
12	Pond Entrance (PI)
13	Pond Exit (PO)
14-15	Surface Drains (SD)
16	South Wheal Fanny Adit Portal (SWFA)
17-23	Final Collection Drain (FCD)

PCA constructs independent linear combinations of the original variables to create principal components. Beginning with the first component each describes a decreasing amount of variation in the data set. (Dong *et al.*, 2007). The first seven components

144

cumulatively explained 75% of the variation in the data set (Table 3.7), and were used to investigate the geochemical character and variability in the data set.

Table 3.7: Initial Eigenvalues from PCA analysis of the Devon Great Consols data set.

	F1	F2	F3	F4	F5	F6	F7
Eigenvalue	8.81	4.73	3.94	2.93	2.37	2.05	1.46
Variability (%)	25.16	13.51	11.27	8.36	6.77	5.86	4.18
Cumulative %	25.16	38.67	49.94	58.30	65.07	70.93	75.11

3.6.6 Geochemical Modelling

The geochemical modelling code PHREEQC Ver.2.17.1 was used to model the speciation of elements and saturation indices for mineral phases in mine drainage waters. The PHREEQC code is based on thermodynamic principals and the underlying assumption is that the system under investigation is in thermodynamic equilibrium. Two thermodynamic databases supplied with the program were utilised, WATEQ4F derived from Ball and Nordstrom (1991) and LLNL, prepared by Johnson at the Lawrence Livermore National Laboratory. The latter includes a wider range of trace elements and associated minerals of interest to this study, (including: Sb, Sn, V and W). The thermodynamic databases describe reactions between aqueous species, or the dissolution of minerals in terms of master species, with experimentally derived equilibrium constants (Parkhurst and Appelo, 1999). In addition to the mineral phases supplied in the database, three sulphide mineral phases and one solution species were added to the WATEQ4F database (as shown below) in order to describe the dissolution of chalcopyrite, sphalerite and arsenopyrite.

```
PHASES
Chalcopyrite
   CuFeS2 +2.0000 H+  =  + 1.0000 Cu++ + 1.0000 Fe++ + 2.0000 HS-
   log_k    -32.5638
   delta_h  127.206 kJ
PHASES
Sphalerite
```

```
    ZnS + H+ = HS- + Zn+2
    log_k     -11.44
    delta_h   35.5222 kJ
PHASES
Arsenopyrite
    FeAsS + 0.5H+ + 1.5H2O = 0.5AsH3 + Fe+2 + 0.5H2AsO3- + HS-
    log_k     -14.4453
    delta_h   28.0187 kJ

SOLUTION_SPECIES
1.0000 H2AsO4- + 1.0000 H+  =  AsH3 +2.0000 O2
    log_k     -155.1907
    delta_h   931.183 kJ
```

3.7   Results and Discussion

3.7.1   Quality Control and Figures of Merit

Analytical balances were calibrated with certified check weights prior to use. Procedural blanks, were prepared in triplicate using 250mL of Milli-Q water in place of a captured water sample. Concentrations of metals were <LOD in procedural blanks with the exception of Ca (all < 5 μmol L^{-1}) and Mg (all < 0.5 μmol L^{-1}) (from polycarbonate filter) for which results were corrected. At least one duplicate sample was analysed during each run and bracketing standard introduced every ten samples to monitor instrumental drift. Carry-over from concentrated standards and samples was monitored during the analysis run and where necessary additional flush times were administered.

Analysis of three samples of a certified reference material were included in each analysis, recoveries are presented in Table 3.8.

 When results from ICP-MS and ICP-OES were produced for a sample, ICP-MS data was used in preference due to the lower LOD. Results outside of the limit of linearity for ICP-MS (outside standard range, Table 3.8) were discarded and ICP-OES results used.

Table 3.8: Limits of detection and CRM recoveries for all analysis of DGC samples. Certified reference material:TMDA-64 (fortified lake water), National Water Research Institute, Canada.

Element/ Anion	CRM Value ($\mu g\ L^{-1}$) ± 2σ limit	Method	Linear /Standard Range	Limit of Detection ($\mu mol\ L^{-1}$)	CRM Recoveries ($\mu g\ L^{-1}$)
Al	265±30	ICP-OES	0.5-5000	0.99,0.39	260, 281
		ICP-MS	0.001-10	0.0004, 0.0008	163, 183
As	150±22	ICP-OES	0.1-1000	2.2,1.3,1.4	158, 147,
Ca	13600*	ICP-OES	0.5-5000	0.0210, 0.0048	13400, 13500
		ICP-MS	0.0005-5	0.0002, 0.0002	237, 265
Cd	251±24	ICP-OES	0.01-100	0.045	234
Co	270±27	ICP-MS	0.001-5	0.0005, 0.0003	237,257
		ICP-MS	0.001-5	0.0004, 0.0006	259, 290
Cu	290±29	ICP-OES	0.1-1000	0.11,0.13, 0.13	311,285,286
Fe	319±30	ICP-OES	0.1-1000	0.46, 0.12, 0.19	308, 317, 312
Mg	3400*	ICP-OES	0.1-500	0.074, 0.047, 0.47	3340, 3380, 3600
		ICP-MS	0.001-2	0.0012, 0.0002	280, 320
Mn	299±26	ICP-OES	0.1-1000	0.041, 0.010, 0.015	295, 290, 287
		ICP-MS	0.0005-1	0.0001	253, 271
Mo	278±22	ICP-OES	0.1-10	0.28, 0.29	252, 294
		FAAS	200-4000	2.0	4400
Na	(4500*)	ICP-OES	0.5-5000	6.1	4520
		ICP-MS	0.0005-1	0.0004, 0.0025	260, 241
Ni	262±23	ICP-OES	0.01-100	0.62, 0.47, 0.36	254, 233, 247
K	580	FAAS	20-2500	0.4	600
		ICP-MS	0.001-0.5	0.0002, 0.0001	283, 296
Pb	297±28	ICP-OES	0.01-100	0.46, 0.50	269, 279
Si	-	ICP-OES	0.5-5000	2.09, 1.46, 0.97	-
Sb	125±20	ICP-MS	0.0005-1	0.0001, 0.0001	121, 138
		ICP-MS	0.0005-5	0.0010, 0.0011	291, 271
V	272±26	ICP-OES	0.01-100	0.40, 0.11, 0.18	276, 256, 262
W	(0.06*)	ICP-MS	0.0005-1	0.0001, 0.0001	0.23, 0.13
		ICP-MS	0.0010-10	0.0019, 0.0025	326, 356
Zn	(313*)	ICP-OES	0.1-1000	0.55, 0.47	302, 306
F⁻	-	IC	10-5000	0.31	-
Cl⁻	-	IC	10-5000	1.3	-
SO_4^{2-}	-	IC	10-5000	1.7	-

*Guidance value only.

Internal standards [193]Ir and [115]In were used to correct for mass flow errors through the ICP-MS and ICP-OES instruments, respectively. ICP-OES operating parameters were optimised for a low concentration element (usually Cd).

Limit of detection was calculated as three times the standard deviation of repeat samples (minimum 7) of the lowest detectable standard. The lowest detectable standard was determined as the lowest standard with a signal to noise ratio > 3:1. In the absence of a CRM for anion analysis, ion chromatography standards were checked against two independently prepared standards. Instrumental parameters for the ICP-MS, ICP-OES and IC are presented in Appendix 3E.

3.7.2 Site Hydrology

Flow from the final collection drain at its discharge point into the River Tamar (location 23) varied from 5.9-33.3 L s^{-1} (Table 3.9). Ditches and surface drains down gradient, around SWF precipitation launders, were generally waterlogged but did not always flow. Up gradient, around WAM and cinders tips, flows in surface drains were highly variable ranging from dryness to 14.3 L s^{-1} (location 8, 13/09/08). Surface drain 14 (SWF) and discharge 5 (WAM tip) were the only surface drains with measurable flow on all site visits (Table 3.9). When water levels observed in surface drains and boreholes (Table 3.10) were compared to local rainfall (Table 3.5), no covariance was found.

A combination of inputs seems to control measured and observed water levels across the site. These comprise rapid surface run-off, shallow groundwater seepage and deeper groundwater movement, which manifest at the observed sample locations at different times with respect to the rainfall that has initiated them. The variability may be exaggerated by the site geology, with high permeability superficial deposits of 1-2 metres depth (including sands and gravels, Figure 3.3), encountered close to the River

Tamar, whilst the site and the site catchment area are underlain by low permeability slate bedrock (BGS, 2009).

Ephemeral streams and waste tip seepages from the cinders and upper heap at Wheal Anna Maria were observed on 28/06/07, 07/02/08, 13/09/08 and 20/07/09. During dry surveys, flow from the tip was limited to a single discharge from an inspection aperture (location 5, photograph 9). Rainfall data (summarised in Table 3.5), suggests that sustained moderate to heavy rainfall in the preceding 7 days is required to generate surface expression of leachate from these waste tips. The low permeability of the lower tailings heap causes seepages from the upper tip to pool on the surface of the lower heap or migrate downstream via two channels either side (photograph 10).

Table 3.9: Flow data (L s^{-1}) calculated for selected locations at Devon Great Consols during water surveys. NR = No result for sample location on date of survey.*NR= dark when sampled, could not accurately determine flow, but dischage was observed.

Flow (L s^{-1})		WAM Tip Discharge	Surface Drain	Final Collection Drain (W-E)					
Sampling Date	Sample No:	5	14	18	19	20	21	22	23
07/02/2008		3.1	0.1	40.8	40.5	NR	33.8	NR	21.6
13/09/2008		2.8	NR	NR	NR	NR	NR	NR	NR
14/01/2009		0.2	0.8	12.1	12.6	14.5	18.8	19.1	33.3
28/02/2009		NR*	1.3	14.7	13.9	15.6	21.3	22.4	30.0
16/05/2009		4.3	0.3	5.45	4.90	6.14	7.90	NR	5.86
20/07/2009		0.3	0.1	NR	NR	6.92	9.19	NR	NR

Table 3.10: Water levels in shallow ground water boreholes installed at Devon Great Consols. Data presented as metres above a 2m ordnance datum (mAOD). X = Borehole destroyed by unknown party. NR = No result.

Water Level (mAOD)

Sampling Date	Borehole No:	1	2	3	4	5	6
14/01/2009		2.00	1.96	0.79	1.57	1.67	1.66
28/02/2009		2.00	1.92	1.29	1.35	2.00	1.66
16/05/2009		X	X	1.21	1.96	1.89	0.66
20/07/2009		X	X	1.32	NR	1.57	1.80

Closer to the River Tamar however, flow patterns in the final collection drain appear to be independent of short-term (14 day) rainfall patterns. For example, similar conditions of low flow rate were observed on the 16/05/09 and 20/07/09, despite contrasting rainfall in the 14 days before the site visit (very dry and very wet respectively). A more detailed check on total rainfall data preceding the 16/05/09 and 20/07/09 visits indicated that both were similarly dry in the 14-30 days before the visit, representing an additional 11 mm and 22 mm of rainfall, respectively (MetOffice, 2009). This suggests that in dry periods such as those preceding the 16/05/09, the water in the final collection drain is maintained by baseflow permeating the artificial and alluvial deposits around and beneath it.

Conversely, high rainfall causes an accumulation of surface runoff in the final collection drain and other ditches; for example that in front of the precipitation launders (location 17). The very high flow observed in the final drain on the 14/1/09, resulted from high rainfall in the 3 days before the visit (36 mm) as the previous 30 days were relatively dry (39 mm). The water level in the north and south banks of the final drain (BH1 and BH2, respectively) remained high, even when shallow groundwater moving

toward the drain from the north west (BH3, Table 6) was relatively low (14/01/09). Boreholes recharged instantaneously upon bailing as the banks and base of the final collection drain are highly permeable. The bank material comprises largely gravels of similar size and composition to the waste material found at the WAM upper tip, mixed with an ochre sludge (See Borehole Log, Appendix 3D and photograph 15-16). This facilitates easy exchange waters between the final collection drain and the surrounding soil and alluvial/artificial deposits. Furthermore, the alluvial deposits underlying the south east of the site (shown in Figure 3.3) provide a potentially high permeability pathway for these waters to the River Tamar.

Permeability was lower toward the south western part of the site. Here the ground was frequently waterlogged and this is likely to be the result of the underlying low permeability strata (clays). Gley soils of alternating colour and character were encountered in BH2 (photograph 16), BH3, BH4 and were most extensive in BH6 (See borehole logs, Appendix 3D for descriptions). BH4 was also noted to contain an impermeable hardpan layer. The low permeability layers exhibited regular horizontal stratification suggesting they may be extensive and could inhibit vertical migration of shallow groundwater and surface drainage. Despite this, recharge in all boreholes (except BH6) was too rapid to accurately measure (Table 3.4). This infers that horizontal flow through higher permeability strata recharges the boreholes and comprises the dominant mode of sub-surface transport through the site toward the River Tamar.

3.7.3   Principal Component Analysis (PCA)

The results of the PCA demonstrated that the geochemical character of samples varied across the site and drainage from the main waste tips: WAM, cinders and precipitation launders, showed particular signatures. Major contributors to the first

principal component (F1) were dissolved Ni (8%), Mn (7%), Co (7%), sulphate (7%), V (6%), Zn (6%), As (6%), Sb (6%), Cd (6%), and Al (5%), accounting for 25% of the total variability of the DGC dataset. These dissolved species represent some of the dissolution products of the mine waste tips as a result of the oxidation of sulphide minerals, with the notable exception of Fe and Cu. So, the first principal component appears to group data based on trace element enrichment. The second principal component (F2), which accounts for 14% of the total variability, was largely attributable to Cu (13%), then Ag (9%), Ca (8%), Al (8%), H^+ (8%), Si (7%), and Cl (7%) concentrations. This appeared to show the prevalence of a particularly Cu rich drainage, emerging from the WAM tip at the top of the site, also characterised with high Ag, Ca, Al and low pH (high [H^+]).

A number of groupings were identified by plotting F1 against F2 (Figure 3.8). Amongst the most prominent are the WAM tip drainage samples, which extend along the positive F2 axis (circle A). Cinders drains are grouped (circle B, Figure 3.8) due to high concentrations of As, Sb and Mo, which were very low in other samples. The samples from the cinders mixing zone, path mixing zone and South Wheal Fanny shaft show character somewhere between group A and group B. BH6 is characterised by low trace metal contamination and dissolved Fe which resolve samples from it along the negative F2 axis (circle C, Figure 3.8). BH6 may be indicative of the geochemistry of ground waters that have not been contaminated with waste leachates.

Also included in group C are the pond samples and South Wheal Fanny Shaft, indicating that they are also relatively free of mine drainage contamination and/or influenced by deep ground waters. BH4 samples and samples from around the precipitation launders (including BH5) are also resolved from the main group, appearing to the left of the plot (circles E and F, respectively). The tightly grouped data near the centre of Figure 3.8 comprises mainly samples from the final collection drain

and BH1-3 (circle D). This suggests some mixing of all waters before entry to the River Tamar. The offset of group D to high F1 and low F2 character could be accounted for by dilution with less contaminated waters, or by the removal of dissolved species, particularly Cu (F1) and also Ni, Mn and As (F2), by natural attenuation along the migration pathway.

The mixing of drainage from WAM, cinders and precipitation launders and dilution by ground water and rainwater leads to a spread of sample character between these groups. Samples taken from the bottom of the site in the final collection drain and BHs 1-3 were closely related in all surveys suggesting the composition of discharge waters to the River Tamar showed little variation.

Principal component F3, which accounted for 11% of the total variability, was most strongly influenced by K (17%), Mo (8%), B (8%), Sb (7%) and As (7%). A plot of F3 vs. F1 and to a lesser extent F3 vs. F2 (neither plot shown) distinguished all cinders drain samples from other samples. Lesser principal components did not display any additional patterns in the data.

In the following sections the results of *in situ* measurement of master variables and laboratory determinations of dissolved metal, metalloid and anion concentrations will be examined in more detail. The groupings by sample type, described in this section and confirmed by the results of the PCA clustering, will be used in subsequent figures. They are listed with further details of sample location in Appendix 3B.

Figure 3.8: Plots of F1 and F2 principal components showing distribution of variables (above) and observations for the Devon Great Consols Data Set. Group A: Wheal Anna Maria Tip drainage, Group B: Cinders drains, Group C: BH6, Pond and South Wheal Fanny Shaft, Group D: BH1-3, Final Collection Drain and South Wheal Fanny Adit, E: BH4, F: BH5 and precipitation launders.

3.7.4   Major Ions

The composition of the surface waters and boreholes with respect to major cations from all surveys at Devon Great Consols are presented as molar percentages in ternary diagrams (Figure 3.9 and Figure 3.10). Overall, the data is grouped towards the bottom left corner of the plot, representing a high molar fraction of Ca and Na + K, with respect to Mg. Average rainwater composition for Plymouth (Coles, 1999) is distinctly different in character, containing a much higher proportion of Mg and Na + K and low Ca. There is a general shift from the main group towards the rainwater character for samples from the pond, ephemeral cinders drain and locations 17 and 18 at the western extent of the final collection drain (locations shown in Figure 3.5). This is consistent with observations of standing water made during site visits and PCA results, which suggested that rainwater collects in the drains and pond and dilutes mine drainage received by the drains.

Figure 3.9: Molar percentage of major cations for surface water samples at Devon Great Consols, grouped by sample type. Mean rainwater composition for Plymouth also shown (Coles, 1999). Blue arrow indicates spread of data towards rainwater composition.

Samples from locations 9 and 10 are separated from the main group by higher Ca concentrations, and this may be explained by recently installed drainage pipes at this location (see photograph 7). This engineering work has introduced foreign material (e.g. plastics, mortar, cement and sand) and disturbed native material, which contains Ca-rich mining waste from the waste tips up slope. This could have caused Ca- rich waters to leach into drains in the immediate vicinity.

Figure 3.10: Molar percentage of major cations for borehole water samples from Devon Great Consols. Mean rainwater composition for Plymouth also shown (Coles, 1999). Arrows indicate spread of data towards Mg-rich waters (red) and rainwater/deep ground water composition (blue).

In terms of major ion composition, waters from BH1,2,3 and BH5 were close to surface water drains from the waste tips, and tip seepages reported from sulphide hosted Cu mines elsewhere in the world (e.g. Stillings *et al.*, 2008). The similarity to surface drains, suggested subsurface transport is an important migration pathway for mine waters at the site. The spread of data extends from Ca-rich waters towards a higher proportion of Mg. This is most evident for BH4 and BH6, the latter also showing a

stronger Na and K character than other samples. Strong Na-K character could be a reflection of flashy recharge with rainwater, or more likely due to the presence of low permeability clays in the area isolating deeper ground waters. Deep ground waters characteristic of fractured argillaceous formations (e.g. Beaucaire *et al.*, 2008), or granitic formations in south west England (Smedley and Allen, 2004), are generally soft and would also plot closest to the rainwater composition marker in Figure 3.9 and Figure 3.10. Therefore, shallow ground waters at DGC appear to show character closest in character to surface drains with some mixing of Mg-rich waters in BH4 and more pristine ground water in BH6.

3.7.5   Master Variables

Conductivity and Total Suspended Solids (TSS)

Conductivity in water samples was highly variable and ranged from 140 to 1040 μS (Figure 3.11). When compared to major ion chemistry, increased conductivity in the WAM tip drainage and locations in receipt of this drainage (dark grey boxes, Figure 3.11), were reflected by increased concentrations of SO_4^{2-} (1795-5285 μmol L^{-1}) and F^- (257-2903 μmol L^{-1}), charge balanced with similarly increased concentrations of Na^+ (377-1095 μmol L^{-1}), Mg^{2+} (114-684 μmol L^{-1}) and lesser increases in a range of other metal cations. Other sample locations were more comparable (although still slightly elevated) with background values such as those in the River Tamar, recorded as 52-284 μS at Greystone Bridge and Gunnislake (1976-2006, EA, 2010). Total suspended solids varied widely in surface water drains, from < LOD (0.72 mg L^{-1}) to 100 mg L^{-1} during predominantly dry surveys, up to a maximum of 36.5 g L^{-1} in WAM tip drainage following heavy rain (location 6, 20/07/09, photograph 17).   In surface drains, particularly around the waste tips, heavy rain caused disturbance and transport of unconsolidated surface material leading to a high dissolved and suspended load in

surface runoff. This effect offset the dilution of contaminated waters from increased rainfall. Borehole waters were also variable in TSS ranging from <LOD (0.72 mg L^{-1}) in BH6 to 34.0 g L^{-1} in BH1.

Figure 3.11: Conductivity measurements recorded at Devon Great Consols for all surveys, grouped by sample type. Dark grey boxes indicate WAM tip drainage and downstream recipients of this drainage. Dashed horizontal lines show conductivity range in the River Tamar close to DGC (1976-2006, EA, 2010) measured at Greystone Bridge and Gunnislake.

pH, Eh and Dissolved Oxygen

pH, redox potential and dissolved oxygen varied widely across all sampling locations and surveys. WAM tip seepages were lowest in pH (pH 3.1-3.9, Figure 3.12) and poised above the buffering threshold of iron hydroxides (~pH 3-3.5, Lottermoser, 2007, Evangalou, 1995). The major iron composition of the seepages suggested that the high Na and Mg release observed resulted from a supplementary buffering mechanism, either ion exchange reactions on mineral surfaces or dissolution of aluminosilicate minerals. Rainfall in the Tamar catchment has a strong marine signature (Smedley and Allen, 2004); therefore deposited salts can contain a high proportion of Na and Mg

which may be displaced by protons in porewaters. Additionally aluminosilicate minerals bearing Na and Mg are very common and could also be responsible for the spikes observed, for example via dissolution of albite in Equation 13 (section 3.4.3). Sample 5, which issues from the inspection hole in the WAM tip (photograph 9), was consistently the lowest in pH. This may be due to the provision of a high permeability pathway and high oxygen ingress by the inspection passage, which would promote generation of acidic waters via oxidation reactions (section 3.4.1).

Upon reaching the final drain and discharging to the River Tamar, the pH of WAM drainage waters had been buffered to pH 3.9-4.5. Boreholes 1-5, also downstream of WAM tip drainage were also buffered to pH 4.0-4.6, suggesting similar buffering mechanisms in surface and shallow ground waters. The slightly higher pH attained by BH1 and BH2 may indicate slower transport via the subsurface to the final drain, which would allow greater buffering from mineral dissolution reactions which may be kinetically slow.

The cinders drainage exhibited quite different character to WAM drainage being lower in overall conductivity (Figure 3.11) and having relatively high pH (pH 5.0-5.4), and slightly lower Eh (486-552 mV, Figure 3.12). As indicated previously by PCA, the cinders mixing zone (CMZ, samples 2-3) and path mixing zone (PMZ, samples 9-10) yielded data between the cinders and WAM end members.

Locations identified as likely to collect and store rainfall in the south west of the site (samples 9-13) were relatively high in pH 4.3-5.2, and exhibited a large range of Eh and DO. Overall surface waters at the site were well oxygenated with flowing surface waters maintaining 69-113 % oxygen saturation, as a result of the rapid transport down slope toward the River Tamar. Reducing conditions and low DO were encountered in BH6 (Eh = 324-451 mV, DO = 1.55-5.87 mg L^{-1}, 14-51 % sat.). Other boreholes were similarly depleted in DO (0.7 - 6.1 mg L^{-1}, 6-52 % sat.).

Figure 3.12: Measured pH (above) and Eh (below) for surface and borehole samples at Devon Great Consols during seven surveys. Wet weather surveys denoted by filled symbols, predominantly dry surveys denoted by hollow symbols. Cind. = Ephemeral Cinders Drain, CMZ = Cinders mixing Zone, WAM = Wheal Anna Maria Waste tip, PMZ = Path mixing zone, SWF Sh/Ad = South Wheal Fanny Shaft and Adit Portal.

Figure 3.13: Dissolved oxygen measurements for surface and borehole samples at Devon Great Consols during four surveys. Remaining explanations as for Figure 3.12.

Waters in the final drain remained constant between surveys and locations with respect to pH, Eh and DO suggesting that upon reaching the drain (and the River Tamar) waters had achieved a relatively stable state of equilibrium between geochemical processes acting upon them.

3.7.6 Dissolved Metals, Metalloids and Selected Anions

WAM and Precipitation Launders Drainage

Figure 3.14: Schematic diagram highlighting migration pathway of Wheal Anna Maria Upper (WAM) and precipitation launder tip drainage.

Consistently elevated dissolved metal concentrations in boreholes and surface drains between the waste tips and the river were observed for Cu and Al (Figure 3.15), Zn and Ni (Figure 3.16), and Cd and Mn (Figure 3.17) with respect to EQS values. A plume of dissolved metal contamination, arising mainly from the WAM upper tip and augmented by the precipitation launders (samples 15 and 17), discharges under all hydrological conditions into the river via the final drain.

Dissolved Al and Cu were particularly high in the Wheal Anna Maria tip seepages (locations 4-8) to a maximum of 1850 µmol L^{-1} and 570 µmol L^{-1}, respectively. The mean concentrations of Al and Cu in the final drain (samples 19-23) were 618 µmol L^{-1} and 77.4 µmol L^{-1}, respectively. Concentrations in this discharge exceed EQS values (Table 3.15, Appendix 3F) by a factor of approximately 33400 and 5000 respectively and fall at the upper end of sampled mine discharge waters in the catchment, with respect to Al and Cu (Table 3.1). Internationally, these concentrations

are moderately high for drainage waters from sulphide hosted metal mines. Literature examples of dissolved Al and Cu in surface waters impacted by metal mine drainage have been reported as 0.330-17900 µmol L^{-1} and 0.0131-2330 µmol L^{-1}, respectively, with highest concentrations recorded in the Rio Tinto, Spain (Cánovas *et al.*, 2008).

Boreholes 1-4 exhibited the same magnitude of contamination to samples from the final drain and were rapidly recharged by inflowing ground waters. BH2 and BH4 situated to the south of the final drain show that contamination also travels in the subsurface beyond the final drain toward the River Tamar. As shown by Figure 3.3, highly permeable alluvial deposits below the drain offer a potential additional pathway into the river.

The proportion of dissolved Al observed downstream in the final drain with respect to drainage waters from the WAM upper tip ($\bar{x} = 800$ µmol L^{-1}) was high, suggesting near conservative transport. In contrast, Cu concentrations in waters generated at the WAM upper tip ($\bar{x} = 224$ µmol L^{-1}) showed a three-fold reduction in the final drain. The reduction in concentration for both metals was attributed to the combined attenuation effect of dilution, raised pH leading to precipitation reactions and sorption to mineral surfaces as waters migrate downstream. The particular reduction of dissolved Cu suggests preferential sorption/or precipitation of this metal to secondary iron phases and/or organic matter, which has been suggested by other studies of mine waters (e.g. Olias *et al.*, 2004) .

Dissolved Zn, Cd and Ni concentrations, were strongly correlated with one another in all waters (r ≥ 0.8), and also very high in drainage from the waste tips. Mean discharge concentrations from the final drain to the River Tamar were 12.5 µmol L^{-1} Zn, 2.01 µmol L^{-1} Ni and 0.020 µmol L^{-1} Cd. Each exceeded EQS for freshwaters, by a factor of 6 for Ni, 28 for Cd and 100 for Zn. The observed concentrations for these

metals were not as high as those recorded in other parts of the catchment in previous targeted surveys (42.8 µmol L^{-1} Zn, 4.77 µmol L^{-1} Ni and 0.080 µmol L^{-1} Cd, Table 3.1).

Unlike Cu, the highest concentrations of these metals were identified in samples closest to the precipitation launders (locations: 14, 15, 17, 18 and BH5) rather than the WAM upper tip seepages. These samples emerged from the PCA as a group with distinct geochemical character. The precipitation launders supplement the contaminant plume migrating from the WAM waste to the river with a Zn, Cd, Ni and additionally Mn- rich discharge.

Using the geochemical modelling code PHREEQC to calculate speciation of dissolved ions, the free divalent cations of Cu, Zn, Mn, Ni and Cd were predicted to be the dominant dissolved species in WAM tip drainage (pH 3.2-4.0), cinders drains (pH 5.0-5.3) and the final drain (pH 3.9-4.5). Some variation of redox state was predicted where more reducing conditions were encountered, for example an increase in Cu(I) with respect to Cu (II) for some borehole samples.

Sulphate ions contributed highly to the overall conductivity of the drainage waters and represent the most abundant anion in solution. Sulphate concentrations ranged from 610-5300 µmol L^{-1} and were highest in WAM and precipitation launders drainage (Figure 3.18). Fluoride concentrations were in some instances similar in magnitude to sulphate (Figure 3.18) and thought to originate from fluorite (CaF_2) identified within the waste tips by other studies (Klink *et al.*, 2005; Page, 2008). Dissolved Ca (858-1651 µmol L^{-1}, $\bar{x}$ = 1167 µmol L^{-1}) in seepages from the WAM upper tip were the same order of magnitude to dissolved F$^-$ (520-1410 µmol L^{-1}, $\bar{x}$ = 834 µmol L^{-1}), suggesting fluorite dissolution could account for a significant proportion of dissolved Ca in the leachates. WAM upper tip drains was undersaturated (S.I. = -2 to -4) with respect to Fluorite, however quantification of F$^-$ by IC, assumes that F is present as the free ion, that was not the thermodynamically favoured species (Al complexes). The

actual concentration of fluoride in drainage waters is likely to be higher than suggested by IC analysis.

Predicted dissolved Al species were the fluoride complexes, (AlF^{2+}, AlF_2^+) accounting for over 90% of dissolved Al in tip drainage, cinders drain and final drain samples. In samples where fluoride concentrations were lower, sulphate complexes became more significant. Kinraide *et al.* (1997) found fluoride and sulphate complexes of Al species to be less phytotoxic than the free ion in a study of Al toxicity in wheat species. This could boost tolerance of plant species to the high Al content of the waters, although the concentrations at DGC are higher than those used in the Kinraide study ($<$ 290 μmol L^{-1}).

Waters were under-saturated with respect to the major Al containing phases which are thought to control Al solubility in low pH-high sulphate waters, namely gibbsite ($Al(OH)_3$, kaolinite ($Al_2Si_2O_5(OH)_5$), alunite ($KAl_3(SO_4)_2(OH)_6$), jurbanite ($Al_3(SO_4)OH.5H_2O$) and basaluminite ($Al_4(SO_4)(OH)_{10}.5H_2O$) (Nordstrom and Ball, 1986). The final drain is poised below pH 4.6, indicating that active dissolution of Al phases is buffering the acidity in this part of the site. Nordstrom and Ball (1986) suggested reduced complexation with sulphate as a factor which may impede the onset of $Al(OH)_3$ hydrolysis and therefore precipitation of Al solids. In the waters at DGC, where fluoride complexes are favoured to sulphate complexation, Al hydrolysis might similarly be impeded, enhancing Al solubility.

The consistency in pH/Eh conditions observed in the final drain (locations 19-23) extends to similarly consistent dissolved sulphate and metal concentrations for Cu, Al, Zn, Mn, Ni and Cd (RSD $\leq$ 12.1%, Table 3.11). Dissolved Pb and As were slightly more variable (RSD 29.0 % and 20.7 %, respectively), due to low concentrations and their strong association with Fe, which showed the greatest variability (RSD = 51.0 %), specifically through co-precipitation and sorption reactions in oxic environments.

This is strong evidence to suggest that a local equilibrium condition has been achieved in the final collection drain. However, the concentrations observed in BH1-4, which draw shallow ground waters in the area around the final drain (0.5-1.5 m depth), show greater variability in concentration. The kinetics of the reactions which maintain the equilibrium condition in the final drain must therefore be rapid with respect to the speed of water movement into it.

Table 3.11: Mean concentration, standard deviations and relative standard deviations of dissolved metals and As in the final collection drain at Devon Great Consols (Sample Locations 19-23, n=17.) Chloride result 445 ± 38 μmol L^{-1}, RSD = 8.5%.

	Cu	Al	Zn	Mn	Ni	Cd	Pb	As	Fe	SO$_4$
Mean ± 1 s.d. (μmol L^{-1})	77.4 ±4.6	618 ±45	12.4 ±1.0	58.5 ±6.6	1.92 ±0.23	0.019 ±0.002	0.0046 ±0.0013	0.23 ±0.05	1.72 ±0.88	2637 ±226
% RSD	6.0	7.3	8.0	11.2	12.1	11.9	29.0	20.7	51.0	8.6

Key among these reactions is likely to be the oxidation of dissolved Fe to Fe(OH)$_3$ phases and the sorption of other metals to the freshly precipitated surfaces. Dissolved Fe concentrations observed across the site (Figure 3.19) show dissolved Fe was largely close to or at the LOD (0.12 μmol L^{-1}) for surface drainage waters. This is consistent with Fe removal as Fe(OH)$_3$(s) phases in oxic waters. The Fe redox state was predicted from thermodynamic equilibria reactions using PHREEQC and confirmed the dominance of Fe(III) over the more mobile Fe(II) when waters were equilibrated with the atmosphere. Locations receiving cinders drainage (locations 1-3) were closest to this theoretical condition, based on the measured pH/Eh/DO and determined solution composition.

However, where dissolved iron was detected Fe(II) was the dominant predicted redox state, either as the free ion or as sulphate and chloride complexes. This was most significant in boreholes and seepages from the WAM upper tip where reducing

conditions strongly favoured Fe(II) complexes, leading to elevated dissolved Fe in these waters. The availability of Fe(III) in solution in the tip drainage and sub-surface flow near to the River Tamar, shows the potential for ongoing precipitation of $Fe(OH)_3(s)$ phases upon reaction with atmospheric oxygen. In the final drain, thick layers (~0.5 m) of ochre are evident in the stream bed and along the banks of the drain (photographs 15 and 16) consistent with this process. Saturation indices calculated by PHREEQC showed the waters in the final drain remain understaurated with respect to $Fe(OH)_3$ phases, but would become saturated if equilibrium with oxygen in the atmosphere was attained.

In the low lying south-west area of the site, metal concentrations were generally lower than in the final drain, consistent with the direction of water movement from the tips being NW to SE. Waters in BH6, also in the south west of the site, were relatively low in all the contaminant metals reflecting less interaction with mine waters. However, there is evidence of contaminated mine water entering the pond (located at sites 12 and 13), most likely via connective drains. Concentrations of Al, Cu, Zn, Ni, and Cd showed some variation between surveys and during one survey (14/01/09), Zn, Ni and Cd (Figure 3.16 and Figure 3.17) were elevated in the pond and drain compared to other surface samples.

Figure 3.15: Dissolved Al (above) and Cu (below) concentrations in Devon Great Consols water samples determined from seven surveys. Remaining explanations as for Figure 3.12. LOD for Al and Cu typically 1.0 µmol L^{-1} and 0.1 µmol L^{-1}, respectively. Long-term freshwater EQS for dissolved Al and Cu equal to 0.00185 µmol L^{-1} and 0.00157 µmol L^{-1}, respectively.

Figure 3.16: Dissolved Zn (above) and Ni (below) concentrations in Devon Great Consols water samples determined from seven surveys. Remaining explanations as for Figure 3.12. LOD for Zn and Ni typically 0.003 μmol L^{-1} and 0.003 μmol L^{-1+}, respectively. Long-term freshwater EQS for dissolved Zn and Ni equal to 0.122 μmol L^{-1} and 0.341 μmol L^{-1}, respectively.

Figure 3.17 Dissolved Cd (above) and Mn (below) concentrations in Devon Great Consols water samples determined from seven surveys. Remaining explanations as for Figure 3.12. LOD for Cd and Mn typically 0.00020 μmol L^{-1} and 0.0012 μmol L^{-1}, respectively. Long-term freshwater EQS for dissolved Cd and Mn equal to 0.00071 μmol L^{-1} and 0.13 μmol L^{-1}, respectively.

Figure 3.18: Dissolved sulphate (above) and fluoride (below) concentrations in Devon Great Consols water samples from six surveys. Remaining explanations as for Figure 3.12. LOD for sulphate and fluoride typically 1.7 μmol L^{-1} and 0.31 μmol L^{-1}, respectively Current UK drinking water standard for fluoride equivalent to 0.08 μmol L^{-1} (DWI, 2009).

Figure 3.19: Dissolved Fe concentrations in Devon Great Consols water samples determined from seven surveys. Remaining explanations as for Figure 3.12. LOD for dissolved Fe typically 0.2 μmol L^{-1}. Long-term freshwater EQS for dissolved Fe equal to 0.000286 μmol L^{-1}.

Cinders Drainage

Figure 3.20: Schematic diagram highlighting migration pathway of cinders tip drainage.

As indicated by PCA, locations to the west of the site (locations 1,2,9,10) receive drainage from the cinders waste tips and concentrations of contaminant metals and sulphate were lower than other locations, but high in As and Sb (Figure 3.21 and Figure 3.22). Overall the two elements were very strongly correlated (r = 1.0) in all samples with an average ratio of As:Sb of 470:1. Maximum recorded concentrations of dissolved As and Sb were 380 μmol L^{-1} and 5.4 μmol L^{-1} respectively at location 1. Based on PHREEQC calculations, the thermodynamically favoured dissolved As species here was As(V) in the form of $H_2AsO_4^-$ or H_3AsO_4 by ten orders of magnitude over As(III). These As(V) species readily adsorb to iron oxides (Lee and Chon, 2006; Asta *et al.*, 2010). Some areas of the cinders waste were stained with ochre (photograph 18), and freshly precipitated iron oxyhydroxides were evident in the final drain (photograph 15).

 Natural attenuation of dissolved As (and Sb) by sorption or co precipitation with these $Fe(OH)_3$ phases is the likely reason why concentrations of As fall below EQS for fresh waters (equivalent to 0.67 μmol L^{-1}, Table 3.15, Appendix 3F), upon reaching the lower part of the site (final drain, $\bar{x} = 0.23$ μmol L^{-1} and pond, $\bar{x} = 0.10$ μmol L^{-1}).

However, some dissolved As and Sb was observed in the stream emerging from the South Wheal Fanny shaft (Max 24.1 μmol L^{-1} As and 0.11 mol L^{-1} Sb) and in borehole samples (Max 5.8 μmol L^{-1} As and 0.009 μmol L^{-1} Sb). This was consistent with increased As(III), with respect to As(V) under more reducing conditions, although As(V) species remained dominant by 3-5 orders of magnitude. The equilibrium position between the As(III) and As(V) redox state, as predicted by PHREEQC, was sensitive to small changes in Eh/pH condition within the range observed in water samples. Arsenite (As(III)) dominates in reducing conditions (Sharma and Sohn, 2009) and is generally stable in solution particularly at low pH (Casiot *et al.*, 2005). Conversely, the stability field of Sb(III) with respect to Sb(V) is much larger than As(III) under Eh/pH

conditions encountered in DGC surveys (Wilson *et al.*, 2010) and the thermodynamically favoured Sb species in all cases was consistently $Sb(III)(OH)_3$, by at least three orders of magnitude.

Arsenic mobility in DGC waters was observed at pH > 5, which is higher than recently reported by others (pH < 3.5, Cheng *et al.* 2009) this may be due to slow kinetics of adsorption or transport on fine colloidal Fe-hydroxides as As(V) (Slowey *et al.*, 2007). The As/Sb ratio remained relatively stable in all samples, since As(III) was not favoured in any water samples captured, and Sb is not so redox sensitive, transformation to As(III) is not likely to be the reason for increased As mobility since this may be expected to increase the As:Sb ratio required more reducing conditions.

Geochemical processes occurring along the transport pathway within the final drain appeared to regulate the observed concentration of As and Sb, as they did for metal contaminants.

Figure 3.21: Dissolved As concentrations, all samples (above) and As, samples < 1.0 μmol L^{-1} As (below) in Devon Great Consols water samples determined from seven surveys. Remaining explanations as for Figure 3.12. LOD for dissolved As typically 0.0008 μmol L^{-1}. Dotted horizontal line represents UK EQS, equivalent to 0.67 μmol L^{-1}.

175

Figure 3.22: Dissolved Sb concentrations in Devon Great Consols samples determined from seven surveys. Remaining explanations as for Figure 12. LOD for dissolved Sb typically 0.0001 µmol L^{-1}. Currently no EQS for dissolved Sb.

Other Trace Elements and Anions

Dissolved concentrations of other elements and anions were included in PCA but not discussed further due to low concentration or being outside the scope of this study. These included: Pb (0.053 µmol L^{-1}, max, WAM drainage), Mo (0.0061 µmol L^{-1}, max, cinders drainage), Co (5.73 µmol L^{-1}, max, BH4), V (0.059 µmol L^{-1}, max , cinders drainage) B (60.0 µmol L^{-1}, max , cinders drainage) and NO$_3^-$ (40.0 µmol L^{-1}, max ,WAM drainage). PO$_4^{2-}$ and Br were <LOD in all samples (LOD = 0.59 µmol L^{-1} and 1.64 µmol L^{-1}, respectively).

3.7.7 Effect on the Water Quality of the River Tamar

The mean concentrations of dissolved Al and Cu in the final drain close to the River Tamar were 618 μmol L^{-1} and 77.4 μmol L^{-1}, respectively (n=17). Therefore approximately 33400 and 5000 fold dilution of this discharge is required to conform to the UK long term EQS for Al and Cu in low alkalinity waters (0.0185 μmol L^{-1} and 0.016 μmol L^{-1}, respectively). Similarly, dissolved Zn ($\bar{x}$ = 12.4 μmol L^{-1}, n=17), Cd ($\bar{x}$ = 0.019 μmol L^{-1}, n=18) and Ni ($\bar{x}$ = 1.93 μmol L^{-1}, n=17), require approximately 100, 25 and 6 times dilution, to achieve EQS limits (0.12 μmol L^{-1}, 0.00071 μmol L^{-1} and 0.34 μmol L^{-1}, respectively).

The highest recorded flow from the drain discharge was 33 L s^{-1} (location 23), which is considerably less than average flow in the River Tamar at Gunnislake (22.6 m^3 s^{-1}) (1956 - 2008, EA). Based on conservative mixing of the two waters (1:685), both dissolved Al and Cu were very likely to cause an EQS failure in the River Tamar as a result of this discharge. Furthermore, even at the highest recorded flow (515 m^3 s^{-1}, representing 1:15600 dilution) the River Tamar requires Al to exhibit non-conservative behaviour in order to meet with regulatory standards. This is attainable because pH in the River Tamar at Gunnislake is generally much higher (pH 7.6-8.7, EA (1997-2008)), than the disassociation constant for gibbsite in acidic waters (Al(OH)$_3$, pK = 4.9, Nordstrom *et al.* (1986)). However, precipitated Al monomers and polymers remain toxic to aquatic organisms as described in section 3.4.4.

Mean dissolved concentrations determined in the River Tamar at Gunnislake Bridge (downstream of DGC, shown in Figure 3.1) from Jam 1997 to Dec 2007 were Cu ($\bar{x}$ = 0.19 $\pm$ 0.05 μmol L^{-1}) Zn ($\bar{x}$ = 0.19 $\pm$ 0.06 μmol L^{-1}), both of which were above long term EQS, Cd ($\bar{x}$ = 0.00066 $\pm$ 0.00037 μmol L^{-1}) Ni ($\bar{x}$ = 0.087 $\pm$ 0.011 μmol L^{-1}) and As ($\bar{x}$ = 0.047 $\pm$ 0.024 μmol L^{-1}) below EQS (EA, 2010). Data for Al was

unavailable, but there were frequent EQS failures in the River Tamar downstream of the final drain discharge for Cu, Zn and Cd during this period. There are also several other mine discharges in the section of the river adjacent to DGC including an adit discharge at Blanchdown (section 3.7.8). Estimating the relative contribution of every input to the contamination in the River Tamar is difficult, particularly diffuse seepages and run off from mine waste. From flow and dissolved data previously gathered at Gunnislake bridge and a survey of major point inputs to the River Tamar, it was estimated that 62 % of dissolved Cu, 59 % dissolved Zn, 55 % of dissolved As and 73 % of dissolved Ni are not accounted for by point discharges including the FCD (Mighanetara, 2009).

The final collection drain at DGC does not collect all the diffuse drainage leaving the site, as comparable metal concentrations were recorded in BH2 and BH4, located in the *phreatic zone* beyond it. The drain may offer the most rapid transport pathway to the river, but the total dissolved contaminant discharge cannot be estimated from flow in the final drain alone, as this may be an under estimate. In particular, base flow through the alluvial deposits which underlay the final drain offer an additional pathway to the River Tamar.

Dissolved metal and metalloid concentrations in borehole samples around the FCD were the same order of magnitude to waters in the drain, and waters recharge almost instantaneously showing high permeability of underlying soils and rocks. These are indicators that the same geochemical processes of Fe precipitation and metal/metalloid sorption/co-precipitation occur in the phreatic zone around the drain as in the drain itself.

Cyclic wetting and aeration of the waste and soils provides greater potential for oxidation reactions to proceed, effectively accelerating the ageing of the materials (Sastre *et al.*, 2004). The fluctuations of water levels observed in the final drain and boreholes will encourage the precipitation of $Fe(OH)_3$ phases and aid natural attenuation

of metals and metalloids via sorption and co-precipitation reactions. However, a high water table also places a greater surface area of contaminated mine waste/soil in the phreatic zone. Desorption and dissolution reactions can mobilise contaminant metals and metalloids and oxidation reactions will consume oxygen. More reducing conditions were at times encountered in the boreholes (1-4) around the FCD and accordingly concentrations of dissolved Fe were increased. Conversely, ochre coloured particulates were often noted to be suspended in purge waters, suggesting cycling between Fe^{2+} and Fe^{3+} dominated conditions. This process may have been caused or enhanced by the mixing action of purging boreholes. The mobility of many metals and metalloid species will increase in reducing conditions, due to the shift from ferric $Fe(OH)_3(s)$ to soluble ferrous Fe^{2+}. The kinetics of the competing reactions and the Eh/pH conditions will determine the composition of waters moving through and from the site.

Maintenance of fast flowing oxic waters through the subsurface and in surface drains is favourable for the attenuation of dissolved metals and metalloids leaving the site. But high permeability also potentially supplies an additional load of contamination to the River Tamar via base flow, particularly if reducing conditions are maintained at depth. The magnitude of the flux, if any, that reaches the River Tamar via baseflow will remain unknown unless a thorough investigation of permeability in the phreatic zone is conducted. However, this study has demonstrated that such an input is likely to provide a portion of the dissolved flux which is unaccounted for by point discharges, particularly for Fe and As which are more mobile under reducing conditions.

3.7.8 Comparison of Dissolved Concentrations with Existing Data and Point Discharges

Concentrations of metals and As in this study in the final collection drain (FCD) and shallow groundwater (BH1-4), were compared with the results from unpublished

data gathered by Mighanetara (July 2005-June 2006, n=12) and the Environment Agency Data (Sept 1992-Dec 1994, n= 27).

Sample location 23 (discharge of final collection drain into River Tamar), was common to all studies and facilitated comparison of data from different time periods. Dissolved concentrations in the final collection drain (FCD) were largely comparable between the three studies, with the exception of Cu, which was significantly lower in the 1992-1994 survey compared with the recent surveys (Figure 3.23). This suggests that as the site matures after total closure (specifically, closure of the Cu-precipitation works ~1980s), and ongoing geochemical processes may be altering the concentrations in the FCD. These processes may include saturation of Cu binding sites on mineral surfaces in the surrounding soils and sediments by Cu and other metals (Benjamin and Leckie, 1981) or major ions (Du Laing *et al.*, 2009), for example Ca released from the WAM tip), disturbance of spoil tips exposing fresh surfaces to weathering, or maturation of secondary iron phases resulting in release of co-precipitated or adsorbed metals (e.g. Moncur, 2009) . Furthermore the continued attenuation of Cu and acidity relies on the rate of supply of soluble iron from the tips and dissolution of acid-buffering minerals to remain greater than the rate of supply of copper.

Flow in the FCD was similar in 2005-2006 (2.6-25.5 L s^{-1}) to this study (5.9-33.3 L s^{-1}), although concentrations were more variable in 2005-2006, showing seasonal increase during the summer months and decrease during winter. Average rainfall during the earlier survey period (July 2005-June 2006), was 3.16 mm d^{-1} (Millhill MIDAS station), which is low compared to the ten year average (3.82 mm d^{-1}, 1999-2009). In contrast, surveys in this study were conducted during years of relatively high average rainfall (July 2006- June 2007 = 4.67 mm d^{-1} (initial survey), and July 2008-June 2009 = 4.31 mm d^{-1}) and concentrations remained relatively constant between surveys. Hydrographs of the River Tamar at Gunnislake (Appendix 3H), demonstrate the large

effect of different rainfall patterns on flow in watercourses. It also clearly illustrates the low summer flow in 1994-1995 and 2005-2006, compared to 2007-2009. Comparison of the three surveys demonstrates that the steady Eh/pH and metal concentrations found in the final collection drain during this study, were not observed during the drier conditions of the 2005-2006 survey.

Dissolved Cu concentrations in groundwater and FCD were significantly higher than those determined in the receiving stream close to the main adit discharge from Devon Great Consols (Blanchdown Adit, BA, Figure 3.23). Concentrations of other metals (except Fe) were close to those determined in the BA discharge and dissolved As and Fe were generally lower in final drain compared to the discharges from both Blanchdown Adit and SWF Adit (a secondary adit in the south west of the site, Figure 3.20). The iron-rich waters emerging from Blanchdown Adit, precipitate as a deep $Fe(OH)_{(s)}$ (ochre) layer upon contact with the atmosphere. This process has the potential to scavenge other metals from solution, reducing the concentrations of some metals (Cu, Zn, Cd, Ni, Mn) before the discharge waters enter the River Tamar. Waters in the final collection drain, are oxic and low in dissolved Fe. Under such conditions, further precipitation of fresh $Fe(OH)_3$ phases is unlikely and the waters will discharge metals into the river at the concentrations reported here. This increases the impact of the final collection drain discharge compared with Blanchdown Adit, when flows are of a similar magnitude.

The average particulate flux of Cu, As, Zn and Ni entering the River Tamar via the final drain were determined during 2005-2006 as 0.098 μmol L^{-1} Cu, 0.0551 μmol L^{-1} As, 0.0629 μmol L^{-1} Zn and 0.0182 μmol L^{-1} (Mighanetara *et al.*, 2009). In all cases the particulate flux leaving the drain is very low compared to the dissolved flux, being most significant for As.

Concentrations of dissolved As were high and dissolved Fe low in waters emerging from South Wheal Fanny Shaft (sample 11), compared to other sample sites. pH and DO were also relatively high (section 3.7.5) and waters from this issue and exhibit character similar to the cinders drainage shown by the PCA.

Similarly, approximately 300 m south west of South Wheal Fanny Shaft, another discharge recorded as "South Wheal Fanny Adit" (Figure 21, SA) was sampled between 1992 and 1994 (EA data). It was similar to other waters sampled in south western area of the site, being characterised by high dissolved As and low dissolved metal contamination. The waters issuing in the south west part of the site appear not to be deep waters from the underground workings, the direction of subsurface flow being east toward Blanchdown Adit. Instead the waters issuing around South Wheal Fanny are likely to be cinders and WAM tip drainage preferentially migrating through the sub-surface via the underground workings (as suggested in Figure 3.20).

Figure 3.23: Dissolved metal and arsenic concentrations in final collection drain (FCD, white boxes), boreholes (grey boxes) and adit discharges (dark grey boxes) at Devon Great Consols. Key: 1 = FCD discharge to River Tamar (Environment Agency, 1992-1994), 2= FCD discharge to River Tamar (Mighanetara, 2005-2006), 3: FCD samples (current study, locations 19-23), BH= Boreholes 1-4 (current study), BA = Blanchdown Adit (Mighanetara, 2005-2006), SS = South Wheal Fanny Shaft, current study, SA = South Wheal Fanny Adit, (Environment Agency, 1992-1994, No data for Cd).

3.7.9   Estimated Annual Contamination Fluxes from the Final Collection Drain and Tip Drainage

Final Collection Drain (FCD)

The estimated contaminant flux leaving the DGC site in the final drain was determined for this study from measured flow close to the discharge point (at location 23) and dissolved concentration of the contaminant on each sampling round. Mean, minimum and maximum loads were calculated per annum based on the data from this study and compared with those from the same location, Blanchdown adit and the River Tamar at Gunnislake during 2005-2006 (Table 3.12). Blanchdown adit was shown to discharge the highest annual flux of Fe, As, Mn, and Ni from surveyed adits in the catchment (Table 3.12, based on unpublished monthly data, Mighanetara, (2005-2006)). Dissolved Cu, Zn and Cd fluxes were also found to be high in the adit discharge, representing 88 %, 75% and 21%, respectively of the highest identified in the Tamar catchment (Ding Dong Mine (Cu), and South Tamar Mine (Zn and Cd)).

The annual flux entering the River Tamar from the FCD for most elements was similar in magnitude to the previous study and represents a significant proportion of the overall flux in the River Tamar immediately downstream. For example, based on 2005-2006 survey data approximately 11 % of the dissolved Cu is attributable to the final collection drain. However in addition to the reduced variability, which was attributed to the wet versus dry sampling periods (see section 3.7.8), the mean and maximum fluxes in this work (2008-2009) were generally higher than found by Mighanetara (2005-2006). For example mean annual Cu and Zn loads calculated from the current study data were 53000 mol y^{-1} and 8840 mol y^{-1}, respectively, compared to 22500 mol y^{-1} and 4450 mol y^{-1} previously. Figure 3.23 showed concentrations in the previous study were generally comparable with this study, while the stability of concentrations between

184

surveys and along the drain suggests the waters were approaching equilibrium with respect to surrounding pore waters. Therefore the additional flux in the latest survey was mostly due to the higher flow in the drain observed in this study (mean annual flow 22.7 L s^{-1}) compared to previously (mean annual flow 13.2 L s^{-1}).

The predicted annual flux of dissolved metals from the FCD was compared to that from Blanchdown Adit and was found to be the same order of magnitude for Zn, Cd, Ni and Mn. However the predicted annual flux of dissolved Cu was much greater in the FCD (4660-75200 mol y^{-1}, Table 3.12) than in the Blanchdown Adit discharge (999-5230 mol y^{-1}). Also the predicted fluxes of dissolved Fe and As were much lower in the FCD (443-5230 mol y^{-1} and 16.9-277 mol y^{-1}, respectively) than from Blanchdown Adit (3890-23900 mol y^{-1} and 279-5233 mol y^{-1}, respectively). These figures give a useful measure of the annual contamination flux reaching the River Tamar as point discharges from the final drain and Blanchdown Adit. They also suggest that if Fe-rich waters from Blanchdown Adit could be mixed with the Cu-rich waters in the final drain and allowed to reach equilibrium with atmospheric O_2, attenuation of the dissolved Cu (and other dissolved metals such as Zn, Ni, Cd and Pb) in the waters of the final drain may be achieved.

Waste Tips

Annual dissolved fluxes of metals and As emanating from the tips were estimated using a different approach, since direct measurement of diffuse flow through a waste tip is prohibitively difficult. The extent of each waste tip area was digitised based on aerial photography and observations made at the site during sampling. Tip catchment areas were defined using ArcGIS v 9.3 with the ArcHydro extension from a 10 m digital terrain model. Estimated average rainfall for the site was calculated based on downloaded Met Office data from MIDAS observation stations (see Chapter 2 for

method). Catchment rainfall for each of the tips is assumed to represent the water flow moving over or through the waste and no correction was made for evaporation or plant uptake. Dissolved concentrations for metals and As were multiplied by the annual rainfall for each tip catchment area to produce a annual flux. Data used in the calculations is provided in Table 3.16 (Appendix 3G).

Mean annual flux and inter-quartile range of metal and As fluxes for each tip were calculated (Table 3.13) and the relative contributions of each tip to the flux observed in the final drain (Table 3.14). Chloride flux was also calculated to compare the behaviour of a conservative ion. The results of the calculation show that mass balance (100%) between the combined tip and drain flux falls within the calculated range for most elements. There are exceptions, most notably for dissolved As, which was considerably higher in combined tip drainage (29400-35900 mol y^{-1}) than in the final drain (45.6-277 mol y^{-1}), suggesting attenuation of two orders of magnitude along the transport pathway. To a lesser extent fluxes of dissolved Pb and Cu are also lower in the final drain compared to leachates produced by the tips. Dissolved Zn and Cd show distribution in waters closest to Cl and therefore exhibit conservative transport.

Speciation of these metals was calculated as being divalent cations by PHREEQC under measured field conditions, and as such these elements would be expected to remain largely mobile in surface and subsurface drainage waters.

The higher predicted flux of As, Cu and Pb from the tips compared with the final drain suggests preferential sorption of these elements to mineral and organic surfaces, an effect that has been particularly documented for these elements in other studies. It cannot be absolutely concluded that the fate of most of the tip drainage is to discharge via the drain, but it appears that for Cl, Al, Mn, Zn, Ni, Cd the mean flux in the drain is larger than that from the tips. Additional inputs of contamination could arise from other areas of waste which fall within the catchment of the final collection drain

(FCD). The most obvious is the Wheal Anna Maria Lower tip (Figure 3), but this exhibits generally very low permeability (1.9-2.3 x 10^{-7} m s^{-1}, Mighaetara (2009)), standing water is consistently observed on its surface (photograph 10) and it comprises layers of firm clayey silt such that migrating waters are unlikely to permeate the tip. Coarser wastes, and contaminated soils are distributed across the site and have not been accounted for in this study, also the banks of the FCD appear to comprise mine wastes which have been washed down from the WAM Upper tip. All could act as an additional sources of contamination.

Some important information for quantification of fluxes within the site emerge from the annual flux data presented in Tables 3.12, 3.13 and 3.14 and previous discussion of elemental behaviour. The cinders waste was the major source of dissolved arsenic at the site by an order of magnitude over Blanchdown Adit. Sorption of As to iron-hydroxides is well documented and appears to attenuate almost all of the As from the tips before reaching the River Tamar, although some sub-surface migration has been demonstrated by borehole water samples. Wheal Anna Maria Upper tip was the largest contributor of dissolved Cu reaching the final drain, some of this appears to be attenuated on route to the River Tamar. Collectively, the tips also have the potential to produce around the same annual flux of Mn, Zn, Ni and Cd as Blanchdown Adit, and it appears these metals within the tip drainages are conservatively transported and discharged to the River Tamar via the final drain.

Uncertainty

Estimates based on the data gathered from this study suggest that at one extreme, up to 65% of the flux of Zn, Mn, Ni, and Cd from the final drain could migrate to the River Tamar as diffuse seepages through the phreatic zone (Table 3.14). There is a lack of information on the magnitude sub-surface flow beyond the FCD to the River

Tamar via high permeability deposits, although the presence of elevated concentrations of dissolved metals and As in the subsurface has been identified in this study.

Large ranges are observed in Table 3.14, this is because tip fluxes are estimated from annual average rainfall and mean (and inter-quartile) dissolved concentrations. These two variables are not independent and the relationship between the two is lost when averaging data in this way. Tips are reactive to hydrological conditions in terms of the concentration and volume of leachate produced. For example, in dry conditions high dissolved loads may accumulate in tip pore waters, but flow from the tips is low. Conversely, in wet conditions higher flow is observed but concentrations may be lower if pore waters do not reach equilibrium. The scenario is complicated further as the kinetics of dissolution and desorption reactions compete with flow rate of percolating waters and these effects are explored in Chapter 5. The situation in the final drain is different; drain fluxes are based on accurate instantaneous flow and concentration determinations so if concentrations depend on flow, this is accounted for.

Scaling up the minimum and maximum instantaneous flux to an annual maximum and minimum is perhaps unrealistic based on the limited number of samples taken and the range of hydrological conditions that may be encountered. Comparison of the mean drain flux gives the best overall picture since the extremes are somewhat smoothed but this does not solve the problem of representivity.

Also, the modelled rainfall data used to calculate tip drainage is based on a 1999-2009 average. Rainfall at the nearest observation station (Millhill) for the main sample period (2008-2009) was 13% higher than the 1999-2009 average. If this is carried through the calculations the result would be an increase in the flux from the tips but would not account for the 'missing' flux observed in the drain and would not alter the overall trends observed.

Table 3.12: Estimated annual dissolved contaminant fluxes entering the River Tamar from the Devon Great Consols final collection drain and Blanchdown Adit . Data marked with asterisk from Mighanetara, 2007. ND = no data. Flow from Blanchdown Adit during 2005-2006 survey = 4.0-145 L s^{-1} (Mighanetara 2009).

Study	Cu (mol y^{-1})	Zn (mol y^{-1})	Mn (mol y^{-1})	Ni (mol y^{-1})	Cd (mol y^{-1})	Pb (mol y^{-1})	Al (mol y^{-1})	As (mol y^{-1})	Fe (mol y^{-1})
2008-2009 Final Collection Drain Range Mean, n=4	15100-75200 **53000**	2660-13300 **8840**	12100-60000 **39400**	405-2000 **1290**	4.14-22.0 **13.8**	1.21- 3.60 **2.68**	125000- 629000 **434000**	45.6-277 **164**	439-1910 **1060**
2005-2006 Final Collection Drain Range* **Mean,** n=12	4660-42600 **22500**	1480-8950 **4450**	102-35000 **19000**	59.7-1400 **638**	2.38-22.0 **7.50**	0.53 -7.13 **2.19**	 ND	16.9-160 **80.7**	443-5012 **2470**
2005-2006 Blanchdown Adit Range* **Mean,** n=12	999-5230 **3780**	2400-22600 **7690**	4820-45900 **23900**	224-1940 **789**	1.01-11.93 **4.33**	<LOD	ND	279-5233 **2570**	3890-239000 **61867**
2005-2006 River Tamar at Gunnislake*	205000	107050	473000	76700	<LOD	232	ND	32000	985000
% Dissolved Flux in River Tamar from FCD, 2005-2006	11	4	4	< 1	-	< 1	-	3	< 1
% Dissolved Flux in River Tamar from Blanchdown Adit, 2005-2006	2	7	5	< 1	-	-	-	8	6

Table 3.13: Estimated annual dissolved contaminant fluxes of selected metals and As produced by the Cinders, Wheal Anna Maria Upper and Precipitation Launders waste tips at Devon Great Consols. Derived from catchment rainfall and dissolved metal concentrations from selected sample locations. Inter-quartile range and mean concentrations used to derive range and mean fluxes (mean shown in bold). Sample locations used: cinders drain (1), WAM tip drainage (4-8), precipitation launders (BH5 and 17).

Tip, Area (m^2), Annual Average Rainfall (mm y^{-1})	Cu (mol y^{-1})	Zn (mol y^{-1})	Mn (mol y^{-1})	Ni (mol y^{-1})	Cd (mol y^{-1})	Pb (mol y^{-1})	Al (mol y^{-1})	As (mol y^{-1})
Cinders Waste Tip 84400 m^2, 1289 mm y^{-1}	1130 – 1390 **1410**	223 – 259 **244**	362 – 487 **422**	27.4 – 31.8 **31.0**	0.213 -0.228 **0.222**	< LOD	16400 – 17200 **16700**	29400 – 35600 **32000**
Wheal Anna Maria Upper Tip 135000 m^2, 1289 mm y^{-1}	34900 – 46400 **38900**	2070 – 2240 **2180**	5570 – 7250 **6410**	157 – 227 **192**	3.35 – 4.32 **3.76**	1.06 -3.42 **2.60**	121000 – 15600 **143000**	50.3 – 286 **231**
Precipitation Launders Tip 116000 m^2, 1264 mm y^{-1}	14900 – 19100 **16800**	1970 – 2600 **2240**	10200 – 14600 **11900**	343 – 479 **398**	3.25 – 4.30 **3.65**	0.48 – 2.08 **1.29**	103000 -148000 **121000**	11.7 – 22.0 **20.5**
Combined Tip Discharge	50900 - 66900 **57100**	4270 - 5135 **4670**	16100 - 22300 **18700**	527 -738 **621**	6.81 -8.85 **7.63**	1.54 - 5.50 **3.90**	240000 - 321000 **281000**	29400-35900 **32200**

Table 3.14: Annual Fluxes of selected metals and As produced by the Cinders, Wheal Anna Maria Upper and Precipitation Launders waste tips as a percentage of annual fluxes determined in the final collection drain. Based on mean (in bold) and inter- quartile ranges. Chloride also shown as representative of a conservative element.

	Cl (%)	Cu (%)	Zn (%)	Mn (%)	Ni (%)	Cd (%)	Pb (%)	Al (%)	As (%)
Cinders Waste Tip	**12.1** (10.7-35.4)	**2.7** (1.8 - 7.5)	**2.8** (1.9 - 8.4)	**1.1** (0.8 - 3.0)	**2.4** (1.6 - 6.8)	**1.6** (1.0 -5.2)	n/a	**3.8** (2.7 - 13.1)	**19500** (12900 -64400)
Wheal Anna Maria Upper Tip	**26.5** (20.1-78.5)	**73.3** (61.6 - 240)	**24.6** (16.9 - 78.0)	**16.3** (12.1 - 46.0)	**14.9** (11.4 - 38.8)	**27.3** (19.6 - 78.5)	**97.1** (87.4-94.9)	**32.9** (24.9 - 96.5)	**141** (103 - 110)
Precipitation Launders Tip	**18.4** (13.2-60.8)	**31.8** (25.5 - 98.6)	**25.4** (19.8 - 74.0)	**30.2** (24.3 - 89.3)	**30.9** (24.0 - 84.7)	**26.4** (19.6 - 78.5)	**48.1** (39.9 - 57.7)	**27.9** (23.5 - 82.2)	**12.5** (7.9 - 25.7)
Combined Tips	**56.9** (44.1-175)	**108** (89.0 - 337)	**58.2** (38.6 - 160)	**47.6** (37.2 – 133)	**48.1** (36.9 - 130)	**55.3** (40.2 - 165)	**145** (127 - 153)	**64.6** (51.1 - 192)	**19600** (13000 - 64500)

3.8   Conclusions and Recommendations

During this study, leachates were observed to issue from the mine waste tips at Devon Great Consols following periods of heavy short term rainfall (> 45 mm in 7 days). The concentrations of dissolved metals in the issuing waters were very high compared to EQS values and highly variable e.g. dissolved Al and Cu in drainage from Wheal Anna Maria (WAM) tip ranged from 591-1145 μmol L^{-1} and 135-387 μmol L^{-1}, respectively. Drainage waters emanating the cinders, WAM and precipitation launders waste tips were in excess of EQS values for dissolved Al, Cu, Zn, Ni, Cd, Mn, Fe and As.

The three areas of waste studied exhibited distinct geochemical signatures; dissolved Cu and Al were particularly high in WAM drainage compared to other discharges in the catchment, whilst the cinders tip produced oxic drainage waters very high in dissolved As (202-378 μmol L^{-1}). Annual fluxes from the tip were predicted using average rainfall data and catchment areas calculated in ArcHydro9 to estimate the annual discharge of waters from the tip. The results showed that the cinders waste could generate an annual flux of dissolved As equal to 32000 mol y^{-1} and Wheal Anna Maria Upper tip an annual flux of Cu equal to 38900 mol y^{-1}, based on concentrations recorded in this study. Drainage waters from the precipitation launders were highest in Mn and Ni equating to predicted fluxes of 11900 and 398 mol y^{-1}, respectively. Other metals were also high in tip drainage with maximum predicted fluxes equal to 143000 mol y^{-1} Al (WAM), 2240 mol y^{-1} Zn (launders) and 376 mol y^{-1} Cd (WAM).

The predicted annual fluxes from the three tips investigated at Devon Great Consols were the same order of magnitude as previously predicted for the main adit discharge at the mine (Blanchdown Adit, Mighanetara (2009)) for Mn, Zn, Ni and Cd.

For some elements, the flux from the tips could represent a significant proportion of the dissolved flux in the River Tamar at Gunnislake, (e.g. Cu estimated at 11%).

However, there was evidence for the natural attenuation of some elements prior to reaching the final collection drain (FCD), which discharged into the River Tamar approximately 350m down gradient from the tips. For As this was sufficient to reduce the discharge concentrations below EQS. Other dissolved species of interest, namely Cu, Al, Zn, Mn, Ni, Cd and sulphate exhibited a steady composition (RSD ≤ 12.1 % across all surveys). This suggested that local equilibrium was achieved in the drain, but evidence from previous studies conducted in relatively dry summers (1994-1995 and 2005-2006), indicate that more variability may be expected in periods of drought.

Based on predicated annual flux, the final collection drain (FCD) appears to capture most of the dissolved contamination flowing through the site, offering a low resistance and oxic pathway for migrating waters. Accurate determination of the proportion of dissolved contamination leaving the site in the FCD versus the total produced from the tips is not permissible with such a limited data set. However, the combined predicted fluxes from the main areas of waste studied was the same order of magnitude to that in the final drain for elements that are less likely to be attenuated by sorption to mineral surfaces or organic matter. Recovery in the final drain for Cl, Zn, and Cd was between 39 and 175 %. This was encouraging, as it suggested that the method used to calculate fluxes from the waste tips was appropriate and that the results were a good approximation of annual fluxes. Additional flux in the drain may arise from contaminated soils and coarser wastes within the catchment of the final drain, including the banks of the drain itself, which appeared to be partially comprised of mine waste similar to that found in the WAM tip.

The FCD is hosted in high permeability artificial (mine waste) and alluvial deposits (river gravels). The shallow groundwaters around the drain were found to be in

local equilibrium with waters flowing in the drain with respect to dissolved metals. They may therefore represent an additional transport pathway to the River Tamar.

Borehole 4 located approximately 10m beyond the final drain at a depth of 1.71 m below a shallow ditch (itself 0.5 m below ground level) was also contaminated with mine waters. This was evidence for horizontal transport of contamination towards the river, since the borehole core removed was characterised by clay and hardpan layers which were inhibited vertical migration of waters. Layers of clay, hardpan and gley soils containing preserved organic matter were also encountered in BH2, BH3 and BH6, suggesting a large spatial extent of impermeable strata and anoxic conditions at shallow depths (< 2m). Groundwater was likely to be the most important transport pathway for Fe and As from the tips as they exhibit higher mobility under reducing conditions. A previous study, estimated 55% of dissolved As to be unaccounted for in the River Tamar by streams and adit discharges (Mighanetara *et al.*, 2009). A portion of this may be due to subsurface transport, since As concentrations were recorded in borehole waters up to 13.7 μmol L^{-1}.

Based on the concentrations of dissolved metals leaving the final drain (location 23) and the relative magnitudes of measured flow in the drain and the river (1:685, mean), both dissolved Al and Cu, were very likely to cause an EQS failure in the River Tamar as a result of this discharge. The higher pH of the river water (pH 7.6-8.7, EA 1997-2008) is likely to reduce the dissolved concentration of metals by enhancing sorption and precipitation. However, there have been frequent recorded failures with respect to EQS for Cu, Zn and Cd downstream of Devon Great Consols (EA, 1997-2008). There are a number of mine sites in the vicinity of Devon Great Consols that contribute to the overall contamination in the River Tamar but the flux discharging from the final drain is a significant contributor of dissolved metal contamination to the River.

Iron solubility in drainage waters at the site were poised around the Fe(II)/Fe(III) solubility boundary for most samples. WAM Upper Tip drainage and subsurface waters contain elevated dissolved Fe(III) which according to PHREEQC calculations and site observations, precipitated as fresh Fe(OH)s upon reaching equilibrium with the atmosphere. This was most obvious in final drain, where thick (tens of centimetres) layers of ochre were deposited on the banks and base of the drain. Sorption of dissolved metals and particularly As was likely to be the dominant attenuation process at the site. The pH of waters in the lower part of the site was buffered to ~ pH 4.5 and indicated that in addition to the concentration of metals a relatively stable pH was also maintained. In the absence of significant carbonate minerals at the site, dissolution of Al-phases maintained the pH balance and resulted in the high discharge of dissolved Al from the drain (434000 mol y^{-1}).

Artificial enhancement of the sorption capacity of freshly precipitated $Fe(OH)_3$ may be a means of removing pollutant metals (e.g. Cu) from solution before discharging to the River Tamar. Factors which might promote this would be a greater surface area of precipitate for sorption, a greater residence time of waters passing through the drain and greater aeration of the waters. This might be achieved by expanding existing ditches to aerate migrating waters moving through the site. However disturbance of the system should be kept to a minimum to prevent the exposure of fresh mineral surface to weathering which may increase pollutant fluxes in the short-term. The waters draining Blanchdown Adit are rich in dissolved Fe and relatively low in dissolved Cu, compared with the waters in the final drain. A scheme to mix the two discharges followed by aeration may reduce the overall pollutant flux discharging into the River Tamar but would require further investigation.

Finally, the mine waste at Devon Great Consols, particularly the WAM upper tip exhibits poor cohesive strength and poor vegetation cover. This results in a high

dissolved and suspended load in tip run off. Mighanetara (2009) estimated the annual loss from the WAM Upper tip to be 200-300 m^3 y^{-1} of material from the three slopes (east, south and west). Management strategies which address the high permeability and low stability of the waste tips are likely to reduce the flux of dissolved contamination arising from them.

3.9 Future Work

A number of assumptions have been made in predicting contaminant fluxes emanating the waste tips. Among them is the extrapolation of limited data for concentrations emerging the tips into yearly fluxes. This work has highlighted that mine waste has the potential to generate large fluxes of pollutant metals and metalloids. It has also indicated that the observed flux is determined largely by the hydrological conditions at the site. In Chapter 5 the leaching potential of selected mine wastes will be examined under laboratory conditions to simulate the action of percolating rainwater. This will help to resolve the range of concentrations of metals and As that may be expected in discharge waters under all hydrological conditions.

Selective dissolution of source minerals and the competitive sorption of dissolved metals and metalloids influence the chemistry of discharge waters. Further investigation of these competitive effects in mixed mineral systems would aid the interpretation of transport processes occurring at abandoned mine sites. It may also be a basis for screening possible remediation strategies.

The speciation of the dissolved metals has not been explored here in great detail but is important in understanding the toxicological effects of pollutants in the aquatic environment. In stream processes and species tolerance should be examined in order to determine the actual eco-toxic effect of the pollutant discharges in the Tamar catchment.

3.10 References

Abraitis, P. K., Pattrick, R. A. D., Kelsall, G. H. and Vaughan, D. J. (2004). Acid Leaching and dissolution of major sulphide ore minerals: processes and galvanic effects in complex systems. *Mineralogical Magazine.* **68** (2) pp 343-51.

Álvarez, E., Fernández Marcos, M. L., Vaamonde, C. and Fernández-Sanjurjo, M. J. (2003). Heavy metals in the dump of an abandoned mine in Galicia (NW Spain) and in the spontaneously occurring vegetation. *The Science of The Total Environment.* **313** (1-3) pp 185-97.

Asta, M. P., Ayora, C., Román-Ross, G., Cama, J., Acero, P., Gault, A. G., Charnock, J. M. and Bardelli, F. (2010). Natural attenuation of arsenic in the Tinto Santa Rosa acid stream (Iberian Pyritic Belt, SW Spain): The role of iron precipitates. *Chemical Geology.* **271** (1-2) pp 1-12.

Balistrieri, L. S., Seal Ii, R. R., Piatak, N. M. and Paul, B. (2007). Assessing the concentration, speciation, and toxicity of dissolved metals during mixing of acid-mine drainage and ambient river water downstream of the Elizabeth Copper Mine, Vermont, USA. *Applied Geochemistry.* **22** (5) pp 930-52.

Ball, J. and Nordstrom, D. (1991). *User's Manual for WATEQ4F with revised thermodynamic database and test cases for calculating speciation of major, trace and redox elements in natural waters. Water-Resourses Investigation Report.* U.S. Geological Survey. pp 91-103.

Bass, J. A. B., Blust, R., Clarke, R. T., Corbin, T. A., Davidson, W., de Schamphelaere, K. A. C., Janssen, C. R., Kallis, E. J. J., Kelly, M. G., Kneebone, N. T., Lawlor, A. J., Lofts, S., Temminghoff, E., Thacker, S. A., Tipping, C. D., Vincent, K. w. and Zhang, H. (2008) *Environmental Quality Standards for trace metals in the aquatic environment* E. Agency Report No. Science Report - SC030194

Beaucaire, C., Michelot, J. L., Savoye, S. and Cabrera, J. (2008). Groundwater characterisation and modelling of water-rock interaction in an argillaceous formation (Tournemire, France). *Applied Geochemistry.* **23** (8) pp 2182-97.

Bech, J., Poschenrieder, C., Llugany, M., Barceló, J., Tume, P., Tobias, F. J., Barranzuela, J. L. and Vásquez, E. R. (1997). Arsenic and heavy metal contamination of soil and vegetation around a copper mine in Northern Peru. *Science of the Total Environment.* **203** (1) pp 83-91.

Benjamin, M. M. and Leckie, J. O. (1981). Multiple-site adsorption of Cd, Cu, Zn, and Pb on amorphous iron oxyhydroxide. *Journal of Colloid and Interface Science.* **79** (1) pp 209-21.

BGS (2003). *Water Quality Fact Sheet: Manganese* British Geological Survey.

BGS (2009). DigMap, Permeability Indices (Version 5), British Geological Survey. NERC.

Booker, F. (1967). *The Industrial Archaeology of the Tamar Valley*. Newton Abbot, David & Charles Ltd.pp 303 pp 130

Buck, C. (2002). *Devon Great Consols Archeological Assessment.*2002R069 Cornwall Archeological Unit, Cornwall County Council. Truro.

Buckley, A. N. and Woods, R. (1984). An x-ray photoelectron spectroscopic study of the oxidation of galena. *Applications of Surface Science.* **17** (4) pp 401-14.

Buckley, A. N., Wouterlood, H. J. and Woods, R. (1989). The surface composition of natural sphalerites under oxidative leaching conditions. *Hydrometallurgy.* **22** (1-2) pp 39-56.

Buffle, J., Chalmers, R. A., Masson, M. R. and Midgley, D. (1988). *Complexation reactions in aquatic systems*, E. Horwood. pp 692

Cama, J. and Acero, P. (2005). Dissolution of Minor Sulphides Present in a Pyritic Sludge at pH 3. *Geologica acta: an international earth sciece journal.* **3** (1) pp 15-26.

Cánovas, C. R., Hubbard, C. G., Olías, M., Nieto, J. M., Black, S. and Coleman, M. L. (2008). Hydrochemical variations and contaminant load in the Río Tinto (Spain) during flood events. *Journal of Hydrology.* **350** (1-2) pp 25-40.

Carrillo, A. and Drever, J. I. (1998). Adsorption of arsenic by natural aquifer material in the San Antonio-El Triunfo mining area, Baja California, Mexico. *Environmental Geology.* **35** (4) pp 251-7.

Casiot, C., Lebrun, S., Morin, G., Bruneel, O., Personné, J. C. and Elbaz-Poulichet, F. (2005). Sorption and redox processes controlling arsenic fate and transport in a stream impacted by acid mine drainage. *Science of the Total Environment.* **347** (1-3) pp 122-30.

CEH.(2011). "National River Flow Archive." Centre for Ecology and Hydrology. Accessed 12/02/2011. Avaliable on the world wide web at: http://www.ceh.ac.uk/data/nrfa/data/search.html.

Chakraborty, P. and Chakrabarti, C. L. (2006). Chemical speciation of Co, Ni, Cu, and Zn in mine effluents and effects of dilution of the effluent on release of the above metals from their metal-dissolved organic carbon (DOC) complexes. *Analytica Chimica Acta.* **571** (2) pp 260-9.

Cheng, H., Hu, Y., Luo, J., Xu, B. and Zhao, J. (2009). Geochemical processes controlling fate and transport of arsenic in acid mine drainage (AMD) and natural systems. *Journal of Hazardous Materials.* **165** (1-3) pp 13-26.

CMWH.(2010). "Cornish Mining World Heritage." Cornwall Council Accessed 12th April 2010. Avaliable on the world wide web at: http://www.cornish-mining.org.uk/project/aboutus.htm.

Coles, S. P. (1999) *Automated Flow Injection Instrument For Monitoring Nitrogen Species in Natural Waters* PhD Thesis.University of Plymouth.pp205-9

Costantini, S., Giordano, R., Beccaloni, E., Perani, C. and Grego, S. (1992). Experimental approach to aluminum phytotoxicity. *Microchemical Journal.* **46** (1) pp 20-9.

Crane, M., Sorokin, N., Atkinson, C. and Maycock, D. (2007). *Proposed Eqs for Water Framework Directive Annex VIII substances: manganese (total and dissolved).*SC040038 Environment Agency. pp 72.

da Silva, G. (2004). Kinetics and mechanism of the bacterial and ferric sulphate oxidation of galena. *Hydrometallurgy.* **75** (1-4) pp 99-110.

Dines, H. G. (1956). *The metalliferous mining region of south-west England*, HMSO.pp 709 pp

Dold, B. (2005). *Basic Concepts of Environmental Geochemistry of Sulphide Mine Waste*. Proceedings of the XXIV Curso Lantinoamericano de Metalogenia UNESCO-SEG, Lima, Peru.

Dong, D.-l., Wu, Q., Zhang, R., Song, Y.-x., Chen, S.-k., Li, P., Liu, S.-q., Bi, C.-c., Lv, Z.-q. and Huang, S.-l. (2007). Environmental Characteristics of Groundwater: an Application of PCA to Water Chemistry Analysis in Yulin. *Journal of China University of Mining and Technology.* **17** (1) pp 73-7.

Du Laing, G., Rinklebe, J., Vandecasteele, B., Meers, E. and Tack, F. M. G. (2009). Trace metal behaviour in estuarine and riverine floodplain soils and sediments: A review. *Science of the Total Environment.* **407** (13) pp 3972-85.

Duester, L., van der Geest, H. G., Moelleken, S., Hirner, A. V. and Kueppers, K. (2011). Comparative phytotoxicity of methylated and inorganic arsenic- and

antimony species to Lemna minor, Wolffia arrhiza and Selenastrum capricornutum. *Microchemical Journal.* **97** (1) pp 30-7.

Dutrizac, J. (1981). The dissolution of chalcopyrite in ferric sulfate and ferric chloride media. *Metallurgical and Materials Transactions B.* **12** (2) pp 371-8.

Dutrizac, J. C. and MacDonald, R. J. C. (1973). The effect of some impurities on the rate of chalcopyrite dissolution. *Canadian Metallurgy Quarterly.* **12** (4) pp 409-20.

DWI (2009). Fluoride Standard for UK Drinking Water. Online at: http://www.dwi.gov.uk/consumers/advice-leaflets/fluoridemap.pdf, Drinking Water Inspectorate

Dybowska, A., Farogo, M., Valsami-Jones, E. and Thornton, L. (2005). Operationally defined associations of arsenic and copper from soil and mine waste in south-west England. *Chemical Speciation and Bioavailability.* **17** (4) pp 147-60.

EA.(2008). "Gauging Station Summary Sheets : River Tamar." Centre for Ecology and Hydrology. Accessed 30/09/2010. Avaliable on the world wide web at: http://www.nwl.ac.uk/ih/nrfa/station_summaries/047/001.html.

EA (2009). *Contaminants in Soil: updated collation of toxicological data and intake values for humans. Inorganic arsenic.*Science Report SC050021 Environment Agency. Bristol.

EA.(2010). "Soil Guidline Value Reports published using the new approach." Environment Agency. Accessed 16/08/10. Avaliable on the world wide web at: http://www.environment-agency.co.uk/research/planning/64015.aspx.

Earle, J. and Callaghan, T. (1988). Impacts of Mine Drainage on Aquatic Life, Water Uses, and Man-Made Structures. *Coal Mine Drainage Prediction and Pollution Prevention in Pennsylvania.* K. B. C. Brady, M. Smith and J. Shueck. Harrisburg, USA, Department of Environmental Protection.

Edwards, R. W., Gee, A. S. and Stoner, J. H., Eds. (1990). *Acid Waters in Wales.* Dordrecht, Kluwer Academic Publishers.

Evangelou, V. P. (1995). *Pyrite oxidation and its control.* Florida, CRC Press. pp 85-86

Evangelou, V. P. and Zhang, Y. L. (1995). A review: Pyrite oxidation mechanisms and acid mine drainage prevention. *Critical Reviews in Environmental Science and Technology.* **25** (2) pp 141 - 99.

Fawell, J. K. (2010). *Aluminium in Drinking-water. Background document for development of*

WHO Guidelines for Drinking-water Quality
 World Health Organisation. Geneva. pp 23.

Filella, M., Belzile, N. and Chen, Y.-W. (2002). Antimony in the envronment: a review focussed on natural waters. I Occurrence. *Earth Science Reviews.* **57** pp 125-76.

Fu, Z., Wu, F., Amarasiriwardena, D., Mo, C., Liu, B., Zhu, J., Deng, Q. and Liao, H. (2010). Antimony, arsenic and mercury in the aquatic environment and fish in a large antimony mining area in Hunan, China. *Science of the Total Environment.* **408** (16) pp 3403-10.

Griffitt, R. J., Luo, J., Gao, J., Bonzongo, J.-C. and Barber, D. S. (2008). Effects of particle composition and species on toxicity of metallic nanomaterials in aquatic organisms. *Environmental Toxicology and Chemistry.* **27** (9) pp 1972-8.

Haaijer, S. C. M., Harhangi, H. R., Meijerink, B. B., Strous, M., Pol, A., Smolders, A. J. P., Verwegen, K., Jetten, M. S. M. and Op den Camp, H. J. M. (2008). Bacteria associated with iron seeps in a sulfur-rich, neutral pH, freshwater ecosystem. *ISME J.* **2** (12) pp 1231-42.

Hamilton Jenkin, A. K. (1974). *Mines of Devon Volume 1: The Southern Area.* Newton Abbot, David & Charles. pp 17-35

Harley, A. D. (2010). *Ambient Water Quality Standards for Iron - Review and Update* Colorado Mining Association, prepared by R Squared Incorporated Denver, USA.

Harris, D. L., Lottermoser, B. G. and Duchesne, J. (2003). Ephemeral acid mine drainage at the Montalbion silver mine, north Queensland. *Australian Journal of Earth Sciences.* **50** (5) pp 797-809.

Herrmann, J. (1987). Aluminium impact on freshwater invertebrates at low pH: A review. *Speciation of Metals in Water, Sediment and Soil Systems*. L. Landner, Springer Berlin / Heidelberg. **11** pp 157-75.

Hiroyoshi, N., Hirota, M., Hirajima, T. and Tsunekawa, M. (1997). A case of ferrous sulfate addition enhancing chalcopyrite leaching. *Hydrometallurgy.* **47** (1) pp 37-45.

Hudson-Edwards, K. A. (2003). Sources, mineralogy, chemistry and fate of heavy metal-bearing particles in mining-affected river systems. *Mineralogical Magazine.* **67** (2) pp 205-17.

Hulshof, A. H. M., Blowes, D. W. and Douglas Gould, W. (2006). Evaluation of in situ layers for treatment of acid mine drainage: A field comparison. *Water Research.* **40** (9) pp 1816-26.

INAP.(2009). "Global Acid Rock Drainage Guide (GARD Guide)." International Network for Acid Prevention. Accessed 14/09/10. Avaliable on the world wide web at: http://www.gardguide.com/.

Kairies, C. L., Capo, R. C. and Watzlaf, G. R. (2005). Chemical and physical properties of iron hydroxide precipitates associated with passively treated coal mine drainage in the Bituminous Region of Pennsylvania and Maryland. *Applied Geochemistry.* **20** (8) pp 1445-60.

Kang, S. and Sproull, R. (1991). Iron Oxidation by Thiobacillus ferrooxidans. *Applied Biochemistry and Biotechnology.* **28-29** (1) pp 907-15.

Kavanagh, P. J., Farago, M. E., Thornton, I. and Braman, R. S. (1997). Bioavaliability of arsenic in soils and mine wastes of the Tamar valley, SW England. *Chemical Speciation and Bioavailability.* **9** (3) pp 77-81.

Kinraide, T. B. (1997). Reconsidering the rhizotoxicity of hydroxyl, sulphate, and fluoride complexes of aluminium. *J. Exp. Bot.* **48** (5) pp 1115-24.

Klink, B. A., Palumbo, B., Cave, M. and Wragg, J. (2005). *Arsenic dispersal and bioccessibility in mine contaminated soils: a case study from an abandoned arsenic mine in Devon, UK*.Research Report RR/04/003 British Geological Survey pp 52.

Klöppel, H., Fliedner, A. and Kördel, W. (1997). Behaviour and ecotoxicology of aluminium in soil and water - Review of the scientific literature. *Chemosphere.* **35** (1-2) pp 353-63.

Kozelka, P. B. and Bruland, K. W. (1998). Chemical speciation of dissolved Cu, Zn, Cd, Pb in Narragansett Bay, Rhode Island. *Marine Chemistry.* **60** (3-4) pp 267-82.

Kraukopf, K. B. and Bird, D. K. (1995). *Introduction to Geochemistry*. New York, McGraw-Hill Inc. pp

Krauskopf, K. B. and Bird, D. K. (1995). *Introduction to Geochemistry*. New York, McGraw-Hill Inc. pp

Kumar, N. and Nath, K. (1987). Toxicity of Nickel to a Fresh Water Teleost, Colisa fasciatus. *Acta hydrochimica et hydrobiologica.* **15** (3) pp 313-5.

Kwong, Y. T. J., Swerhone, G. W. and Lawrence, J. R. (2003). Galvanic sulphide oxidation as a metal-leaching mechanism and its environmental implications. *Geochemistry: Exploration, Environment, Analysis.* **3** (4) pp 337-43.

Langdon, C. J., Piearce, T. G., Meharg, A. A. and Semple, K. T. (2001). Survival and behaviour of the earthworms Lumbricus rubellus and Dendrodrilus rubidus from arsenate-contaminated and non-contaminated sites. *Soil Biology and Biochemistry.* **33** (9) pp 1239-44.

Lasier, P. J., Winger, P. V. and Bogenrieder, K. J. (2000). Toxicity of Manganese to <i>Ceriodaphnia dubia</i> and <i>Hyalella azteca</i>. *Archives of Environmental Contamination and Toxicology.* **38** (3) pp 298-304.

Lee, G., Bigham, J. M. and Faure, G. (2002). Removal of trace metals by coprecipitation with Fe, Al and Mn from natural waters contaminated with acid mine drainage in the Ducktown Mining District, Tennessee. *Applied Geochemistry.* **17** (5) pp 569-81.

Lee, J. S. and Chon, H. T. (2006). Hydrogeochemical characteristics of acid mine drainage in the vicinity of an abandoned mine, Daduk Creek, Korea. *Journal of Geochemical Exploration.* **88** (1-3) pp 37-40.

Lin, Z. (1997). Mineralogical and chemical characterization of wastes from the sulfuric acid industry in Falun, Sweden. *Environmental Geology.* **30** (3) pp 152-62.

Lollar, B. S., Ed. (2005). *Environmental Geochemistry.* Oxford, Elsevier.

Lottermoser, B. G. (2007). Mine Wastes: characterization, treatment and environmental impacts. Berlin, Springerpp 304.

Ma, X., Geiser-Lee, J., Deng, Y. and Kolmakov, A. (2010). Interactions between engineered nanoparticles (ENPs) and plants: Phytotoxicity, uptake and accumulation. *Science of the Total Environment.* **408** (16) pp 3053-61.

Mayes, W. M., Gozzard, E., Potter, H. A. B. and Jarvis, A. P. (2008). Quantifying the importance of diffuse minewater pollution in a historically heavily coal mined catchment. *Environmental Pollution.* **151** (1) pp 165-75.

Mayes, W. M., Johnston, D., Potter, H. A. B. and Jarvis, A. P. (2009). A national strategy for identification, prioritisation and management of pollution from abandoned non-coal mine sites in England and Wales. I.: Methodology development and initial results. *Science of the Total Environment.* **407** (21) pp 5435-47.

Mayes, W. M., Potter, H. A. B. and Jarvis, A. P. (2010). Inventory of aquatic contaminant flux arising from historical metal mining in England and Wales. *Science of the Total Environment.* **408** (17) pp 3576-83.

Mehta, A. P. and Murr, L. E. (1983). Fundemental studies of the contribution of galvanic interaction to acid-bacterial leaching of mixed metal sulphides. *Hydrometallurgy.* **9** pp 293.

MetOffice (2009) MIDAS Land Surface Observations Data British Atmospheric Data Centre. Accessed: Avaliable online at http://badc.nerc.ac.uk/data/ukmo-midas/.

Mighanetara, K. (2009) *Impact of Metal Mining on the Water Quality of the Tamar Catchment* PhD Thesis Thesis.University of Plymouth.pp248

Mighanetara, K., Braungardt, C. B., Rieuwerts, J. S. and Azizi, F. (2009). Contaminant fluxes from point and diffuse sources from abandoned mines in the River Tamar catchment, UK. *Journal of Geochemical Exploration.* **100** pp 116-24.

Milam, C. D. and Farris, J. L. (1998). Risk identification associated with iron-dominated mine discharges and their effect upon freshwater bivalves. *Environmental Toxicology and Chemistry.* **17** (8) pp 1611-9.

Mohan, D. and Chander, S. (2006). Removal and recovery of metal ions from acid mine drainage using lignite--A low cost sorbent. *Journal of Hazardous Materials.* **137** (3) pp 1545-53.

Moncur, M. C., Jambor, J. L., Ptacek, C. J. and Blowes, D. W. (2009). Mine drainage from the weathering of sulfide minerals and magnetite. *Applied Geochemistry.* **24** (12) pp 2362-73.

Moreno-Jiménez, E., Peñalosa, J. M., Manzano, R., Carpena-Ruiz, R. O., Gamarra, R. and Esteban, E. (2009). Heavy metals distribution in soils surrounding an abandoned mine in NW Madrid (Spain) and their transference to wild flora. *Journal of Hazardous Materials.* **162** (2-3) pp 854-9.

Navarro Flores, A. and Martínez Sola, F. (2010). Evaluation of Metal Attenuation from Mine Tailings in SE Spain (Sierra Almagrera): A Soil-Leaching Column Study. *Mine Water and the Environment.* **29** (1) pp 53-67.

Nordstrom, D. K., Alpers, C. N., Ptacek, C. J. and Blowes, D. W. (1999). Negative pH and Extremely Acidic Mine Waters from Iron Mountain, California. *Environmental Science & Technology.* **34** (2) pp 254-8.

Nordstrom, D. K. and Ball, J. W. (1986). The Geochemical Behavoir of Aluminium in Acidified Surface Waters. *Science.* **232** pp 54-6.

Nordstrom, D. K. and Southam, G. (1997). Geomicrobiology of sulfide mineral oxidation. *Reviews in Mineralogy and Geochemistry.* **35** (1) pp 361-90.

Nordstrom, D. K. and Wilde, F. D.(2005). "Reduction-Oxidation Potential (Electrode Method)." *USGS National Field Manual.* Accessed 12th March 2008. Avaliable on the world wide web at: http://water.usgs.gov/owq/FieldManual/Chapter6/6.5_contents.html.

O'Neill, P. (1998). *Environmental Chemistry.* London, Blackie Academic and Professional. pp

Olias, M., Nieto, J. M., Sarmiento, A. M., Ceron, J. C. and Canovas, C. R. (2004). Seasonal water quality variations in a river affected by acid mine drainage: the Odiel River (South West Spain). *Science of the Total Environment.* **333** (1-3) pp 267-81.

Page, K. (2008). *County Geological Sites in West Devon and their contribution to the Cornwall and West Devon Mining Landscape's World Hertitage Site, Notes from the Devonshire Association Excursion* SEOES, University of Plymouth.

Page, K. N. (2004). *Geodiversity Audit and interpretative review of the mining districts of the Tamar and Tavy rivers in West Devon. Part 1 - Geodiversity Audit and selection of County Geological Sites. A report to Devon County Council.*

Palumbo-Roe, B., Klinck, B. and Cave, M. (2007). Arsenic speciation and mobility in mine wastes from a copper-arsenic mine in Devon, UK: a SEM, XAS, sequential chemical extraction study. *Trace Metals and other Contaminants in the Environment.* P. Bhattacharya, A. B. Mukherjee, J. Bundschuh, R. Zevenhoven and H. L. Richard, Elsevier. **9** pp 441-71.

Parkhurst, D. L. and Appelo, C. A. J.(1999). "User's Guide to PHREEQC (Version 2)- A Computer Program for Speciation, Batch-Reaction, One-Dimensional Transport, and Inverse Geochemical Calculations." USGS. Accessed. Avaliable on the world wide web at: http://wwwbrr.cr.usgs.gov/projects/GWC_coupled/phreeqc/html/final.html.

Perdue, E. M., Beck, K. C. and Helmut Reuter, J. (1976). Organic complexes of iron and aluminium in natural waters. *Nature.* **260** (5550) pp 418-20.

Pettersson, C., Håkansson, K., Karlsson, S. and Allard, B. (1993). Metal speciation in a humic surface water system polluted by acidic leachates from a mine deposit in Sweden. *Water Research.* **27** (5) pp 863-71.

Poléo, A. B. S., Østbye, K., Øxnevad, S. A., Andersen, R. A., Heibo, E. and Vøllestad, L. A. (1997). Toxicity of acid aluminium-rich water to seven freshwater fish

species: A comparative laboratory study. *Environmental Pollution.* **96** (2) pp 129-39.

Poschenrieder, C., Gunsé, B., Corrales, I. and Barceló, J. (2008). A glance into aluminum toxicity and resistance in plants. *Science of the Total Environment.* **400** (1-3) pp 356-68.

Price, G. D. (2002). The distribution of trace metal pollutants within intertidal sediments of the Tamar Estuary, SW England. *Geoscience in south-west England.* **3** pp 319-22.

Richardson, P. H. G. (1995). *Mines of Dartmoor and the Tamar Valley after 1913.* Torquay, Devon Books.pp 160 pp 50-52

Rieuwerts, J., Austin, S. and Harris, E. (2009). Contamination from historic metal mines and the need for non-invasive remediation techniques: a case study from Southwest England. *Environmental Monitoring and Assessment.* **148** (1) pp 149-58.

Rodgers, N. J., Apte, S. C., Stuaber, J. L. and Storey, A. W. (2005). *Copper Speciation and Toxicity in the Fly River: A review.*ET/IR745R   Centre for Avanced Analytical Chemistry Energy Techology, CSIRO.

Romero, F. M., Armienta, M. A. and Gonzalez-Hernandez, G. (2007). Solid-phase control on the mobility of potentially toxic elements in an abandoned lead/zinc mine tailings impoundment. *Applied Geochemistry.* **22** (1) pp 109-27.

Rosseland, B. O., Blakar, I. A., Bulger, A., Kroglund, F., Kvellstad, A., Lydersen, E., Oughton, D. H., Salbu, B., Staurnes, M. and Vogt, R. (1992). The mixing zone between limed and acidic river waters: complex aluminium chemistry and extreme toxicity for salmonids. *Environmental Pollution.* **78** (1-3) pp 3-8.

Roussel, C., Neel, C. and Bril, H. (2000). Minerals controlling arsenic and lead solubility in an abandoned gold mine tailings. *The Science of The Total Environment.* **263** (1-3) pp 209-19.

Rout, G. R., Samantaray, S. and Das, P. (2001). Aluminium toxicity in plants: a review. *Agronomie.* **21** pp 3-21.

Sastre, J., Hernández, E., Rodríguez, R., Alcobé, X., Vidal, M. and Rauret, G. (2004). Use of sorption and extraction tests to predict the dynamics of the interaction of trace elements in agricultural soils contaminated by a mine tailing accident. *Science of the Total Environment.* **329** (1-3) pp 261-81.

Schlekat, C. E., Van Genderen, E., De Schamphelaere, K. A. C., Antunes, P. M. C., Rogevich, E. C. and Stubblefield, W. A. (2010). Cross-species extrapolation of chronic nickel Biotic Ligand Models. *Science of the Total Environment.* **408** (24) pp 6148-57.

Shand, P., Edmunds, W. M., Lawrence, A. R., Smedley, P. L. and Burke, S. (2007). *The natural (baseline) quality of groundwater in England and Wales.*Research Report No. RR/07/06   British Geological Survey

Sharma, V. K. and Sohn, M. (2009). Aquatic arsenic: Toxicity, speciation, transformations, and remediation. *Environment International.* **35** (4) pp 743-59.

Sharples, M., Maskell, J., Lunt, P. and Williams, A.(2008). "Devon Great Consols Virtual Tour." LabPlus, University of Plymouth. Accessed 13th March 2009. Avaliable   on   the   world   wide   web   at: http://www.ssb.plymouth.ac.uk/labplus/sharples/DGC/DGCOverview.htm.

Sherrell (2000). *Devon Great Consols and Bedford United Mines Report on the Results of a Desk Study and Surface Reconnaissance Inspection in Relation to Past Metalliferous MIning Activity* Frederick Sherrell Limited. Tavistock.

Shtangeeva, I., Bali, R. and Harris, A. (2011). Bioavailability and toxicity of antimony. *Journal of Geochemical Exploration.* **In Press, Corrected Proof** pp.

Sigg, L., Black, F., Buffle, J., Cao, J., Cleven, R., Davison, W., Galceran, J., Gunkel, P., Kalis, E., Kistler, D., Martin, M., Noel, S., Nur, Y., Odzak, N., Puy, J., Van Riemsdijk, W., Temminghoff, E., Tercier-Waeber, M. L., Toepperwien, S., Town, R. M., Unsworth, E., Warnken, K. W., Weng, L. P., Xue, H. B. and Zhang, H. (2006). Comparison of analytical techniques for dynamic trace metal speciation in natural freshwaters. *Environmental Science & Technology.* **40** (6) pp 1934-41.

Singer, P. C. and Strumm, W. (1970). Acid Mine Drainage: The rate-determining step. *Science.* **163** pp 1121-3.

Slowey, A. J., Johnson, S. B., Newville, M. and Brown Jr, G. E. (2007). Speciation and colloid transport of arsenic from mine tailings. *Applied Geochemistry.* **22** (9) pp 1884-98.

Smedley, P. L. and Allen, D. (2004). *Baseline Report Series 16: The Granites of South-West England.*Commissioned Report No. CR/04/255 British Geological Society

Soil Remediation Circular 2009 (2009). Dutch National Institute for Public Health & the Environment

South_West_Water (2009). *Water Resources Plan 2010-2035* South West Water

Sparrow, C. and Wilkins, J. (2001). *Devon Great Consols & Bedford United Mineralogical Assessment.*CEC/447 Cornwall Environmental Consultants. pp 4-9.

Stillings, L. L., Foster, A. L., Koski, R. A., Munk, L. and Shanks Iii, W. C. (2008). Temporal variation and the effect of rainfall on metals flux from the historic Beatson mine, Prince William Sound, Alaska, USA. *Applied Geochemistry.* **23** (2) pp 255-78.

Strigul, N., Vaccari, L., Galdun, C., Wazne, M., Liu, X., Christodoulatos, C. and Jasinkiewicz, K. (2009). Acute toxicity of boron, titanium dioxide, and aluminum nanoparticles to Daphnia magna and Vibrio fischeri. *Desalination.* **248** (1-3) pp 771-82.

Stumm, W. and Morgan, J. J. (1996a). Aquatic Chemistry. New York, Wiley & Sons. pp 691.

Stumm, W. and Morgan, J. J. (1996b). Aquatic Chemistry. New York, Wiley & Sons. pp 885-7.

"Tamar Valley Area of Outstanding Natural Beauty."2010). Tamar Valley Services. Accessed 5th June 2010. Avaliable on the world wide web at: http://www.tamarvalley.org.uk/themesec.asp?pid=3&sid=40.

Tong, L.-l., Jiang, M.-f., Yang, H.-y., Yu, J., Fan, Y.-j. and Zhang, Y. (2009). Dynamic corrosion of copper-nickel sulfide by Acidithiobacillus ferrooxidans. *Transactions of Nonferrous Metals Society of China.* **19** (2) pp 438-45.

Torma, A. F. (1988). Leaching of metals *Biotechnology*. H. J. Rehm and G. Reed. Weinheim, Germany, VCH Verlagsgesellsschaft. **6B** pp 367-99.

UKTAG (2008). *Proposals for Environmental Quality Standards for Annex VIII Substances.*SR1-2007 UK Technical Advisory Group on the Water Framework Directive.

Urbano, G., Meléndez, A. M., Reyes, V. E., Veloz, M. A. and González, I. (2007). Galvanic interactions between galena-sphalerite and their reactivity. *International Journal of Mineral Processing.* **82** (3) pp 148-55.

van Herwijnen, R., Laverye, T., Poole, J., Hodson, M. E. and Hutchings, T. R. (2007). The effect of organic materials on the mobility and toxicity of metals in contaminated soils. *Applied Geochemistry.* **22** (11) pp 2422-34.

Ventura-Lima, J., Bogo, M. R. and Monserrat, J. M. (2011). Arsenic toxicity in mammals and aquatic animals: A comparative biochemical approach. *Ecotoxicology and Environmental Safety.* **74** (3) pp 211-8.

Wardell-Armstrong (1992). *Gunnislake Intake Pumping Station River Tamar, Pollution Riak Study Phase II - Stability Assessment of Selected Tips for the National Rivers Authority, South West Region* Wardell Armstrong Cardiff.

Wauer, G., Heckemann, H.-J. and Koschel, R. (2004). Analysis of Toxic Aluminium Species in Natural Waters. *Microchimica Acta.* **146** (2) pp 149-54.

WDBC.(2006). "Tamar Valley Mining Heritage Project Project Background Information." West Devon Borough Council

Accessed 12th August 2010. Avaliable on the world wide web at: http://www.westdevon.gov.uk/upload/public/attachments/services/tvmhpprojecti nfo.pdf.

Weng, L., Temminghoff, E. J. M., Lofts, S., Tipping, E. and Van Riemsdijk, W. H. (2002). Complexation with Dissolved Organic Matter and Solubility Control of Heavy Metals in a Sandy Soil. *Environmental Science & Technology.* **36** (22) pp 4804-10.

Wilson, S. C., Lockwood, P. V., Ashley, P. M. and Tighe, M. (2010). The chemistry and behaviour of antimony in the soil environment with comparisons to arsenic: A critical review. *Environmental Pollution.* **158** (5) pp 1169-81.

Younger, P. L., Banwart, S. A. and Hedin, R. S. (2002). *Mine water: Hydrology, polllution and remediation*. Bodmin, Klewer Academic Publishers. pp 67-73

Zhu, W. F., Deng, Q., Shao, S., Mo, C., Pan, X., Li, W. and Zhang, R. (2009). Environmental characteristics of water near the Xikuangshan antimony mine, Hunan Province. *Huanjing Kexue Xuebao / Acta Scientiae Circumstantiae.* **29** (3) pp 655-61.

3.11 Chapter 3 Appendices

3A.   Historical Maps provided on following pages

Figure 3.24: Historical Map of Devon Great Consols (1884)

Major areas of Cinders waste, Wheal Anna Maria upper and lower waste and South Wheal Fanny Precipitation Launders referred to in this study outlined in red.

County Series

1:2500 Scale

1854-1901

1s Edition

Published 1882-1884

Figure 3.25: Historical Map of Devon Great Consols (1891)

Major areas of Cinders waste, Wheal Anna Maria upper and lower waste and South Wheal Fanny Precipitation Launders referred to in this study outlined in red.

County Series

1:10560 Scale

1849-1899

1st Edition

Published 1888-1891

© Crown Copyright and Landmark Information Group Limited (2010). All rights reserved. (1888-1901)

Figure 3.26: Historical Map of Devon Great Consols (1906)

Major areas of Cinders waste, Wheal Anna Maria upper and lower waste and South Wheal Fanny Precipitation Launders referred to in this study outlined in red.

County Series

1:2500 Scale

1893-1915

1ˢ Revision

Published 1906

© Crown Copyright and Landmark Information Group Limited (2010). All rights reserved. (1906)

Figure 3.27: Historical Map of Devon Great Consols (1907)

Major areas of Cinders waste, Wheal Anna Maria upper and lower waste and South Wheal Fanny Precipitation Launders referred to in this study outlined in red.

County Series

1:10560 Scale

1846-1969

1^{s} Revision

Published 1907

© Crown Copyright and Landmark Information Group Limited (2010). All rights reserved. (1907)

Figure 3.28: Map of Devon Great Consols site showing archaeological features logged by Buck (2002).

3B.   Devon Great Consols Sample Location Descriptions

Sample	Description
1	Cinders Drain (Picture 4), ephemeral, only sampled when wet conditions allowed.
2-3	Cinders Mixing Zone (Picture 6), ephemeral, only sampled when wet conditions allowed.
4-7	Seepage from Wheal Anna Maria waste tip (from E to W) captured only following heavy rainfall (e.g. Picture 7). Sample 5 emerges from inspection hole (Pictures 10), some flow measurable during all surveys.
8	Drain collecting discharge from W end of Wheal Anna Maria tip, quickly lost to sub-surface flow, sometimes dry.
9-10	Drainage channel draining SE, downhill on W edge of WAM waste, passes under trackway, via engineered gully with plastic pipe, and migrates as largely sub-surface flow towards South Wheal Fanny precipitation launders. Position of sample varied according to flow conditions.
11	Stream emerging from South Wheal Fanny shaft
16	Adit portal at South Wheal Fanny (Picture 11)
12	Pond inflow (commonly standing water or seepage), collecting waters at W of site near to South Wheal Fanny.
13	Pond Outflow (commonly standing water or seepage) collecting waters at W of site near to South Wheal Fanny.
14	Surface stream flowing NW to SE into final drain through wooded area. Stream passes next to Borehole No. 3 shortly before entering final drain.
15	Wide surface drain flowing NW to SE entering final drain immediately to the E of the precipitation launders, heavily vegetated and waterlogged. Close to BH5.
17	Final drain in front of precipitation launders, possible trap for rainwater or leachate from precipitation launders depending on conditions.
18 -19	Final drain in front of precipitation launders, before and after flow from 15 enters.
19-23	Final drain along course, upstream and downstream of 14 (20 and 21), at Boreholes 1 and 2 (22) and before entering the River Tamar (23).
BH1 and BH2	Interception of shallow groundwaters moving beneath final drain, BH1 N and BH2 S of drain.
BH3	Interception of groundwaters moving from NW towards River Tamar. Directly beneath surface drain 14.
BH4	Interception of groundwaters moving to SE, beyond final drain.
BH5	Shallow perched water table within precipitation launders/waste tip. Close to drain 15.
BH6	"Clean" deep borehole driven to bedrock to SW of WAM waste tips, in clayey waterlogged soil. Intended to intercept deeper, background groundwaters.

3C.   Photographs

Photograph 1 Wheal Anna Maria waste viewed from the west with eastern extent of cinders waste in foreground. Taken 05/04/09 A J M Turner	
Photograph 2 Cinders waste tips, viewed from the east. Taken 20/07/09 M W Sharples, University of Plymouth.	

| **Photograph 3**

Close up of cinders waste showing bright blue-green efflorescent (copper) salts. Similar also found on and around Wheal Anna Maria, particularly on course wastes.

Taken 05/04/09

A J M Turner | |
| **Photograph 4**

View looking north-west towards top of cinders waste. Ephemeral Stream (Sample 1) in front of cinders, with small inspection hole or adit, circled top of picture.

Taken 20/07/09

A J M Turner | |

Photograph 5	
View looking west, showing ephemeral stream from cinders tips mixing with drainage from other tips to north and west of Wheal Anna Maria tip (Sample 2). Taken 20/07/09 A J M Turner	
Photograph 6	
Cinders drain migrating along eastern extent of tailings tip (between sample 3 and 9). View from south west to north east (vegetated bank of tailings shown on right). Taken 08/02/08 A J M Turner	

Photograph 7	
Plastic drainage pipe carrying cinders drainage toward precipitation launders (sample 10). Taken 08/02/08 A J M Turner	
Photograph 8 Tip seepage emerging from W side of Wheal Anna Maria tip (sample 4). Taken 20/07/09 A J M Turner	

Photograph 9

Wheal Anna Maria waste tip inspection hole discharge (sample 5).

Taken 20/07/09

A J M Turner

Photograph 10

View looking south east, from top of Wheal Anna Maria upper tip showing drainage into and around waterlogged lower (tailings) waste tip (toward sample location 8). Direction of flow indicated by blue arrows.

Taken 08/02/08

A J M Turner

217

Photograph 11 Remains of precipitation launders (eastern section) showing plateau underlain by mixed waste material. View from east to west. Taken 08/02/08 A J M Turner	
Photograph 12 Drainage ditch in front of precipitation launders. View from east to west (toward pond). Taken 08/02/08 A J M Turner	

Photograph 13 Adit Portal discharge near to South Wheal Fanny (Sample 16). Light green discolouration suspected to be efflorescent salts, precipitated on side of side of portal receiving sunlight. Standing water in front of portal (not shown), held in mine leat/terraced bank. Taken 20/07/09 A J M Turner	
Photograph 14 Final collection drain at sample location 22 (also location of BH1 and BH2), looking west toward precipitation launders. Taken 20/07/09 A J M Turner	

219

Photograph 15 Final collection drain at sample location 21, showing ochre deposits on banks. Taken 20/07/09 A J M Turner	
Photograph 16 DGC Borehole 2 installation (South bank of Final Collection Drain). Core from BH2 showing streaked clayey gley soil and organic material below soft ochre. Oily-film visible on water within borehole indicative of iron and sulphur rich wetlands and bogs (Haaijer *et al.*, 2008). Taken 13/01/09 A J M Turner	

Photograph 17 Wheal Anna Maria waste tip combined drainage with high suspended load flowing into lower (tailings) waste tip. Taken 20/07/09 A J M Turner	
Photograph 18 Ochre stained mine waste eastern part of cinders. View looking north. Taken 20/07/09 M W Sharples	

3D.   Devon Great Consols Groundwater Borehole Logs

Borehole	Augered Depth (m)	Observations
DGC BH1	0-0.53	Soft orange ochre, containing coarse GRAVEL. Unable to penetrate further with hand auger.
DGC BH2	0-0.50	Soft orange ochre.
	0.50-0.76	Mid brown and black streaked CLAYEY gley soils.
	0.76 -1.22	Streaked CLAY with high organic content comprising un-decomposed leaf litter. Increased GRAVEL content with depth (photograph 16)
	1.22 (end)	Grey coarse GRAVEL, unable to penetrate further with hand auger.
DGC BH3	0-0.76	Dark grey gley soil and CLAY.
	0.76-1.06	Brown-orange ochre.
	1.60-1.65	Dark grey gley soil and CLAY. Appears anerobic.
	1.65 (end)	Organic matter comprising un-decomposed leaf litter, twigs.
DGC BH4	0-0.85	Wet yellow CLAY
	0.85	Orange/brown HARDPAN, difficult to auger
	0.85-1.21 (end)	Stiff yellow CLAY, appears dry
DGC BH5	0-0.58	Coarse sub-angular COBBLES and GRAVELS, comprising tip waste and country rock.
DGC BH6	0-1.62	Mid-dark brown CLAY
	1.62-1.89	Organic matter containing un-decomposed leaf litter. H_2S odour.
	1.89-1.98	Humic streaked black CLAY.
	1.98-2.00 (end)	Gravels (probably alluvium)

3E.   Instrumental Parameters for ICP-MS, ICP-OES and IC

The parameters presented here are typical for the experimental runs conducted however signals were optimised for each run therefore actual conditions may vary slightly from those shown

ICP-OES Varian 725-ES

Nebuliser	Sturman-Masters V-Groove
Power	1.6-1.7 kW
Plasma Flow	22.5 L min^{-1}
Auxillary Flow	1.5 L min^{-1}
Nebuliser Flow	0.75 L min^{-1}
Viewing Height	10 mm
Replicate Read Time	2-10 s
Stabilisation Delay	10-15 s

ICP-MS Thermo Fisher X Series 2

Nebuliser	Meinhard (glass, fine capillary)
Spray Chamber	Jacketed conical with an impact bead
Forward Power	1.35 kW
Reflected Power	4 W
Auxiliary Flow	1.0 L min^{-1}
Coolant Flow	12.0 L min^{-1}
Nebuliser Flow	0.864 L min^{-1}
Number of Sweeps	100
Dwell Time	10 ms

Dionex DX-500 IC

Mobile Phase	0.01 M Na$_2$CO$_3$
Column	Dionex Ionpac AS9-HC
Column Temperature	25°C
Injection Volume	200 µL
Run Time	18 min
Plates (typically)	5000-8000
Detector	Electrochemical (ED50)

3F. Environmental Quality Standards proposed for the Water Framework Directive in respect of freshwaters.

Table 3.15: Environment Agency existing or proposed* Water Framework Directive Environmental Quality Standards for freshwaters (*latest quoted). Ranges apply according to water hardness, lower value applicable to low alkalinity waters. Published standards in μg L^{-1}, converted here to μmol L^{-1} for comparison with results from this study.

Element/Species (relative atomic mass)	Annual Average or Long Term Exposure Limit		Maximum Allowable Concentration or Short Term Exposure Limit	
	(μg L^{-1})	(μmol L^{-1})	(μg L^{-1})	(μmol L^{-1})
Al (26.98)	0.05	0.00185	0.25	0.00927
As (74.92)	50	0.667	-	-
Cd (112.40)	≤ 0.08-0.25	0.000712-0.00222	0.045- 1.5	0.000400-0.0134
Cl (35.45)	2	0.0564	5	0.141
Cu (63.55)	1-28	0.0157-0.441	-	-
Fe (55.85)	0.016	0.000286	0.041	0.000734
Mn (54.94)	7	0.127	24	0.436
Ni (58.69)	20	0.341	-	-
Pb (207.2)	7.2	0.0348	-	-
Zn (65.37)	8-125	0.122-1.91	-	-

3G.   Data Used to Calculate Estimated Annual Flux from Mine Waste Tips at Devon Great Consols.

Table 3.16: Estimated annual flux for selected metals and As leaving three tips at Devon Great Consols. Inter quartile range and mean concentrations used to derive fluxes. Sample locations used: Cinders drain (1), WAM tip drainage (4-8), precipitation launders (BH5 and 17).

	DGC Cinders	DGC WAM	DGC Precipitation Launders
Tip Catchment Area (m^2)	84400	134535	115825
Average Annual Rainfall (mm)	1289	1289	1264
Range Cu (μmol L^{-1})	10.4 – 12.8	201 - 267	102 - 131
Mean Cu (μmol L^{-1})	12.9	224	115
Range Cu Flux (mol y^{-1})	1130 - 1390	34900 – 46400	14900 - 19100
Mean Cu Flux (mol y^{-1})	**1410**	**38900**	**16800**
Range Zn (μmol L^{-1})	2.05 - 2.38	12.0 – 12.9	13.4 – 18.0
Mean Zn (μmol L^{-1})	2.24	12.6	15.3
Range Zn Flux (mol y^{-1})	223 - 259	2074 - 2242	1968 - 2634
Mean Zn Flux (mol y^{-1})	**244**	**2180**	**2240**
Range Mn (μmol L^{-1})	3.33 – 4.47	32.1 – 41.8	69.4 – 99.6
Mean Mn (μmol L^{-1})	3.88	37.0	81.4
Range Mn Flux (mol y^{-1})	362 - 487	5570 - 7250	10200 - 14600
Mean Mn Flux (mol y^{-1})	**422**	**6410**	**11900**
Range Ni (μmol L^{-1})	0.252 - 0.292	0.91 – 1.31	2.34 – 3.28
Mean Ni (μmol L^{-1})	0.285	1.11	2.72
Range Ni Flux (mol y^{-1})	27.4 – 31.8	157 - 227	343 - 479
Mean Ni Flux (mol y^{-1})	**31.0**	**192**	**398**
Range Cd (μmol L^{-1})	0.0020 – 0.0021	0.019 – 0.025	0.022 – 0.029
Mean Cd (μmol L^{-1})	0.00204	0.023	0.025
Range Cd Flux (mol y^{-1})	0.213 – 0.228	3.35 – 4.32	3.25 – 4.30
Mean Cd Flux (mol y^{-1})	**0.222**	**3.76**	**3.65**
Range As (μmol L^{-1})	270 - 328	0.290 – 1.65	0.080 – 0.150
Mean As (μmol L^{-1})	294	1.33	0.140
Range As Flux (mol y^{-1})	29400 - 35600	50.3 - 286	11.7 – 22.0
Mean As Flux (mol y^{-1})	**32000**	**231**	**20.5**
Range Al (μmol L^{-1})	151 - 158	695 - 902	702 -1010
Mean Al (μmol L^{-1})	154	823	828
Range Al Flux (mol y^{-1})	16400 - 17200	121000 - 156000	103000 - 148000
Mean Al Flux (mol y^{-1})	**16700**	**142700**	**121000**
Range Pb (μmol L^{-1})	<LOD	0.0060-0.020	0.00015-0.0209
Mean Pb (μmol L^{-1})	<LOD	0.015	0.0141
Range Pb Flux (mol y^{-1})	-	1.06-3.42	0.48-2.08
Mean Pb Flux (mol y^{-1})	**-**	**2.60**	**1.29**

3H.   River Hydrographs

River Tamar at Gunnislake, 1994-1995 and 2004-2009 (CEH, 2011).

-End of Chapter 3-

226

Chapter 4

Mine Waste Tips as a source of

Metal and Arsenic Contamination,

Case Study 2: Wheal Betsy

4. Mine Waste Tips as a source of Metals and Arsenic Contamination, Case Study 2: Wheal Betsy

4.1 Abstract

Cholwell Brook, a tributary of the River Tavy, receives drainage waters from mine waste tips at Wheal Betsy, an abandoned Pb-Ag mine. The hydrology of the site was much simpler then at Devon Great Consols, with a short migration pathway (<10m) from tips to Cholwell Brook. Waste tips at the site are very heterogeneous, due in part to the varied mineralogy of the site, but are generally more permeable in the northern zone compared to the southern zone.

Background surface and groundwaters entering the site were already above environmental quality standards (EQS) for dissolved Cu and Mn. This was due to the mineralisation of bedrock geology in the area. However, dissolved metals in the waters of Cholwell Brook increased through the mine site such that Cholwell Brook failed long term EQS for Al, Zn, Cu, Pb, and Cd during seven surveys conducted between 2007 and 2009. The highest exceedance was for dissolved Cd (0.018 μmol L^{-1}, equal to 250 x EQS), dissolved Mn (11.0 μmol L^{-1}, equal to 87 x EQS) and dissolved Zn (3.9 μmol L^{-1}, equal to 55x EQS).

The concentration and estimated annual flux of dissolved Pb (0.45 μmol L^{-1}, and 783 mol y^{-1}, respectively), and the estimated flux of dissolved Cd (470 mol y^{-1}) were higher than identified elsewhere in the catchment by previous studies. Arsenic and Fe mobility was limited due to the shallow and oxic nature of surface and ground waters at the site.

Concentrations and fluxes of dissolved metals increased with increased rainfall and this was attributed to higher water tables in the base of the northern mine waste tips.

The reactivity of the stream waters to rainfall highlights the importance of considering hydrological factors in such investigations. Concentrations of dissolved metals in shallow groundwaters confirmed the mine waste to be a source of mobile contaminant metals to Cholwell Brook, but seepage from underground workings may also contribute to base flow, and are worthy of future investigation.

4.2   Introduction and Aims

In Chapter 3 the diffuse mine waters emanating from the mine waste at Devon Great Consols were investigated and concentrations of dissolved metal and metalloids were determined. From this data and measured and modelled hydrological data for the site, annual fluxes emerging from the tips were predicted. The same approach was adopted at the second study site, Wheal Betsy, an abandoned Pb-Ag mine with contrasting hydrology and mineralogy. The aims, objectives and methodology are identical to those presented in Chapter 3, in sections 3.3 and 3.6 respectively except where indicated in section 4.4.

4.3   Background Information: Wheal Betsy

4.3.1   Location and Ownership

A summary of the location and key environmental features of the site were provided as a case study in Chapter 2 (section 2.6.3). Wheal Betsy is situated within Dartmoor National Park, approximately 1.5 km N of the village of Mary Tavy (Figure 4.1), and 9 km NE of the ancient stannary town of Tavistock.

The site is owned by South West Water (SWW), who are responsible for the capping and securing the exposed mine shafts. The engine house and chimney on the site are owned by the National Trust. The land to the east of Cholwell Brook (Figure 4.2) is part of Cholwell Farm, which comprises private farmland and riding stables is

owned by the Powell family. Permission from SWW was gained to install shallow ground water boreholes and conduct regular site visits. Permission was also granted by the Powell family to gain access to Cholwell Brook from the E bank in order to safely take water samples from the brook and to access borehole water from a tap located in the stable yard.

Figure 4.1: Wheal Betsy site located NE of Mary Tavy, as it appears on current OS 1: 50000 scale map. © Crown Copyright and Landmark Information Group Limited (2010). All rights reserved.

4.3.2   History

Wheal Betsy was worked for lead and silver from the 13th Century (Hamilton Jenkin, 2005). The recorded output of the mine to its closure in 1877 was 400 t Pb and 113 kg Ag (Booker, 1967). The mine underwent several changes of name and owner during its operation and between 1816 and 1837 was operated in conjunction with Wheal Friendship a neighbouring mine to the south. The mines exploited part of the "Great Crosscourse" (Richardson, 1995), one of the N-S tending mineral lodes found throughout south west England . The north–south cross-courses are younger than the

229

east-west deposits (like those exploited at Devon Great Consols) being emplaced in the post-granite phases of mineralisation and are typically characterised by veins of quartz with Pb-Zn-Ag sulphides, fluorite and siderite (Durrance and Laming, 1982).

Twelve shafts were sunk along the N-S tending mineral lode, extending to approximately 270 m depth near to the engine house, which was built in the 1840s. A historical map dated 1884 and a schematic of the underground layout are shown in Figure 4.22 and Figure 4.23, respectively (Appendix 4A).

The historical map shows many small buildings and features indicating that extensive mineral processing was conducted at the site during its operation. There are also reports that ores were smelted on site using peat cut from nearby deposits (Hamilton Jenkin, 2005). The current extent of the waste tips approximately matches the outline from 1884, although from site inspections it appears that some waste material has been removed, particularly from the most westerly area, adjacent to the main road (A386).

4.3.3   Site Topography, Hydrology and Mine Waste Mineralogy

Cholwell Brook, flows approximately north to south through the site and is hosted in a steep valley. The brook is a tributary of the River Tavy and joins it approximately 2 km downstream. The brook is recognised as a geological site of special scientific interest (SSSI), as it clearly displays a thrust contact (fault boundary) between the Bealsmill Formation, and the lower Greystone Formation created during the *Variscan Orogeny* (DCC, 2011).

The mine waste at Wheal Betsy comprises a collection of tips which vary in size, appearance and size grading. At the northern end of the site, the tips are exclusively found on the western bank of Cholwell Brook near the engine house shown in Figure 4.2 and photograph 1 (all photographs in Appendix 4B). These tips are steeply sloping and contain coarse gravels, pebbles and small sub-angular and angular cobbles.

There is evidence of ongoing erosion of the tips as a result of slope instability and physical weathering. Freeze-thaw fracturing of the consolidated tip material has also been observed during winter site visits. The major mineralogical components of the mine waste, visible to the naked eye, are slate, quartz, siderite ($FeCO_3$) with small amounts of galena (PbS,), arsenopyrite (AsFeS) and sphalerite (ZnFeS).

Where stable, the tips were partially vegetated with a mixture of gorse, heather and grass. On sparsely vegetated areas of waste, *bryophyte* species and lichens are also observed. To the south of the site the tips appeared to be generally finer grained, and vary greatly in colour from bright yellow clays, through coarser orange sands to grey platy weathered slates. Cholwell Brook passed directly through the waste in the southern part of the site (Figure 4.2 and photograph 2). The southern tips, being of finer particle size, may represent the tailings from mineral processing at Wheal Betsy. Alternatively, they may be characteristic of the mineralisation surrounding the fault boundary which comprise a tectonic mélange consisting of clasts of sandstone, chert, dolerite, limestone and volcanics set in a soft clay gouge matrix (DCC, 2011). A wooden chute is still visible from the brook approximately halfway along the south tips (Photograph 3). The southern waste tips contain largely slate and sandstone which comprise the *country rock*. Hard pan horizons and crusts are visible in both the north and south spoil material (see example in photograph 4).

Mineralogical studies have revealed that a host of other minerals are present within the tips including iron pyrite (FeS_2), calcite ($CaCO_3$), löllingite ($FeAS_2$), chalcopyrite ($CuFeS_2$), rhodochrosite ($MnCO_3$), marcasite (FeS_2) and vivianite ($Fe_3(PO_4)_2.8H_2O$) (Page, 2008). The contribution of each of these minerals to the overall volume of waste is unknown and extremely difficult to estimate due to the heterogeneity of the tips.

The predominantly slate bedrock was encountered at shallow depths (< 1 m), and was visible along the steep sided valley and in the base of Cholwell Brook. There were no superficial deposits. Profiles of transects marked in Figure 4.2 are show in Figure 4.3 and demonstrate the steep sided valley (average slope 12-15°) in which the site is located. The OS 10 m contours used to plot the transects have included some of the spoil topography in addition to the land surface; this is most obvious on transect A-B which cuts through the largest area of waste.

Figure 4.2: Schematic diagram showing mine waste tips at Wheal Betsy comprising coarser waste in northern tips (orange) and finer tailings in south tips (grey). Large blue arrows represent direction of shallow ground water flow.

The direction of shallow groundwater movement was expected to follow the topography of the site, draining into Cholwell Brook (shown as thick blue arrows in

Figure 4.2). Deeper ground water is likely to be influenced by the deep mine workings below the site. It is possible that there is hydraulic connectivity with the workings of Wheal Friendship located approximately 1km to the south of the site, however records suggest that the mines were worked independently of one another (Booker, 1967).

Figure 4.3: Cross sections through Wheal Betsy site as marked on Figure 4.4. Note the step A-B transect at approximately 150 m, this is due to the contour data including the main mine waste heaps.

4.4 Methods

4.4.1 Reagents

See Chapter 3, section 3.6.1.

4.4.2 Cleaning Protocol

See Chapter 3, section 3.6.2

4.4.3 Sampling Protocol and Sample Treatment

Sampling Strategy

Waters from Cholwell Brook were sampled at the intervals marked in Figure 4.4. Samples 1 and 2 were taken upstream of the visible and known extent of the mine waste and underground workings. Samples 12 and 13 were downstream of the mine waste.

Figure 4.4: Schematic overview of Wheal Betsy next to Cholwell Brook (River Tavy), showing location of major waste tips, surface water (red) and borehole samples (blue), ephemeral streams and drainage channels.

Where found, surface drains entering the brook were also sampled (samples 14-17, orange boxes), and brook samples were taken upstream and downstream of these

234

inputs. The aim was to delineate the surface point inputs from the diffuse inputs as the brook flows alongside the mine waste. There were no obvious adit discharges into the brook.

The northern part of the site provided the best opportunity to capture shallow ground waters entering the brook from the base of the mine waste. Five boreholes were installed as shown in Figure 4.4 and listed with depths, in Table 4.1.

Table 4.1: Borehole depth data and observations. CB= Cholwell Brook. Core logs are presented in Appendix 4C.

Borehole	Depth (at installation)/Location	Additional Comments
1	0.52 m. West bank of CB, adjacent to sample 7	Dry on all subsequent surveys.
2	0.88 m. In vegetated area between base of waste tips and CB	Waters clear, borehole sometimes dry. Rapid recharge.
3	0.83 m. Base of coarse waste tip. Sparsely vegetated with heather.	Waters dark brown to clear, some dark brown suspended particles. Rapid recharge.
4	1.15 m. In grassy area adjacent to sample 6.	Waters ocherous to clear, some light brown suspended particles. Rapid recharge
5	0.95 m. At base of waste tips beneath engine house.	Waters clear with some light brown suspended particles. Sometimes dry. Rapid recharge.
6	Waters from upstream ground water reservoir.	Waters clear.

Boreholes were drilled using a combination of a portable pneumatic drill and hand-auguring. Cased boreholes were installed and waters sampled and treated as described in Chapter 3, section 3.6.3. Each ended when slate bedrock was encountered. All cores removed contained a high proportion of loose mine waste of varying size fractions (for detailed content, see Appendix C). Boreholes 3 and 5 were drilled into the

foot of the largest mine waste tips to capture waters percolating through the mine waste. Boreholes 1, 2 and 4 targeted waters moving through the shallow subsurface shortly before entering Cholwell Brook.

BH1 proved dry in all subsequent visits. A sixth borehole was attempted upstream of the site but failed to encounter ground water after drilling to 2 metres. However, an underground reservoir was located in approximately the same area, up catchment from the mine site. The reservoir, which used to serve the town of Mary Tavy is piped directly to a tap at Cholwell Farm via plastic pipes. With the owner's permission, this was used to sample the background groundwater quality at the site and was allowed to flow for several minutes before measurements and samples were taken.

Rainfall and Temperature

Rainfall data was downloaded for the 14 days preceding each site visit from the nearest MIDAS land surface data station (MetOffice, 2009), located at Blackdown: Wheal Jewell Reservoir (SX 521814), approximately 1.3 km NE of the site. Rainfall data and water temperatures for each sampling round are summarised in Table 4.2.

The ten year average rainfall (1999-2009) recorded at Blackdown was 4.6 mm d^{-1} which is higher than the catchment average of 4.0 mm d^{-1}. The frequency of a heavy rain event (> 20 mm d^{-1}) during the same ten year period was on average 17 days, placing it in the "Extreme Risk" category for rain intensity within the Tamar catchment (see Chapter 2, section 2.5.5). As for Devon Great Consols, the sampling campaign set out to encompass the range of hydrological conditions.

Sample temperatures were relatively consistent between boreholes and surface waters, compared with DGC waters. The exception was winter, where ground waters obtained from the upstream underground reservoir (minimum 0.4 °C), were colder than other samples. Surface waters (6.5-13.0 °C) were not much warmer than groundwater (0.4 - 14.6 °C), even in summer, and some borehole waters were warmer than stream

waters. This indicated rapid transport of the waters from source and through Cholwell Brook and insufficient time for waters to equilibrate with warmer air temperatures. Slower transport in shallow groundwater could account for the difference, but it may also indicate local warming by reactions taking place within the waste, specifically pyrite oxidation which is highly exothermic (1409 kJ mol^{-1}, (Wels *et al.*, 2003)).

Table 4.2: Surface water sample temperatures and rainfall data for Wheal Betsy preceding each site visit. Rainfall data obtained from nearest MIDAS land surface station at Blackdown: Wheal Jewell reservoir (SX 521814), located 1.4 km NE of site. Ten year (1999-2009) average for station = 4.6 mm d^{-1} and Tamar catchment = 4.0 mm d^{-1}.*Sampling conducted a few days after extensive snow-melt. [1]Borehole samples in parenthesis.

Sampling Date	Sample Temp (°C)[1]		Rainfall in 7 days before sampling (mm)							Rainfall on day (mm)	7 Day Total (mm)	14 Day Total (mm)
		Day:	7	6	5	4	3	2	1	0		
03/07/2007	10.6 – 11.7		20.5	14.5	1.6	1.4	14.7	11.9	7.6	8.3	72	143
27/08/2008	11.3 – 12.6 (11.2 – 14.5)		7.8	0.5	0.0	18.8	2.4	0.0	0.0	2.5	30	85
16/10/2008	(12.1 – 14.2)		0.1	0.0	0.0	0.2	0.5	7.3	1.0	0.3	9.1	89
10/12/2008	6.9 – 7.7 (0.4 – 10.2)		17.3	19.0	3.6	0.0	0.1	5.3	2.7	1.2	48	74
12/02/2009*	6.3 – 7.5 (4.1 – 8.9)		6.1	0.1	1.4	10.7	22.1	0.9	0.0	0.0	41	60
09/05/2009	10.0 – 10.8 (10.2 – 12.2)		0.0	0.0	0.0	1.6	2.2	2.1	0.0	0.0	5.9	29
23/07/2009	11.2 – 13.0 (10.5 – 14.6)		30.1	8.6	4.3	4.2	10.0	14.2	0.0	31	71	127

Sampling conducted on the 03/07/2007 comprised the initial investigative survey; conditions were very wet in the 14 days before the survey (143 mm) and a number of surface discharges were evident which were not seen again during other rounds. Relatively dry conditions preceded the 09/05/09 survey (29 mm in 14 days. All other surveys were conducted in relatively wet conditions, following average (60 mm,

based on 4.6 mm d^{-1}) to above average total rainfall in the previous 14 days (64-127 mm).

Audible and visible freeze thaw erosion was witnessed from the slopes of the north waste tips during the winter surveys (10/12/08 and 12/02/09), the latter of which followed thawing of heavy snowfall over a number of days. Very heavy rain (and hail) fell on the 23/07/09 during sampling of Cholwell Brook resulting in high surface run-off from the waste tips and visibly turbid stream water.

Sampling, In-situ determination and Sample Treatment

All procedures followed those previously described for Devon Great Consols samples in Chapter 3, section 3.6.3.

4.4.4   Instrumentation and Analysis

pH, Eh and DO meter calibration and elemental analysis conducted as described in Chapter 3, Section 3.6.4.

4.4.5   Principal Component Analysis

Principal component analysis (PCA) (XLSTAT version 2010.4.01) was applied to the Wheal Betsy data set using the same method described for the Devon Great Consols data in Chapter 3, section 3.7.3. Observations were organized into groups according to sample type, as listed in Table 4.3. Borehole data was grouped individually by borehole number.

The first seven components cumulatively explained 82% of the variation in the data set (Table 4.4), and were used to investigate the geochemical character and variability of the data.

Table 4.3: Sample Type Groupings for the Wheal Betsy Data set.

Sample Location Numbers	Sample Type Grouping (PCA label)
1	Cholwell Brook, upstream of Cholwell Farm (USF)
2	Cholwell Brook, upstream of waste tips (USW)
3-7	Cholwell Brook, alongside waste tips, N of bridge (CBN)
8-12	Cholwell Brook, alongside waste tips, S of bridge (CBS)
13	Cholwell Brook, downstream of waste tips (DSW)
14	Surface collection drain from N waste (SDN)
15-17	Surface collection drains from S waste (SD15,SD16,SD17)

Table 4.4: Initial Eigenvalues from PCA analysis of the Wheal Betsy data set.

	F1	F2	F3	F4	F5	F6	F7
Eigenvalue	11.68	4.38	2.85	2.37	1.57	1.29	1.14
Variability (%)	37.69	14.11	9.19	7.65	5.05	4.18	3.68
Cumulative %	37.69	51.80	60.99	68.64	73.69	77.87	81.55

4.4.6 Geochemical Modelling

The geochemical modelling code PHREEQC Ver.2.17.1 was applied to the Wheal Betsy data set. Speciation of elements and saturation indices for mineral phases in mine drainage waters were calculated from thermodynamic principals using the same databases and amendments described in Chapter 3, section 3.6.6.

4.5 Results and Discussion

4.5.1 Quality Control and Figures of Merit

Recoveries and limits of detection for all analyses of Wheal Betsy water samples are presented in Table 4.5. All other analytical procedures and instrumental

conditions were the same as for Devon Great Consols water samples, as presented in Chapter 3, section 3.7.1.

Table 4.5: Limits of detection and CRM recoveries for all analysis of DGC samples. Certified reference material:TMDA-64 (fortified lake water), National Water Research Institute, Canada. CRM recoveries in bold indicate concentration was close to limit of linearity for instrument. *Guidance value on CRM certificate only.

Element/ Anion	CRM Value (µg L^{-1}) ± 2σ limit	Method	Linear /Standard Range	Limit of Detection (µmol L^{-1})	CRM Recoveries (µg L^{-1})
Al	265±30	ICP-MS	0.028-22	0.11	297
As	150±22	ICP-MS	0.01-2.0	0.011	171
B*	300	ICP-OES	0.1-1000	0.71, 0.73, 0.90, 0.79	280, 306, 312, 308
Ca	13600*	ICP-OES	0.5-5000	0.076, 0.22, 0.019, 0.0048	13810, 14520, 14070, 14071
Cd	251±24	ICP-MS	0.001-2	0.0087	229
Co	270±27	ICP-MS	0.003-10	0.088	278
Cu	290±29	ICP-MS	0.001-5	0.016	257
		ICP-OES	0.1-1000	0.20, 0.11, 0.11, 0.13	304, 317, 289, 293
Fe	319±30	ICP-OES	0.1-1000	0.18, 0.47, 0.14, 0.19	315, 308, 357, 320
Hg	-	ICP-MS	0.001-5	0.001	-
Mg	(3400*)	ICP-OES	0.1-500	0.18, 0.02, 0.63	3553, 3351, 3702
Mn	299±26	ICP-MS	0.001-10	0.019	297
		ICP-OES	0.1-1000	0.030, 0.041, 0.028, 0.015	310, 295, 290, 296
Mo	278±22	ICP-MS	0.0001-1	0.0016	254
Na	(4500*)	FAAS	200-4000	2.0	4400
		ICP-OES	0.5-5000	6.1	4740
Ni	262±23	ICP-MS	0.0005-2	0.0013	279
K	580	FAAS	20-2500	0.4	600
Pb	297±28	ICP-MS	0.003-10	0.0012	282
Si	-	ICP-OES	0.5-5000	0.20, 1.30, 0.97	-
Sb	125±20	ICP-MS	0.0005-1	0.0019	130
Sn*	292	ICP-MS	0.001-5	0.0012	282
V	272±26	ICP-MS	0.001-1	0.010	297
W	(0.06*)	ICP-MS	0.0005-1	0.0058	0.14
Zn	(313*)	ICP-MS	0.0010-10	0.0053	332
		ICP-OES	0.1-1000	0.22, 1.4, 0.55, 0.47	330, 288, 309, 320
F$^-$	-	IC	10-5000	0.31	-
Cl$^-$	-	IC	10-5000	1.3	-
SO$_4$$^{2-}$	-	IC	10-5000	1.7	-

4.5.2   Site Hydrology

Increased rainfall conditions in the days preceding each sampling visit resulted in a measured change in the levels observed in boreholes and the flow of Cholwell Brook. Flow rates for Cholwell Brook and surface drains are tabulated in Table 4.6. The flow in Cholwell Brook was extremely variable (12-459 l s^{-1}) and variation was both spatial and temporal. Maximum flows were recorded approximately halfway through the site in most rounds (underlined, Table 4.7), whilst in others (03/07/07 and 10/12/08) flow in the middle section of the brook was relatively low.

It is known that extensive underground mine excavations exist on the site with a number of shafts extending N-S from the Engine House (see Figure 4.22, Appendix 4A). The engine house is approximately 440 m along the length of the sampled section of Cholwell Brook. If it assumed that this approximately marks the onset of the mine workings at Wheal Betsy, from this point onwards the base flow of Cholwell Brook may be affected. The significant storage capacity underground could augment or abate the flow in Cholwell Brook depending on the water level in the underground workings. Also, the underground workings at Wheal Betsy may have hydraulic connectivity to another mine located approximately 300m to the south (Wheal Friendship). This might explain why the flow in Cholwell Brook tends to decrease towards the S end of the site, despite receiving surface run-off from the surrounding land and dropping evenly in height by approximately 30 m.

The highest flow (459 L s^{-1}) was recorded on 23/07/09. The intense rainfall experienced during this visit began during sampling at sample 13, and continued through sampling (upstream) to sample 3. The speed with which flow visibly increased in the brook infers a very rapid transport time for waters entering the watercourse. Therefore the variability in flow recorded in Cholwell Brook on this occasion was likely to be enhanced by the influx of surface waters following the onset of heavy rain and

hail.   The amount of rainfall falling on the site in the preceding days to each site visit was also reflected in the borehole water levels (Table 4.6).

BH2 was completely dry on two occasions during periods of low rainfall, whilst the highest levels were observed following the wettest period captured by the sampling schedule, on 23/07/2009, amounting to 72 mm of rain in the preceding 7 days.   It   is important to note, particularly when comparing data with Devon Great Consols, that the boreholes at Wheal Betsy were largely hosted within the waste tips themselves. The tips (cinders, WAM upper and precipitation launders) at Devon Great Consols were situated above the water table (although internal perched tables may have existed). In contrast evidence from borehole levels and borehole logs (Appendix 4C) suggests that a significant proportion of the mine waste in northern tips at Wheal Betsy lies in the *phreatic zone*. Therefore, with the exception of surveys following very dry periods (< 30 mm in 7 days), the mine waste at the base of the tips is subjected to continuous flushing by groundwaters.

Table 4.6: Water levels in shallow ground water boreholes installed at Wheal Betsy. Data presented as metres above a 1m ordnance datum (mAOD). Total rainfall recorded for 7 days prior to visit in parenthesis. Highest water level in bold for each location.

Water Level (mAOD)

Sampling Date	Borehole No: 2	3	4	5
27/08/2008 (30 mm rainfall)	0.23	0.43	0.44	0.29
16/10/2008 (9 mm rainfall)	0.00	0.24	0.29	0.16
10/12/2008 (48 mm rainfall)	**0.35**	0.26	0.39	0.26
12/02/2009 (42 mm rainfall)	0.34	**0.44**	0.45	0.29
09/05/2009 (6 mm rainfall)	0.00	0.25	0.30	0.13
23/07/2009 (72 mm rainfall)	**0.35**	0.40	**0.60**	**0.34**

Table 4.7: Flow data (L s^{-1}) calculated for Cholwell Brook and surface drains at Wheal B/etsy during water sampling rounds. *Sampling conducted a few days after extensive snow-melt. (-) = No result for sample location on particular round due to contstraints of accessability. Drain 16 appears to be surface runoff entering brook next to bridge; flow rate could not be measured due to thick vegetation (mainly gorse) at entrance point. Maximum flow for each visit is underlined.

Flow (L s^{-1})		Cholwell Brook (N-S)													Surface Drains			
Distance along Cholwell Brook (m):		0	190	295	305	435	445	575	640	730	785	795	950	1025	300	440	635	790
Sampling Date	**Sample No:**	**1**	**2**	**3**	**4**	**5**	**6**	**7**	**8**	**9**	**10**	**11**	**12**	**13**	**14**	**15**	**16**	**17**
03/07/2007		48	-	53	13	13	35	35	-	-	<u>190</u>	<u>190</u>	79	-	1.2	1.3	-	0.7
27/08/2008		-	38	64	85	-	<u>176</u>	115	-	-	-	-	-	-	0.5	-	-	-
10/12/2008		-	-	-	<u>125</u>	-	64	61	83	103	-	-	-	97	0.1	-	-	-
12/02/2009*		-	68	-	74	-	145	<u>313</u>	121	87	-	-	-	105	2.6	-	-	-
09/05/2009		-	20	-	12		35	<u>49</u>	15	41	-	-	-	39.6	0.1	-	-	-
23/07/2009		-	-	32	32	-	<u>459</u>	76	131	107	-	-	-	107	0.6	-	-	-

4.5.3   Principal Component Analysis (PCA)

Separation of samples in PCA, appeared to be largely based on the enrichment of all dissolved ions (with the exception of trace Hg), leading to a positive F1 shift and the DO concentration of the waters, leading to a positive F2 and slightly negative F1 shift. This is shown by the variable and observation plots of F1 vs. F2 in Figure 4.5. Major contributors to the first principal component (F1) were dissolved Ni (7%), Ca (7%), Sr (7%), Zn (7%), sulphate (7%), Cd (7%), Pb (6%), Mn (6%), Fe (5%), Ba (5%), Co (5%) and Mg (5%), accounting for 38% of the total variability of the WB data set.

These dissolved species are all likely dissolution products of the mine waste tips as a result of the oxidation of mixed sulphide minerals. Dissolved Ni, Zn, sulphate, Cd, and Pb all figure strongly as may be expected given the type of mining conducted (Pb-Ag-Zn). As for the DGC data set, dissolved Cu again plays less of a role in describing the variability of the data than other metals derived from the common metal sulphide ore minerals. Dissolved Ca, Sr and Ba also contribute largely to F1, suggesting a carbonate source, attributable to marine rainwater or possibly released from buffering reactions of acidic mine waters (e.g. Equation 12, Chapter 3, section 3.4.3). However the overall carbonate content of the host rocks are low in this area (BGS, 2010) and therefore the acid neutralising potential is also likely to be low. The second principal component (F2), which accounts for 14% of the total variability, was mostly attributable to dissolved oxygen (15%), conductivity (15%) and temperature (9%). The distribution of variables and observations with respect to F1 and F2 are shown in Figure 4.5. Overall there is limited separation of the data set because the main variables of interest (Zn, Pb, Cu, Cd, Mn, As, [H^+], sulphate) are orientated similarly on the variables plot (upper graph, Figure 4.5).

A nucleation of samples (Figure 4.5, circle A) with slight negative F1 character and slightly positive F2 character was observed and the majority of these samples

comprise Cholwell Brook waters. When examined in detail there was no obvious trend between location on the diagram and distance along the water course. However samples up stream of the visible mine waste (labelled as USW, Figure 4.5) tend to spread towards the negative axis of both F1 and F2. Borehole samples spread from negative F1 and F2 character to towards slightly positive F1 character and positive F2 character. There was no obvious location specific trend in the character of borehole waters. The difference between samples was attributed to the residence time of groundwaters within the waste, which is likely to control the degree of saturation with respect to dissolved species and sample temperature.

Plots of F3 vs. F1 (not shown here) and F4 vs. F1 (also not shown) grouped Cholwell Brook samples and resolved borehole samples similarly to the F2 vs F1 plot shown. No further division of the samples into discernable groupings was observed when lesser principal components were compared. Principal component F3, which accounted for 9% of the total variability, was most strongly influenced by Ag (14%), Sn (14%) and B (13%). Principal component F4 accounted for 8% of the total variability and was most strongly influenced by nitrate (15%), Sn (14%), Ag (13%) and B (10%). Ag and Sn generally exhibit very low solubility, and are present in very small amounts in some of the samples but were <LOD for most. The distribution of dissolved B throughout the samples and its high contribution to the variability of the data set suggests something within the site is acting as a source either within the waste or an alternative source. In other studies of surface and ground water geochemistry, elevated B has been attributed to sulphur-rich coal mines (Craw *et al.*, 2006), domestic and industrial effluents and the weathering of boron-containing minerals, such as tourmaline, clays and Fe-oxides (Jahiruddin *et al.*, 1998; Shand *et al.*, 2007) . Waters at Devon Great Consols and Wheal Betsy both show variable B concentrations (3.1-60.0 μmol L^{-1} and (0.04-9.1 μmol L^{-1}, respectively), but both are within range of naturally

occurring UK groundwaters (Shand *et al.*, 2007).

Figure 4.5: Plots of F1 and F2 principal components showing distribution of variables (above) and observations for the Wheal Betsy Data Set. Group A: Cholwell Brook samples.

4.5.4   Major Ions

The composition of the surface waters and boreholes with respect to major cations from all sampling rounds at Wheal Betsy are presented as molar percentages in ternary diagrams (Figure 4.6 and Figure 4.7). Overall, the data is grouped towards the bottom right corner of the plot, representing a high molar fraction of Na and K similar in composition to average rainwater, determined for Plymouth from Coles (1999).

Both boreholes and surface waters show a spread of data toward slightly higher Ca with respect to Na and K. The largest shift is observed from ground waters upstream of the mine, (12.4-13.6 μmol L^{-1}) to BH2 and BH3, highest in Ca (78.1-178 μmol L^{-1}). The plots suggest that interaction with soils or mine waste increase the proportion of dissolved Ca, a trend that was also seen for the Devon Great Consols data set (shown in grey for reference in Figure 4.7).

Overall, waters flowing through the Wheal Betsy site remain close to their source composition; either rainwater, groundwater or a mixture of the two. These findings concur with the hydrological observations to suggest that, due to rapid transport times and situation of the site in the upper reaches of the catchment (River Tavy), rainfall needs to travel a short distance before reaching the boreholes and Cholwell Brook. Therefore, waters are unlikely to reach equilibrium with respect to the mineral phases encountered in the waste.

Figure 4.6: Molar percentage of major cations for surface water samples from Wheal Betsy, grouped by sample type. Mean rainwater composition for Plymouth also shown (Coles, 1999).

Figure 4.7: Molar percentage of major cations for borehole water samples from Wheal Betsy. Mean rainwater composition for Plymouth also shown (Coles, 1999). Cholwell Brook samples (grey circles), Devon Great Consols surface drains (grey triangles) and boreholes (grey squares) also shown for comparison.

4.5.5   Master Variables

Conductivity and Total Suspended Solids (TSS)

Conductivity in all water samples ranged from 101 to 1480 µS (Figure 4.8). This was similar to the range observed in drains at Devon Great Consols (140-1040 µS) and much higher than in the River Tavy (5.0-17.7 µS cm^{-1}, Jan 1997-Dec 2006, EA). Borehole waters had higher conductivity than samples taken from Cholwell Brook and surface drains. However, unlike the Devon Great Consols site, samples showed a high degree of consistency with respect to sampling rounds, with the highest conductivities measured during the driest sampling condition (09/05/09, open triangles, Figure 4.8). The conductivities recorded on the 23/07/09 were slightly higher than other 'wet' rounds and this may be attributed to the high intensity rainfall which fell during the visit causing increased turbidity. The major contributors to conductivity were major ions: Na^+ (183-660 µmol L^{-1}), Cl^- (13.0-837 µmol L^{-1}), Ca^{2+} (12.4-178 µmol L^{-1}), Mg^{2+} (36.3-116.5 µmol L^{-1}), and dissolved Si (44.2-115 µmol L^{-1}).

Total suspended solids were low in upstream groundwater (<LOD (0.72 mg L^{-1}) -17.2 mg L^{-1}) and in upstream brook samples (all <LOD). Suspended particulates varied widely in concentration in waters from the boreholes (7.6 mg L^{-1} - 6.6 g L^{-1}). Brook samples through the site were generally low (<LOD-32.8 mg L^{-1}) but were increased as a result of heavy rainfall (23/07/09) and snow melt (12/02/09), to a maximum of 176 mg L^{-1} (sample 6, 12/02/09). However this is 200 times less than recorded in surface drains from WAM Upper tip at Devon Great Consols. Tips at DGC were more obviously susceptible to wind and water erosion, due to the lack of vegetation, low cohesion of tip material and unstable slope angles (physical properties determined by Mighanetara (2009)). At Wheal Betsy, the top surfaces of the north and south tips are largely vegetated and have extensive hardpan layers, giving increased protection, although erosion from the exposed slopes is a visibly on-going process.

Figure 4.8: Conductivity measurements recorded at Wheal Betsy during seven surveys.

pH, Eh and Dissolved Oxygen

The pH fluctuated widely across all sampling locations and rounds (pH 3.2-6.1, Figure 4.9). This is attributed to the fast and turbulent transport of waters through the site both in the brook and in surface and subsurface drainage from the tips. Accordingly brook and surface drains remained oxic with positive Eh (320-750mV, Figure 4.9) and high dissolved oxygen 8.9-13.5 mgL^{-1} (Figure 4.10). The pH of both upstream groundwater (pH 4.3-6.1) and upstream surface water (pH 4.6-6.1) entering the site were generally acidic due to the rainfall pH (around pH 5, EA (2008)) and catchment dominated by acidic soils and carbonate poor bedrock. Readings were varied and occasionally high, suggesting a flashy catchment response to incoming rainfall and a short residence time in subsurface systems. The highest pH values (>pH 6, 27/08/08)

may indicate the influence of some carbonate or aluminium silicate buffering in the upstream waters. Instrument error or drift also cannot be ruled out, but recorded drift was in all cases <0.3 pH units over the course of 18hrs, and so was unlikely to adversely distort the data. Furthermore, these values are within the range of published pH for groundwaters draining Dartmoor granites (pH 4.3-7.2, Smedley and Allen, (2004)).

BH2 (pH 4.0-4.5) and BH3 (pH 3.8-4.7) had significantly lower pH than waters in the northern stretch of Cholwell Brook, but otherwise there was no spatial control on the occurrence of low pH waters, with acidity (as $[H^+]$), spanning three orders of magnitude in the stream waters during the period of investigation.

Measured Eh in boreholes showed that reducing conditions were not prevalent, although the sampling round on the 23/07/09 returned lower Eh results in BH4 (288 mV) and BH5 (378 mV), compared with all boreholes and across previous rounds. Boreholes on this occasion were sampled before the onset of heavy rain and therefore may have been more stagnant than the high rainfall figures suggest. Dissolved oxygen was generally lower in boreholes than Cholwell Brook and surface drains; this was despite high Eh results. Field determination of Eh by this method are generally considered inaccurate beyond determination of extremes of reducing and oxic conditions (Christensen *et al.*, 2000). Therefore detailed analysis of the Eh results, particularly in very oxic waters, should be approached with caution.

Overall, waters migrate only a short distance from mine waste to Cholwell Brook (< 10m) and are rapidly transported downstream. There is less time for wasters to approach chemical equilibrium with waste minerals and soils, compared to waters migrating through the Devon Great Consols site. The result is a greater variability in the chemio-physical character of the waters. Variability is also exhibited by the concentrations of dissolved metals, metalloids and anions.

Figure 4.9: Measured pH (above) and Eh (below) in Wheal Betsy surface and borehole samples determined from seven surveys. Wet weather sampling rounds denoted by filled symbols, dry rounds denoted by hollow symbols.

Figure 4.10: Dissolved oxygen in Wheal Betsy surface and borehole samples determined from seven surveys. Samples 1 and 2 upstream of mine waste and known workings, U/S GW represents background groundwater concentrations. Wet weather sampling rounds denoted by filled symbols, dry rounds denoted by hollow symbols.

4.5.6   Dissolved Metal, Metalloid and Selected Anion Concentrations

In this section the concentrations of dissolved metals and metalloids in the drainage waters of Wheal Betsy will be discussed. PCA indicated that variations in geochemistry were largely due to residence time and DO content, and separated ground waters from stream waters. Since this indicates a much simpler system than at Devon Great Consols, drainage waters are examined by elemental groupings, rather than isolation of waters with a specific geochemical signature.

Aluminium and Iron

Dissolved Al concentrations in ground and surface waters (Figure 4.11) were up to three orders of magnitude lower than those observed at Devon Great Consols. However, all waters still exceeded EQS values for dissolved Al concentrations (0.009 μmol L^{-1}, short-term maximum, Chapter 3, Appendix 3D). PHREEQC calculations showed dissolved Al was most likely to occur as the trivalent free ion, but mono- and di-hydroxides were also predicted. In samples with highest sulphate, i.e. groundwaters in receipt tip drainage, the formation $AlSO_4$ was also favoured.

The pH range of the waters lies in the expected range of an aluminium buffered system (~pH 4.5-6.0, depending on mineral phases present). Carbonate buffering is unlikely to buffer significantly in this catchment, based on the slate dominated bedrock geology and acidic soils (Chapter 2, section 2.4.3), so dissolution of Al-containing phases is likely to be the dominant buffering mechanism. This was confirmed using the PHREEQC code and waters in Cholwell Brook were calculated to be saturated with respect to kaolinite ($Al_2Si_2O_5(OH)_4$), just saturated (SI > 0, < 1) with respect to gibbsite ($Al(OH)_3$) and basaluminite ($Al_4(SO_4)(OH)_{10}.4H_2O$), but undersaturated with respect to alunite ($KAl_3(SO_4)_2(OH)_6$) and jurbanite ($AlSO_4(OH)\cdot5H_2O$). Gibbsite, as the first hydroxyl product, is likely to precipitate in the range pH 4.5-5.0 (Nordstrom and Ball, 1986) but in the turbulent waters of the brook, it is possible that some of this may remain in solution as monomeric or colloidal species. Importantly, the monomeric form is primarily responsible for Al toxicity in aquatic systems (Wauer *et al.*, 2004).

Dissolved Al concentrations in borehole waters (1.6-21.8 μmol L^{-1} Al) were generally higher than in surface waters from the same survey and were calculated to be undersaturated with respect to all Al phases. This demonstrates that equilibrium of the waters with respect to the mineral assemblage was not achieved under conditions captured by the seven surveys.

Dissolved Fe concentrations were higher than the long-term EQS value (equivalent to 0.000286 μmol L^{-1}) with a range of < LOD (0.04)-1.2 μmol L^{-1} in surface waters and 0.6- 44.3 μmol L^{-1} in boreholes (excluding upstream groundwater, Figure 4.11). Boreholes at Wheal Betsy were shallow and oxic, with measured Eh similar to surface waters. Dissolved oxygen levels were variable (4.2 – 11.4 mg L^{-1}), but waters did not become sufficiently reducing for Fe^{2+} to be the dominant redox state (from PHREEQC modelling). However, higher dissolved Fe in borehole samples was co-variant with lower dissolved oxygen and increase in Fe^{2+} relative to Fe^{3+} in solution.

The elevated concentrations of dissolved Fe may have arisen because waters were not at equilibrium. However, samples were not filtered for 12 hours post-collection and were not depleted in DO, so this is unlikely since oxidation of Fe^{2+} to a Fe^{3+} precipitate (Fe(OH$_3$), is a relatively rapid process, (e.g. approximately 10^{-9} mol L^{-1} s^{-1} to 3.27±0.01×10^{-6} mol L^{-1} s^{-1}, Kirby and Brady (1998)), particularly in the presence of catalysing bacteria known to thrive in acidic mine waters. Closer inspection of the data set reveals that the median Fe concentration for each borehole was low (1.4-1.9 μmol L^{-1}) compared to the range, and that the highest Fe concentrations were recorded in the first sampling round, shortly after the installation of the boreholes. It is likely that a colloidal fraction of Fe permeated the 0.2 μm filters used to isolate the dissolved fraction and that this was enhanced by disturbance of the boreholes during installation. The relatively low rainfall at this time (14 days previous to 28/08/08) may not have been sufficient to adequately flush the borehole prior to sampling. If these high results are excluded, Fe concentrations are only slightly elevated in BH3, BH4 and BH5 with respect to surface drains and Cholwell Brook.

The surface drains were not enriched in either dissolved Al or dissolved Fe, and there was no obvious effect, either positive or negative from these inputs (samples 14-17, Figure 4.12).

Figure 4.11: Dissolved Al (top) and Fe (bottom) concentrations in Wheal Betsy surface and borehole samples determined from seven surveys. Remaining explanations as for Figure 4.10. LOD for Al and Fe typically 0.1 μmol L^{-1} and 0.2 μmol L^{-1}, respectively. Long-term freshwater EQS for dissolved Al and Fe equal to 0.00185 μmol L^{-1} and 0.000286 μmol L^{-1}, respectively.

Figure 4.12: Dissolved Al and Fe in Cholwell Brook waters during seven surveys. Dashed vertical lines show inputs from surface drains (14, 15,16 and 17). Annual average EQS shown as dotted horizontal lines. Remaining explanations as for Figure 4.10.

Dissolved Zn, Pb, Cd, Cu, Ni, and Mn Concentrations in Cholwell Brook and Surface Drains

Dissolved concentrations of pollutant metals (Zn, Pb, Cu, Cd, Ni and Mn) increased with distance along Cholwell Brook in this study (Figure 4.13 to Figure 4.17).

Dissolved Zn and Pb in incoming stream waters were at or below EQS values (0.122 μmol L^{-1} and 0.0348 μmol L^{-1}, respectively), but consistently exceeded this threshold upon reaching the visible extent of the mine waste and workings (sample 3, Figure 4.17). Both elements showed further enrichment in the waters as they passed through the site to a maximum of 3.9 μmol L^{-1} for Zn and 0.45 μmol L^{-1} for Pb, representing 55 x and 12x current long term EQS values for low alkalinity waters. These figures are slightly lower than Rieuwerts *et al.* (2009), who determined maximum dissolved concentrations of Zn and Pb equal to 6.7 μmol L^{-1} and 1.2 μmol L^{-1}, respectively, from three surveys in 2004. The accumulation of dissolved Pb was greater through the southern waste tips, suggesting mine wastes may be more Pb-rich in this part of the site. Upon leaving the site, dissolved Pb in Cholwell Brook was higher than concentrations recorded in targeted surveys, streams and rivers in the Tamar catchment by the EA (maximum equivalent to 0.0965 μmol L^{-1}, 1974-2008, Table 3.1).

Dissolved Zn is above the range recorded for major tributaries of the River Tamar, but lower than drainage from some adits within the Tamar catchment (e.g. 42.8 μmol L^{-1}, recorded for adit drainage from Drakewalls mine, EA). It is also lower than concentrations in the final collection drain at Devon Great Consols ($\bar{x}$ = 12.4 μmol L^{-1}). However the final drain at DGC, discharges to a major watercourse (River Tamar), resulting in an approximate 680 times dilution based on mean flow. Cholwell Brook is a tributary of the River Tavy, relying on catchment dilution and natural attenuation of pollutants to reduce dissolved concentrations downstream of the mine. The mean flow in the River Tavy at the nearest gauging station (Denham/Ludbrook SX476681), some

15 km further downstream, was 6.97 m^{3}s^{-1} (1981-2009, CEH (2011)), still much lower than the River Tamar at Gunnislake (22.6 m^{3}s^{-1}, CEH (2011)). Therefore, the impact of dissolved Zn (and other eco-toxic elements) on aquatic life may be greater in Cholwell Brook.

Concentrations of dissolved Cd were <LOD (0.009 μmol L^{-1}) upstream of the site, but also increased with distance along the watercourse to a maximum of 0.018 μmol L^{-1} (Figure 4.17). This level is low compared to some international river systems polluted by mine waters. For example 6.58 μmol L^{-1} was recorded in the Rio Tinto, SW Spain (Cánovas *et al.*, 2008) and 8.99 μmol L^{-1} in surface waters at a Bolivian mining area (Salvarredy-Aranguren *et al.*, 2008). However, concentrations in the brook are approximately 250 times greater than the annual average EQS value for low alkalinity waters, and at higher concentrations than previously recorded by the EA during targeted and routine surveys of watercourses in the Tamar catchment.

Dissolved Cu (Figure 4.14), Ni (Figure 4.15) and Mn (Figure 4.16) concentrations in Cholwell Brook were low by comparison to the final drain at DGC. Waters increased in Cu concentration the brook to a maximum of 0.29 μmol L^{-1} at location 12, representing 18 x EQS value (0.016 μmol L^{-1}), but was considerably lower than the average discharge concentration in the final drain of Devon Great Consols (70-85 μmol L^{-1}). Dissolved Ni, which had showed greater variability in concentration with respect to other metals at Devon Great Consols, increased in concentration through the site like other contaminant metals, but was not clearly ordered from low to high by increasing rainfall (Figure 4.17). Maximum concentrations recorded for dissolved Ni in Cholwell Brook (0.08 μmol L^{-1}) did not exceed the EQS value (0.34 μmol L^{-1}). Similarly, concentrations of dissolved Mn in all samples (0.26-11.0 μmol L^{-1}) were at least an order of magnitude lower than found in the waters at DGC, but all samples were higher than the current long term average EQS (0.127 μmol L^{-1}).

Closer inspection of the ordering of sample rounds with respect to Zn in Cholwell Brook (Figure 4.13, lower graph and Figure 4.17) demonstrate that higher concentrations in the Brook were observed during wet surveys. In fact the concentration of Zn in the Brook doubled from the driest to the wettest periods. A similar trend was observed for all the major contaminant species (Zn, Pb, Cu, Cd, Ni and Mn (Figure 4.17), As (Figure 4.18) and sulphate (Figure 4.19)).

There are no other mine discharges located within the catchment of the brook or tips than could augment metal concentrations in waters entering the site. The acidic groundwater, soils and mineralisation of the country rock in the area cause background concentrations of some trace elements to be elevated and include: Al (up to 47.1 μmol $^{-1}$), Cu (up to 8.2 μmol L^{-1}), Zn (up to 24.5 μmol L^{-1}), Mn (up to 0.108 μmol L^{-1}) and Pb (up to 0.0177 μmol L^{-1}) (Smedley *et al.*, 2004). This enrichment accounts for elevated dissolved Zn, Cu and Mn with respect to EQS in the upstream waters at Wheal Betsy.

Surface drains were generally higher in dissolved contaminants than the Brook. Surface drain 14, flows along the northern boundary of visible waste (Figure 4.4). This drain was generally lower in dissolved contamination than other surface drains and similar to those seen for the low sample numbers in Cholwell Brook. The remaining drains, which were ephemeral in nature, comprised surface run-off from main areas of waste (sample 15 and 16) and the only input from the east bank (sample 17). The drains were generally enriched in contaminant metals with respect to Cholwell Brook, particularly Pb, which was higher in sample 17 than any other sample (2.8 μmol L^{-1}). Sample 17 may be discharging from a collapsed adit but or may be a collection of surface drainage channelled through a fracture in the exposed bedrock. The latter is more likely as dissolved Fe is usually elevated in adit discharges, but was similar in drain 17 to other samples (Figure 4.11). In either case, this was further evidence for Pb-rich deposits being concentrated in the southern zone of the site.

Dissolved Zn, Pb, Cd, Cu, Ni, and Mn Concentrations in Shallow Groundwaters

Elevated groundwater concentrations with respect to the Brook and EQS values were recorded in shallow groundwater throughout the sampling rounds for dissolved Zn (up to 30.4 μmol L^{-1}, BH4), Pb (up to 2.3 μmol L^{-1}, BH3), Cu (up to 2.4 μmol L^{-1}, BH4), Cd (up to 0.17 μmol L^{-1}, BH4), Ni (up to 0.41 μmol L^{-1}, BH2 and BH3), and also Mn (up to 11.0 μmol L^{-1}, BH4). Dissolved metal concentrations were two to five times the concentrations observed in the Brook, with the exception of Cd which was approximately five to ten times higher in the borehole waters.

BH3 and BH5 were installed into the base of the mine waste, while BH2 and BH4 were installed a short distance away (<10 m) alongside Cholwell Brook. There was no evidence of significant natural attenuation, leading to reduced concentration from the boreholes at the base of the tip, to the boreholes next to Cholwell Brook. Concentrations of individual dissolved metals in borehole waters varied significantly between surveys with a minimum RSD of 24% (Table 4.8). Chloride concentrations also varied (RSD = 31 %) and since Cl is generally considered to be conservative, this indicated that evapo-transpiration may be an important process affecting porewater concentrations in the waste tips (see later anion discussion). RSD was considerably higher for the redox sensitive elements Fe and As, 156 % and 203 % respectively.

Table 4.8: Mean concentration, standard deviations and relative standard deviations of dissolved metals and As in BH2-BH5 at Wheal Betsy (n = 21, n = 17(Cl, SO$_4$)). Chloride result 489 ± 152 μmol L^{-1}, RSD = 31 %.

Dissolved metal/metalloid:	Zn	Mn	Cu	Al	Ni	Cd	Pb	As	Fe	SO$_4$
Mean ± 1 s.d. (μmol L^{-1})	21.4 ±5.3	4.96 ±2.66	0.920 ±0.624	6.49 ±4.89	0.179 ±0.088	0.127 ±0.031	1.15 ±0.48	0.209 ±0.325	4.88 ±9.93	176 ±46
% RSD	25	70	68	75	49	24	42	156	203	26

The composition of the borehole waters varied spatially and temporally with respect to these metals. Concentrations of dissolved Zn, Cd and Ni were generally

higher in all boreholes during wet surveys (filled symbols in Figure 4.13 to Figure 4.16) when a high water table was observed at the base of the tips (from Table 4.7). However this was not the case for all metals. Dissolved Cu and Pb, were highest in BH3 (base of tip) during a wet survey and highest in BH4 (next to brook) under drier conditions. This was attributed to slightly lower pH observed in drier surveys (16/08/08 and 09/05/09) enhancing desorption of these elements, which are known to be strongly associated mineral surfaces, particularly Fe-oxides.

Low rainfall is likely to result in increased transport times, such that dissolved metals in the pore waters accumulate toward equilibrium. This is consistent with the relatively low Eh and dissolved oxygen observed in BH4 compared with other boreholes during all surveys, since oxygen is likely to be consumed by oxidation reactions with pyritic material in the mine waste (identified in the core log, Appendix 4C). A smaller variation in pH between surveys also suggests a steady state is attained more easily in pore waters surrounding BH4 when the transport of ground waters is slower.

If the concentration of pollutant metals was constant in surface and shallow groundwaters, as for the final drain at DGC, then the expected effect of higher rainfall would be to dilute the contamination in the Brook; instead the reverse trend was observed. Therefore, the variability being detected in Cholwell Brook is attributed to the dynamics of flushing leachate from the mine waste tips. The generation of dissolved load from the mine waste is reactive to changing hydrological conditions. Oxic rainfall supplied oxygen to drive sulphide oxidation and in conjunction with a higher water table promoted the reaction of a greater total surface area of waste material. High rainfall also drove hydraulic transport of the contamination away from the source and into Cholwell Brook.

The dominant species for the contaminant metals Zn, Pb, Cu, Cd, Ni and Mn were calculated using PHREEQC geochemical modelling. There was little variation in the predicted speciation of these metals in the sampled waters. A range of complexes were predicted but, the divalent free ion was the dominant species by one or two orders of magnitude for Zn, Pb, Cu, Cd, Mn, and Ni, in surface waters and boreholes. Also important were chloride complexes for Cd ($CdCl^+$), and Mn ($MnCl^+$), sulphate complexes for Zn ($ZnSO_4$), Pb ($PbSO_4$) and Mn ($MnSO_4$). Borehole samples were reacted with a gas phase equivalent to the composition of air in PHREEQC; however there was little effect on the major species predicted for aforementioned metals suggesting they were close to equilibrium with respect to atmospheric oxygen.

The flux arising from flooded mine workings must also be considered. This could contribute to the base flow of Cholwell Brook and react similarly to higher water levels and oxic recharge. Cycling of oxidation and flushing in underground workings due to fluctuating water levels increases the contamination flux from underground workings (Wheal Jane remediation program, United Utilities Industrial Ltd, *personal comm.*). Secondary minerals may be precipitated in the unsaturated zone as water level falls and subsequently remobilised as waters rebound (Evans *et al.*, 2006). Surface expression of the water table in the workings at Wheal Betsy could augment the concentrations in Cholwell Brook via this mechanism. It is virtually impossible to determine accurately the relative contribution of two sources (mine waste leachate vs. emerging mine waters). The waste tip material has much greater mineral surface area and exposure to the atmosphere, proven by the high permeability and oxic waters encountered in borehole waters. However, the reactive catchment and underground voids may similarly recharge dissolved oxygen to the mine workings. Furthermore, back-filling of the underground workings with mine waste was (and remains) a common practice. This would increase the reactive surface area of minerals compared to unfilled

workings. Further investigation of the transport pathway of waters in Cholwell Brook would be required to elucidate the contribution, if any, from underground workings.

Figure 4.13: Dissolved Zn (above) and dissolved Zn zoomed to show samples < 5 µmol L⁻¹ (below) for surface and borehole samples at Wheal Betsy during seven surveys. Dotted horizontal lines represent annual average EQS for Zn (0.122 µmol L⁻¹). Remaining explanations as for Figure 4.10.

Figure 4.14: Dissolved Pb (above) and Cu (below) concentrations for surface and borehole samples at Wheal Betsy during seven surveys. Dotted horizontal lines represent annual average EQS for Cu and Pb (0.016 and 0.035 μmol L^{-1} respectively). Remaining explanations as for Figure 4.10.

Figure 4.15: Dissolved Cd (above) and Ni (below) for surface and borehole samples at Wheal Betsy during seven surveys. Dotted horizontal lines represent annual average EQS for Cd and Ni (0.00071 and 0.341 μmol L^{-1} respectively). Missing Cd data points for samples 1-3,5,14,16,US G/W < LOD (0.009 μmol L^{-1}). Remaining explanations as for Figure 4.10.

Figure 4.16: Dissolved Mn for surface and borehole samples at Wheal Betsy during seven surveys. Remaining explanations as for Figure 4.10. Dotted horizontal lines represent annual average EQS for Mn (0.0127 μmol L^{-1}).

Figure 4.17: Dissolved Zn, Pb, Cu, Cd and Ni for Cholwell Brook during seven surveys. Annual average EQS shown as dotted lines. Remaining explanations as for Figure 4.10.

268

Arsenic (and Antimony) Concentrations and Speciation

Dissolved As concentrations were largely <LOD (0.011 µmol L^{-1}) in Cholwell Brook but were consistently detected in the southern-most sampling point (sample 13) to a maximum of 0.055 µmol L^{-1}, (Figure 4.18). This is an order of magnitude lower than current EQS concentration (equivalent to 0.667 µmol L^{-1}). The surface drain (Sample 17), also in the south of the site, returned the highest result for dissolved As (2.0 µmol L^{-1}), but was only observed to flow during one visit. As discussed in the previous sections, this drain may be the surface expression of deeper ground waters, which are higher in dissolved As. Surface waters were otherwise very low in As (<LOD). Co-precipitation reactions of As with Fe (and Pb), are thermodynamically favoured and have been noted in other studies of sulphidic mine waste e.g. Roussel *et al.* (2000). Inspection of the saturation indexes generated by PHREEQC showed that all samples were undersaturated with respect to a number of secondary iron and arsenic phases including jarosites (e.g. K-Jarosite, $KFe_3(SO_4)_2(OH)_6$) and scorodite ($FeAsO_4{:}H_2O$). So although As (and Pb) mobility is evident at the southern extent of the site it is possible that this is short-lived, tending towards less mobile As(V) species upon reaching thermodynamic equilibrium or being bound within or sorbed to secondary Fe precipitates.

Upstream groundwater in this catchment can be enriched in As (up to 0.08 µmol L^{-1}, Smedley *et al.* (2004)), due to interactions with metamorphic aureoles surrounding the Dartmoor, Gunnislake and Kit Hill granites and the black shales outside of them (Moon, 2010). However, due to the strong association of As to Fe-oxides in oxic environments, shallow groundwaters have low dissolved concentrations, as was the case at Wheal Betsy, where upstream groundwaters were <LOD. Shallow boreholes at Wheal Betsy, particularly BH4 were elevated in As with respect to surface samples to a maximum of 1.19 µmol L^{-1}. Geochemical modelling revealed that, as for the boreholes

at Devon Great Consols, a higher proportion of As(III) to As(V) under more reducing

conditions, which was concurrent with observed increased mobility. Upon simulated

equilibrium with atmospheric oxygen (PHREEQC), the dominant As redox state

becomes As (V) in all samples, with H_3AsO_4 being the dominant species with lesser

amounts of $H_2AsO_4^-$.

Figure 4.18: Dissolved As for surface and borehole samples at Wheal Betsy during seven surveys. Remaining explanations as for Figure 4.10. Missing As data points < LOD (0.011 µmol L^{-1}).

At Devon Great Consols, a strong covariance existed between the occurrence of

dissolved As and dissolved Sb in solution (molar ratio of 470:1). A similar relationship

at Wheal Betsy would suggest a maximum dissolved Sb concentration of approximately

0.004 µmol L^{-1}, in the waters. Results from ICP-MS analysis suggested the presence of

trace Sb in the waters of Wheal Betsy around this level (0.006 µmol L^{-1}). However, this

was below the calculated limit of detection for Sb (0.019 µmol L^{-1}) and the relationship

between As and Sb could not be confirmed.

Anions

Concentrations of dissolved sulphate and chloride are shown in Figure 4.19. Fluoride, phosphate, nitrite and bromine were below detection limits in all samples. Nitrate concentrations ranged from 8.3- 28.5 μmol L^{-1} in surface waters and 2.4-45.5 μmol L^{-1} in boreholes and, as for Devon Great Consols, the most likely source was surface run-off from agricultural land.

Concentrations of dissolved sulphate were 26.3-53.9 μmol L^{-1} in the surface samples at Wheal Betsy, slightly higher than background groundwaters (25.5-44.4 μmol L^{-1}), while borehole waters were significantly higher (102-271 μmol L^{-1}). As the second most abundant counter ion (after chloride), and the product of sulphide oxidation reactions, there was a close correlation between sulphate and contaminant metals in solution (r $\geq$ 0.9 for Zn, Cu and Cd, r ≥ 0.8 for Pb and Ni and r $\geq$ 0.7 for Mn, all p values << 0.05), and Ca (r ≥ 0.8, p << 0.05) which was thought to arise from buffering reactions within the mine waste.

Dissolved sulphate displayed the same pattern of increased concentration along the course of Cholwell Brook as seen for these metals and was more prevalent as a complexing species towards the south of the site and in the borehole samples. Overall the concentration range was much lower than that recorded for Devon Great Consols drainage (610-5300 μmol L^{-1}), consistent with a lower total dissolved metal load.

The presence of dissolved chloride, a conservative element derived from atmospheric sea-water inputs, is an indication of the amount of surface water input at each of the sample locations (Guan *et al.*, 2009) while increased concentration can indicate evapo-transpiration of shallow groundwaters (Shand *et al.*, 2007). Surface drain 14 and BH5, BH4 and BH3 showed enrichment in Cl compared to the mean concentration (374 μmol L^{-1}) to a maximum of 837 μmol L^{-1} (BH5). This suggests that concentration of pore waters occurs in the northern waste tips as a result of evapo-

transpiration. The formation of efflorescent salts from saturated porewaters can lead to a temporary sink for contaminants which may be subsequently dissolved. This would enhance the release of contamination from the tips following rainfall.

Figure 4.19: Dissolved sulphate (above) and chloride (below) for surface and borehole samples at Wheal Betsy during five surveys. No anion analysis for initial survey or 16/10/08. Remaining explanations as for Figure 4.10.

Borehole levels and stream flow were also low at this time and suggest a higher residence time for shallow ground waters, in the absence of rainwater 'flushing' the waste tips. Relatively high conductivity and pH , low DO and low dissolved Al, as compared to other rounds, were also recorded and are consistent with a longer residence time allowing dissolution and desorption processes to approach equilibrium.

Other Trace Elements

Dissolved Co was between 0.011-0.130 μmol L^{-1} across all surveys and sample locations. Phosphate, Nitrite, F, Sn, Mo, V, W, Sb and U were also analysed but all were below <LOD in all samples.

4.5.7 Estimated Annual Contamination Fluxes from Diffuse Pollution at Wheal Betsy and the Relative Contribution from North and South Waste Tips

Cholwell Brook

Dissolved metal and As fluxes leaving the site via Cholwell Brook were calculated for each survey based on dissolved concentrations and flows downstream of the mine (sample 13, Table 4.9). Fluxes were also calculated for the boundary between north and south areas of mine waste (sample 8, Table 4.9), in order to investigate the relative contributions of the north and south tips to overall flux. For comparison with data from the final drain discharge at Devon Great Consols (DGC), daily results have been scaled-up to annual ranges and mean annual dissolved flux (Table 4.10).

The estimated average annual flux of dissolved Cd discharging into Cholwell Brook (470 mol y^{-1}) was considerably higher than the annual flux estimated for the final collection drain (DGC, 13.8 mol y^{-1}) and Blanchdown adit (DGC, 4.33 mol y^{-1}). It

as also higher than an adit from another abandoned lead-silver mine[1] (20.2 mol y^{-1}, Mighanetara, unpublished work). As such, dissolved Cd entering Cholwell Brook from Wheal Betsy represents the largest flux of Cd so far reported for a mine in the Tamar catchment

Table 4.9: Estimated daily dissolved contaminant fluxes leaving the Wheal Betsy site via Cholwell Brook (at sample location 13). Relative contribution of north tips/workings (WBN, sample 8), to overall flux determined for each survey. Range and mean results presented (mol d^{-1}).

Daily Dissolved Flux in Cholwell Brook (mol d^{-1})	Zn	Pb	Cu	Mn	Cd	Ni	As	Al	Fe
WBN (8), range	2.23-29.9	0.0523-2.36	0.06-1.09	0.83-7.96	0.0316-0.129	0.0730-0.732	<LOD	1.39-32.5	0.37-7.29
WBN (8), mean	16.6	0.933	0.539	4.48	0.0853	0.388	<LOD	15.7	4.33
WBN + WBS (13), range	7.61-31.2	0.738-3.26	0.48-1.81	2.13-6.47	0.0342-0.150	0.190-0.551	<LOD-0.503	3.77-18.4	0.37-7.29
WBN + WBS (13), mean	**22.2**	**3.25**	**1.29**	**5.11**	**0.10**	**0.445**	**0.215**	**12.7**	**2.66**
% WBN, range	29-104	7-77	14-76	39-131	0-176	39-134	(0)	37-98	45-351
% WBN, mean	73	40	41	89	72	90	(0)	81	171

Estimated annual dissolved Zn flux from Wheal Betsy (2780-11400 mol y^{-1}) was approximately equal in magnitude to flux from the final collection drain (FCD) at DGC (2660-13300 mol y^{-1}, Table 4.10), and approached that of the highest point discharge of dissolved Zn previously identified by Mighanetara *et al.* (2009) in the waters of Luckett Stream, 11900 mol y^{-1}. Dissolved Fe and As flux from both the FCD and Cholwell Brook were similarly low due to the maintenance of oxic conditions in the steam waters, whilst dissolved fluxes of Cu and Al were two and three orders of magnitude lower

---

[1] South Tamar Consols worked one of the richest lead silver deposits in the catchment, until inundation by waters from the River Tamar in 1856 prematurely ceased operation. Large quantities of Pb-Ag ore remained below ground in situ and as broken rock (Booker, 1967).

from Wheal Betsy than DGC (Table 4.10). Despite this, the receiving watercourse at Wheal Betsy is more vulnerable to ecological damage than the River Tamar in receipt of Devon Great Consols discharge from the final drain, due to the lack of immediate in-stream dilution.

Table 4.10: Estimated annual dissolved contaminant fluxes leaving the Wheal Betsy site via Cholwell Brook (at sample location 8 and 13). Range and mean results presented (mol y^{-1}). For comparison, 2008-2009 Devon Great Consols Final Collection Drain results (from Chapter 3) are also shown below with the ratio of mean results for final dissolved discharges from both sites.

Annual Dissolved Flux in Cholwell Brook (mol y^{-1})	Zn	Pb	Cu	Mn	Cd	Ni	As	Al	Fe
WBN (8), range	812-10910	19.1-860	11.5-46.9	304-2904	23.6-400	26.7-267	<LOD	508-11900	137-2662
WBN (8), mean	6040	340	31.1	1640	197	142	<LOD	5750	1580
WBN + WBS (13), range	2780-11400	269-1190	12.5-54.8	779-2360	174-660	69.2-201	<LOD-183	1376-6704	307-1980
WBN + WBS (13), mean	**8100**	**783**	**37.6**	**1870**	**470**	**163**	**78.6**	**4630**	**970**
Devon Great Consols Final Collection Drain (FCD), range	2660-13300	1.21-3.60	15100-75200	12100-60000	4.14-22.0	405-2000	45.6-277	125000-629000	439-1910
Devon Great Consols Final Collection Drain, mean	**8840**	**2.68**	**53000**	**39400**	**13.8**	**1290**	**164**	**434000**	**1060**
Ratio of mean FCD : mean WBN+WBS	1:1	1:292	1410:1	21:1	1:34	8:1	2:1	94:1	1:1

Figure 4.20 compares the 7-day and 14-day total rainfall data (right graph), with flow in Cholwell Brook (middle graph) at halfway (sample 8) and at the downstream extent of the waste (sample 13), for four surveys of directly comparable data. High flow (23/07/09) and low flow (09/05/09) in Cholwell Brook was consistent with the high and low short term rainfall, while snow melt waters increased flow during one survey

relative to rainfall (12/02/09). Rainfall had a two-fold effect on flux, increasing the volume of leachate produced and the concentrations of dissolved metals in the Brook.

Figure 4.20: Graphs displaying relationship between 7-day and 14-rainfall (left), flow in Cholwell Brook (middle) and combined flux of Zn, Pb, Mn, Ni, Cu, Al and Fe (right). (F) = pore waters within waste tips above the water table were frozen, (M) = flows augmented by melt waters, (D) = dry, (W) = wet. Error bars for flow assume 7.5 % RSD on flow meter, but do not account for error in cross-sectional area of stream.

Higher pH (Figure 4.9) in waters of the northern part of Cholwell Brook was covariant with decreased flow and was attributed to a lower volume of acidic leachate entering the brook from the north tips. High rainfall and snow melt both generated high groundwater levels in the waste and resulted in low pH for waters in the brook. This is consistent with the previous study at Wheal Betsy by Rieuwerts *et al.* (2009), where the lowest pH and highest concentrations of dissolved Zn and Pb were recorded during the wettest survey (Dec 2004, rainfall average 4.07 mm d^{-1}, Met Office (2006)).

Low pH was maintained downstream of the south waste tips (sample 13, Figure 4.9) but was variable and highest when melt waters augmented flow, perhaps as a result of increased dilution from surface run-off.

A higher combined dissolved contaminant flux of Zn, Pb, Cu, Mn, Cd, Ni, As, Al and Fe in Cholwell Brook (Figure 4.20, right) was concurrent with high rainfall and high stream flow (Figure 4.20, left and centre, respectively). The flux from the northern zone was highly variable compared with the total flux (Table 4.9 and Figure 4.21) and was dependent on rainfall and flow conditions. The north zone supplied the majority of

dissolved flux of Zn, Cd, Mn, Ni, while Pb, As and Cu were more significantly augmented through the southern zone, most likely due to their enrichment in the mineralogy of the southern waste tips. This may be a consequence of the boundary of two geological formations being at the site (described in section 4.1.3), marked by Cholwell Brook. Tips to the east of this boundary are found only in the southern part of the site and the only surface drain from the east bank (sample 17, Figure 4.4) was highest in dissolved Pb (Figure 4.14) and As (Figure 4.18).

Figure 4.21: Percentage of overall dissolved flux attributed to tips and workings in northern part of the site. Error in flux determined as product of analytical LOD and flow error. Error bars on WBN flux (% of total) calculated as sum of flux error at location 8 and 13.

When conditions were dry (09/05/09), or surface temperatures cause tip porewaters to freeze (10/02/09), flow through the northern tips was reduced. This resulted in the southern tips supplying a higher proportion of the overall flux leaving the site (Figure 4.20, right). The southern tips, being comprised of finer waste material (see Chapter 5, section 5.6.2), including layers of compacted clays and iron-pan, generally produce a smaller proportion of the overall flux because water ingress and leachate transport was inhibited by low permeability.

The relative flux of dissolved metals and chloride with respect to one another remained relatively stable (Figure 4.21) when the magnitude of total flux varied considerably (Figure 4.20, right). The exception was Cd, where melt waters significantly enhanced the flux of Cd from the northern part of the site (Figure 4.21, lower graph, 12/02/09). There was no obvious reason for this behaviour.

For some surveys, the flux of dissolved Fe for sample 8 (south of the north tips), was significantly greater than at for sample 13, (400 m downstream of the south tips). This is highlighted by the large bars for dissolved Fe in Figure 4.21 for the wettest survey (23/07/09), and the survey following snow-melt (12/02/09). This may be partially attributed to the lower flow recorded at location 13 compared with location 8 (Figure 4.20, middle). However high flux of dissolved Fe was covariant with a higher suspended load of fine particulates (section 4.5.5). Rapid precipitation of Fe-oxide minerals and sorption to stream sediments or organic matter may have been a mechanism by which in-stream reduction of dissolved Fe occurred between locations 8 and 13.

The mobility of other metals may have been similarly reduced through co-precipitation and sorption reactions to $Fe(OH)_3$ minerals or organic matter. This is consistent with the fall in dissolved concentration of Zn, Pb, Cu, Cd, and Ni observed from location 12 (downstream extent of waste) to location 13 (Figure 4.17). However, the same fall was not observed for As. This may be a consequence of slower reaction kinetics, or competition with other dissolved species, in particular dissolved organic matter (DOM). DOM was not directly measured, but was likely to be abundant in the stream waters given the land use of the immediate area, (sheep grazing and riding stables directly adjacent to Cholwell Brook, Figure 4.4). DOM tends to compete with dissolved arsenic species for active sites on adsorbents and thus increases arsenic mobility (Sharma and Sohn, 2009). The attenuation of Fe by precipitation and the

sorption of other dissolved contaminants was consistent with processes controlling contaminant mobility in the final drain at Devon Great Consols. However the attenuation effect in Cholwell Brook could only be inferred from limited data. The association of contaminant metals and As to secondary Fe precipitates is explored further in Chapter 5.

The concentration and flux data suggests that leachate from the northern waste tips, were responsible for the magnitude and variability in dissolved contamination observed in Cholwell Brook. Deeper groundwater from the abandoned workings may augment flux, but under conditions of low flow, concentrations and fluxes (Figure 4.20, right) of dissolved metals in the brook were reduced. Therefore dissolved metals and As were lower in base flow and were augmented by tip drainage. It was concluded that fluctuation in rainfall and water table controls the levels of dissolved contamination eluting from the tips into the watercourse in a highly reactive catchment. It is still possible that the underground workings supply an additional flux to the brook, but may discharge further downstream, perhaps mixing with discharges from Wheal Friendship and would require further investigation.

Predicted Annual Flux from the Waste Tips

As for the selected tips at Devon Great Consols, an estimation of the fluxes arising from the tips at the site was attempted using the catchment area defined by ArcHydro9 (ArcGIS), average annual rainfall data (MIDAS, Met Office) and dissolved contaminant concentrations derived from borehole samples (BH2-5). The calculation was made for the tips in the northern part of the site only, as no borehole data was recorded for the southern tips. Data for all the contaminants of interest are shown in Table 4.11, alongside data for the tips at Devon Great Consols.

The calculations demonstrate the potential for the tips to account for all the dissolved contaminant flux observed in Cholwell Brook up the boundary with the southern waste tips.

There was a large margin of error on such calculations due to the scaling up of limited BH and stream water samples to represent metal concentrations emanating from the entire northern waste deposit. This is a particular problem for this site as the observed concentrations in boreholes and surface waters fluctuated widely, and were attributed to the hydrological variation between surveys. The high upper range of mass balance (e.g. 898 % for Zn, Table 4.11) occurs because of the disparity between the method of estimation used to determine annual flux in Cholwell Brook, compared to that used for the waste tips.

Very dry and very wet conditions were shown to effect on concentrations and flow in the brook. Direct measurement of the stream waters captured variability in both concentration and flow. However, the estimated tip flux was calculated from average annual rainfall data therefore the variability in the rainfall data is lost from the calculation. Variability in estimated tip flux is derived only from the variability in dissolved concentrations in borehole waters, as captured during five of seven surveys.

Despite the limitations the mean estimated flux for tips and Cholwell Brook, was general consistent between to within an order of magnitude for typically mobile elements such as Zn (138 %) and Mn (91%). The exception appears to be Cd for which the predicted flux from the tips is very low as a proportion of flux in Cholwell Brook (8.5-25%). This is important because the concentration and flux of Cd in Cholwell Brook is particularly high compared to others in the catchment (section 4.5.6). Determining the source and/or mechanism that led to the high concentrations of dissolved Cd in the stream waters would require further investigation.

Elements that typically precipitate at pH values measured in the brook ($\bar{x}$ = pH 4.9), such as Al, or elements known to co-precipitate or associate with Fe-oxyhydroxides such as Pb and Cu were over accounted for in tip flux compared to flux determined for Cholwell Brook. This was also the case at Devon Great Consols and the apparent attenuation is consistent with literature information on the sorption behaviour of these particular elements.

Estimates of annual flux can only improve with additional data, but there is strong evidence to suggest that the flux of contamination emanating the waste tips, particularly in the northern part of the Wheal Betsy site, is responsible for most of the contaminant flux transported downstream via Cholwell Brook.

Table 4.11: Estimated annual flux for selected metals and As leaving tips at Wheal Betsy North. Mean and inter quartile ranges of dissolved mean concentrations used to derive fluxes shown. Sample numbers used: BH2 – BH5. Mass balance of annual fluxes from north tips with respect to Cholwell Brook downstream of north tips.. Based on mean (in bold) and inter- quartile ranges. *Tip catchment encompasses two annual average rainfall zones, mean of two values used in calculation.

	Wheal Betsy North Tips	Cholwell Brook (8)	Mass Balance	Ratio of [WBN tips] to [Cholwell Brook]	DGC Cinders Tips	DGC WAM Tips	DGC Precipitation Launders Tips
Tip Catchment Area (m^2)	243580	-	-	-	84400	134535	115825
Average Annual Rainfall (mm y^{-1})	1650*	-	-	-	1289	1289	1264
Range Zn (µmol L^{-1})	18.1-23.5	1.71-2.86	-	11:1 - 8:1	2.05 - 2.38	12.0 – 12.9	13.4 – 18.0
Mean Zn (µmol L^{-1})	20.9	2.29	-	9:1	2.24	12.6	15.3
Range Zn Flux (mol y^{-1})	7291-9450	**812-10910**	87-898 %	-	223 - 259	2074 - 2242	1968 - 2634
Mean Zn Flux (mol y^{-1})	**8384**	**6040**	**138 %**	-	**244**	**2178**	**2244**
Range Ni (µmol L^{-1})	0.1435-0.1867	0.0504-0.0648	-	3:1 - 3:1	0.252 - 0.292	0.91 – 1.31	2.34 – 3.28
Mean Ni (µmol L^{-1})	0.1792	0.0565	-	3:1	0.285	1.11	2.72
Range Ni Flux (mol y^{-1})	57.7-75.0	26.7-267	28-216 %	-	27.4 – 31.8	157 - 227	343 - 479
Mean Ni Flux (mol y^{-1})	**72.0**	**142**	**51 %**	-	**31.0**	**192**	**398**
Range Cd (µmol L^{-1})	0.109-0.140	<LOD-0.0122	-	(<LOD)- 11:1	0.0020 – 0.0021	0.019 – 0.025	0.022 – 0.029
Mean Cd (µmol L^{-1})	0.124	0.0103	-	12:1	0.00204	0.023	0.025
Range Cd Flux (mol y^{-1})	43.6-56.1	174-660	8.5-25 %	-	0.213 – 0.228	3.35 – 4.32	3.25 – 4.30
Mean Cd Flux (mol y^{-1})	**49.9**	**470**	**10 %**	-	**0.222**	**3.76**	**3.65**

Range Mn (μmol L^{-1})	2.74-4.06	0.596-0.706	-	5:1 - 6:1	3.33 – 4.47	32.1 – 41.8	69.4 – 99.6
Mean Mn (μmol L^{-1})	3.72	0.658	-	6:1	3.88	37.0	81.4
Range Mn Flux (mol y^{-1})	1100-1632	304-2904	64-361 %	-	362-487	5570-7250	10200-14600
Mean Mn Flux (mol y^{-1})	**1493**	**1640**	**91 %**	-	**422**	**6410**	**11900**
Range Al (μmol L^{-1})	4.49-7.38	1.07-4.00	-	4:1 - 2:1	151-158	695-902	702-1010
Mean Al (μmol L^{-1})	6.61	1.95	-	3:1	154	823	828
Range Al Flux (mol y^{-1})	1805-2964	1376-6704	44-131 %	-	16400 - 17200	121000 - 156000	103000-148000
Mean Al Flux (mol y^{-1})	**2658**	**970**	**274 %**	-	**16700**	**142700**	**121000**
Range Pb (μmol L^{-1})	0.971-1.169	0.040-0.209	-	24:1 - 5:1	<LOD	0.006-0.020	0.003-0.009
Mean Pb (μmol L^{-1})	1.343	0.112	-	11:1	<LOD	0.015	0.014
Range Pb Flux (mol y^{-1})	390-540	19.1-860	63-2040 %	-	<LOD	1.06-3.42	0.48-2.08
Mean Pb Flux (mol y^{-1})	**470**	**340**	**138 %**	-	**<LOD**	**2.60**	**1.29**
Range Cu (μmol L^{-1})	0.618-1.020	0.0940-0.0633	-	7:1 - 16:1	10.4-12.8	201-267	102-131
Mean Cu (μmol L^{-1})	0.866	0.0760	-	11:1	12.9	224	115
Range Cu Flux (mol y^{-1})	248-410	11.5-46.9	22-875 %	-	1130-1390	34900-46400	14900-19100
Mean Cu Flux (mol y^{-1})	**348**	**31.1**	**1120 %**	-	**1410**	**38900**	**16800**
Range As (μmol L^{-1})	0.0690-0.276	<LOD	-	-	270 - 328	0.290 – 1.65	0.080 – 0.150
Mean As (μmol L^{-1})	0.185	<LOD	-	-	294	1.33	0.140
Range As Flux (mol y^{-1})	27.7-111	<LOD-183	60% +	-	29400 - 35600	50.3 - 286	11.7 – 22.0
Mean As Flux (mol y^{-1})	**74.4**	**78.6**	**95%**	-	**32000**	**231**	**20.5**

4.6 Conclusions and Recommendations

Wheal Betsy is situated in a step sided valley in an area of above average rainfall compared to other areas in the Tamar catchment and low permeability slate-dominated bedrock. Background surface and groundwaters were enriched in dissolved Cu and Mn above current EQS values upon reaching the site. This was attributed to the mineralisation of the host geology in the area which have been shown previously to enrich granite hosted groundwaters in certain trace elements including Al, Cu, Zn, Mn, and Pb (Smedley *et al.*, 2004). Dissolved concentrations of all the contaminant metals of interest (Al, Zn, Cu, Pb, Mn, Ni, and Cd) increased with distance along Cholwell Brook as the watercourse passed through the mine site at Wheal Betsy. As a result Cholwell Brook failed long term EQS for Al, Zn, Cu, Pb, and Cd during all surveys. The highest exceedance was for dissolved Cd (0.018 μmol L^{-1}, equal to 250 x EQS), dissolved Mn (11.0 μmol L^{-1}, equal to 87 x EQS) and dissolved Zn (3.9 μmol L^{-1}, equal to 55x EQS).

The concentration and estimated flux of dissolved Pb (0.45 μmol L^{-1}, and 783 mol y^{-1}, respectively) and the estimated flux of dissolved Cd (470 mol y^{-1}) were higher than identified elsewhere in the catchment by previous studies. Arsenic and Fe mobility was limited due to the shallow and oxic nature of surface and ground waters at the site.

The hydrology of the site was much simpler then at Devon Great Consols, with a short migration pathway (<10m) from tips to Cholwell Brook. Groundwater table and stream flow were highly reactive to short-term rainfall patterns and concentrations of dissolved contaminant metals were increased in the brook during wet surveys. Concentrations and fluxes of dissolved metals increased with increased rainfall and this was attributed to higher water tables in the base of the northern mine waste tips. Under conditions of low flow, the contribution from the southern tips to overall contaminant flux

increases. The south tips appeared to contribute most to fluxes of Pb, Cu and As, suggesting enrichment in these elements compared to the north tips.

The waste tips at the site were very heterogeneous at the site, but the tips in the northern zone exhibited greater permeability than the more clay-rich wastes in the south of the site. This may have been due in part to the unique geological setting of the site, lying on the thrust boundary of two distinct bedrock formations. The boundary of the Bealsmill Formation, and the lower Greystone Formation, is situated along Cholwell Brook; having resulting from the same geological event that created the mineralised deposits of south west England (Variscan Orogeny, DCC (2011)). Alternatively tip heterogeneity could be a feature of the division of processing waste, i.e. separation of course and fine waste, produced and deposited during the site's operation (to 1877).

The north tips were rapidly flushed by percolating waters and which supplied oxygen for oxidation and dissolution of sulphide minerals. Dissolved contaminants (Zn, Pb, Cd, Cu, Mn, Ni and Pb) in porewaters of the mine waste were enriched with respect to waters in Cholwell Brook by up to 25x (Al, Table 4.11). Despite this, waters were not at equilibrium with mineral phases in the waste and were rapidly transported into Cholwell Brook via shallow subsurface flow and ephemeral surface drains. No reduction in dissolved metal was observed between waters percolating the base of the mine wastes and those close to the bank of the brook. In fact borehole logs revealed that the vegetated areas between the tips and the Brook (in the northern part of the site) were underlain by fractured (probably waste) rock.

Waters in BH4 appeared to be closest to the equilibrium position for ground waters at the site, resulting in waters with similar pH (~pH 4.5) to those observed in the lower part of the Devon Great Consols site. In both scenarios, it is most likely that equilibrium with Al phases controls the pH of the waters, but that equilibrium is more readily achieved by

drainage waters at Devon Great Consols due to the longer transport pathway from tip to watercourse (~400m to River Tamar).

There is spatial and temporal variation in the sources of contaminant metals at the Wheal Betsy site which complicates the prediction of their magnitude and mobility based on limited sampling. However the reactivity of the stream waters to rainfall highlights the importance of considering hydrological factors in such investigations. Dissolved concentrations in borehole waters confirmed the mine waste to be a source of mobile contaminant metals to Cholwell Brook, but seepage from underground workings may also contribute to base flow (particularly As and Pb) towards the south of the site, particularly as a major geological fault and extensive under-ground workings lie beneath the site.

However, concentrations of Fe which are often elevated in adit discharges as a result of more reducing conditions remained low in all samples taken from Cholwell Brook. They were also low in drain 17, a suspected adit in the southern part of the site. Also lower concentrations of dissolved contaminants in the Brook were observed during low flow conditions, when the contribution from base flow, including underground workings, might have been higher. The magnitude of flux arising from underground workings, if any, was concluded to be small but worthy of further investigation.

Overall, the estimated flux from the north tips is likely to account for most or all of the flux observed in Cholwell Brook for most elements (except Cd). Management strategies that reduce the permeability of the northern waste tips may offer the best chance of reducing the annual flux of dissolved contaminants into Cholwell Brook. However, given that much of the waste is in direct contact with the waters of the Brook, disturbances of the tips should be avoided, as this could cause an acute pollution event. Furthermore, the site is extremely important to a number of stakeholders (walkers, horse-riders, geologists (SSSI), industrial archaeologists and the National Trust (owners of the Engine House),

such that invasive treatment methods are likely to be met with opposition from interested parties.

Based on the findings of this study, management of the site should include the following measures to address dissolved pollution discharging from the site:

- Regular monitoring of dissolved metal and metalloid concentrations leaving the site in Cholwell Brook

- Determination of the downstream extent and magnitude of reduced water quality due to contamination released from the site.

- Protection and maintenance of the site with respect to public access to minimise erosion of the tips. Specifically, taking measures to reduce unauthorised use of cycles and motor vehicles and encouraging appropriate use of footpaths and bridleways.

- Investigation of the ecological importance of the site.

- If necessary, investigation of suitable in-stream methods that might be feasible for the treatment of waters leaving Wheal betsy in Cholwell Brook.

Concentrations of dissolved Pb, Zn, Cd, Cu, Ni and Mn decreased in the waters of the brook a short distance downstream of the mine waste (< 200 m). This may indicate natural attenuation via sorption to organic matter, or mineral surfaces such as Fe oxyhydroxides, constrains the downstream impact of the pollution leaving Wheal Betsy. Such mechanisms could be used to cleanse waters leaving the site. Treatment of the waters of Cholwell Brook rather than the waste tips also offers the advantage that any pollution arising from the underground workings would also be treated. This may be particularly relevant for the flux of dissolved Cd which, based on evidence from this study was not accounted for by tip leachates.

4.7 Future Work

 As stated above, a number of uncertainties remain in the determination of the contribution of dissolved contamination from the waste tip to the overall contamination leaving the site. Therefore future work will attempt to address some of the uncertainties raised. In particular, how the quality of downstream waters is affected by the dissolved metal pollution from Wheal Betsy and how this varies with rainfall patterns and distance from the site. Also, determine if there is significant mixing of waters in Cholwell Brook with deep groundwaters. Specifically, implement tracer tests to establish transport times of waters at Wheal Betsy and determine if waters are conservative in Cholwell Brook, or if interaction with deeper ground water flowing through underground workings contributes significantly to contaminant flux.

4.8 References

BGS (2010). DigMap GB-50 (Geology), British Geological Survey. NERC.

Booker, F. (1967). *The Industrial Archaeology of the Tamar Valley*. Newton Abbot, David & Charles Ltd.

Cánovas, C. R., Hubbard, C. G., Olías, M., Nieto, J. M., Black, S. and Coleman, M. L. (2008). Hydrochemical variations and contaminant load in the Río Tinto (Spain) during flood events. *Journal of Hydrology*. **350** (1-2) pp25-40.

CEH.(2011). "National River Flow Archive." Centre for Ecology and Hydrology. Accessed 12/02/2011. Avaliable on the world wide web at: http://www.ceh.ac.uk/data/nrfa/data/search.html.

Christensen, T. H., Bjerg, P. L., Banwart, S. A., Jakobsen, R., Heron, G. and Albrechtsen, H.-J. (2000). Characterization of redox conditions in groundwater contaminant plumes. *Journal of Contaminant Hydrology*. **45** (3-4) pp165-241.

Coles, S. P. (1999) *Automated Flow Injection Instrument For Monitoring Nitrogen Species in Natural Waters* PhD Thesis.University of Plymouth.pp205-9

Craw, D., Rufaut, C. G., Haffert, L. and Todd, A. (2006). Mobilisation and attenuation of boron during coal mine rehabilitation, Wangaloa, New Zealand. *Science of the Total Environment*. **368** (2-3) pp444-55.

DCC.(2011). "Educational Register of Geological Sites - A guide to Geological Fieldwork in Devon." Devon County Council Accessed. Avaliable on the world wide web at: http://www.devon.gov.uk/geo-wheal-betsy.pdf.

Durrance, E. M. and Laming, D. J. C. (1982). *The Geology of Devon*, University of Exeter.

EA.(2008). "South West Obsevatory Environment Module." Accessed 30th March 2009. Avaliable on the world wide web at: http://www.swenvo.org.uk/environment/river_water.asp#quality.

Evans, K. A., Watkins, D. C. and Banwart, S. A. (2006). Rate controls on the chemical weathering of natural polymineralic material. II. Rate-controlling mechanisms and

mineral sources and sinks for element release from four UK mine sites, and implications for comparison of laboratory and field scale weathering studies. *Applied Geochemistry.* **21** (2) pp377-403.

Guan, H., Love, A. J., Simmons, C. T. and Kayaalp, A. S. (2009). Factors influencing chloride deposition in a coastal hilly area and application to chlorine deposition mapping. *Hydrology and Earth System Science Disscussions.* **6** pp5851-80.

Hamilton Jenkin, A. K. (2005). *Mines Of Devon*. Trowbridge, Cromwell Press.

Jahiruddin, M., Smart, R., Wade, A. J., Neal, C. and Cresser, M. S. (1998). Factors regulating the distribution of boron in water in the River Dee catchment in north east Scotland. *Science of the Total Environment.* **210-211** pp53-62.

Kirby, C. S. and Brady, J. A. E. (1998). Field determination of Fe2+ oxidation rates in acid mine drainage using a continuously-stirred tank reactor. *Applied Geochemistry.* **13** (4) pp509-20.

MetOffice (2006) MIDAS Land Surface Observations Data (1853-current). British Atmospheric Data Centre. Accessed: Avaliable online at http://badc.nerc.ac.uk/data/ukmo-midas/.

MetOffice (2009) MIDAS Land Surface Observations Data British Atmospheric Data Centre. Accessed: Avaliable online at http://badc.nerc.ac.uk/data/ukmo-midas/.

Mighanetara, K. (2009) *Impact of Metal Mining on the Water Quality of the Tamar Catchment* PhD Thesis Thesis.University of Plymouth.pp248

Moon, C. J. (2010). Geochemical exploration in Cornwall and Devon: a review. *Geochemistry: Exploration, Environment, Analysis.* **10** (3) pp331-51.

Nordstrom, D. K. and Ball, J. W. (1986). The Geochemical Behavoir of Aluminium in Acidified Surface Waters. *Science.* **232** pp54-6.

Page, K. (2008). *County Geological Sites in West Devon and their contribution to the Cornwall and West Devon Mining Landscape's World Hertitage Site, Notes from the Devonshire Association Excursion* SEOES, University of Plymouth.

Richardson, P. H. G. (1995). *Mines of Dartmoor and the Tamar Valley after 1913*. Torquay, Devon Books.

Rieuwerts, J., Austin, S. and Harris, E. (2009). Contamination from historic metal mines and the need for non-invasive remediation techniques: a case study from Southwest England. *Environmental Monitoring and Assessment.* **148** (1) pp149-58.

Roussel, C., Neel, C. and Bril, H. (2000). Minerals controlling arsenic and lead solubility in an abandoned gold mine tailings. *The Science of The Total Environment.* **263** (1-3) pp209-19.

Salvarredy-Aranguren, M. M., Probst, A., Roulet, M. and Isaure, M.-P. (2008). Contamination of surface waters by mining wastes in the Milluni Valley (Cordillera Real, Bolivia): Mineralogical and hydrological influences. *Applied Geochemistry.* **23** (5) pp1299-324.

Shand, P., Edmunds, W. M., Lawrence, A. R., Smedley, P. L. and Burke, S. (2007). *The natural (baseline) quality of groundwater in England and Wales*.Research Report No. RR/07/06 British Geological Survey

Sharma, V. K. and Sohn, M. (2009). Aquatic arsenic: Toxicity, speciation, transformations, and remediation. *Environment International.* **35** (4) pp743-59.

Smedley, P. L. and Allen, D. (2004). *Baseline Report Series 16: The Granites of South-West England*.Commissioned Report No. CR/04/255 British Geological Society

Wauer, G., Heckemann, H.-J. and Koschel, R. (2004). Analysis of Toxic Aluminium Species in Natural Waters. *Microchimica Acta.* **146** (2) pp149-54.

Wels, C., Lefebvre, R. and Robertson, A. (2003). An overview of prediction and contral of air flow in acid-generating waste-rock dumps. *Environmine Online Journal.*

4.9   Chapter 4 Appendices

4A.   Figures and Historical Maps

Figure 4.22: Schematic of shaft positions and depths, from N to S at Wheal Betsy. Adapted from Richardson (1995).

Figure 4.23: Historical map showing site features at Wheal Betsy in 1884, shortly after closure in 1877, only the northern Engine House remains from the buildings shown © Crown Copyright and Landmark Information Group Limited (2010) All rights reserved. 1884. Also shown are current course of Cholwell Brook (blue line) and current extent of identified mine waste tips (shaded areas).

4B.   Photographs

Photograph 1 View looking NW showing Engine House and northern most mine waste tips, borehole (No.5) installation taking place in foreground. Taken 26/08/08 A J M Turner	BH5
Photograph 2 View to S along Cholwell Brook showing direct contact with mine wastes toward the south of the site. Taken 03/09/07 A J M Turner	South Waste Tips

Photograph 3: Wooden Chute visible in Wheal Betsy (south) mine waste, chute contains cemented mine waste. Taken 03/09/2007 A J M Turner	
Photograph 4: Mine waste tips at south of site looking N. Consolidated and clay rich tip material with visible hard pan horizons. Partially vegetated with heather. Taken 09/05/09 A J M Turner	

293

Photograph 6: Core removed from BH3 Taken 26/08/08 A J M Turner	
Photograph 8: Core removed from BH5 at base of engine house waste tips. Taken 26/08/08 A J M Turner	

4C.   Wheal Betsy Groundwater Borehole Logs

Borehole	Augered/Drilled Depth (m)	Observations
WB BH1 **DRY**	0 - 0.52	Exposed consolidated orange/brown coarse SAND and fine GRAVELS comprising processing waste.
	0.52 (end)	Grey slate/shale BEDROCK
WB BH2 ** Water strike at 0.78 m **	0 - 0.06	Light brown SOIL/grass root zone
	0.06 - 0.14	Dark brown SOIL
	0.18 - 0.20	Orange brown angular COBBLES
	0.20 - 0.30	Orange brown poorly sorted very coarse SAND with frequent large angular grey/orange COBBLES
	0.30 - 0.88 (end)	Stratified dark grey/orange weathered shale BEDROCK
WB BH3 (Photograph 5) ** Water strike at 0.75 m **	0-0.17	Dark brown soil/heather root zone
	0.17 - 0.30	Dark brown/orange clayey sandy SOIL with frequent small-medium angular PEBBLES comprising mainly slate
	0.30 - 0.50	Grey/brown large PEBBLES comprising pyrite rich rock tending to 50% large COBBLES of pyritic rock and 50% clayey orange fine-medium SAND.
	0.50 - 0.74	Dark brown humic material (possibly an earlier surface horizon)
	0.74 - 0.83 (end)	Dark grey weathered shale BEDROCK.
WB BH4 **Water strike at 0.50 m**.	0-0.20	Light brown SOIL/grass root zone
	0.20 - 0.25	Dark brown SOIL
	0.25 - 1.15	Light brown/orange poorly sorted gravels with medium to very large PEBBLES comprising mine waste.
	1.15 (end)	Grey slate BEDROCK
WB BH5 (Photograph 6) **Water strike at 0.75 m**	0 – 0.05	Medium brown SOIL/grass root zone
	0.05 - 0.20	90% Grey/brown small to large angular

		COBBLES with 10% grey/light brown sandy GRAVELS
	0.20 – 0.77	Orange poorly sorted coarse SAND with frequent large PEBBLES and COBBLES of dark grey platey slate.
	0.77 – 0.95 (end)	Dark grey laminated slate BEDROCK
WB BH6 (Up catchment, close to site of underground reservoir) ** DRY ** Aborted	0 – 0.15	Dark brown SOIL with high humic content and grass roots.
	0.15 - 0.40	Dark brown soft CLAY
	0.40 – 0.95	Light brown/orange soft CLAY with occasional large sub-angular PEBBLES
	0.95 (end)	BEDROCK, unable to drill through – hole abandoned.
WB BH7 (Up catchment, close to site of underground reservoir) ** DRY ** Aborted	0 – 0.15	Dark brown SOIL with high humic content and grass roots.
	0.15 – 1.50	Light brown/orange soft CLAY with occasional sub-angular COBBLES
	1.50 – 2.00 (end)	Light grey weathered slate interbedded with light brown soft flakey CLAY

4D.   River Hydrograph

River Tavy at Denham/Ludbrook 2009

-End of Chapter 4-

Chapter 5

The Geochemistry and Leaching

Behaviour of Selected Mine Wastes

from the Tamar Catchment

5 The Geochemistry and Leaching Behaviour of Selected Mine Wastes from the Tamar Catchment

5.1 Abstract

Column experiments, based on the European standard up-flow percolation test (TS 14405), were applied to mine waste from an abandoned Pb-Ag mine and an abandoned Cu-As mine from southwest England. The aim was to investigate the range and magnitude of dissolved metals and metalloids leachable from mine waste tips. The dynamic leaching test was chosen to mimic the transport of low ionic strength rain or groundwater (simulated by MilliQ) through mine waste, thereby providing a laboratory proxy for field conditions. A range of metals (Al, Cd, Cu, Mn, Ni, Pb, Zn) and arsenic were determined in the column leachate, covering a range of solid to liquid ratios of 0-10 L kg^{-1}, applicable to different hydrological field conditions.

The highest concentrations of Al (6260 μmol L^{-1}), Cu (312 μmol L^{-1}), Zn (206 μmol L^{-1}), Ni (7.72 μmol L^{-1}) and Cd (0.712 μmol L^{-1}) in the leachate were observed at low L:S ratios where porewaters become saturated with respect to mineral phases in the mine waste. Leachate concentrations decreased exponentially for most elements throughout the experiment, except Pb, which maintained high concentrations (up to 81 μmol L^{-1}). Batch extractions with L:S ratios of 2, 5 and 10 L kg^{-1} were applied to the same materials using MilliQ, CH_3COOH and $MgCl_2$. For batch MilliQ extractions, concentrations in the supernatant were generally comparable to results from column experiments, but some differences were observed and attributed to the dynamic mode of leaching in the column.

Concentrations of metals in shallow ground waters collected during field surveys of the two sites were of the same order of magnitude as concentrations obtained

from the column experiments. For mine waste in tips situated above the water table, concentrations were best approximated as high L:S ratios. Concentrations of dissolved metals in shallow ground waters and surface drains were usually well approximated by low L:S ratios, showing that the column experiments provide a good approximation of the range of field conditions. Concentrations of dissolved As were higher in the field (up to 380 μmol L^{-1}) than in the laboratory experiments (up to 41 μmol L^{-1}) while dissolved Pb was much lower in the field (up to 2.8 μmol L^{-1}) compared to the laboratory. Both were attributed to differences in pH between comparable laboratory (pH 1.8-4.5) and field systems (pH 3.2-5.4). This discrepancy highlighted the limitations of using laboratory experiments to predict pollutant sources at abandoned mine sites.

5.2 Introduction

The geochemical composition of drainage waters from mine waste tips are controlled by the characteristics of the material (mineral surfaces, particle size) and the hydrological conditions encountered at the site. Kinetics are fundamental to leachate composition, and determine the balance between processes of mineral dissolution/precipitation, surface desorption/adsorption and dilution. The dissolved concentration of an element may be equilibrium controlled, when the solubility of the element is determined by chemical saturation of the aqueous phase with respect to the solid phase. The release may also be transport controlled when hydrological conditions determine the rate of flow through a tip and therefore the concentration of metals found in solution (Evans et al., 2006). In addition, the ionic strength (*or ion activity product*) of pore water solutions affects the solubility of dissolving mineral phases and this too depends on the movement of fluid through mine waste (Essington, 2003). At both study

sites in this study, drainage waters were undersaturated with respect to $Fe(OH)_3$ and Al mineral phases, and dissolved concentrations were therefore transport controlled.

Due to the complexity of factors affecting leachate composition, in-situ monitoring of mine waters offers the best means of determining the magnitude of contamination emanating from waste tips. However, site investigations can be expensive and require detailed knowledge of the site hydrology to capture drainage from the tips in a representative manner. Often abandoned mine sites are un-secured, leading to authorised and unauthorised use of the waste tips by the public. This can impede in situ monitoring over long periods because equipment may be lost or damaged.

Commonly, the potential of contaminated solids to leach dissolved contaminants is estimated from laboratory-based equilibrium techniques. A range of laboratory methods are available and these are reviewed in section 5.4. In this chapter, dissolved metal and As concentrations were determined via two contrasting laboratory leaching techniques and results compared to the field concentrations determined at two study sites, Devon Great Consols (DGC, Chapter 3) and Wheal Betsy (WB, Chapter 4). The waste material used in the laboratory experiments was a composite removed from the selected tip wastes at each site to allow comparison against the field data. The combined results are used to aid understanding of the geochemical controls on leachate composition for the mine wastes studied. This will aid future management and/or remediation strategies for mine waste tips. The exercise also shows the advantages and disadvantages of the laboratory techniques used and examines their suitability for future studies of mine waste leachate.

5.3   Aims and Objectives

The aims of this chapter were to:

- Characterise the mineralogy and physical characteristics of a selection of mine waste samples from sites in the Tamar catchment.

- Investigate the use of laboratory based static and dynamic experiments to generate leachates under controlled conditions and critically assesses their suitability for predicting contaminant concentrations in the field.

The contaminants of interest were Al, Cd, Cu, Zn, Ni, Pb, Mn, Fe and As, which were identified in the field studies as elevated in drainage waters or important to contaminant mobility. Other trace elements including Sb, Sn, V, and W were also considered in the determination of total content of the mine waste.

Samples of the waste tip material found at Devon Great Consols and Wheal Betsy were used in this study (see Chapter 3 and Chapter 4 respectively for detailed site descriptions). This allowed results from the laboratory leaching experiments to be compared against the results gained from in situ sampling of mine waste leachates. The research objectives of this chapter were to:

1. Select or design a suitable dynamic experiment to mimic in the laboratory, the leaching behaviour of mine waste in the field.

2. Select a batch extraction method suitable for routine analysis of contaminated solids.

3. Collect mine waste material from each of the study sites to be representative of the waste tips. In particular preserve the biogeochemical integrity of the sample through the laboratory tests.

4. Investigate the physical and mineralogical characteristics of the sample materials used in the leaching experiments.

5. Determine concentration ranges and total extractable amounts (mol kg^{-1}) for dissolved contaminants found in mine waste leachate.

6. Investigate the effect of biogeochemical factors on leachate composition namely: pH, Eh, solid: liquid ratio and sample drying.

7. Compare the results of static and dynamic laboratory tests to one another and to field data and determine the advantages and disadvantages of each approach.

8. Use the combined results to determine the geochemical controls on contaminant mobility from mine waste materials studied.

5.4   Literature Review - Field and Laboratory Methods for the Determination of Leachable Metals and Metalloids from Mine Waste

A brief review of field and laboratory techniques applicable to the determination of contaminant mobility from mine waste is presented in the following paragraphs. The methods used in this chapter are introduced and the rationale for their selection discussed.

5.4.1   In-Situ Techniques

Ideally, elemental concentrations and chemical parameters should be determined in-situ, since the act of sampling and storing samples potentially compromises their physical, chemical and biological integrity. Unfortunately, few parameters can be determined accurately in the field. Portable equipment allows the measurement of physio-chemical parameters, such as pH, redox potential, conductivity and dissolved oxygen. Ion selective electrodes may be used for determination of individual metal ions including Al^{3+} and Cu^{2+} (Honeychurch and Hart, 2003; Peijnenburg *et al.*, 2007). These measurements require saturated conditions and are most suited to aqueous environments. Similarly, colorimeter field instruments are a convenient method of gathering data in the field and can be used for a range of aqueous analaytes, including

301

metals. However, limits of detection are typically higher than laboratory instruments (e.g. Fe 30 μg L^{-1}, Al 10 μg L^{-1} manufacturers LOD, Hach GmbH) and quality assurance of results is difficult to achieve.

Lysimeters have also been proven to be an effective tool for assessing the transport of mobile metals through the soil (Miro *et al.*, 2005). On-site lysimeter experiments are performed by inserting an impermeable barrier into the soil to collect percolating fluids. Although lysimeters have been employed in acid rock drainage studies (Sracek *et al.*, 2004), their installation typically requires mechanical assistance and their installation may alter the properties of the overlying material, thereby destroying the natural conditions in-situ experiments are meant to preserve.

Disturbance may also be a problem for the application of semi-permeable devices, such as diffusive gradient thin films (DGT), which have been successfully used to study the mobility and bioavailability of metals in the soil (Zhang *et al.*, 1995; Gao *et al.*, 2006; Gao *et al.*, 2007). DGTs are based on the establishment of equilibrium of exchangeable ions between a removable medium (generally a layer of resin or gel) and the sediment pore waters. The gel/resin layer allows ions and complexes to diffuse freely, whilst limiting their uptake rate, thus allowing for replenishment of the soil solution (Peijnenburg *et al.*, 2007). The metals are extracted from the exchange medium and their concentration in the environmental matrix is related to the extracted amount via Fick's first law of diffusion (Zhang *et al.*, 1995). DGTs are particularly useful for gaining high resolution data for the spatial distribution of elements, since they may be installed with minimum disturbance to the host environment. They may be used to determine any dissolved species for which there is a selective binding agent available (including As, Cd, Co, Cr, Cu, Pb, Mn, Ni, Zn); however, the effectiveness of the binding agent is pH dependent. For example, Cd binds relatively weakly and can only be measured down to pH 4.5 (Zhang, 2003). DGTs are commonly applied to studies of

bioavailable and labile metals in saturated environments, recent studies have shown the technique may be successfully applied to the assessment of mine waters and waste deposits where saturated conditions exist (Søndergaard *et al.*, 2008; Yapici *et al.*, 2008; Sherwood *et al.*, 2009).

5.4.2 Laboratory Techniques

Laboratory based extraction methods are widely employed to assess the release of metal contamination from soils, sludges and sediments. They may comprise a single stage extraction, or the application of a number of different extractants aimed at liberating metal ions bound to different mineral phases. Strong acids, such as HF, HNO_3, HCl, or chelating agents (e.g. EDTA, DPTA, NTA) release trace metals into solution in concentrations high enough to permit detection by routinely applied analytical techniques. Total digestion of minerals requires treatment with HF to liberate all elements from silicate lattices. However this is both time consuming and hazardous and arguably unnecessary in the determination of mobility under environmentally relevant conditions. Digestion with aqua regia (typically a 3:1 mixture of concentrated HCl and HNO_3) is most commonly employed to determine pseudo-total metal relying on oxidative decomposition of all but the most resilient mineral phases (Mudroch and Azcue, 1997).

It is also possible to target more labile metal pools using milder extractants, such as $CaCl_2$, $MgCl_2$ or NH_4NO_3. These are particularly valuable in the assessment of plant bioavailability (Peijnenburg *et al.*, 2007). However, the extracted metal fraction is operationally defined by the choice of the extractant, instead of being functionally defined, i.e. plant available, mobile or exchangeable. A comparison study by Moral *et al.* (2002) investigated the use of a number of mild reagents (NH_4Cl, $CaCl_2$, $SrCl_2$ and DPTA) to extract Cd, Ni, Pb, Co and Cr from contaminated soils. DPTA was the most

effective extractant, but only in terms of liberating the highest concentrations. The results of extraction studies must be applied with care to natural systems. The study by Moral *et al.* (2002) also showed that the extracted concentrations depended on the extraction procedure applied, the source of pollution and the type of soil, particularly the pH and carbonate content

Sequential extractions have been applied extensively to environmental samples contaminated by mining operations, including soils, sediments and mine wastes (Fanfani *et al.*, 1997; Dold, 2003; Pagnanelli *et al.*, 2004; Pueyo *et al.*, 2008). The elemental distribution in a sample is defined in terms of association with mineral phases, as determined operationally by the sequential application of extractants of increasing strength. However the technique is often criticised for the lack of selectivity of some leaching agents and readsorption of released metal ions onto the substrate (Rauret and Rubio, 1997; Miro *et al.*, 2005). The scheme initially described by Tessier *et al.* (1979), Table 5.1, was shown to be inadequate for studying either Cu or As fractionation in mine waste as it severely underestimated the Fe-oxide associated fraction (Dybowska *et al.*, 2005). The scheme has often been modified but this has reduced the comparability of results between studies. In light of a widely accepted need for improvement and standardisation, a revised version of the scheme has been developed (BCR 3-step sequential extraction procedure), along with dedicated certified reference materials (e.g. BCR-601, BCR-701) (Rauret *et al.*, 1999; Pueyo *et al.*, 2001; Ciceri *et al.*, 2008). The operationally defined target phases of each step in the Tessier and BCR modified schemes are presented for comparison in Table 5.1.

Despite the attempts at standardisation of sequential leaching methods, many limitations remain in their application to the assessment of the metal leaching potential of a given solid phase. Small operational deviations of method (e.g. extraction time, washing between steps) may influence results. Moreover, the interpretation of what

constitutes the 'leachable fraction' is controversial, since it depends on the characteristics of the solid material and element of interest. Table 5.2 shows literature data obtained for labile metal fractions, as extracted by a variety of sequential batch methods from soils contaminated by mining operations. These figures illustrate the lack of comparability between studies due to differences in methodology. In a review, Bacon and Davidson (2008) concluded that sequential extractions remain a useful technique for identifying the potential mobility of elements; however results should be interpreted with caution in light of their limitations.

This project seeks to quantify dissolved metals released progressively from mine spoil deposits under natural environmental conditions. Sequential extractions provide information on operationally defined fractions that are deemed to be 'exchangeable', 'water-soluble' or 'acid-soluble'. Depending on the chosen extraction scheme, they are typically carried out as batch experiments at a fixed liquid to solid ratio (typically L:S = 10:1) and hence do not elucidate the leaching behaviour of elements under variable hydrological conditions (Evans *et al.*, 2006; van der Sloot *et al.*, 2006). Therefore, laboratory-based extraction techniques that employs a variety of liquid to solid (L:S) ratios may be more suitable to mimicking the dynamic environmental conditions mining waste is exposed to in-situ.

Performing extractions in a dynamic mode can help to address certain limitations of batch extraction methods, notably the fixed L:S ratio and readsorption of extracted elements onto mineral phases due to prolonged contact (Chomchoei *et al.*, 2002). Dynamic-column leaching experiments have been accepted as a good method for estimating metal mobility over realistic timescales (Gibert *et al.*, 2004; Hartley *et al.*, 2004; Evans and Banwart, 2006; Michel *et al.*, 2007; Slowey *et al.*, 2007). Typically, experiments involve packing non-metallic columns with a representative amount of field material (usually 0.5 – 10 kg). The columns may be undisturbed cores or

305

composite bulk material. A volume of leaching fluid (e.g. $CaCl_2$, deionised water, or NH_4Cl_2) is applied under pressure and leachates collected as fractions for chemical analysis. This type of test is employed by the Dutch Environment Agency as a standard leach test for inorganic components from granular materials (NEN 7343). A similar published European standard method exists (CEN/TS 14405, 2004) and has been implemented in studies of solid waste materials (Dijkstra *et al.*, 2008). Variations of dynamic extractions include those based on flow injection analysis (FIA) including rotating coil systems (Fedotov *et al.*, 2005), stirred flow cells (Sukreeyapongse *et al.*, 2002) and packed microcolumns which are a scaled down and automated form of the more conventional column leaching technique (Chomchoei *et al.*, 2007).

For this study, a dynamic extraction test closely following that described by CEN/TS 14405 was adopted and has since been applied to similar studies of Pb-Zn mine wastes by the British Geological Survey (Palumbo-Roe *et al.*, 2009). The technique generates leachates over a range of L:S ratios and can accommodate coarse sample material (< 4mm) without the need for aggressive milling or crushing. The acidic nature and elevated conductivity of the leachates is the result from the interaction of rainwater of comparatively low ionic strength with the mineral phases and porewaters in the waste. The solid phase is the dominant control on composition such that MilliQ water was deemed suitable as a proxy for rainwater.

Aside from the limitations of a small sample size, heterogeneity and sample disturbance common to all laboratory based methods, this technique mimics the dynamic situation of waste in the field and was deemed most likely to give the most realistic result for concentrations of labile elements of interest. The main limitation of the dynamic extraction is that the mineral phase associations suggested by sequential extractions are not so readily inferred from column experiments. Without automation, the technique is also more labour intensive and time consuming than commonly applied

batch methods. So, in addition to the dynamic extractions, batch experiments may be conducted on the same material using a range of extractants which are thought to target particular phases. The batch extraction methods applied in this chapter are summarised in Table 5.3. The selection is designed to both aid understanding of contaminant release processes, and to look at the consistency of results between methods.

Supplementary analyses are required to confirm mineralogical phase associations controlling element release. Although direct methods of solid phase association exist, including several powerful X-ray techniques e.g. X-ray adsorption near-edge structure (XANES) and X-ray adsorption fine structure (EXAFS), they are expensive and not widely available (Bacon and Davidson, 2008). However mineralogical examination using X-ray techniques e.g. powder X-ray diffraction to examine crystalline composition, and an energy dispersive spectroscopy (EDS) detector coupled to SEM, to provide elemental associations and textural information, are useful alternatives that are more accessible.

Table 5.3: Extraction reagents used in equilibrium batch experiments listed with their source and the targeted metal(loid) fraction.

Source of Method:	Extractant / Method	Target Fraction
EA/National Rivers Authority R&D Note 301, 1994	MilliQ H_2O, shaken for 16 h	Water soluble
Step one of the Tessier *et. al* sequential extraction scheme, 1979	1.0 mol L^{-1} $MgCl_2$, pH 7.0 (adjusted with 1 mol L^{-1} NaOH), shaken for 1 h	Exchangeable
Step one of the revised BCR sequential extraction scheme	0.11 mol L^{-1} CH_3COOH , shaken for 16 h	Exchangeable, water soluble and acid-soluble
Commonly applied technique in studies of contaminated solids e.g. Pulford *et al.* (2009)	Aqua Regia (3:1 con. HCl : conc HNO_3), cold digest for 1h followed by hot digest (100°C) for 2 h	Pseudo - total (all except silicate bound metals)

Table 5.1: Comparison of the Tessier and Revised BCR 3 step sequential extraction procedures. From (Bacon and Davidson, 2008).

Tessier (1979)			Revised BCR (Rauret *et al.*, 1999)			
	Reagent	Fraction label and nominal target phase(s)		Reagent	Fraction label	Nominal target phase(s)
Step 1	1.0 mol L^{-1} MgCl$_2$, pH 7.0	Exchangeable	Step 1	0.11 mol L^{-1} CH$_3$COOH	Exchangeable, water soluble and acid-soluble	Soluble and exchangeable cations and carbonates
Step 2	1.0 mol L^{-1} CH$_3$COONa adjusted to pH 5 with CH$_3$COOH	Bound to carbonates	Step 2	0.5 mol L^{-1} NH$_2$OH-HCl at pH 1.5	Reducible	Fe-Mn oxyhydroxides
Step 3	0.04 mol L^{-1} NH$_2$OH-HCl in 25% CH$_3$COOH (96°C)	Bound to Fe-Mn oxides	Step 3	H$_2$O$_2$ (85˚C) then 1.0 mol L^{-1} CH$_3$COONH$_4$	Oxidisable	Organic matter and sulphides
Step 4	HNO$_3$/H$_2$O$_2$ (85˚C) then 3.2 mol L^{-1} CH$_3$COONH$_4$ in 20% HNO$_3$	Bound to organic matter and sulphides	(Step 4) *	*Aqua Regia*		
Step 5	HClO$_4$/HF	Residual				

* Although not officially a step in the sequential extraction, it is recommended that the residue at the end of step 3 is digested with *aqua regia* and the sum of the four fractions be compared with the results of a separate *aqua regia* digestion of the material.

Table 5.2: Metal concentrations reported in other studies of mine spoil and contaminated soils for single 'exchangeable' (ex) and 'available' (av) fractions, or as part of a sequential extraction scheme (se). All units mg kg^{-1}. ns = non-specified.

Author	Location	Sample and Fraction	Depth (cm)	L:S ratio	pH	Cu	As	Zn	Pb	Cd	Mn
Dybowska *et al.*(2005)	Devon Great Consols, SW England.	Contaminated soil and spoil (ex, se, MgCl$_2$)	0-15	ns	3.2-6.8	1.72-71.67 (0.04-9.99%)	7.35-3588 (0.05-5.36 %)	-	-	-	-
Alvarez *et al.* (2003)	An abandoned mine in Galicia (NW Spain).	Cu rich spoil (ex, 1M NH$_4$Cl)	0-20	10:1	3.0-5.0	17.7 - 1866	-	0-106	-	-	1.8-133
Bech *et al.*(1997)	Copper mine, Piura (Northern Peru).	Cu rich soil and Spoil (av, NH$_4$OAc-EDTA)	10	5:1	3.33-5.86	0.48 - 53	<0.25 - 13	0.08-5.9	0.61-4.9	< 0.05-3.8	0.83- 10
Moreno-Jiménez et al.(2009)	Monica pyrite mine, NW Madrid (Spain).	Soils close to mining dumps (ex, 0.1 M (NH$_4$)$_2$SO$_4$	0-30	10:1	3.89-5.99	0.46-6.32	-	1.24-149.4	-	0.06-7.23	1.44-6.6

5.5 Methods

5.5.1 Reagents

All aqueous solutions were prepared with Milli-Q water (Millipore, R $\geq$ 18.2 MΩ cm^{-1}, reverse osmosis followed by ion exchange). Standard solutions and reagents were prepared in a Class 5 (BS EN 150 14644) laminar flow hood (model BassAir 06VB), according to trace metal clean techniques to minimize contamination. Multi-element calibration standards were prepared as serial dilutions from standard solutions (1000 or 10000 μg L^{-1}, Romil Pure Chemistry, Fisher and BDH) and acidified to < pH 2 with Q-HNO$_3$ (Q denotes purified by sub-boiling distillation, Romil SPA).

MgCl$_2$(s) (analytical grade, Fisher) and CH$_3$COOH (100 % glacial, Aristar) were used to prepare batch extraction solutions of 1.0 Mol L^{-1} MgCl$_2$ and 0.11 Mol L^{-1} CH$_3$COOH respectively.

Analytical grade acids were used for washing of equipment unless stated otherwise.

5.5.2 Cleaning Protocol

Polyethylene skirted centrifuge tubes (50 mL), used for sample collection and standard preparation, were cleaned by immersion in a series of cleaning solutions (Decon 90, 2% v/v, >24 h; HCl, 6 mol L^{-1}, $\geq$7 days, HNO$_3$, 2 mol L^{-1}, $\geq$7days). Perspex™ columns used in leach experiments (section 5.5.4) were rinsed with detergent (Decon 90, 2%) and immersed into HNO$_3$, pH 2, $\geq$7days. Filtration units (polycarbonate, Nalgene), and all coloured components (centrifuge tube lids, silicone rubber 'o' rings, polyethene fixings) were rinsed with detergent (Decon 90, 2%) and immersed in HCl, 2mol L^{-1}, $\geq$3 days . All items were rinsed with deionised water prior to the Decon 90 step and rinsed with MQ water after each of these subsequent steps.

Items were dried in a Class 5 laminar flow hood and stored in two plastic zip-lock bags prior to use.

5.5.3   Sample Collection and Sample Treatment

Samples of mine waste material were taken from two study sites, Devon Great Consols and Wheal Betsy. At Devon Great Consols, four composite samples of ca. 1.5 kg were taken from the Wheal Anna Maria upper and cinders waste tips (Figure 3.5, Chapter 3). At Wheal Betsy, five composite samples of ca.1.5 kg were taken from both the northern and southern tip areas. Sampling used a stainless steel trowel to liberate material at shallow depths (Wheal Anna Maria, Cinders and Wheal Betsy north tip: 10-50 cm depth, Wheal Betsy south tip: 10-40 cm depth). Surface crusts, root layers and large pebbles (>16 mm, Wentworth Scale) were omitted by hand sorting. The material was collected into zip lock bags and stored cool with ice packs before transfer to a laboratory refrigerator (4°C). Descriptions of the material encountered at each sampling location are provided in Appendix A. The individual mine waste samples were sieved, and the <4 mm fraction combined to form composite samples with mineralogy representative of the Wheal Anna Maria (WAM) and Cinders (CIN) waste tips at Devon Great Consols and the north and south tip areas at Wheal Betsy (WBN and WBS). The composite samples were homogenized by quartering and recombining (5 repetitions), placed in an airtight HDPE container and returned to the refrigerator pending dynamic and static leaching experiments. The < 4 mm fraction, as used in the column and batch extraction experiments, constituted 92%, 72%, 39% and 53% by weight of the total sample material removed from WAM, CIND, WBN and WBS waste tips, respectively.

A portion (~100 g) of each individual and each composite sample was retained in two zip lock polythene bags for particle size analysis, SEM and XRD analysis and determination of moisture content.

Selected homogenised individual and composite samples (50 g) were dried in porcelain crucibles (cleaned with Milli-Q and IMS) at 40°C for 72 h. The filled crucibles were removed from the oven to a desiccator to cool before samples were transferred to zip lock polyethylene bags. A subsample (10 g) was sieved to 2 mm and reserved for SEM-EDS analysis. A separate subsample (20 g) was reduced to a fine homogeneous powder by a Tema™ disc mill (30 s, tungsten carbide discs). The powder was sieved to 63 μm and reserved for XRD analysis.

5.5.4   Dynamic Up-flow Column Experiments

Experimental Design

The experimental design for up-flow column extraction was based on a standard European method (CEN/TS 14405, 2004) and follows recommendations for column design and operation of the test. Columns were manufactured from Perspex™ tubes (30 cm length, 5 cm i.d.) and lids secured with nylon screws. Nylon mesh (180 μm) fixed into the lids on the inlet and outlet functioned as screen for the solid material. HDPE and silicon tubing was used for transport of the eluent (MQ water) and leachate samples to and from the column. Polypropylene HPLC nuts, ferrules and connectors and were used to connect the components of the flow circuit.

Leaching solution (MQ water constantly aerated with compressed air) was transported by a peristaltic pump at a constant flow rate (2.0 mL min^{-1}) into the inlet at the bottom of the column. Out flowing solution (leachate) was filtered in-line in two stages (0.4 μm, and 0.2 μm, Whatman Nucleopore) using two filter holders (47 mm, Swinnex). The leachate was either directed through a flow chamber for in-line determination of Eh and pH and to waste, or was collected at set times to provide fractions for analysis.

Figure 5.1: Schematic diagram of dynamic upflow percolation experiment

A schematic of the experimental set up is shown in Figure 5.1. One column is shown here for clarity, although during each experiment three columns were run in parallel. The leachate reservoir and sample collection was housed in a small laminar flow hood to minimise contamination. The initial flow rate was established by determination of MilliQ flow through an empty column, flow was also determined during each sample collection. The time taken for the sample to travel from the column outlet to the collection vessel was used to calculate the void volume of the system (shown in red, < 10 mL in all cases).

Column Packing

Triplicate empty columns were weighed complete with lids, filters and fixings. Laboratory film was placed over the inlet and outlet ports to minimise contamination during filling and weighing. A dedicated blank line comprising HDPE tubing (50 cm), complete with two column fittings was also weighed with each column. Sample material was introduced from one end of the column in layers (~5 cm) until the column was full. A 125 g weight was used to compact each sample layer. The weight comprised

an acetate disc (4.7 cm diameter) fixed to the base of a 125 mL HDPE bottle filled with DI water. The bottle was dropped 50 times on each layer from a height of approximately 10 cm. The nylon filter was placed on top of the sample and the lid carefully secured. Two O rings inside each column lid provide a water tight seal. The filled column was reweighed together with the blank line in order to establish the weight of the solid sample.

Column Saturation

Within hours of column packing, columns were secured vertically into purpose built housing and laboratory film removed from the inlet and outlet ports. The outlet line from the peristaltic pump was fixed to the inlet port at the base of the column. The blank line was fixed to the outlet port at the top of the column. The pump was turned on and the column allowed to saturate with leach solution (MilliQ water). When fluid began to enter the blank line, the pump was stopped. The pump tubing was disconnected from the inlet port of the column and replaced with the blank line to create a closed loop. The saturated column was removed from its housing, weighed to estimate the void volume of the column (assuming hydraulic connectivity between void spaces and no trapped air). From this measurement, the intial liquid:solid ratio could be determined. The columns were re-secured into the housing and left in-situ at room temperature for 72 hr +/- 1 hr prior to the start of the test in order to allow pore waters to equilibrate with the solid sample. The optimum saturation time was determined from trial experiments of 24, 48, 72 and 168 h.

Experimental Run

After saturation for 72 h, the blank line was uncoupled from each column and replaced with the circuit tubing as shown in Figure 5.1. The pump was switched on and the experiment timed. The eluent was passed through the inline pH meter with the first

10 mL directed to waste in order to purge the void volume from filters and outlet tubing. Sample fractions (~30 mL) were collected by directing flow to a sample collection vessel (50 mL polyethylene skirted centrifuge tubes, pre-weighed). The time taken to collect each fraction was timed and used to estimate the outflow velocity of each column. Once collected, sample fractions were immediately transferred to a refrigerator and within hours of collection a 2 mL aliquot was transferred to a glass HPLC vial and refrigerated pending quantification of anions by ion chromatography (Dionex DX-500 system, Dionex Ionpac AS9-HC column).

The pH of the eluent was monitored (Hanna HI9025 instrument fitted with a VWR electrode) and recorded at time intervals throughout the experiment. Triplicate columns were run at staggered time intervals (~4hrs); Eh was measured during the experiment for at least one replicate (Hanna HI9025 instrument fitted with a redox-ORP electrode, VWR).

A recommended sampling scheme based on dry mass and passing eluent volume is given in CEN/TS 14405, 2004. Time intervals for each column were calculated from a solid: liquid ratio based on dry mass and the cumulative volume of passing leachate. Some deviation was made from the recommended scheme to include more frequent sampling, particularly at the beginning of each experiment. All fractions were accurately timed. Total experiment run time was calculated during the test from an average of sample collection times measured during the experiment. The recommended experiment endpoint was reached when 10 L kg^{-1} had passed through each column. Total leachate volume for all experiments was > 10 L kg^{-1}. Typically this was achieved within 5 days, depending on flow rate.

The remaining sample was acidified to pH 2 with Q-HNO$_3$ pending analysis of metal(loid) content by ICP-OES (Varian 725-ES Inductively Coupled Plasma Optical Emission Spectrometer) and ICP-MS (VG Plasma Quad PQ2+ Turbo Inductively

Coupled Plasma Mass Spectrometer) in an ISO9001:2000 accredited analytical research facility.

Cleaning

The column flow circuit was cleaned before and after each experimental run. Q-HNO$_3$ (10% v/v) was introduced to the circuit as a cleaning solution via peristaltic pump (< 0.1mL min^{-1}, total contact time $\geq$3 days). This was followed by a rinse with MQ water (< 0.1mL min^{-1}, total contact time $\geq$1 day). Inline filters were installed prior to the pre-experimental cleaning step and removed before post-experimental cleaning.

5.5.5   Batch Extractions

Soil pH

Soil pH was determined according to a modification of the EPA method 9045D. 10 mL of deionised water was added to 10 g of each sample (<4 mm fraction) in a 25 mL glass beaker and stirred for 5 min. The soil suspension was covered and allowed to settle for 1 hr. The pH of the samples was measured using a Hanna HI9025 instrument fitted with a thermocouple and pH electrode (Hanna H1230). The pH electrode was calibrated daily with pH 4.0 and 7.0 buffers (BDH Laboratory).

Equilibrium Extractions

Composite Wheal Anna Maria (WAM), Cinders (CIND), Wheal Betsy north (WBN) and south (WBS) tip material was dried (40°C, 72 h). Sub-samples of the homogenized material (4, 8 and 10 g) were accurately weighed into 50 mL centrifuge tubes. An aliquot of MilliQ was added via pipette to achieve L:S ratios of 10, 5 and 2 respectively e.g. 40 mL to 4 g to achieve L:S of 10. Each was prepared in triplicate alongside procedural blanks. Samples and blanks were laid horizontally and shaken for 16 h (orbital shaker), then immediately centrifuged (3000 rpm, 15 min). The

supernatant was carefully removed via auto-pipette and acidified (Q-HNO$_3$, pH 2) for metal(loid) analysis.

The experiment was repeated on WAM, CIND and WBS material using two different extraction schemes; these are listed in Table 5.3. All samples were centrifuged, sampled and analysed identically.

Aqua - Regia Digests

Sub-samples (0.5g) of the dried composite WAM, CIND, WBN and WBS tip material were accurately weighed into acid-washed Tecator™ glass tubes (in triplicate). To each 4 mL of HCl (35 %, Romil SpA) and 1 mL of HNO$_3$ (70 %, Romil SpA) was added and allowed to digest for 1 hr at room temperature. A further 0.5mL of HNO$_3$ was added to each tube before refluxing for 2 hrs at 95-100 °C. Once cool, solutions were quantitatively transferred to 50 mL volumetric flasks through glass fibre filters (Whatman 41, Ashless) and made to volume with dilute HNO$_3$ (2%, Romil SpA in MilliQ). Solutions were transferred to 50 mL polyethylene skirted centrifuge tubes and 10- and 100-fold dilutions prepared with dilute HNO$_3$ pending analysis for metals and metalloids.

Three replicates of a CRM were digested using the same method applied to the samples. The percentage recoveries are shown in section 5.6.1 (Table 5.4).

5.5.6   Instrumentation and Analysis

Moisture content was determined in triplicate gravimetrically after drying (105°C, 24 h) sieved and homogenized samples (10 g). The organic matter content was determined gravimetrically as loss on ignition (LOI, 1 hr ramp to 450 °C, then 8 h).

Homogenised and sieved samples (< 63 μm), were pressed gently into plastic specimen holders and examined for crystalline mineral phases by XRD using a Siemens

D5000 diffractometer and CuKα radiation at the Camborne School of Mines, University of Exeter (CSM). Data was collected for 1 hr using a 2-70° 2 θ program.

Polished blocks were prepared for SEM analysis from selected samples (1 g of < 2mm homogenised sample, gently disaggregated with pestle and mortar). These included the composite material used in the leaching experiments, (pre- and post-column run) a number of individual samples of mine waste collected from the two study sites and for comparison a number of pre-prepared samples gathered from other mine waste tips in the Tamar Valley by Mighanetara (2009) during a previous PhD project.

Samples were mixed with graphite (1.5 g) and subsequently mixed with Epofix™ resin and hardener. The mixture was poured into a mould of 30 mm diameter and allowed to de-gas for 30 min then oven dried (50°C, 4 h). Once set samples were ground and polished to produce a cross sectioned sample surface for analysis (*pers. comm*. Pendray, 2009). Grain mounts were also prepared on selected samples by sprinkling a light coating of particles (< 2 mm) onto self adhesive conductive carbon tabs fixed to aluminium mounts. All prepared samples were carbon coated before being introduced to the SEM. Samples were examined for texture and elemental composition using a JEOL JSM-5400LV scanning electron microscope with a JEOL energy dispersive spectrometer at CSM. The system was used in hi vacuum mode and LinkISIS software used to interpret the raw data. Samples were initially scanned in secondary electron imaging mode. The detector was switched to backscatter image composition mode for imaging.

Metal and metalloid analysis of batch and column leachate was carried out by ICP-OES (Varian 725-ES Inductively Coupled Plasma Optical Emission Spectrometer) and ICP-MS (Thermo Fisher X Series 2 Inductively Coupled Plasma Mass Spectrometer) in an ISO9001:2000 accredited analytical research facility. Yttrium and indium (100 μg L^{-1}) were used as internal standards. Matrix matched standards were

prepared for CH$_3$COOH and MgCl$_2$ batch extractions. Dissolved anions were determined by ion chromatography (Dionex DX-500 system, Dionex Ionpac AS9-HC column). Na and K analysis was performed by flame photometer (Corning 400). ICP-OES and ICP-MS analyses were verified against a certified reference material for trace elements (TMDA-64, National Water Research Institute, Canada). Instrumental operating conditions are given in Chapter 3, Appendix 3E.

5.6   Results and Discussion

5.6.1   Quality Control and Figures of Merit

pH and Eh Meters

The pH meter was calibrated daily before use and checked after use using standard solutions (pH 4 and 7, BDH). The maximum recorded daily drift in calibration was 0.3 pH units. The Eh meter was checked daily before use by measuring against ZoBell's solution, using the method described in Chapter 3 (3.7.1).

Analytical Figures of Merit

Instrument drift was monitored by re-injection of a multi-elemental standard after every ten samples. Typically instrumental drift was < 5%, depending on element and concentrations, where drift exceeded 10%, samples were re-analysed. Recoveries for certified reference materials are shown in Table 5.4. Internal standards, check standards and limits of detection determined as described in Chapter 3 (3.7.1). Procedural blanks for column experiments comprised a sample of the final rinse wash of column circuits with filters installed (MilliQ). In all batch experiments including aqua regia digestions, matrix matched blanks were subjected to the same procedure and analysis. Results were corrected for procedural blanks.

Table 5.4: Limits of detection and CRM recoveries for all analysis of samples in Chapter 5. Certified reference materials: LGC6156 (Harbour Sediment) and LGC6137 (Estuarine Sediment), LGC Standards, UK and TMDA-64 (fortified lake water), National Water Research Institute, Canada. % result in parenthesis based on mean values. * Certificate guidance value only. ** Denotes LOD for 0.11 M acetic acid standard matrix, $^+$Denotes LOD for 1 M $MgCl_2$ standard matrix.

Element/ Anion	TDMA-64 Certified Value (μg L^{-1}) $\pm$ 2σ limit	LGC6156 (or LGC 6137†) Certified Value (mg kg^{-1}) $\pm$ 95% confidence level	Method	Linear / Standard Range (μmol L^{-1})	Limit of Detection (μmol L^{-1})	TDMA-64 Recoveries (μg L^{-1})	LGC6156 / 6137 Recoveries (mg kg^{-1})
Al	265$\pm$30	19000 $\pm$3700	ICP-OES	0.5-5000	1.4, 1.5, 1.1, 0.39, 0.99, **0.62, $^+$1.5,	304, 261, 296, 273, 260, 268, 269.	14200$\pm$1440 (67%)
As	150$\pm$22	38.3$\pm$5.8	ICP-OES	0.1-1000	1.5, 1.5, 1.3, **1.2, $^+$2.1, 2.3	163, 147, 158, 181, **<LOD**	35$\pm$19 (91 %)
Ca	13600*	43000$\pm$2600	ICP-OES	0.5-5000	0.032, 0.22, 0.18, 0.0048, 0.021, **0.021, $^+$0.19, 0.43	13600, 14200, 13600, 13500, 13400, 14300, 13000,	44900$\pm$7230 (105 %)
Cd	251$\pm$24	2.9$\pm$0.5	ICP-MS	0.0005-5	0.0006, 0.0032,	242, 236	-
			ICP-OES	0.01-100	**0.062, $^+$0.16	257, 256	2.5$\pm$0.5 (86 %)
Co	270$\pm$27	28.3$\pm$2.8	ICP-MS	0.001-5	0.24,	264	-
			ICP-OES	0.05-500	0.46, 0.22, 0.32,**0.15, $^+$0.31	264, 263, 244, 280, 270	-
Cu	290$\pm$29	2400$\pm$122	ICP-MS	0.001-5	0.074, 0.033	307, 312	-
			ICP-OES	0.1-2000	0.26, 0.11, 0.16, 0.13, 0.13,**0.13, $^+$0.21	308, 311, 267, 286, 285, 285, 273	2460$\pm$290 (103 %)
Fe	319$\pm$30	†30700$\pm$1600	ICP-OES	0.1-1000	0.31, 0.47, 0.20, 0.19, 0.13, **0.18, $^+$0.24	347, 308, 338, 312, 317, 313, 289	25400$\pm$1200 (83 %)
Mn	299$\pm$26	553$\pm$27	ICP-OES	0.1-1000	0.48, 2.3, 0.07, 0.015, 0.010, **0.011,$^+$0.022	316, 295, 303, 287, 290, 306, 270, 300	528$\pm$76 (95 %)
Mo	278$\pm$22	-	ICP-OES	0.1-10	0.28, 0.29, **0.17	301, 252	-
Na	4500*	20100$\pm$1150	FAAS	200-4000	2.0	4400	-
			ICP-OES	0.5-5000	5.7, 6.1, 7.7, **6.1	4500, 4500, 4700, 4700	19775$\pm$1010 (98 %)

Element/ Anion	TDMA-64 Certified Value (µg L^{-1}) ± 2σ limit	LGC6156 (or LGC 6137[†]) Certified Value (mg kg^{-1}) ± 95% confidence level	Method	Linear / Standard Range (µ mol L^{-1})	Limit of Detection (µmol L^{-1})	TDMA-64 Recoveries (µg L^{-1})	LGC6156 / 6137 Recoveries (mg kg^{-1})
Ni	262±23	161±13	ICP-OES	0.01-100	0.54, 0.62, 0.24, 0.36, 0.47,**0.37, [+]0.94	277, 254, 260, 247, 233, 259, 271	133±80 (83 %)
			ICP-MS	0.001-0.5	0.0047, 0.0027	323, 326	127±66 (174 %)
Pb	297±28	[†]73.0±3.6	ICP-OES	0.01-5000	0.95, 0.50, 0.46	285, 279, 269	-
Si	-	-	ICP-OES	0.5-5000	2.7, 2.1, 3.0, 1.0, 1.5, **1.3,[+]4.5,	-	-
Sb	125±20	-	ICP-OES	0.5-50	1.6	126	-
Sn	292*	-	ICP-OES	0.05-500	0.72, 0.79, 0.85, **0.91, [+]1.7	308, 275, 294, 295, 246	-
V	272±26	91.5±10.0	ICP-OES	0.01-100	0.35, 0.40, 0.15, 0.18, 0.11, **0.10, [+]0.20	270, 276, 274, 262, 256, 281, 282	72±12 (79 %)
			ICP-MS	0.0005-1	0.0001	0.11	-
W	0.06*	-	ICP-OES	0.5-50	3.7	<LOD	-
			ICP-MS	0.0010-10	0.026, 0.028	330	-
Zn	313*	3530±195	ICP-OES	0.1-1000	0.77, 1.4, 0.65, 0.46, 0.55, **0.38, [+]1.31	329, 307, 321, 306, 302, 327, 239	2730±120 (77 %)
F^{-}	-	-	IC	10-5000	0.31	-	-
Cl^{-}	-	-	IC	10-5000	1.3	-	-
SO$_4^{2-}$	-	-	IC	10-5000	1.7	-	-

5.6.2 Mine Waste Characterisation

Moisture and Organic Content

The moisture content of the sample material was 5.6% (WAM), 13.4% (CIND), 13.2% (WBN) and 14.7% (WBS). Organic content was determined by LOI as 2.8% (WAM), 10.3% (CIND), 4.7% (WBN) and 7.5% (WBS).

Acid Extractable Metals and Metalloids

The relative abundance of metals and metalloids in the four composite samples of waste material used in this study are shown in Table 5.2.

Figure 5.2: Acid extractable metals and metalloids determined by aqua regia digestion for composite mine waste samples used in batch and column experiments. Bars represent mean of triplicate results, error bars represent +/- 1 s.d. Note logarithmic scale on y-axis.

The aqua regia digestion method provides a "pseudo-total" for the mass of each element extractable from the sample if weathering was accelerated. The extracted loads are presented on a $\log_{10}$ scale in order to show the relative abundance of major and trace elements which span many orders of magnitude. The acid extractable content of Cu, Zn, Pb

and As (Table 5.5) shows that the content of Cu and As were of a comparable range while Pb content was only notable in material from Wheal Betsy. The variability in the content observed for some elements is partly due to the combined effect of small sample size and mineralogical heterogeneity of the samples.

Table 5.5: Summary of mean acid extractable content for Cu, Zn, Pb and As from selected mine wastes. All units mmol kg^{-1}. Highest result for each element in bold.

	Cu	Zn	Pb	As
WAM	35.8 ± 18	0.572 ± 0.10	0.354 ± 0.07	272 ± 65
CIND	**50.8 ±1.1**	7.93 ± 0.20	1.69 ± 0.15	**383 ± 8.2**
WBN	13.1 ± 2.2	16.6 ± 6.1	126 ± 80.5	66.4 ± 9.0
WBS	27.0 ± 7.5	**22.4 ± 6.6**	**224 ± 29.3**	104 ± 29

In addition to these elements which are commonly identified in mine waters a range of trace elements were detected. These included Cd and Ni which were mobile in field drainage waters. Cd and Ni content was highest in WBN (40.8 µmol kg^{-1}) and CIND (93.4 µmol kg^{-1}) respectively. Dissolved concentrations of Sb, V, W, and Sn in field drainage waters were very low (<LOD, for most samples). However, the content of trace elements, particularly Sn and W, may be of interest to future site management strategies, their abundance in CIND waste samples was equivalent to 0.086 % and 0.023% and is just above the current cut off for economic recovery (0.08% Sn and 0.02% W, Wolf Minerals Ltd, 2010). A full list of elemental content determined for all element/sample combinations is listed in Table 5.10.

Particle Size Analysis

All composite sample materials were poorly sorted with a range of particle sizes in the < 4mm fraction. Figure 5.3 shows WBS material had the largest fine (< 250 µm) fraction comprising 24.7% silts and clays. WAM was generally coarser, comprising mainly coarse and very coarse sands and only 4.6 % silt and clay.

Sample	% Mass of Total Sample							
	Gravel (> 4 mm)	Gravel (2-4 mm)	Very Coarse Sand (1-2 mm)	Coarse Sand (0.5 - 1 mm)	Medium Sand (250 -500 µm)	Fine Sand (125 - 250 µm)	Very Fine Sand (63 - 125 µm)	Silt and Clay (< 63 µm)
WAM	0.0	11.0	26.6	34.7	17.7	4.5	1.8	4.6
CIND	0.8	19.6	17.3	16.5	14.4	6.4	7.3	16.6
WBN	0.1	26.6	25.3	15.0	11.0	3.3	3.1	14.2
WBS	0.5	19.7	19.1	14.2	12.1	3.6	4.8	24.7

Figure 5.3: Above: Results of particle size analysis for composite mine waste samples used in batch and column experiments. Groupings according to the Wentworth particle size scale. Below: Particle size results displayed graphically as coarse (red and orange) and fine (< 250 µm, blue) fractions.

X-Ray Diffraction

XRD patterns were obtained for pre- and post- column leached WAM, WBN, WBS, and CIND samples (dried, ground and sieved to <63 μm). One sample (WAM, Figure 5.4) was run in duplicate and reproducibility was good. Raw data was interpreted using Brucker AXS Eva software to peak match existing reference XRD patterns. However, the sample patterns were dominated by crystalline quartz (blue pattern, Figure 5.4) which is commonly associated with hydrothermal veins and was present in all the samples analysed.

File: 2 DGC column pre run rep 1.raw - Type: 2Th/Th locked - Start: 2.000 ° - End: 70.000 ° - Step: 0.020 ° - Step time: 2. s - Temp.: 21 °C (Room) - Time Started: 3426 s - 2-Theta: 2.000 ° - Theta: 1.000 ° - Chi: 0.00 ° - Phi:

File: 2 DGC column pre run rep 2.raw - Type: 2Th/Th locked - Start: 2.000 ° - End: 70.000 ° - Step: 0.020 ° - Step time: 2. s - Temp.: 21 °C (Room) - Time Started: 3426 s - 2-Theta: 2.000 ° - Theta: 1.000 ° - Chi: 0.00 ° - Phi:

Quartz ref - File: 2 DGC column pre run.raw - Type: 2Th/Th locked - Start: 2.000 ° - End: 70.000 ° - Step: 0.020 ° - Step time: 2. s - Temp.: 21 °C (Room) - Time Started: 3422 s - 2-Theta: 2.000 ° - Theta: 1.000 ° - Chi: 0.00 °

Figure 5.4: Stacked XRD patterns obtained for Quartz reference material (blue) and DGC composite material replicates (red and black).

Minor constituents (< 5%) and amorphous mineral phases such as secondary iron oxyhydroxides could not be positively identified by XRD. Major phases that were identified are shown in Table 5.6. There was no discernable difference in the patterns

325

obtained for pre- and post-column materials. Relative abundances could not be calculated as samples were not prepared with an internal standard.

Table 5.6: Minerals identified by powder XRD using Brucker AXS Eva software. (S) indicates secondary (iron) mineral phase.

Sample	Mineral Classes	Mineral Groups	(Crystalline) Mineral Phases Identified
WAM	Oxide	Quartz	Quartz
	Silicate	Tourmaline	Dravite, Schorl, Uvite
		Mica	Muscovite-silicon rich
		Zeolite	Gismondine
		Chlorite	Chamosite
	Halide	Fluorite	Fluorite
	Sulphide	Sulphide	Arsenopyrite
	Phosphate	Arsenate	Juanitaite (S)
CIND	Oxides	Quartz	Quartz
		Simple Oxides	Maghemite (Fe(III)Oxide Fe_2O_3)
	Halide	Fluorite	Fluorite
	Silicate	Pyroxene	Enstatite
WBN	Oxides	Quartz	Quartz
	Sulphate	Alunite	Jarosite
	Halide	Complex halides	Douglasite
	Phosphate	Arsenate	Beudantite (S)
	Silicate	Mica	Muscovite (silicon rich), illite
		Chlorite	Chamosite
	Sulphide	Sulphide	Galena
WBS	Oxides	Quartz	Quartz
	Phosphate	Arsenate	Beudantite (S)
	Sulphate	Alunite	Jarosite
	Silicate	Mica	Muscovite (silicon rich), illite

Scanning Electron Microscopy

Wheal Anna Maria Upper (WAM)

Surface mounts and sectioned blocks were examined by SEM to investigate the physical appearance and elemental composition of the mine wastes. The surface mounts of WAM tip waste (< 4 mm fraction) showed angular grains of typically around 0.5-1 mm in diameter (Figure 5.5). The surfaces exhibited a variety of textures with surface crusts and detritus commonly associated with the grains

Figure 5.5: WAM sample grains

Surface crusts, as shown on the quartz grain in Figure 5.6, were examined in cross section and revealed a coating of Fe-oxides rich in As (≤ 26 % atomic composition, quantitative EDX) with lesser amounts of Cu (≤ 2.5 %) and Zn (≤ 0.85 %). There was no evidence of surface exposed primary sulphide minerals, although minerals surfaces beneath flaking surfaces were usually richer in As. The flecks of detritus were mainly comprised of silicate minerals (often illite and muscovite) or Fe-oxides, again with As and Cu associated.

Figure 5.6: BSI WAM Quartz grains exhibiting surface crusts and detritus.

Cross sectioned polished blocks of WAM waste revealed the internal composition and textures of the grains. The WAM sample comprised mainly silicates (illite and muscovite and quartz) and fluorite. There were occasional grains of altered arsenopyrite and most mineral grains exhibited the Fe-oxide rims with trace As, Cu and Zn (Figure 5.7). The highly fractured arsenopyrite with feathered edges and rims of amorphous Fe-O was indicative of oxidative alteration. There was very little evidence of other sulphide phases within the sample. Where found, chalcopyrite and sphalerite were altered to a greater extent than the arsenopyrite, suggesting preferential weathering of the Cu, Zn and occasionally Mn containing phases (Figure 5.7). The high concentrations of Cu, Zn and Mn determined in field samples of leachates from the WAM tip must are likely to be from the dissolution of these phases. There appears to be some attenuation of dissolved metals via association with the secondary Fe phases and in general the content of As, Cu and Zn was increased in Fe-oxides closest to the remnants of the primary sulphide minerals.

Figure 5.7: Top Left: BSI of cross-sectioned WAM grains showing silicate minerals (dark) with Fe-oxide coatings (lighter rims). Bright grain is a highly altered grain of arsenopyrite. Top right: detailed image of the alteration zones around the crystalline arsenopyrite. Bottom left : BSI of multi - mineral assemblage (left). Bottom right: highly weathered chalcopyrite and sphalerite (lightest areas), Fe-oxides and quartz (dark areas).

Cinders (CIND)

The cinders material exhibited a greater range of particle size and textures than the WAM waste (Figure 5.8, left). The internal structures were varied and unusual, often appearing bubbled, and likely to be the result of processing in the arsenic calciners (Figure 5.8, right).

Figure 5.8: Left: BSI of cinders waste. Right: Large grain showing porous texture consistent with high-temperature alteration and evolution of gas (in a furnace), smaller altered grain of arsenopyrite also shown to left.

There was very little bright material on the back-scattered images of the cinders (CIND) waste indicating a paucity of heavy elements. Chalcopyrite and sphalerite were absent, but occasional grains of wolframite and arsenopyrite were evident. The mineral assemblage was dominated by silicate minerals and fluorite. Where found, arsenopyrite was fractured and weathered with alteration to As rich Fe-oxide. Elsewhere in the sample, Fe-oxides were present largely as amorphous whole grains with textures resembling soil particles, or high-temperature furnace products (Figure 5.8, right). There was a paucity of Fe-oxide surface coatings on other mineral grains. Interestingly, despite the absence of copper-, zinc- and manganese- containing primary sulphide minerals, Fe-oxides enclosed in some grains were rich in these elements. This suggests that the primary sulphide was once present in these grains but has been preferentially weathered from the sample leaving behind voids and secondary Fe-oxides with Cu, Zn and Mn associated with them.

Surface mounts of the bright red material which was a constituent of the CIND composite were also examined as the red-orange colour resembled altered arsenic sulphides identified in other As-rich waste (Greenhill Arsenic Works, DeNull (2007)). The textures were indicative of high-temperature alteration, being bubbled and pitted, and As

content was concentrated in detrital material on the surface. Therefore it is concluded that

the sample is composed of an inert man-made material (e.g. brick dust).

Wheal Betsy North (WBN)

The BSI of WBN prepared as surface mounts show a range of particle shapes and

sizes, generally less than 500 μm diameter and comprising mainly mica and quartz (Figure

5.9, top left).

Figure 5.9: Top Left: BSI of WBN waste material showing mixed particle size. Top Right: Pb rich Fe-oxide coatings on mineral surfaces. Bottom left: BSI of WBN waste material showing assortment of mineral grains with surface coatings of Fe-Pb-S-O phase. Bottom right: Highly altered galena surrounded by secondary Fe-Pb-S-O phase.

Surface crusts were ubiquitous with surface cracks similar to those observed in the WAM material. The crusts were generally brighter than the host minerals and bright particles of detritus were also commonly associated with the grains (Figure 5.9, top right and bottom left). Investigation of these crusts with EDX revealed the bright areas to have a high Pb content (≤ 13 % atomic composition).

The EDX spectra revealed a fairly consistent atomic ratio of Fe, Pb, O and S in surface coatings (average 21:10:39:11), in addition to variable amounts of As (3.9-9.8%) with trace amounts of Zn (≤ 1.2 %) and Cu (≤ 1.6 %) also common. Of all commonly identified secondary phases, the composition was most consistent with the secondary phase beudantite ($PbFe_3(AsO_4)(SO_4)(OH)_6$), identified by XRD and identified in previous studies of other Pb-bearing mine waste e.g. Roussel *et al.* (2000). However, plumbojarosite ($Pb_{0.5}Fe^{3+}_3(SO_4)_2(OH)_6$), beaverite-(Cu) ($Pb(Fe^{3+},Cu)_3(SO_4)_2(OH)_6$) and beaverite-(Zn) ($Pb(Fe_2^{3+},Zn)(SO_4)_2(OH)_6$) are also possible phases, which may not be detectable via XRD due to a lack of crystalinity.

Primary sulphide minerals made up a very small part of the sample, and where encountered, galena (PbS) was highly altered (Figure 5.9, bottom right). EDX targeting the centre of this mineral grain also revealed that trace amounts of Zn and Cu were present (both present at 0.5-0.7%). Since Cu and Zn are not trace constituents of galena, it suggests chalcopyrite and sphalerite have been preferentially weathered away. A very small number of fragmented and highly altered sphalerite particles were found, but no chalcopyrite. Since Cu , Zn, Mn, Ni, Cd and Pb were enriched in the waters percolating the WBN tips (Chapter 4), these elements must either be released via dissolution of the remaining sulphide minerals or release of these species from the secondary minerals, either due to phase change or desorption.

Wheal Betsy South (WBS)

There was a higher proportion of fine material (< 100 μm diameter) in the WBS sample and numerous aluminium silicate phases were identified, commonly highly textured and intimately associated with other phases within grains. Also observed in the WBS samples, was a higher count of grains comprised mainly of amorphous Fe-Pb-S-O phases (26:7:44:13 atomic %). The composition was slightly less Pb-rich than the WBN sample. Fe-Pb-S-O coatings were ubiquitous, and as for all sample materials, there was no visible difference in pre- and post- column leached samples (Figure 5.10, top and bottom left) such that they were not visibly altered by the conditions of the column test. There was very little galena present. A rare example is shown in Figure 5.10 (bottom left) enclosed in a secondary Fe-Pb-S-O phase. Close inspection of the outer phase shows the highly amorphous texture (Figure 5.10, bottom left), and some grains exhibited an outermost coating of Fe-O around the secondary Pb phase. Copper and Zn were only present in trace amounts associated with the secondary phases.

The degree to which the samples in this study were representative of the tip waste from elsewhere in the Tamar catchment was examined by comparison to existing samples, prepared similarly during a previous study by Mighanetara (2009). These comprised material from New Great Consols, Luckett (historically mined for Sn, Cu, As, Ag and W), Old Gunnislake Mine (Cu,As,W), Okel Tor (Cu, Sn, As) and Gawton (Cu,As,Sn). Sulphide minerals comprised a only a small fraction (< 5%) of the cross-sectioned grains examined. This is consistent with the findings of Mighanetara (2009), who examined ten mine waste samples from five mine sites in the Tamar Valley using semi-quantitative field scans by QEMSCAN[®]. For most samples in the study sulphide content was low but could be highly variable (<0.1 - 29%, for a single phase) between mines and between samples from the same site.

Figure 5.10: BSI of WBN material pre-column (top left) and post-column experiment (top right). Bottom right: BSI of surface mounted WBS grain showing cracked surface coating. Bottom right: Rare fragment of galena (bright area) enclosed by secondary Fe-Pb-S-O phase and altered quartz grain (large dark area).

The degree of alteration observed in primary sulphide minerals in this work was variable but in all samples including those prepared in this study, arsenopyrite was more commonly encountered than Cu- Mn- and Zn- sulphides. The Old Gunnislake sample had the lowest sulphide content, with arsenopyrite limited to small highly altered grains (Figure 5.11, top left). It also contained evidence of angular glassy material likely to be processing waste (furnace slag). Like the CIND sample, secondary Fe-oxide coatings were not obvious in this sample. The secondary coatings observed in the WAM, WBN and WBS

material were encountered in the Okel Tor, Luckett and Gawton. In the Okel Tor waste, whole grains of secondary Fe-oxide phase were encountered which were rich in As, Cu, Zn and Mn or a combination of all. Figure 5.11 (top right) shows a cross sectioned grain comprising secondary Fe-oxide minerals rich in Zn at the centre, suggesting that this is the remains of a highly weathered sphalerite grain. This sample also had characteristic textures which indicate the growth of socrodite ($FeAsO_4.2H_2O$) on arsenopyrite (Figure 5.11, bottom left). The waste material from Luckett had the greatest variety of mineral types. There was little arsenopyrite but arsenic was commonly associated with secondary Fe-O-As and Fe-Pb-As-S-O phases. The material from Gawton was similar in composition and texture to the samples from WAM. Figure 5.11 (bottom right) shows the degree of alteration exhibited by the arsenopyrite and the Fe-oxide coatings on the particles. Elsewhere in the sample small amounts of chalcopyrite and sphalerite were encountered. These were much less abundant than arsenopyrite with a high degree of alteration, again indicating preferential weathering. Overall the textures and elemental composition of phases encountered in the WAM, CIND, WBN and WBS do appear to be representative of those found in other mine wastes.

There is some variation in the mineralogy and degree of alteration but the wastes appear to fall into two categories: those with extensive secondary Fe-O coatings and those without. The diversity of the minerals found does depend on the particular mineralogy of the site, but the relative abundance in all samples seems to indicate the preferential weathering of Cu- Zn- and Mn- containing sulphide phases, over arsenopyrite. This is not consistent with literature solubility constants (K_{sp}) of the pure sulphide mineral phases. Solubility generally follows the order Sphalerite > Galena = Arsenopyrite > Pyrite >> Chalcopyrite (PHREEQC, Stumm and Morgan (1996)). However there is variation in literature K_{sp} values depending on temperature, and crystal structure. Sulphide phases identified in the mine wastes were rarely pure sulphide end members, and solubility

products cannot be used as a substitute for oxidative weathering rates when assessing the reactivity of sulphide mineral phases.

The most striking finding of the SEM investigation is how small the fraction of primary sulphides is in all the samples. Therefore the behaviour and stability of the secondary phases is most likely to control the mobility of many of the toxic elements (Cu, Zn, As, Pb) of interest to this study.

Figure 5.11: Top left: BSI of highly altered sphalerite grain within Okel Tor waste. Top right: BSI of Old Gunnislake sample showing highly altered arsenopyrite. Bottom left: BSI showing alteration of arsenopyrite (crystalline light areas) to scorodite (flecked areas) in Okel Tor waste. Bottom right: BSI showing Fe-oxide coating (approximately 10 micron) and alteration of arsenopyrite grain.

5.6.3   Column and Batch Experiments

Conditions and Reproducibility

Column and batch experiments were carried out at ambient temperatures of 18.2-23.0 °C. Test conditions of flow rate, pH and Eh were reproducible between replicate columns of the same waste material (Table 5.7). Small differences in the dry mass, saturated pore volume, linear velocity and flow rate of the leachate from different materials resulted from variation in particle size and packing on flow through the waste. High backpressures were observed when the filled columns were connected to the flowing circuit. This caused one column to fail (leaking seal and sheared nylon retaining screw) at the beginning of the experimental run (CIND 2) leaving only two replicates for the CIND material.

Table 5.7: Up-flow percolation test characteristics for each column: flow rate, moisture content, temperature, dry mass, saturated pore water volume, linear velocity, initial L:S ratio, median pH and pH and Eh ranges.

Tip Material:	DGC Wheal Anna Maria (WAM)			DGC Cinders (CIND)		
Replicate No.	1	2	3	1	2	3
Mean flow rate (mL min^{-1})	1.51	1.71	1.70	1.43	-	1.49
Dry mass of solid sample (kg)	0.855	0.837	0.873	0.663	0.665	0.676
Saturated pore water volume (L)^1	0.250	0.259	0.245	0.209	0.204	0.202
Linear Velocity (cm h^{-1})^2	10.9	11.9	12.5	12.3	-	13.3
Initial L:S ratio (L kg^{-1})^3	0.29	0.31	0.28	0.32	0.31	0.30
pH range	2.4-3.7	2.5-3.5	2.5-3.5	4.0-4.5	-	4.0-4.5
Median pH ^{4}		3.1			4.2	
Eh range (mV)	500 -730	580-750	565-700	405-670	-	365-575

Tip Material:	Wheal Betsy North (WBN)			Wheal Betsy South (WBS)		
Replicate No.	1	2	3	1	2	3
Mean flow rate (mL min^{-1})	1.44	1.39	1.61	1.45	1.31	1.69
Dry mass of solid sample (kg)	0.866	0.833	0.810	0.848	0.842	0.850
Saturated pore volume (L)[1]	0.085	0.086	0.094	0.079	0.081	0.079
Linear Velocity (cm h^{-1})[2]	30.5	29.1	30.8	33.0	29.1	38.5
Initial L:S ratio (L kg^{-1})[3]	0.10	0.10	0.12	0.09	0.10	0.09
pH range	1.9-2.6	1.8-2.5	1.9-2.6	2.0-2.5	2.3-2.6	2.3-2.6
Median pH [4]		2.3			2.4	
Eh range (mV)	715 -800	-	-	720 -780	-	-

[1] Water volume in saturated column, determined gravimetrically

[2] Determined from saturated pore volume per unit length of column (mL cm^{-1}) and the average flow rate (mL h^{-1})

[3] Initial L:S ratio calculated from saturated pore volume and dry sample mass

[4] Median pH determined from all three replicates at L:S ratio >0.2 L kg^{-1}.

Column and Batch pH and Redox Potential

There was little variation in pH during the course of the column experiments (open symbols, Figure 5.12). WBN and WBS material produced leachates of similarly acidic pH values (pH 1.9-2.6). WAM leachate had a slightly higher pH (pH 2.4-3.7), and leachate from the CIND sample material was highest in pH (pH 4.0 - 4.5) The pH data shown in Figure 5.12 clearly shows that the method of leaching experiment has a significant effect on the pH of the solution in the system. Column pH was lower than batch experiments (closed symbols, Figure 5.12) whilst both batch and column pH were lower than the pH measurements taken of comparable leachates in the field. For example seepages from the base of the WAM tip were pH 3.2-4.0, (DGC locations 3-7, n=14), drains issuing from the CIND waste were pH 5.0-5.3 (DGC location 1, n=3), and boreholes in the base of WBN tips were pH 3.2-5.1, (WB BH3 and BH5, n=11).

Figure 5.12: pH measurements recorded during column experiments (n=3 WAM, WBN and WBS, n=2 CIND) and soil pH experiments (n=3, error bars represent +/- 1 s.d). Note change of scale after break on x-axis.

The redox potential in the columns leachate remained positive (365 - 800 mV, Figure 5.13) throughout the experiment, indicating that the columns were not oxygen limited. However CIND and to a lesser extent, WBN and WBS, produced progressively more oxic leachate during the experiment. The gradual increase in Eh observed indicates the rate of oxygen consumption (by oxidation reactions) were kinetically slower than the rate of supply of oxygenated waters to the column. Therefore the rate of oxidation reactions and not the rate of oxygen supply is the rate limiting factor controlling release of contaminant metals in column leachates. The deliberate oxygen saturation of inflowing eluent raised the Eh of the column leachates above values recorded in field drains flowing from the tips (e.g. WAM 560 - 740 mV, CIND 485 - 552 mV, WBN 455 -555 mV). Concentrations and extractable loads resulting from the columns may therefore be regarded as the upper limit (or "worst case") leachate composition under saturated oxic conditions.

Figure 5.13: Redox potential measurements as Eh (mV) recorded during column experiments (corrected for saturated AgCl electrode half cell potential). Note change of scale after break on x-axis.

The high variability in pH and Eh observed for the WAM columns is attributed to a limitation of the method used to make measurements for this sample. pH and Eh meters were swapped between replicate columns during the experiment and resulted in less stable and more variable readings. In subsequent column experiments (WBN, WBS and CIND), pH and Eh probes remained in situ and monitored one replicate (two for CIND) for the duration of the experiment. During all experiments, probes were only removed periodically to check calibration with pH 4.0 and Zobell's (Eh) reference solutions. The probes were not recalibrated as values remained within 0.3 pH and 10 mV of the start values for the reference solutions. Therefore the variation in Eh and pH observed for CIND, WBN and WBS may be confidently interpreted as indicative of geochemical processes occurring within the columns.

The pH and Eh values the two individual CIND columns are displayed in Figure 5.12 and Figure 5.13 to demonstrate that it is possible to have distinctly geochemical environments in the column system despite homogenisation of the sample and identical

treatment of the columns. When translated from the controlled laboratory to the field environment, where there is much greater scope for heterogeneity within mine waste, it is apparent that the geochemical environment could vary greatly within individual tips of even the most visually homogeneous material. Even small changes in pH or Eh could result in a shift in element behaviour through altered speciation, sorption or desorption, this in turn could dramatically alter the mobility of toxic elements from mine waste tips. This behaviour is explored in the following sections where elements are grouped according to the dominant geochemical processes controlling their mobility.

5.6.4 Elemental Mobility in Dynamic Column Experiments and Batch Experiments

Elemental Release Curves and Cumulative Elemental Loads

Dissolved elemental concentrations (μmol L^{-1}, filtered in-line to 0.2μm) in column leachate were plotted against the liquid to solid ratio (L:S), normalised for dry mass (L kg^{-1}). The resulting release curves were highly reproducible for replicate columns for all elements, as exemplified in Figure 5.14 for Cl and Zn leached from WAM tip material. There were a small number of exceptions, which are noted in the following sections. Error bars are not shown as staggered collection times and the slight differences in flow rate meant that the calculated L:S values differed between replicate columns. Results from replicate columns were combined to produce a single data set for each sample of waste. The shape of the Cl curve in Figure 5.14 may be considered to be representative of the transport of an unretained species through the column. A shallower curve (seen for Zn) indicates greater interaction with the waste solid in the column.

Dissolved concentrations (μmol L^{-1}) of metals and metalloids determined for column (points) and batch experiments (points with error bars) will be presented together in the following sections. Also shown are the mean, maximum and minimum concentrations determined in comparable samples from the field studies. Field data are

displayed as horizontal lines since it was not possible to determine the L:S ratio in situ. For the material from Devon Great Consols (WAM and CIND), comparable field values comprise dissolved elemental concentrations for the WAM tip drains (DGC locations 4-7, n=13), and the cinders drain (DGC location 1, n=4). At Wheal Betsy, data from boreholes located at the base of the WBN tips(WB BH2-5, n=21), were used to compare to leachate from WBN waste material. No borehole or drainage data was available to directly compare WBS material. Instead dissolved concentrations are shown for a section of Cholwell Brook where the WBS waste is in direct contact with the stream (WB locations 9 and 10, n=5). NB. WBS field data will be affected by upstream sources (WBN) and in-stream dilution.

Figure 5.14: Concentration of dissolved Cl and Zn in leachate from replicate columns of WBN tip material versus cumulative liquid to solid (L:S) ratio. Concentrations were corrected for dry mass in the column. LOD_{Zn} = 0.53 μmol L^{-1}, LOD_{Cl} = 1.3 μmol L^{-1}.

Metal and metalloid concentrations determined in column leachate at a cumulative L:S ratio are not directly comparable with those determined in the batch experiments. Concentrations determined in column leachates accounts for the leachate passing through the system at the point of sampling, ignoring that which has already passed. Conversely in the batch experiment the dissolved fraction is retained in a closed system. For direct comparison of the relative extraction efficiencies of the two methods, the cumulative extractable mean loads (μmol kg^{-1} dry weight) were calculated and are presented for the

columns (as points) and batch experiments (as bars). In addition, the results of the $MgCl_2$ and CH_3COOH batch extractions are shown alongside those for MilliQ to compare the relative extraction efficiencies of these methods and interpret the mechanisms that control metal and metalloid release.

5.6.5   Iron and Aluminium Release

SEM observations of Fe- and Al- associations with Cu, Zn, Mn and Pb indicated that the solubility of mineral phases containing iron and aluminium would strongly influence the mobility of other metals and metalloids associated with them. Field data in Chapter 3 and Chapter 4 also indicated that the drainage waters draining from the mine wastes were poised at a pH indicative of either an Fe-buffered system (~ pH 3) e.g. WAM tips or an Al-buffered system (pH 4.5-5.0) e.g. CIND and WBN tips. Leaching of dissolved Al and Fe in the column and batch experiments established the intrinsic stability of Al and Fe phases in the sample materials under different conditions.

Iron

Since Fe speciation is sensitive to both pH and redox conditions, the implications of Eh/pH variation are best described with the aid of the Pourbaix diagram shown in Figure 5.15. The waters from field and column study are shown to be predominantly in the stability field of the solid iron-hydroxide phase (no Eh data for batch experiments, hence not shown). The boundaries within the Pourbaix diagram are approximations based on a simplified system and the exact position may vary slightly from that shown. However the placement of the species boundary is consistent with the PHREEQC geochemical modelling results for field samples (Chapter 3, section 3.76 and Chapter 4 section 4.5.6) which calculated the dominance of the Fe^{3+} species over Fe^{2+} in surface waters at equilibrium with the atmosphere.

Figure 5.15: Pourbaix diagram showing aqueous iron species in a Fe-O_2-H_2O system at 25°C, 10^{-6} M Fe (adapted from Beverskog and Puigdomenech (1996)). Dashed blue lines represent stability field of H_2O. Column samples from all L:S ratios and mean field data shown. Error bars represent +/- 1 s.d.

With all samples lying close to the Fe^{2+}/Fe^{3+} boundary only a small reduction of Eh or pH may result in dissolution of Fe-hydroxide phases. Such phases were shown by SEM to be a major sink of As, Pb, Zn, and Cu under current field conditions but could become a major source if conditions were to change. The concentration and load plots for Fe are shown in Figure 5.16 and Figure 5.17 respectively. Under the conditions of the column test, Fe mobility was very low for all the study samples, despite low pH compared with the field. WBN material did release a little Fe at the start of the experiment, perhaps due to a slight reduction of pH/Eh in the saturated column; however this was rapidly suppressed by the inflow of oxygen as the experiment progressed. Given the low pH generated by the sample material, it is likely that oxidation of pyrite or other iron sulphide phases occurred during the saturation phase of the column. Such reactions would have consumed oxygen and supplied dissolved Fe into solution.

Batch experiments liberated more Fe but the output was still very low representing < 0.02% of the pseudo total content (1-3 mol kg^{-1}) and Fe remains largely immobile under field and laboratory conditions encountered in this work. The higher result for batch over column could be a consequence of reduced Eh. However, the reaction vessel included an atmospheric headspace, allowing O_2 to mix with the waters. The reaction time was also much shorter than the column saturation time (12 hr shaking, immediate centrifuging and isolation of supernatant). Therefore establishment of reducing conditions in the batch vessels was unlikely. A more plausible explanation is inclusion of colloidal iron-oxides suspended in the "dissolved fraction". The finest fraction of iron-oxyhydroxides and clays observed under SEM may have been disaggregated in the batch experiments. Isolation of the leachate by centrifuge, versus filtration for the columns, may have artificially enhanced the proportion of 'dissolved' Fe.

The field data was most closely matched by the column results, although occasional spikes of Fe were observed, demonstrated by the maximum horizontal lines in Figure 5.16. As for the laboratory data, these may be attributed by physical disturbance of the material (e.g. purging of the boreholes) or a slight reduction in pH or Eh moving equilibrium towards the more mobile Fe^{3+} in solution. A single high result of 47.3 µg L^{-1} dissolved Fe was recorded for WAM seepages at pH 3.7 and Eh 637 mV and a singular maximum of 44.3 µg L^{-1} dissolved Fe was determined for WBN at pH 4.6 and Eh 490 mV (BH4). Both these samples plot inside the region of Fe_2O_3, which implies that disturbance of the waste caused the spike in Fe observed. This infers that some colloidal Fe was passing through the 0.20 µm filter.

Reduction in either pH or Eh would enhance Fe mobility (Figure 5.15). In the batch reaction vessel (50 mL centrifuge tube, vigorously shaken), oxygen in the headspace would be supplied to all the samples, and therefore low Eh conditions are unlikely but could not be confirmed.

Figure 5.16: Dissolved iron concentrations determined in column (multiple points), batch (points at 2, 5 and 10 L kg⁻¹) and field samples (horizontal lines) for sample materials WAM, CIND, WBS and WBN (clockwise from top left). Error bars represent +/- 1 s.d.

Cumulative Batch and Column Release

The relative mobility of Fe between experiments and sample type might therefore be explained by the initial pH condition and the capacity of the samples to buffer the pH of the extractant solution. Acetic acid consistently liberated the most Fe because it was the most acidic solution added (pH = 2.86). The acid generating capacity of the sample materials followed the order WBS ~ WBN > WAM > CIND, such that of the three samples compared WBS amends MilliQ H$_2$O to the lowest pH (pH 3.11, L:S 10:1), and CIND to

the highest pH (pH 4.70, L:S 10:1). The CIND material appears to reduce extraction efficiency of acetic acid. This may be attributed to a pH effect whereby the pH is increased by the weathering reactions occuiring within this system. Under these conditions, the extractable Fe load was more comparable to results with MilliQ and $MgCl_2$ extractants.

In the batch extractions (Figure 5.17), acetic acid (CH_3COOH, 0.11 M) liberated the most dissolved Fe from the solid for all samples tested. In the absence of significant carbonate minerals (from XRD and SEM evidence) acidic treatment targets exchangeable ions and soluble mineral phases. $MgCl_2$ (1.0 M, pH 7) was least able to liberate Fe from WAM and CIND waste but was more effective than MilliQ in the WBS sample. From the targeted phases presented in Table 5.3, WBS waste apparently contains a much larger exchangeable fraction of Fe than other samples. The magnitude of Fe released (WAM>>WBS>CIND>WBN) was not proportional to the total acid extractable total Fe content (CIND>>WBN>WAM>WBS). (See Table 5.10, Appendix B for values).

The lack of consistency between MilliQ and $MgCl_2$ extractions indicate that ionic strength also plays an important role in Fe solubility. $MgCl_2$ (1 M, pH 7.0) was both the least acidic and the highest molarity extractant applied. The results for WBS show that $MgCl_2$ liberated more Fe than MilliQ despite the later being a more acidic system. Also extraction efficiency generally increased with increased L:S ratio. This is often cited as a limitation of batch experiments, whereby saturation of the solvent inhibits further dissolution of mineral phases. This is consistent with the results for CIND, WBN and WBS but the trend was not observed for the WAM sample (Figure 5.17, top left).

In summary, although there is evidence for both pH and ionic strength effects, the results from the batch extractions indicate a complex release mechanism for Fe which cannot be easily resolved or generalised for different sample types.

Figure 5.17: Cumulative extracted Fe load (µmol kg^{-1} of dry material) for column leachates (points) and batch extractions (bars) at L:S ratios of 2, 5 and 10. Error bars represent +/- 1 s.d. Note no data for WBN MgCl$_2$ and WBN CH$_3$OOH.

The unpredictability of these trends also extends to batch extractions of Al, Cu, Zn, Mn, Ni and Cd, although the reproducibility of triplicate samples remained good. The oxidation of Fe-, metal- and As-sulphide phases, identified in the waste by SEM, was the primary source of dissolved metals and arsenic. However, release behaviour is complicated by association of the elements with secondary phases (Fe-oxides) and clays. In fact, the

content of some elements (As, Pb, Cu, Zn and Mn) in secondary coatings may be higher than the content in primary minerals based on the surface area observed under SEM, although this would require further work to quantify. The behaviour of Al, Cu, Zn, Mn, Ni and Cd is explored in the following paragraphs and Pb and As in section 5.6.7.

Aluminium

Aluminium is not directly sensitive to redox changes but mineral phases containing aluminium often buffer acidic mine waters in the environment to pH 4.0-4.5. Al was clearly soluble at the < pH 5 conditions of the batch and column experiments, as shown by the release curves in Figure 5.18. The CIND waste released leachate with the most dissolved Al and highest pH. There was a decrease in median pH from CIND to WAM and from WAM to WBN and WBS of approximately one pH unit (Table 5.7). This was equivalent to a 10-fold increase in the hydrogen ion activity and resulted in approximately 10-fold increase in the amount of Al released from the columns. The paucity of carbonate phases in the samples and the ready dissolution of Al phases indicate that Al-buffering is the dominant pH control on leachates.

The column release curves shown in Figure 5.18 are similar for WAM and CIND samples. The maximum concentration achieved during saturation of the column decays rapidly as flow is initiated until dynamic equilibrium position is reached. At this point the rate of supply of dissolved Al is equal to the rate of removal from the column in the leachate. This shape of release curve was typical of many of the elements studied in this work. However the WBS release curve is different from the ten-fold exponential decrease in concentration seen for the other samples (Figure 5.18), bottom right). This indicates an Al resupply mechanism that is unique to the WBS sample. This may be a consequence of the larger fine fraction within the sample providing higher reactive surface area for rapid dissolution or desorption of metals from clay minerals. Alternatively aluminium silicate

phases controlling Al solubility in the WAM and CIND samples may be more crystalline than in the WBS sample, and show slower dissolution kinetics. However, the actual amount of buffering is much lower in WBS than seen for CIND and WAM waste since the pH remains low (circa pH 2.5 throughout the experiment, Figure 5.12).

The results of the batch (MilliQ) and column experiments are similar in terms of the cumulative release of Al (Figure 5.19) and the unique behaviour of the WBS sample is reflected in by a linear cumulative curve. Unusually, the extraction efficiency of $MgCl_2$ actually exceeded that of acetic acid for the WBS sample. This is further evidence of the effect of high ionic strength on the sample and suggests that Al, like Fe, is in a more readily exchangeable form in the WBS sample compared to WAM and CIND. It also demonstrates the lack of comparability between extraction schemes and the lack of selectivity for a particular fraction. From Table 5.3, exchangeable Al would be expected to be included in the acetic acid extracted fraction and yet the acetic acid extraction liberates less than half that of the $MgCl_2$ extraction for WBS.

As for Fe, acetic acid was more effective as an extractant of Al from WAM and CIND with MilliQ>$MgCl_2$ for WAM and CIND samples and $MgCl_2$>MilliQ in the WBS sample. However, unlike dissolved Fe the mobility of dissolved Al was higher in the columns than in the batch experiments, except in the WBS sample. A high fine fraction (24.7 % silts and clays) was observed as detritus on the surface of grains within the WBS sample (SEM, section 5.6.2). Disturbance of the coating may have mobilised colloidal Al, similarly to colloidal Fe.

Figure 5.18: Dissolved aluminium concentrations determined in column (multiple points), batch (points at 2, 5 and 10 L kg-1 and field samples (horizontal lines) for sample materials WAM, CIND, WBS and WBN (clockwise from top left). Error bars represent +/- 1 s.d.

Figure 5.19: Cumulative extracted Al load (µmol kg^{-1} of dry material) for column leachates (points) and batch extractions (bars) at L:S ratios of 2, 5 and 10. Error bars represent +/- 1 s.d.

5.6.6 Exchangeable Divalent Cations (Cu, Zn, Mn, Ni, Cd,)

Like Al, the shape of the column release curves for Cu, Zn, Mn, Ni, Ni and Cd typically showed a ten-fold exponential decrease from the start of the experiment, where a saturated equilibrium had been established, to a dynamic equilibrium at a cumulative L:S ratio around 10. The steepest initial drop was observed for quickly eluted elements which demonstrate a low affinity for the solid sample (as exemplified Cl in Figure 5.14).

Variation in the initial curve gradient differed with sample type, for example the release curves for Cu and Zn are shown for CIND (Figure 5.20, middle) where elution was consistently more rapid (with respect to L:S ratio) than WAM and WBN (Figure 5.20, top and bottom respectively). The same trend was observed for Mn and Cd and Ni (where above LOD). The dissolution of the primary sulphide phases in the waste has not been considered

The comparison between dissolved concentrations in the column and batch experiments versus the field demonstrated that it most cases the field concentrations (represented by horizontal lines) were coincident with high L:S ratio in the release curves. Low L:S in the column experiments was indicative of elements released after saturated equilibrium, equivalent to the "first flush" from a mine waste tip following heavy rain. The results for WAM, where field leachates can only be collected as issues form the base of the tip following heavy rain, best reflect this (Cu and Zn in Figure 5.20, top). Likewise field samples of CIND drainage waters were collected from ephemeral streams flowing under wet conditions approximately 10 m from the base of the tips. The field results are comparable with L:S ratios of approximately 5:1. Dilution from waters flowing around and under the tips, which reduces the concentrations observed at WBN in the boreholes directly in front of the tips, were matched by high L:S ratio in the curve. Finally at WBS (Figure 5.21) the in stream dilution of mine waters leaving the waste tips is diluted beyond the lowest extent of the Cu and Zn release curves observed in the columns.

The point at which the field ranges cross the column leachate curve varied between elements released from the same sample of waste. For example in the WBN column (Figure 5.20, bottom) the mean field concentration for Zn crosses the release curve at L:S 7:1, while the field concentration of Cu is too low to cross the curve. This demonstrates that some elements are released more slowly into interstitial waters of the waste when rain water percolates. Different elements exhibit different levels of interaction with the mineral

353

surfaces inside the waste and therefore, the solid matrix exhibits selectivity for some elements over others.

Figure 5.20: Dissolved Zn and Cu column release curves for WAM (top), CIND (middle) and WBN (bottom). Also shown are concentrations determined in batch experiments (points with error bars) and concentrations ranges determined in field samples of drainage from respective waste tips (horizontal lines). Error bars represent +/- 1s.d.

354

Figure 5.21: Dissolved Zn and Cu column release curves for WBS. Also shown are concentrations determined in batch experiments (points with error bars) and concentrations ranges determined in field samples of drainage from respective waste tips (horizontal lines). Error bars represent +/- 1s.d.

SEM/EDX examination of the metal- and arsenic-rich coatings on mineral grains suggested dissolution and desorption processes at the surface of mineral grains are important in determining mobility Cu, Zn and Mn. Overall Cu, Zn, Mn, Ni and Cd affinity for the solid phase followed the order: WBS >> WBN > WAM > CIND (based on slope of release curves). This does not obey the order that would prevail if surface charge on mineral surfaces was the most important factor determining interaction between dissolved cations and the solid. The point of zero charge (PZC) is defined as the pH at which the net charge of all charge sources (oxides and clays) is zero (Gast, 1977). Below the PZC mine waste has an overall positive charge and is an anion adsorber and above the PZC the mine waste has an overall negative charge and is a cation adsorber (Taylor and Eggleton, 2001). The PZC of some of the mineral phases identified in the samples by XRD (from Table 5.6) and some commonly found within sulphidic mine wastes are listed in Table 5.8.

The PZC for iron and aluminium oxide minerals is generally higher (5 - 10) than the pH recorded during the leach experiments. Under such conditions the secondary iron oxide phases identified by SEM are likely to be positively charged and relatively poor adsorbers of cations.

Table 5.8: PZC values for some minerals found in sulphidic mine waste. Sources: (T) adapted from Taylor *et al.*(2001) and references therein, (A) from Alverez-Silva *et al.* (2010), (K) from Kosmulski and references therein (2011). Range shown where more than one result exists. Bold font indicates minerals identified by XRD in samples from this study.

Mineral Class	Mineral Name	PZC
Oxides	**Quartz, SiO_2**	**1 - 2.9** [T, K]
	Gibbsite, $Al(OH)_3$	5 - 9.5 [T]
	Goethite, $FeO(OH)$	6.2 - 9.6 [T, K]
	Ferrihydrite, $Fe_2O_3.0.5H_2O$	6.9 - 8.7 [T, K]
	Lepidocrocite, $FeO(OH)$	7.8 [K]
	Iron Hydroxide (Colloidal)	6 [K]
Silicates	Kaolinite, $Al_2Si_2O_5(OH)_4$	< 2 - 4.6 [T, K]
	Montmorillonite, $(Na,Ca)_{0.33}(Al,Mg)_2(Si_4O_{10})(OH)_{2.}nH_2O$	2-6 [T]
	Muscovite	**< 3 - 4.5**
	Chlorite (Chamosite), $(Fe,Mg)_5Al(AlSi_3O_{10})(OH)_8$	4.7 [A]
Halides	**Fluorite, CaF_2**	**10.5** [K]
Sulphides	**Galena, PbS**	**2.2 -6.1*** [K]
	Sphalerite, (Zn,Fe)S	**2.2 - 3**
	Chalcocite, Cu_2S	< 2

Therefore the most acidic column material would be predicted to have the lowest adsorption of divalent cations and the order of affinity for the column would follow the order CIND>WAM>WBS>WBN, but this was not the order observed (WBS >> WBN > WAM > CIND). Literature evidence (Table 5.8) suggests that quartz, silicates (including clays) and sulphides are more likely to have a negative surface charge at the pH conditions measured in the column and batch experiments and therefore will strongly adsorb cations. Clays in particular are good cation adsorbers due to the permanent (negative) charge imbalance in clay mineral structures (Evangelou, 1995).

High clay content can therefore give rise to good adsorptive properties and also is beneficial in reducing permeability through mine waste. WBS had the highest fine fraction, comprising silts and clays (Figure 5.3) and demonstrated dissolution behaviour that was consistent with a high exchange capacity associated with clay content. However, the fine fraction was also relatively high for the CIND sample and pH was highest, yet the retention of cationic species in the CIND column was poor. Furthermore, the WAM sample had a very low fine fraction (Figure 5.3) but displayed greater retention of cationic species than CIND.

This trend may be explained when the iron oxide coatings, ubiquitous in the WAM, WBN and WBS samples are reconsidered. Such coatings were less abundant in the CIND sample. This is consistent with the higher pH measured in the pore waters of the CIND sample. Able to buffer its pore waters to > pH 4.5 by dissolution of Al bearing phases, dissolution and precipitation of secondary Fe-oxide phases is less likely to occur.

Despite the PZC values for iron oxide minerals in Table 5.8, there was a clear association between Cu, Zn, Mn and secondary iron oxides in the SEM/EDX images of the mine wastes in this study. The PZC is known to vary across a mineral surface and oxides vary greatly in charge sites per unit weight and charge sites exhibit different electro-static bonding strengths for a particular metal-cation surface (Benjamin and Leckie, 1980). Particularly strong adsorption (specific adsorption) may be independent of the PZC and thus sorption can take place below the PZC (Kuo and Baker, 1980). Based on this information and the SEM observations, iron-oxide surfaces do play an important role in the sorption of Cu, Zn, Mn, Cd, Ni. The lack of Fe-O-cation bond strength is counteracted by the high abundance and high surface area of iron-oxides available for sorption. Furthermore, in mine waste tips, were cyclic wetting and drying of minerals is common, the precipitation of fresh Fe-oxides as secondary phases (evident for WAM, WBN and WBS) provides a constantly renewed sink for aqueous metal cations. This is in agreement

with Klinck *et al.* (2005) who observed thin banded films of iron oxides on and between mineral grains in WAM waste material during SEM analysis. This study concluded iron oxides were precipitated as hydrous gels under saturated conditions and subsequently dry and shrink in situ, giving rise to the characteristic coatings observed.

Fractional Release and Selective Adsorption Effects for Al, Cu, Zn, Mn, Ni, Cd

The cumulative leached load for each of the elements Al, Cu, Zn, Mn, Ni and Cd determined from the column experiments (μmol kg^{-1} dry sample) are listed alongside the total acid extractable content determined from the aqua regia digests (mmol kg^{-1} dry sample) in Table 5.10 (Appendix B). When ordered from highest to lowest, there is a strong relationship between total content and the released load indicating fractional release from the waste (Table 5.9).

However, this relationship does break down when the concentration of the metal of interest is low in the leachate, typically < 5 μmol L^{-1}. The order of affinity for the solid phase for all samples is shown also in Table 5.9. These are based on the initial concentration gradient (shallow gradient indicates high affinity). There is evidence to suggest that a selective adsorption of some metals retards mobility while increasing the mobility of others. This would account for the non-fractional behaviour observable at low concentrations. For example, when released in leachate at similarly low concentrations, Cd seems to be selectively retained over Ni and Cu selectively retained over Mn (Table 5.9, in bold). Cu generally shows a greater affinity for the solid phase than the other cationic elements (with the exception of Pb, section 5.6.7). The behaviour of Al is complicated somewhat by its tendency to form complex ions, such as sulphate pairs and hydroxyl-Al monomers and polymers (Nordstrom, 1982). Accordingly its relative mobility with respect to other cationic species was highly variable.

358

The CIND material had the lowest overall interaction with dissolved cationic species (Figure 5.20) and also failed to exhibit any selective adsorption effects between Cu, Zn, Cu, Ni. Baker (1980) stated that in most cases fractional adsorption decreases as the total metal concentration increases. This is consistent with the observations in this study as CIND waste generated leachate with three times more cationic strength (18500 μmol kg^{-1}) than the other samples (Table 5.9). The CIND sample had the highest Fe content (3354 mmol kg^{-1}) but the lowest content of Fe-oxide coatings on mineral grains, a feature that was also identified by SEM for waste containing furnace slag (cinders) from another site (Old Gunnislake sample, section 5.6.2). The reduced content of iron in the cinders material is explained by the reactions that occur when arsenopyrite is heated in air during the calcining process. Arsenic and sulphur are simultaneously liberated to the gaseous phases (at 450°C), leaving either iron oxides (hematite or magnetite), or if raised to around 500°C , pyrrhotite (Fe$_{1-x}$S) (Mular *et al.*, 2002). The reactivity of pyrrhotite in mine waste (Equation5, Chapter 3), is dependent on the stoichiometry (Lollar, 2005), while the direct removal of Fe-As pyrites prevents later dissolution and precipitation within the tip. If selective adsorption is particular to the iron-oxides in the samples then the lack of such coatings in the CIND waste may also account for the low selectivity and overall retention.

Further evidence of selective sorption is evident when the cumulative extracted loads (μmol kg^{-1}) for Cu, Zn, Mn, Ni and Cd in the column experiments are compared to the batch experiments. As a general rule, extraction efficiency in the batch experiments increased with L:S ratio for all the elements discussed so far (including Fe and Al). This was explained by the equilibrium limitation of the batch method which suppresses elemental dissolution in a closed system.

Table 5.9: Order of column leached metals and acid extractable metals for Al, Cu, Zn, Mn, Ni and Cd in mine waste samples.

Sample	Order of Column Leached Load (µmol kg^{-1}) (High to Low)	Order of Acid Extractable Content (mmol kg^{-1}) (High to Low)	Order of Affinity for Solid Phase in Column (Low to High)	Total Column Cationic Load (µmol kg^{-1})*
WAM	Al>Cu>Mn>Zn>Ni>Cd	Al>Cu>Mn>Zn>Ni>(Cd<LOD)	Al<Ni=Zn<Mn<Cu, (Cd<LOD)	6310
CIND	Al>Cu>Mn=Zn>Ni>(Cd<LOD)	Al>Cu>Mn>Zn>Ni>Cd	Cu=Mn=Zn=Ni<Al, (Cd<LOD)	18500
WBN	Zn>Al>Mn>Cu>**Ni>Cd**	Zn>Al>Mn>Cu>**Cd>Ni**	Ni<Zn=Cd=Al<Mn<Cu	3930
WBS	Al>Zn>**Mn>Cu**>Ni>Cd	Al>Zn>**Cu>Mn>Cd>Ni**	**Ni<Mn**<Zn<**Cd<Cu**<Al	6340

*Sum of detectable dissolved Ca, Mg Na, K, Al, Si, B, Ba, Cd, Co, Cr, Cu, Fe, Mn, Mo, Ni, Pb, Sr, V and Zn.

The leachate leaving the columns showed an exponential decrease in concentration for most elements during the experiment (exception Pb, see section 5.6.7). This shows that the rate of the transport through the column was faster than the rate of elemental release and the ionic strength of the leachate decreased through the experiment. Therefore, column experiments under the conditions of this study did not suffer the same equilibrium limitation as the batch experiments. As a result, the cumulative extracted load of dissolved cations should be higher for the column experiment than batch experiments at the same L:S ratio, but this was not always the case.

The results for WAM, WBN and WBS are presented in Figure 5.22. The column experiment does indeed liberate more Zn (also Cd, not shown) in all cases than the equivalent batch experiment. However this is not true of all metals and the results show that mobility of Cu (and Mn, not shown) was often suppressed in the column experiments being most evident at low concentrations in WBS leachate (Figure 5.22, bottom) and shows similar behaviour to dissolved Fe (Figure 5.16).

Overall the mobility of Zn and Cd is enhanced in the column experiments because the elements have a relatively low affinity for mineral surfaces and desorption into solution is promoted by decreasing ionic strength in the passing fluid. Conversely Cu and Mn show a higher affinity to mineral surfaces within the sample and are preferentially retained and/or preferentially sorbed on to fresh Fe-oxide as they are precipitated in the column. The gentle leaching action in the column aids the retention of amorphous and colloidal material within the waste. Disturbance of the sample in the laboratory and the field promotes mobilisation of fine content (iron oxides and clays) which in turn promoted the mobility of associated metals.

Figure 5.22: Cumulative extracted Cu and Zn load (μmol kg^{-1} of dry material) for column leachates (points) and batch extractions (bars) at L:S ratios of 2, 5 and 10. Error bars represent +/- 1 s.d.

5.6.7 Lead and Arsenic

So far the behaviour of As and Pb has not been explored. Of all the elements of interest, As and Pb demonstrated the most 'atypical' release curves in the column experiments. They also were major components of the overall acid extractable load (mmol kg^{-1}) shown in Figure 5.2. Arsenic content (acid-extractable) in all the waste samples was comparable to Al content (max 2.9% acid extractable, CIND), while WBN and WBS were very Pb-rich (2.6 % and 6.1% acid extractable As, respectively).

Lead

In the last part of section 0, the selectivity of mineral surfaces, particularly iron oxides, for dissolved eco-toxic metal cations was explored. In particular, Mn and Cu were identified as having a high affinity for amorphous iron oxides. However, in Figure 5.21 the results for Cu in leachates from the WBN material show that a more Cu was extracted in the column experiment than the batch, an observation that is counterintuitive to the argument so far presented. This behaviour can be explained by introducing the results for dissolved Pb. The Pb content of WAM (and CIND) waste was very low (0.35 and 1.7 mmol kg^{-1}, respectively) and dissolved Pb was <LOD in all column and batch extractions from these samples. However in WBN and WBS samples, Pb was both highly abundant (126 and 224 mmol kg^{-1}, respectively) and highly mobile. The concentration of Pb in the WBN column and batch leachates (33-40 μmol L^{-1}, Figure 5.23) was slightly higher than Cu (3 - 18 μmol L^{-1}, Figure 5.20). Pb and Cu cations have been shown to compete for same type of binding site on iron oxides (Baker, 1980) and in the presence of high concentrations of dissolved Pb, Cu exhibited higher mobility in the WBN experiments.

Inspection of the leachate curves for WBN and WBS in Figure 5.23 demonstrates the unique behaviour of Pb. At the beginning of the column experiments,

dissolved Pb initially decreased until a L:S ratio of 2:1 was reached, then it began to increase (Figure 5.23). WBN leachate decreased initially but rebounded to a concentration similar to the initial value. With the exception of Fe, all other elements so far discussed for the WBN sample have displayed a 'typical' exponential decay release curve. Therefore the mechanism supplying Pb to solution from WBN does not affect the mobility of other metal cations, with the exception of Cu, to a detectable level. There was a noticeable step change in pH recorded in the WBN leachate at the L:S ratio where Pb begins to increase. At the same time the concentration of Fe in the leachate, which was initially slightly soluble, tended to zero as oxic waters flow through the column. Precipitation of Fe-oxides is an acid generating process (Chapter 3, Equation 3) and yet the pH of the system rose, apparently buffered by some other mechanism.

Figure 5.23: Dissolved Pb concentrations (left axis) and pH (right axis) determined in column (multiple points), batch (points at 2, 5 and 10 L kg^{-1}) and field samples (horizontal lines) for sample materials WBS and WBN. Error bars represent +/- 1 s.d. WAM and CIND batch and column results not show, all <LOD. All CIND field results <LOD, WAM field range = 0.003-0.053 µmol L^{-1}, mean = 0.015 µmol L^{-1}.

From available evidence and the low release of dissolved Al and Fe, this seems most likely to be cationic exchange with protons, resulting in the atypical release curves observed for all the cations determined in the WBS leachate.

Sulphate (graph not presented) also increased and subsequently exponentially decays in the WBN leachate. Accurate determination of the phase controlling Pb solubility is beyond the capabilities of this study but the elemental leaching behaviour and SEM observations suggest a secondary Pb-(As)-Fe-SO_4 phase, possibly beudantite ($PbFe_3(AsO_4)(SO_4)(OH)_6$) buffers pH and controls Pb mobility.

The release curve for Pb from WBS material was similar to WBN (Figure 5.23), showing an initial decrease followed by a steady increase for the remainder of the column experiment to a maximum of 81.2 μmol L^{-1}. pH fluctuates but the step change at L:S 2:1 was not observed. In the WBS column experiments Al, Cu, Zn, Mn and Cd all showed release behaviour that was similar to that of Pb, being rapidly mobilised by exchange reactions. This indicated that these elements are closely associated in a geochemical environment unique to the WBS sample. Interestingly the selective sorption of Cu was also evident, despite the concentration of Pb (65 - 81 μmol L^{-1}, Figure 5.23) being two orders of magnitude greater than Cu (0.2 - 0.8 μmol L^{-1}, Figure 5.21). The treatment of WBS material with $MgCl_2$ liberated twenty times more Pb than the batch and column extractions using MilliQ (Figure 5.24). To a lesser extent, Al and Fe were also selectively liberated from WBS material by $MgCl_2$ (Figure 5.17 and Figure 5.19, respectively), but $MgCl_2$ was the least efficient extraction agent for Cu and Zn.

The evidence suggests a rather complex array of concurrent reactions in the WBS sample. There is evidence for the presence of Fe-Oxides with associations of Cu, As, Zn from SEM/EDX observations, and these are common to all the mine wastes studied. There is also evidence of the selective sorption of Cu and Mn to Fe-oxides. In addition, a highly mobile and exchangeable source of Pb, Al, Cu, Zn, Mn and Cd was

elucidated from the shape of the elemental release curves and the results of $MgCl_2$ extractions. The high fine fraction suggests that clay minerals might be a sink for high loads of Pb and that the lower pH established in the laboratory experiments triggers release along with lesser amount of Al, Fe, Cu, Zn, Mn and Cd. Acid treatment of clays creates new pores and increases surface acidity by replacement of cations, like Al^{3+}, Fe^{3+} and Ca^{2+} from the structure with protons (Mills *et al.* (1950). The association of Al with the mechanism also suggests associations with amorphous Al-hydroxides may be important in influencing mobility. This is consistent with acid dissolution of part of Al_2O_3, from the crystal lattice of clays noted by Oubagaranadin *et al.* (2010) in a study of the adsorption properties of acid-activated clay.

Figure 5.24: Cumulative extracted Pb load (µmol kg^{-1} of dry material) for column leachates (points) and batch extractions (bars) at L:S ratios of 2, 5 and 10. Error bars represent +/- 1 s.d.

Importantly, field samples taken from surface waters and boreholes at Wheal Betsy showed that Pb mobility is generally much lower in the field than in the laboratory experiments (WBN and WBS). There was a gradual increase in dissolved Pb in Cholwell Brook as it passed through the site, particularly on contact with the WBS

tips but the maximum recorded concentration was 0.46 µmol L^{-1} (equivalent to 94.3 µg L^{-1}). The proposed WFD EQS is 7.2 µg L^{-1} (Potter, 2008 *Pers. Com.*). The maximum recorded concentration in the field exceeded the EQS (582 µg L^{-1} Pb, from a drainage issue into Cholwell Brook). However, the maximum dissolved concentrations produced in the column experiments were equivalent to 8290 µg L^{-1} (WBN) and 16600 µg L^{-1} (WBS). Clearly there is an enormous potential source of Pb bound up in the mine waste at the site. Retention of the Pb largely within the waste tips is attributable to the higher pH in the field (pH 3.2 - 6.1), versus the laboratory experiments (pH 1.8 - 3.1). Higher pH with respect to the PZC of the mineral surfaces (Fe-oxides and clays, Table 5.8) promotes stronger binding of metal cations (Oubagaranadin *et al.,* 2010), and less dissolution of primary sulphide minerals. Other contributory factors are the apparent selectivity of some adsorption reactions for Pb over other cations commonly co-occurring in acid mine/rock drainage such as Cu, Mn, Zn and Cd. Also the physical characteristics of the mine waste cannot be overlooked - in particular permeability. The high clay content of the WBS material presents a low permeability barrier to water ingress in the field and therefore reduces the volume of leachate generated. Highly vegetated tips (e.g. WBS, see sample descriptions table in Appendix A) also indicate favourable attributes of high tip stability and low permeability.

Arsenic

Despite being an abundant element within all the mine waste samples, mobility of As was generally low in the surface and ground waters with maximum concentrations of dissolved As of 1.81 µmol L^{-1} at Wheal Betsy and 5.75 µmol L^{-1} at Devon Great Consols (except cinders drainage). Drains from the cinders waste tips at Devon Great Consols were however exceptionally high in dissolved As and produced a maximum of 378 µmol L^{-1} (equivalent to 28300 µg L^{-1}). Arsenic speciation is sensitive to both pH

and redox change, with As(III) exhibiting higher mobility than As(V). Although within the range of mine waters in Cornwall (0.1 - 95600 µg L^{-1}) and comparable to other sulphide ore producing areas (e.g. Rio Tinto, Spain, max 22000 µg L^{-1}) (Bowell, 2003), the concentrations measured in the field in WAM drainage were very high for oxic waters, where As(V) is prevalent. Importantly, the cinders tip leachates measured in the field were ten times more concentrated than leachates from the column and batch experiments using composite material from the cinders tip (max 41 µmol L^{-1}, Figure 5.25). Arsenic was the only element studied that showed higher mobility in the field than in the laboratory experiments.

Figure 5.25: Dissolved arsenic concentrations determined in column (multiple points), batch (points at 2, 5 and 10 L kg^{-1} and field samples (horizontal lines) for sample CIND sample. WAM, WBS and WBN column and batch all <LOD. Error bars represent +/- 1 s.d. Mean field results for WAM, WBS and WBN all <LOD.

The pourbaix diagram in Figure 5.26 shows the stability fields of aqueous arsenic for a simplified As-O_2-H_2O system. The Eh/pH conditions recorded for field and column experiments are plotted and are grouped within the $H_2As(V)O_4^-$ field.

Therefore there is no evidence to suggest speciation is the reason for the discrepancy between field and laboratory results.

Arsenic was highly abundant in the Fe-oxides observed in all the samples studied by SEM/EDX and as an anionic species is most strongly adsorbed at low pH and to minerals with high PZC. The pH in the field was higher (pH 5.0-5.4, cinders drain, Devon Great Consols) than in the laboratory experiments (pH 4.0-4.9), and may be the reason for the higher mobility observed in the field.

Figure 5.26: Pourbaix diagram showing aqueous arsenic species in a As-O$_2$-H$_2$O system at 25°C, 1bar pressure (adapted from Smedley and Kinniburgh (2002)). Dashed blue lines represent stability field of H$_2$O. Column samples from all L:S ratios and mean field data shown, error bars represent +/- 1 s.d.

Also, in CIND sample material, Fe-oxides were generally confined to whole mineral grains and less abundant as films on other minerals, resulting in a lower surface area for adsorption. The distribution and content of Fe-oxides was a consequence of mixing and homogenising the composite sample from sub-samples with visibly

369

different mineralogy (Table 5.10, Appendix A). Incorporation of Fe-oxide rich soils from the surface of the wastes may have enhanced the samples' intrinsic ability to retain dissolved As. In the field scenario, saturation of the available $H_2As(V)O_4^-$ binding sites on existing Fe-oxides within the waste and the slow generation of fresh Fe-oxide surface would lower retention of freshly generated dissolved As. A number of other studies of mine waters (e.g. Asta *et al.* (2010), Slowey *et al.* (2007) Lee and Chon (2006)) have also reported that As was naturally attenuated in acidic streams receiving mine waters by sorption onto newly formed Fe-precipitates (schwertmannite, goethite and jarosite).

In the batch experiments As was liberated under acidic conditions from all three samples using MilliQ and acetic acid extractions (Figure 5.27). All materials demonstrated a very clear trend of increased extraction efficiency with increased L:S volume. WAM and WBN leached similar extractable loads in batch experiments, and for all samples, mobility in the column was lower than in the batch experiments. Associated with the Fe-oxides, the gentle mode of leaching in the column (which also reflects percolation through waste tips in the field) reduced As mobility by enhancing the retention of Fe-oxides within the solid matrix. This is particularly important for As associated with the colloidal fraction of Fe oxides (commonly 20-200 nm, Slowey *et al.* (2007)) which may or may not be recorded as "dissolved" or "mobile" depending on the method of separation.   All three waste materials were As-rich comprising 2.9 % (CIND), 0.78% (WBS) and 0.48% (WAM) acid extractable As by weight, but CIND material released disproportionately more As than the relative As content of the samples Again this may be attributable to the distribution of Fe-oxides in the samples. Physical disaggregation and partial digestion of the mineral phases under acidic conditions (min pH 2.8, with acetic acid), mobilises As during the batch experiments. WAM and WBS with abundant Fe-oxides distributed as surface coatings offered higher surface area for

retention and readsorption of As, than the Fe-O content of CIND, present predominantly as distinct particles.

In an acidic environment, iron oxide surfaces are largely protonated (being below PZC) and should therefore promote sorption and retention of anionic As species. If the pH of the system were to fall below pH 2 or become oxygen limited, the dominant aqueous As species becomes electronically neutral ($H_3As(V)O_4$ and $H_3As(III)O_3$). This should enhance mobility in the laboratory experiments. However the CIND had the highest intrinsic buffering ability and the pH of the acetic acid (0.11 mol L^{-1}) added was pH 2.83, so achievement of pH <2 is unlikely. The waters in the column and batch experiments were also unlikely to be oxygen poor and Fe solubility (as Fe(III)) which would be indicative of low redox/pH conditions, was low. Therefore the dominant As species was likely to be anionic (as $H_2As(V)O_4^-$) in both field, column and batch experiments and this is consistent with other studies of As mobility and attenuation in surface waters (e.g. Asta *et al.* (2010), Casiot *et al.* (2005)).

The $MgCl_2$ extractions yielded the least dissolved As compared to other extraction schemes tested, so unlike dissolved Pb, dissolved As is not preferentially bound to the solid phase in an easily exchangeable form. Therefore in agreement with other studies of As mobility from mine wastes (e.g. Bowell (2003)) and soils (e.g. Warren *et al.* (2003)), sorption to Fe-oxides controls the mobility of As in leachates. In the case of the cinders tips at Devon Great Consols, where attenuation of As is not intrinsic, the transport pathway to the River Tamar (See map in Figure 3.20, Chapter 3) attenuates dissolved As in surface drains and shallow ground waters to < 6 μmol L^{-1} (< 550 μg L^{-1}), upon reaching the final drain.

There were several possible sources of the dissolved As measured in the cinders drains that might lead to the exceedance of the intrinsic sorption capacity of the CIND waste. Dissolution of remaining arsenopyrite within the waste or from the tips and

remains of the old As calciners (Figure 3.5, Chapter 3). However this is likely to be

kinetically slow, based on the persistence of the mineral in mine wastes compared to

other sulphides (e.g. chalcopyrite and sphalerite) and the relatively high pH (~pH 4.5).

Alternatively, reducing conditions deeper within the tip or from seepages beneath the

tip, promote As mobility.

Figure 5.27: Cumulative extracted As load (µmol kg^{-1} of dry material) for column leachates (points) and batch extractions (bars) at L:S ratios of 2, 5 and 10. Error bars represent +/- 1 s.d. WBN all results for batch and column <LOD.

The dissolved arsenic is transported via pore waters to the oxic surface drains where

sorption sites are already saturated with As and therefore even if As(III) is oxidised to

As(V), mobility remains high. In addition, evidence from other studies indicate as

secondary iron oxides age and become more crystalline under acidic conditions, their capacity to absorb contaminants decreases which would could result in As release. (Moncur *et al.*, 2009).

5.6.8 Longevity of Mine Waste as a Pollution Source

The number of column flush cycles required to deplete the source of each element was calculated as the acid-extractable total divided by the cumulative load determined the column leach experiments (to L:S 10:1), (See Table 5.10, Appendix B for values). This data is displayed in Figure 5.28. This calculation assumes that the elemental release will be of the same magnitude in each flush and that saturation of pore waters is achieved prior to each flush cycle. More complex numerical models have been applied to mine wastes in the literature, including 'shrinking core' kinetics of pyrite oxidation (Gerke *et al.*, 2001). However the empirically derived data in this study and the simple calculation provides a good tool to estimate of the relative residence times of elements of interest in the waste.

Iron is largely retained in the waste material and therefore exhibits a very high residence time. Arsenic residence time is of the order of several hundred column flushes in waste material poor in Fe-oxide coatings (CIND). These increase to a minimum of tens of thousands of column flushes where extensive Fe-oxides have been precipitated via low temperature alteration of Fe-phases (WAM, WBN and WBS).

The number of flush cycles varies for each element between sample types due to the complexity of surface interactions discussed in this chapter. Residence times of Cu, Zn, Mn, Ni, Cd and Pb are of the order of tens to hundreds of column flushes. Residence times are highest in clay-rich material (WBS) even under acidic leaching conditions which were more acidic in the laboratory than measured in the field.

Figure 5.28: Elemental resistance of elements to oxidative leaching in mine waste. Note logarithmic y-axis. As in WBN and WBS columns and Pb in WAM and CIND columns, all <LOD, therefore very high resistance. Cd <LOD in aqua regia digest of WAM, therefore very poor resistance.

5.6.9 Hydrological Considerations and Uncertainty

Under field conditions, the residence time of metals and arsenic in clay rich material is likely to be greatly enhanced due to the low porosity of the material and the higher pH of percolating waters. This is consistent with field observations, where WBS tips supply a lower flux of dissolved metals and As to Cholwell Brook than the WBN tips (Chapter 4, section 4.5.7).

Reducing oxygen ingress into waste tips (to reduce sulphide oxidations reactions) has been the target of many research projects and remediation schemes. Reduced oxygen availability could result in an enrichment of un-oxidised sulphide

minerals within the waste tips. If so, the longevity of the source-term may be much longer than the metal content of the upper weathered horizon, calculated here, would suggest. However studies have also shown that oxygen does not necessarily become limited at depth within waste tips, and thermally driven processes can draw oxygen through the base of the tip (Shaw *et al.*, 2002). Oxygen ingress within waste tips can vary widely spatially as well as with depth, and the establishment of preferential channels of high permeability can distribute oxygen deep within the tip (Song and Yanful, 2011 2011). An example of where this may be important is the inspection hole in the WAM upper tip, which continually discharges leachate and allows atmospheric oxygen into the waste (Chapter 3, photograph 9).

All solids collected in this study were from near surface locations in the oxic weathering zone of the tips. The study assumed that the near-surface waste would control the geochemistry of leachates. However, once initiated, oxidation of pyrite can occur through bacterially mediated schemes with a limited oxygen supply (Section 3.4.1, Chapter 3). The extent to which reactions occur at depth within the tips is currently unknown because deep drilling of the tips was prohibitively expensive. Another consideration is the erosion rates of the tip; continual removal of the surface of the waste exposes deeper layers of the waste to oxic conditions. If the underlying waste has a higher content of sulphide minerals, having been previously protected from the atmosphere, then the exhaustion of contamination in the oxic surface layer may never be achieved.

Horizontal heterogeneity of minerals is a common feature of pyritic mine wastes and exerts a strong control on the geochemistry of pore waters (Gerke *et al.*, 2001). Stratification into layers of different geochemical character can result from the type of waste deposited (e.g. fine grained tailings, course rock discard, furnace waste), the method of deposition i.e. compaction by heavy machinery and geochemical alteration

over time. Stratification with respect to particle size distribution gives rise to two modes of fluid transport in unsaturated tips; gravitational and preferential flow through course material and capillary flow through fine grained material (Poisson *et al.*, 2009). Capillary flow can reduce generation of AMD/ARD in unsaturated wastes by creating layers of low permeability, restricting oxygen ingress and fluid movement known as capillary buffering effects (Lefebvre *et al.*, 2001; Fala *et al.*, 2005). Also, the development of cemented layers (*iron-* or *hard- pans*), observed in WAM, WBN and WBS waste tip, have been shown to be particularly influential to the retention of As and Pb, and in the reduction of metal movement and oxygen ingress within the tips (Blowes *et al.*, 1991; Kohfahl *et al.*, 2010).

Overall, the hydrological complexity of water movement through mature mine waste tips, coupled with the heterogeneity of the waste, makes accurate prediction of eco-toxic leachate geochemistry and longevity of the source term very difficult. The observed concentrations in the field largely matched or were below, those derived from column experiments. This is encouraging evidence to support the assumption that weathering of the oxic surface layers controls the geochemistry of mine waste leachates. If deposits within the tips are richer in primary sulphides, this is not expressed as higher contaminant concentrations in field leachates at either site, with the exception perhaps of As from the cinders waste (discussed in section 5.6.7).

Capturing a representative sample of a waste tip covering several hundred square metres in a few kilograms of material is a long-standing limitation of laboratory experiments. The results of this study have shown that with careful treatment replicate leaching experiments can produce reliable and reproducible results, but have also shown that very small changes in Eh and pH can have a dramatic effect on element mobility.

5.7   Conclusions and Recommendations

The content of acid extractable metals and metalloids vary considerably between samples of mine waste as a result of different local geology, mineral processing of wastes and the weathering of the material after deposition.

There are two underlying factors controlling concentration of dissolved contaminants in mine waste leachate: mineralogy of the solid, which determines the solubility of elements, and fluid movement through the waste which determines the degree of saturation of pore waters with respect to waste mineralogy and atmospheric oxygen. The interaction of the two factors, and the dynamic nature of the later, results in complex release behaviour for co-eluting elements from mine waste including eco-toxic elements such as Al, As, Cu, Cd, Ni, Pb and Zn.

Grains of mine waste containing primary sulphide minerals constituted a very low proportion of the total assemblage in all the wastes examined in this study. This was also observed in additional samples of mine waste from other sites in the Tamar catchment, prepared for an earlier study.   Examination by SEM provided clear evidence for in-situ weathering of sulphide minerals, resulting in voids and replacement with secondary iron oxide minerals within mineral grains. Arsenopyrite exhibited less alteration than other sulphide minerals (galena, chalcopyrite, sphalerite), and preferential leaching of the non-As sulphides appears be a common feature of all the mine waste samples examined. This may reflect the difference in dissolution rates of different mineral phases, including the selective dissolution of one sulphide over another via formation of galvanic cells (discussed in section 3.4.1, Chapter 3). However, the relatively high abundance of arsenopyrite for some samples may also be a consequence of the historical period in which the tip waste was deposited. Arsenopyrite was not always treated as an economic mineral and was discarded as a by-product of early copper-extraction, becoming more important in the late stage of mining in the

Tamar Valley (post ~ 1900). Reprocessing of waste, including crushing to a finer particle size, extraction of copper, tin and tungsten and re-tipping has also been documented until the 1970's in the Tamar Valley, and this would affect the rates of weathering within the tip material.

In all cases the waste material examined represented only the surface (< 0.5m) mineralogy of the waste. Conditions are oxic and desorption from Fe-oxide coatings on grains and clays appear to be the most important mechanism for determining leachate composition. The stability of the secondary Fe- phases under oxic and acidic (pH < 4) conditions in the field and laboratory experiments effectively locks Fe in situ within the waste. Cyclic wetting and drying of waste tips allows successive dissolution and precipitation of Fe(III) oxides and results in characteristic surface Fe-oxide coatings on all mineral grains within the waste. This provides dissolved ions in solution with an amorphous mineral surface where exchange reactions allow for sorption and desorption of mobile species in and out of pore waters.

Anionic As species appear to bond very strongly with the positively charged Fe-oxide surface at low pH. In waste derived from arsenic calcining, the pH of leachates was higher than other waste samples (pH 4.0-4.5) and resulted in lower retention of anionic As species. It was also suggested that historic high temperature alteration of FeS phases to Fe-oxides (in furnaces) forces oxidation reactions to completion, reducing the capacity of the waste furnace cinders to generate acidity and freshly precipitated Fe-oxides, after deposition. The paucity of fresh Fe-oxide was a feature of the cinders waste from SEM investigations and led to lower retention of dissolved As from cinders waste in laboratory and batch experiments.

Adsorption to Fe-oxides is also an important retention mechanism for other elements, most notably Cu and Zn, which are commonly associated with secondary minerals in mine waste even when there is little evidence of primary sulphide minerals

(e.g. chalcopyrite, bornite, sphalerite, galena) in the sample. Sorption occurs at low pH (min pH 2.3) even though the PZC for most of the minerals in the waste is much higher. Under these conditions, protonation of the mineral surfaces is favoured and the bond-strength of the cation to the mineral surface is low, increasing with increasing pH. This explains why the CIND waste had the highest total extractable Cu content (50.8 mmol kg^{-1}), but released less into leachates (pH 4.0-4.5) than the WAM tip material (38.5 mmol kg^{-1}, pH 2.4- 3.7).

In mine wastes with a high fine fraction (silts and clays) sorption to clays may be as important as sorption to Fe-oxides. This was particularly so for Pb, but elemental release curves from the column experiments also suggested associations with Al, Cu, Zn, Mn, Cd and Ni also affect the mobility of these elements. Desorption of Pb was readily observed under low pH conditions in the column and batch experiments (pH 1.9 - pH 3.0, WBN and WBS). Release of Pb appeared to have a small buffering effect (~ 0.5 pH units) in the WBS leachate but not in WBN leachate. This was attributed to the higher (double) concentration of Pb and higher content of fines in the WBS sample.

Overall release of the mobile elements (Cu, Zn, Mn, Cd, Ni) is largely proportional to their relative abundance within the tip waste. At low concentrations (Typically < 5 μmol L^{-1}) competitive sorption between Pb, Cu, Zn, Mn, Ni and Cd becomes apparent. A high affinity for the solid phase was exhibited by Pb, Cu and Mn, whilst Zn and Cd and Ni were preferentially desorbed and mobilised into pore waters passing dynamically through a column. This is in agreement with other studies where the preferential sorption of one element to Fe-oxides leads to the increase contaminant load of another (e.g. Hartley *et al.* (2004)).

In cases where extensive field investigations are not viable, the up-flow percolation experiment provides a means of mimicking the conditions of dynamic flow through mine spoil. Results from column experiments and field samples were similar

for most metals (Cu, Zn, Mn, Ni and Cd) and may provide a useful tool for prediction of leachate composition. The highest concentrations of Al (6260 μmol L^{-1}, CIND), Cu (312 μmol L^{-1}, WAM), Zn (206 μmol L^{-1}, WBN), Ni (7.72 μmol L^{-1}, CIND) and Cd (0.712 μmol L^{-1}, WBN) in the leachate were observed at low L/S ratios. Concentrations at dynamic equilibrium were one order of magnitude below the maxima, with the exception of Pb which remained high (max 81.2 μmol L^{-1}, WBS). Lowest observed leachate concentrations in the field and laboratory remained elevated by one order of magnitude, with respect to current EQS values. For all elements, the dynamic equilibrium concentration from column experiments was more closely matched to field conditions than results obtained from the batch extractions.

However, the discrepancies between column and batch experiments were small enough to suggest that batch experiments could be useful for developing management strategies where it is necessary to survey large areas for contaminant mobility. However, the column test provides additional information on relative desorption behaviour of elements. Column experiments could be a valuable tool in the examination of the effect of amendments to the waste used in remediation schemes.

The largest difference between laboratory and field experiments was observed for Pb concentrations, where mobility was much reduced in the borehole samples in comparison with the high loads recorded for both batch and column experiments. This was attributed to the higher pH measured in the borehole waters (pH 3.8-5.1) compared with the more acidic leachates derived in the laboratory. This is likely to result from the mixing and dilution of leachates with other catchment waters, both at the surface and below the water table. The differences observed between laboratory and field based assessment approaches, demonstrates the limitations of applying laboratory data to the field scale. It also highlights the necessity to consider the effect of different physico-chemical and hydrological situations on the contamination potential of mine spoil.

The results of this study have shown that disturbance (e.g. removal of waste, purging boreholes, shaking tests and homogenising) or pH adjustment of the pore waters could dramatically affect the mobility of Fe, Pb and As, which are currently stored in secondary mineral phases within waste tips. In turn, remobilisation of these elements, with a high affinity for mineral surfaces, may have an acute knock-on effect on other less strongly sorbed species such as Cu, Zn and Cd, potentially leading to a devastating release of eco-toxins to the environment. Since the geochemistry of mine waste tips is so complex, perhaps the best approach for future management is to concentrate on stabilisation of the tips to reduce erosion of the weathered surface layers, combined with sensitive methods of reducing permeability such as promotion of natural re-vegetation and plant succession. In this way the likelihood of acute pollution events may be reduced and the concentrations of most metals would reduce with time as the surface layer is leached, effectively capping the waste tips.

5.8   Future Work

In future studies of mine wastes, column experiments may be speeded up via automation of sample collection. The high backpressures encountered in this study could be addressed by reviewing the method of packing the columns to allow for lower bulk density and faster flow. Reproducibility of the columns was generally very good so reducing the size of the columns may also be permissible, particularly for finer wastes. However, such method changes should be approached with caution given the low abundance of sulphide mineral grains within the samples, which as a source, could strongly effect released concentrations of metals and arsenic from mine waste samples.

The examination of reducing conditions within waste tips is worthy of further study as it may be crucial to As mobility from wastes based on the Fe-oxide associations and leaching behaviour of cinders (CIND) waste in this study. This may be

achieved by conducting batch and/or column experiments under anoxic conditions or if possible simulating cyclic oxic - reducing conditions. Ideally some field investigation of tip permeability and geochemistry with depth would help confirm or counter the argument that leaching under oxic conditions is the dominant control on leachate composition.

The rate of arsenopyrite oxidation appears to be slower than chalcopyrite, galena and sphalerite based on visual evidence of the waste under SEM. This is potentially evidence for electrochemical controls on leachate composition and armouring via galvanic effects. The effect of a mixed sulphide system on rates of dissolution for individual minerals is worthy of further investigation.

Greater understanding of the physical behaviour and hydrology of waste tips would certainly aid future management strategies. Accurate determination of the erosion rates of tips would be beneficial and could be easily achieved using available GPS and laser scanning technologies. Tracer tests may also be applied to help unravel the very complex hydrology of mine sites where sub-surface and surface waters interact, for example at Wheal Betsy where extensive underground voids are situated below the main watercourse (Cholwell Brook) and appear to influence the flow.

Finally, the capture of a 'first-flush' of mine waste following a heavy rain event would be an ideal way of monitoring the concentrations of eco-toxic metals entering a watercourse. This can be achieved via deployment of an automated in-situ sampling device into a receiving stream.

5.9   References

Alvarez-Silva, M., Uribe-Salas, A., Mirnezami, M. and Finch, J. A. (2010). The point of zero charge of phyllosilicate minerals using the Mular-Roberts titration technique. *Minerals Engineering.* **23** (5) pp 383-9.
Álvarez, E., Fernández Marcos, M. L., Vaamonde, C. and Fernández-Sanjurjo, M. J. (2003). Heavy metals in the dump of an abandoned mine in Galicia (NW Spain)

and in the spontaneously occurring vegetation. *The Science of The Total Environment.* **313** (1-3) pp 185-97.

Asta, M. P., Ayora, C., Román-Ross, G., Cama, J., Acero, P., Gault, A. G., Charnock, J. M. and Bardelli, F. (2010). Natural attenuation of arsenic in the Tinto Santa Rosa acid stream (Iberian Pyritic Belt, SW Spain): The role of iron precipitates. *Chemical Geology.* **271** (1-2) pp 1-12.

Bacon, J. R. and Davidson, C. M. (2008). Is there a future for sequential chemical extraction? *The Analyst.* **133** pp 25-46.

Baker, R. A., Ed. (1980). *Contaminants and Sediments Volume 2 Analysis, Chemistry Biology.* Ann Arbor, Michigan, Ann Arbor Science.

Bech, J., Poschenrieder, C., Llugany, M., Barceló, J., Tume, P., Tobias, F. J., Barranzuela, J. L. and Vásquez, E. R. (1997). Arsenic and heavy metal contamination of soil and vegetation around a copper mine in Northern Peru. *Science of the Total Environment.* **203** (1) pp 83-91.

Benjamin, J. C. and Leckie, J. O. (1980). Adsorption of metals and oxide interfaces: effect of the concentrations of adsorbate and competing metals. *Contaminants and Sediments* B. R. A. Ann Arbor MI, Ann Arbor Science Publishers. pp 305.

Beverskog, B. and Puigdomenech, I. (1996). Revised pourbaix diagrams for iron at 25-300 °C. *Corrosion Science.* **38** (12) pp 2121-35.

Blowes, D. W., Reardon, E. J., Jambor, J. L. and Cherry, J. A. (1991). The formation and potential importance of cemented layers in inactive sulfide mine tailings. *Geochimica Et Cosmochimica Acta.* **55** (4) pp 965-78.

Bowell, R. (2003). The influence of speciation in the removal of arsenic from mine waters. *Land Contamination & Reclamation.* **11** (2) pp 231-8.

Casiot, C., Lebrun, S., Morin, G., Bruneel, O., Personné, J. C. and Elbaz-Poulichet, F. (2005). Sorption and redox processes controlling arsenic fate and transport in a stream impacted by acid mine drainage. *Science of the Total Environment.* **347** (1-3) pp 122-30.

Chomchoei, R., Hansen, E. H. and Shiowatana, J. (2007). Utilizing a sequential injection system furnished with an extraction microcolumn as a novel approach for executing sequential extractions of metal species in solid samples (vol 526, pg 177, 2004). *Analytica Chimica Acta.* **583** (1) pp 216-.

Chomchoei, R., Shiowatana, J. and Pongsakul, P. (2002). Continuous-flow system for reduction of metal readsorption during sequential extraction of soil. *Analytica Chimica Acta.* **472** (1-2) pp 147-59.

Ciceri, E., Giussani, B., Pozzi, A., Dossi, C. and Recchia, S. (2008). Problems in the application of the three-step BCR sequential extraction to low amounts of sediments: An alternative validated route. *Talanta.* **76** (3) pp 621-6.

DD CEN/TS 14405:2004, Characterisation of waste - Leaching behaviour test - Up-flow percolation test (2004).

DeNull, R. (2007). The Greenhill Arsenic Works.

Dijkstra, J. J., Meeussen, J. C. L., Van der Sloot, H. A. and Comans, R. N. J. (2008). A consistent geochemical modelling approach for the leaching and reactive transport of major and trace elements in MSWI bottom ash. *Applied Geochemistry.* **23** (6) pp 1544-62.

Dold, B. (2003). Speciation of the most soluble phases in a sequential extraction procedure adapted for geochemical studies of copper sulfide mine waste. *Journal of Geochemical Exploration.* **80** (1) pp 55-68.

Dybowska, A., Farogo, M., Valsami-Jones, E. and Thornton, L. (2005). Operationally defined associations of arsenic and copper from soil and mine waste in south-west England. *Chemical Speciation and Bioavailability.* **17** (4) pp 147-60.

Essington, M. E. (2003). *Soil and Water Chemistry: An Integrative Approach*, CRC Press. pp

Evangelou, V. P. (1995). *Pyrite oxidation and its control*. Florida, CRC Press. pp

Evans, K. A. and Banwart, S. A. (2006). Rate controls on the chemical weathering of natural polymineralic material. I. Dissolution behaviour of polymineralic assemblages determined using batch and unsaturated column experiments. *Applied Geochemistry.* **21** (2) pp 352-76.

Evans, K. A., Watkins, D. C. and Banwart, S. A. (2006). Rate controls on the chemical weathering of natural polymineralic material. II. Rate-controlling mechanisms and mineral sources and sinks for element release from four UK mine sites, and implications for comparison of laboratory and field scale weathering studies. *Applied Geochemistry.* **21** (2) pp 377-403.

Fala, O., Molson, J., Aubertin*, M. and Bussière*, B. (2005). Numerical Modelling of Flow and Capillary Barrier Effects in Unsaturated Waste Rock Piles. *Mine Water and the Environment.* **24** (4) pp 172-85.

Fanfani, L., Zuddas, P. and Chessa, A. (1997). Heavy metals speciation analysis as a tool for studying mine tailings weathering. *Journal of Geochemical Exploration.* **58** (2-3) pp 241-8.

Fedotov, P. S., Fitz, W. J., Wennrich, R., Morgenstern, P. and Wenzel, W. W. (2005). Fractionation of arsenic in soil and sludge samples: continuous-flow extraction using rotating coiled columns versus batch sequential extraction. *Analytica Chimica Acta.* **538** (1-2) pp 93-8.

Gao, Y., Leermakers, M., Elskens, M., Billon, G., Ouddane, B., Fischer, J. C. and Baeyens, W. (2007). High resolution profiles of thallium, manganese and iron assessed by DET and DGT techniques in riverine sediment pore waters. *Science of the Total Environment.* **373** (2-3) pp 526-33.

Gao, Y., Leermakers, M., Gabelle, C., Divis, P., Billon, G., Ouddane, B., Fischer, J. C., Wartel, M. and Baeyens, W. (2006). High-resolution profiles of trace metals in the pore waters of riverine sediment assessed by DET and DGT. *Science of the Total Environment.* **362** (1-3) pp 266-77.

Gast, R. G. (1977). Surface and Colloid Chemistry. *Minerals in Soil Environments.* D. J. B and W. S. B. Madison, WI, American Society of Agronomy. pp 27.

Gerke, H. H., Molson, J. W. and Frind, E. O. (2001). Modelling the impact of physical and chemical heterogeneity on solute leaching in pyritic overburden mine spoils. *Ecological Engineering.* **17** (2-3) pp 91-101.

Gibert, O., de Pablo, J., Luis Cortina, J. and Ayora, C. (2004). Chemical characterisation of natural organic substrates for biological mitigation of acid mine drainage. *Water Research.* **38** (19) pp 4186-96.

Hartley, W., Edwards, R. and Lepp, N. W. (2004). Arsenic and heavy metal mobility in iron oxide-amended contaminated soils as evaluated by short- and long-term leaching tests. *Environmental Pollution.* **131** (3) pp 495-504.

Honeychurch, K. C. and Hart, J. P. (2003). Screen-printed electrochemical sensors for monitoring metal pollutants. *TrAC Trends in Analytical Chemistry.* **22** (7) pp 456-69.

Klinck, B. A., Palumbo, B., Cave, M. and Wragg, J. (2005). *Arsenic dispersal and bioaccessibility in mine contaminated soils: a case study from an abandoned arsenic mine in Devon, UK*.Research Report RR/04/003   British Geological Survey pp 52.

Kohfahl, C., Graupner, T., Fetzer, C. and Pekdeger, A. (2010). The impact of cemented layers and hardpans on oxygen diffusivity in mining waste heaps A field study

of the Halsbrücke lead-zinc mine tailings (Germany). *Science of the Total Environment.* **408** (23) pp 5932-9.

Kosmulski, M. (2011). The pH-dependent surface charging and points of zero charge: V. Update. *Journal of Colloid and Interface Science.* **353** (1) pp 1-15.

Kuo, S. and Baker, A. S. (1980). Sorption of copper, zinc and cadmium in some acid soils. *American Soil Science Society Journal.* **44** pp 969.

Lee, J. S. and Chon, H. T. (2006). Hydrogeochemical characteristics of acid mine drainage in the vicinity of an abandoned mine, Daduk Creek, Korea. *Journal of Geochemical Exploration.* **88** (1-3) pp 37-40.

Lefebvre, R., Hockley, D., Smolensky, J. and Lamontagne, A. (2001). Multiphase transfer processes in waste rock piles producing acid mine drainage: 2. Applications of numerical simulation. *Journal of Contaminant Hydrology.* **52** (1-4) pp 165-86.

Lollar, B. S., Ed. (2005). *Environmental Geochemistry*. Oxford, Elsevier.

Michel, K., Roose, M. and Ludwig, B. (2007). Comparison of different approaches for modelling heavy metal transport in acidic soils. *Geoderma.* **140** (1-2) pp 207-14.

Mighanetara, K. (2009) *Impact of Metal Mining on the Water Quality of the Tamar Catchment* PhD Thesis Thesis.University of Plymouth.pp248

Mills, G. A., Holmes, J. and Cornelius, E. B. (1950). The Acid Activation of Some Bentonite Clays. *The Journal of Physical and Colloid Chemistry.* **54** (8) pp 1170-85.

Miro, M., Hansen, E. H., Chomchoei, R. and Frenzel, W. (2005). Dynamic flow-through approaches for metal fractionation in environmentally relevant solid samples. *TrAC Trends in Analytical Chemistry.* **24** (8) pp 759-71.

Moncur, M. C., Jambor, J. L., Ptacek, C. J. and Blowes, D. W. (2009). Mine drainage from the weathering of sulfide minerals and magnetite. *Applied Geochemistry.* **24** (12) pp 2362-73.

Moral, R., Gilkes, R. J. and Moreno-Caselles, J. (2002). A comparison of extractants for heavy metals in contaminated soils from Spain. *Communications in Soil Science and Plant Analysis.* **33** (15-18) pp 2781-91.

Moreno-Jiménez, E., Peñalosa, J. M., Manzano, R., Carpena-Ruiz, R. O., Gamarra, R. and Esteban, E. (2009). Heavy metals distribution in soils surrounding an abandoned mine in NW Madrid (Spain) and their transference to wild flora. *Journal of Hazardous Materials.* **162** (2-3) pp 854-9.

Mudroch, A. and Azcue, J. M. (1997). *Manual of physio-chemical analysis of aquatic sediments*, CRC Press.pp 287 pp

Mular, A. L., Halbe, D. H. and Barratt, D. J., Eds. (2002). *Mineral Processing Plant Design, Practice, and Control.* Littleton, Colorado, Society for Mining, Metallurgy, and Exploration, Inc (SME).

Nordstrom, D. K. (1982). The effect of sulfate on aluminum concentrations in natural waters: some stability relations in the system Al2O3-SO3-H2O at 298 K. *Geochimica Et Cosmochimica Acta.* **46** (4) pp 681-92.

Oubagaranadin, J. U. K., Murthy, Z. V. P. and Mallapur, V. P. (2010). Removal of Cu(II) and Zn(II) from industrial wastewater by acid-activated montmorillonite-illite type of clay. *Comptes Rendus Chimie.* **13** (11) pp 1359-63.

Pagnanelli, F., Moscardini, E., Giuliano, V. and Toro, L. (2004). Sequential extraction of heavy metals in river sediments of an abandoned pyrite mining area: pollution detection and affinity series. *Environmental Pollution.* **132** (2) pp 189-201.

Palumbo-Roe, B., Klinck, B., Banks, V. and Quigley, S. (2009). Prediction of the long-term performance of abandoned lead zinc mine tailings in a Welsh catchment. *Journal of Geochemical Exploration.* **100** (2-3) pp 169-81.

Peijnenburg, W., Zablotskaja, M. and Vijver, M. G. (2007). Monitoring metals in terrestrial environments within a bioavailability framework and a focus on soil extraction. *Ecotoxicology and Environmental Safety.* **67** (2) pp 163-79.

Pendray, S. (2009). Senior Geology Technician, Camborne School of Mines, University of Exeter. To A. Turner.

Poisson, J., Chouteau, M., Aubertin, M. and Campos, D. (2009). Geophysical experiments to image the shallow internal structure and the moisture distribution of a mine waste rock pile. *Journal of Applied Geophysics.* **67** (2) pp 179-92.

Potter, H. A. B. (2008). ANNEX I to Directive 2000/60/EC: Environmental Quality Standards for Priority Substances and Certain other pollutants. . A. Turner.

Pueyo, M., Mateu, J., Rigol, A., Vidal, M., Lopez-Sanchez, J. F. and Rauret, G. (2008). Use of the modified BCR three-step sequential extraction procedure for the study of trace element dynamics in contaminated soils. *Environmental Pollution.* **152** (2) pp 330-41.

Pueyo, M., Rauret, G., Luck, D., Yli-Halla, M., Muntau, H., Quevauviller, P. and Lopez-Sanchez, J. F. (2001). Certification of the extractable contents of Cd, Cr, Cu, Ni, Pb and Zn in a freshwater sediment following collaboratively tested and optimised three-step sequential extraction proceedure. *Journal of Environmental Monitoring.* **3** pp 243-50.

Pulford, I. D., MacKenzie, A. B., Donatello, S. and Hastings, L. (2009). Source term characterisation using concentration trends and geochemical associations of Pb and Zn in river sediments in the vicinity of a disused mine site: Implications for contaminant metal dispersion processes. *Environmental Pollution.* **157** (5) pp 1649-56.

Rauret, G., Lopez-Sanchez, J. F., Sahuquillo, A., Rubio, R., Davidson, C., Ure, A. and Quevauviller, P. (1999). Improvement of the BCR three step sequential extraction procedure prior to the certification of new sediment and soil reference materials
Journal of Environmental Monitoring. **1** pp 57-61.

Rauret, G. and Rubio, R. (1997). Sources of error in speciation analysis. *Quimica Analitica.* **16** pp 119-30.

Roussel, C., Neel, C. and Bril, H. (2000). Minerals controlling arsenic and lead solubility in an abandoned gold mine tailings. *The Science of The Total Environment.* **263** (1-3) pp 209-19.

Shaw, S., Wels, C., Robertson, A. and Lorinezi, G. (2002). *Physical and Geochemical Characterisation of Mine Rock Piles at the Questa mine, New Mexico; An Overview.* Proceedings of the Proceedings of the Ninth International Conference on Tailings and Mine Waste, Fort Collins, Colorado, Taylor & Francis.

Sherwood, J. E., Barnett, D., Barnett, N. W., Dover, K., Howitt, J., Kew, P. and Mondon, J. (2009). Deployment of DGT Units in Marine Waters to Assess the Environmental Risk from a Deep Sea Tailings Outfall. *Analytica Chimica Acta.* **562** (1-2) pp.

Slowey, A. J., Johnson, S. B., Newville, M. and Brown Jr, G. E. (2007). Speciation and colloid transport of arsenic from mine tailings. *Applied Geochemistry.* **22** (9) pp 1884-98.

Smedley, P. L. and Kinniburgh, D. G. (2002). A review of the source, behaviour and distribution of arsenic in natural waters. *Applied Geochemistry.* **17** (5) pp 517-68.

Søndergaard, J., Elberling, B. and Asmund, G. (2008). Metal speciation and bioavailability in acid mine drainage from a high Arctic coal mine waste rock

pile: Temporal variations assessed through high-resolution water sampling, geochemical modelling and DGT. *Cold Regions Science and Technology.* **54** (2) pp 89-96.

Song, Q. and Yanful, E. K. (2011). Oxygen influx and geochemistry of percolate water from reactive mine waste rock underlying a sloping channelled soil cover. *Applied Geochemistry.* **26** (5) pp 655-65.

Sracek, O., Choquette, M., Gélinas, P., Lefebvre, R. and Nicholson, R. V. (2004). Geochemical characterization of acid mine drainage from a waste rock pile, Mine Doyon, Québec, Canada. *Journal of Contaminant Hydrology.* **69** (1-2) pp 45-71.

Stumm, W. and Morgan, J. J. (1996). Aquatic Chemistry. New York, Wiley & Sons. pp 885-7.

Sukreeyapongse, O., Holm, P. E., Strobel, B. W., Panichsakpatana, S., Magid, J. and Hansen, H. C. B. (2002). pH-Dependent Release of Cadmium, Copper, and Lead from Natural and Sludge-Amended Soils. *J Environ Qual.* **31** (6) pp 1901-9.

Taylor, G. and Eggleton, R. A., Eds. (2001). *Regolith Geology and Geomorphology.* Chichester, John Wiley & Sons.

Tessier, A., Campbell, P. G. C. and Bisson, M. (1979). SEQUENTIAL EXTRACTION PROCEDURE FOR THE SPECIATION OF PARTICULATE TRACE-METALS. *Analytical Chemistry.* **51** (7) pp 844-51.

van der Sloot, H. A., Meeussen, J. C. L., van Zomeren, A. and Kosson, D. S. (2006). Developments in the characterisation of waste materials for environmental impact assessment purposes. *Journal of Geochemical Exploration.* **88** (1-3) pp 72-6.

Warren, G. P., Alloway, B. J., Lepp, N. W., Singh, B., Bochereau, F. J. M. and Penny, C. (2003). Field trials to assess the uptake of arsenic by vegetables from contaminated soils and soil remediation with iron oxides. *The Science of The Total Environment.* **311** (1-3) pp 19-33.

Yapici, T., Fasfous, I. I., Murimboh, J. and Chakrabarti, C. L. (2008). Investigation of DGT as a metal speciation technique for municipal wastes and aqueous mine effluents. *Analytica Chimica Acta.* **622** (1-2) pp 70-6.

Zhang, H. (2003). DGT - for measurements in waters, soils and sediments. Avalible online at: http://www.dgtresearch.com/dgtresearch/dgtresearch.pdf. Accessed 01/08/2011.

Zhang, H., Davison, W., Miller, S. and Tych, W. (1995). IN-SITU HIGH-RESOLUTION MEASUREMENTS OF FLUXES OF NI, CU, FE, AND MN AND CONCENTRATIONS OF ZN AND CD IN POREWATERS BY DGT. *Geochimica Et Cosmochimica Acta.* **59** (20) pp 4181-92.

5.10   Chapter 5 Appendices

A. Sample Descriptions

Site	Sample	Sample Depth (cm)	Description	% by weight, < 4mm	% Contribution by weight to composite sample (< 4mm fraction)
Devon Great Consols Wheal Anna Maria Tip (WAM)	DGC1	10-50	Orange/brown very coarse SAND locally consolidated. *Hard pan* encountered at ~50cm. Well sorted. Occasional areas of CLAY on surface with patches of grass. Elsewhere, no vegetation.	92	100
	DGC2				
	DGC3				
	DGC4				
Devon Great Consols Cinders Waste Tip (CIND)	CIND1	10-50	Dark brown GRANULES with frequent small pebbles of angular dark brown platy minerals (possibly slate). Poorly sorted. No vegetation.	69	31
	CIND2		Dark brown medium SAND. Well sorted. No vegetation.	71	36
	CIND3		Red and reddish-brown coarse SAND with occasional orange, yellow and red efflorescent salts. Moderately sorted. No vegetation.	69	12
	CIND4		Brown medium SAND with occasional red SAND and occasional yellow and orange efflorescent salts. Moderately sorted. Occasional grass roots.	81	21

Site	Sample	Sample Depth (cm)	Description	% by weight, < 4mm	% Contribution by weight to composite sample (< 4mm fraction)
Wheal Betsy North Tips (WBN)	WBN1	10-50	Very poorly sorted orange/ brown coarse SAND (60%) with frequent small and large cobbles comprising hardpan[1] and gangue minerals including quartz, veined shale/slate, quartz. Surface stained with iron oxyhydroxide. Actively eroding tip face. No Vegetation.	42	25
	WBN2	10- 50	Very poorly sorted brown medium SAND (80%) with frequent large angular pebbles of hard pan and gangue minerals including quartz veined shale/shillit, slate, and quartz. Surface stained with iron oxyhydroxide. Actively eroding tip face, No vegetation.	55	28
	WBN3	10- 50	Medium brown granules and very coarse sand (80%) with frequent (20%) small and medium angular pebbles of gangue minerals including hard pan and quartz veined shale/slate and slate and iron oxyhydroxide. Actively eroding tip face. No Vegetation.	26	12
	WBN4	10- 50	Moderately sorted light brown coarse SAND (60%) with frequent small to medium angular pebbles of gangue material comprising slate/shale. Actively eroding tip face. No Vegetation.	30	14
	WBN5	10- 50	Very poorly sorted light brown coarse (30%) and medium (30%) SAND with occasional grey and light brown angular large pebbles (20%) and occasional large cobbles (5%) and boulders (5%). Actively eroding tip face. No Vegetation.	42	22

Site	Sample	Sample Depth (cm)	Description	% by weight, < 4mm	% Contribution by weight to composite sample (< 4mm fraction)
Wheal Betsy South Tips	WBS1	10-40	Orange/brown medium coarse SAND. Loosely consolidated with some consolidated outcrops above the surface. Occasional small pebbles and cobbles of quartz hosted mineralised rock. Some discrete zones of light brown clayey medium SAND. Tip eroding. Vegetated with heather, gorse and grasses.	73	21
	WBS2	10-40	Brown fine to medium SAND with very occasional platy cobbles of gangue minerals (slate) and very occasional small pebbles of slate. Consolidated at 20-30 cm depth.	61	18
	WBS4	10-20	Yellow fine and medium SAND with occasional large angular pebbles (5%) and angular cobbles (5%). Weathered surface extends to 5-10cm. Eroding bank of tip. Vegetated with heather and gorse.	44	16
	WBS5	30-40	Consolidated orange/yellow medium SAND with occasional (2%) large angular pebbles and small angular cobbles of hardpan occurring in discreet pockets. Weathered to 5cm depth. Mid tip plateau appears stable. No vegetation.	65	21
	WBS7	10-20	Grey coarse SAND with frequent small angular platy pebbles of slate/shale. Actively eroding steep slope. No vegetation.	34	12
	WBS8	15-30	Grey/brown coarse SAND with frequent small pebbles of gangue minerals including shale and quartz. Loose at weathered surface becoming consolidated beyond 5cm depth.	43	14

B. Cumulative Loads and Relative Acid Extractable Contents for Selected Elements.

Table 5.10: Cumulative dissolved loads and acid extractable content for selected elements from mine waste samples.

Sample	Element	Cumulative extracted load from column (mean, µmol kg^{-1})	Acid Extractable Total (AAT), from aqua regia (mean, mmol kg^{-1})	Acid Extractable Content in aqua regia (% by weight)	Proportion of AAT leached in column experiment (%)	Number of column cycles required to exhaust supply	Order of resilience to oxic weathering (high to low)
WAM	Fe	5.88	1530	8.5	3.84×10^{-4}	3.98×10^8	1
	Al*	1350	421	1.1	3.21×10^{-1}	3.12×10^2	2
	Cu	781	38.5	0.24	2.03	4.93×10^1	5
	Zn	28.7	0.572	0.0037	5.02	1.99×10^1	7
	Mn	98.4	7.31	0.040	1.35	7.43×10^1	4
	Ni	0.654	0.0234	0.00014	2.84	3.52×10^1	6
	Cd	0.0145	<LOD	<LOD	-	-	(low)
	Pb	<LOD	0.354	0.0073	-	-	(high)
	As	1.65	272	2.0	2.55×10^{-3}	3.92×10^4	3
	Sb	-	0.172	0.0021	-	-	-
	V	-	0.368	-	-	-	-
	Sn	-	2.42	0.029	-	-	-
	W	-	0.456	0.0084	-	-	-
CIND	Fe	0.0700	3354	18.7	2.09×10^{-6}	4.79×10^7	1
	Al	8330*	691	1.9	1.21	8.30×10^1	7
	Cu	156	50.8	0.32	3.07×10^{-1}	3.25×10^2	5
	Zn	55.2	7.93	0.052	6.96×10^{-1}	1.44×10^2	6
	Mn	49.0	16.3	0.090	3.01×10^{-1}	3.33×10^2	4
	Ni	4.08	0.0934	0.00055	4.37	2.29×10^1	8
	Cd	0.0760	0.0261	0.00029	2.91×10^{-1}	3.43×10^2	3
	Pb	<LOD	1.69	0.035	-	-	(high)
	As	291	383	2.9	7.60×10^{-2}	1.32×10^3	2
	Sb	-	1.22	0.015	-	-	-
	V	-	0.706	-	-	-	-
	Sn	-	7.25	0.086	-	-	-
	W	-	1.28	0.023	-	-	-

Chapter 5

Sample	Element	Cumulative extracted load from column (mean, μmol kg^{-1})	Acid Extractable Total (AAT), from aqua regia (mean, mmol kg^{-1})	Acid Extractable Content in aqua regia (% by weight)	Proportion of AAT leached in column experiment (%)	Number of column cycles required to exhaust supply	Order of resilience to oxic weathering (high to low)
WBN	Fe	35.2	1743	9.7	2.01×10^{-3}	4.95×10^{4}	1
	Al*	484	197	0.52	2.46×10^{-1}	4.07×10^{2}	2
	Cu	74.6	13.1	0.083	5.69×10^{-1}	1.76×10^{2}	4
	Zn	518	16.6	0.11	3.12	3.20×10^{1}	7
	Mn	114	5.23	0.029	2.18	4.59×10^{1}	5
	Ni	0.311	0.0106	0.00018	2.93	3.41×10^{1}	6
	Cd	1.95	0.0408	0.00046	4.78	2.09×10^{1}	8
	Pb	363	126	2.6	2.88×10^{-1}	3.47×10^{2}	3
	As	<LOD	66.4	0.50	-	-	(high)
	Sb	-	1.28	0.016	-	-	-
	V	-	0.157	0.00080	-	-	-
	Sn	-	<LOD	-	-	-	-
	W	-	<LOD	-	-	-	-
WBS	Fe	0.878	1280	7.2	6.86×10^{-5}	1.46×10^{6}	1
	Al*	181	143	0.39	1.26×10^{-1}	7.90×10^{2}	3
	Cu	4.12	27.0	0.17	1.53×10^{-2}	6.55×10^{3}	2
	Zn	59.1	22.4	0.15	2.64×10^{-1}	3.79×10^{2}	5
	Mn	1.89	1.35	0.0074	1.40×10^{-1}	7.14×10^{2}	4
	Ni	0.132	0.0203	0.00012	6.50×10^{-1}	1.54×10^{2}	7
	Cd	0.866	0.0197	0.00022	4.40	2.27×10^{1}	8
	Pb	730	224	6.1	3.26×10^{-1}	3.07×10^{2}	6
	As	<LOD	104	0.78	-	-	(high)
	Sb	-	2.52	0.031	-	-	-
	V	-	0.172	0.00088	-	-	-
	Sn	-	0.41	0.0049	-	-	-
	W	-	<LOD	-	-	-	-

-End of Chapter 5-

Chapter 6

Final Conclusions and

Recommendations

6 Final Conclusions and Recommendations

6.1 Prioritisation of Mine Waste Tips and Their Effect on Water Quality

The GIS exercise in Chapter 2 provided a priority list of the mine sites in the Tamar Catchment that pose the most risk to watercourse quality based on physical and environmental factors. A simplified version of this model has since been used by the Environment Agency to prioritise sites in five catchments in south west England. The methodology has the potential for wider application as it meets most of the requirements of Article 20 of the Mining Waste Directive (2001/21/EC), which states guidelines for pre-selection of potentially harmful abandoned mine sites.

The priority list for the Tamar catchment placed streamed workings located on Dartmoor and the mine waste tips at Wheal Betsy, near Mary Tavy, highest. Waste at streamed workings may present a low risk to watercourses due to the composition and age of the waste rock, and may be downgraded upon further investigation. A number of non-streamed abandoned mine sites within the Gunnislake and Mary Tavy region, were included in the "Extreme" risk category. These were the locations of the two study sites, Devon Great Consols (DGC) and Wheal Betsy, respectively. Waste at Wheal Betsy was in direct contact or in very close proximity to the watercourse receiving leachates and as a result displayed little attenuation potential. It's location on Dartmoor meant it received higher and more intense rainfall than other areas and the characteristics of the soil and local geology resulted in rapid transport of waters through the shallow subsurface. This was reflected in its high score in the prioritisation (4400/6000) and was confirmed by the elevated concentrations of metals recorded in Cholwell Brook and the reactivity of the overall contaminant flux to short-term rainfall patterns.

The studied tips at Devon Great Consols were located further from the receiving water course (River Tamar), allowing for greater natural attenuation of drainage waters

along the drainage pathway and resulting in a low score for proximity. Their location within the Tamar Valley was also relatively sheltered and therefore scored lower for rainfall, wind and sun exposure in the model. However, the large area of bare waste and soil found at the site and the low permeability of the underlying bedrock meant there was a high run-off potential and meant that the site still scored highly in the model (3468/6000 for precipitation launders and 3298/6000 for WAM and Cinders) and were also classified in the top category for risk.

Published information confirmed high levels of metal and arsenic contamination within the waste tips found at both sites. Furthermore, the location of Devon Great Consols was coincident with existing water quality data and EQS failures in the River Tamar for Cu, Zn and Cd a short distance downstream at Gunnislake (EA, 1997-2008).

Leachates were captured from the mine waste tips in repeated surveys during 2007-2009 and were found to be highly enriched in dissolved contaminant metals. The composition of leachates varied between tips according to the mineralogy of the waste. Cinders waste at DGC was particularly high in dissolved As ($\bar{x} = 294$ μmol L^{-1}) and Sb ($\bar{x} = 0.527$ μmol L^{-1}), while dissolved Cu was highest in DGC Wheal Anna Maria tip leachates ($\bar{x} = 224$ μmol L^{-1}), dissolved Al ($\bar{x} = 828$ μmol L^{-1}), Mn ($\bar{x} = 81.4$ μmol L^{-1}) and Ni ($\bar{x} = 2.72$ μmol L^{-1}) was highest in DGC precipitation launders and dissolved Zn ($\bar{x} = 20.9$ μmol L^{-1}) and Cd ($\bar{x} = 0.124$ μmol L^{-1}) was highest in shallow groundwaters flowing through the base of the Wheal Betsy (North) tips.

Reducing dissolved Al and Cu from the final collection drain (FCD) at DGC and dissolved Cd from Wheal Betsy should be the priority of regulators wishing to improve the ecological and chemical status of the receiving water courses (Cholwell Brook) and (River Tamar) based on this study. Dissolved concentrations of Al and Cu were very high upon entering the River Tamar from the FCD (618 μmol L^{-1} and 77.4 μmol L^{-1}, respectively). Based on the concentrations observed and conservative mixing of the

waters, dissolved Cu and Al will cause the River Tamar to consistently fail EQS values. In stream precipitation and sorption to stream sediments may reduce the dissolved concentration but precipitation of metals, particularly Al and Fe may still be harmful to aquatic life. For example conversion of dissolved Al to high molecular weight polymeric species can cause fish mortality, via clogging of the gills (Rosseland *et al.*, 1992; Klöppel *et al.*, 1997).

Other dissolved elements present in discharging waters from the drain including Zn, Cd, Mn and Ni are likely to be diluted below EQS values upon conservative mixing with river water but in combination with other known mine discharges could also result in regulatory failures. Removal of some or all of the dissolved metals in waters of the final collection drain is likely to significantly improve the ecological and chemical status of the River Tamar downstream of the discharge point. This could reduce the frequency and magnitude of regulatory failures. For example, based on 2005-2006 survey data at least 11 % of the dissolved copper in the River Tamar at Gunnislake may be attributed to the final collection drain (Mighanetara, 2009).

At Wheal Betsy, concentrations of dissolved Cd were <LOD (0.009 μmol L^{-1}) upstream of the site, but also increased with distance along Cholwell Brook, a tributary of the River Tavy, to a maximum of 0.018 μmol L^{-1} upon leaving the site. This is approximately 250 x the current EQS value. Dissolved Zn, Cu and Pb also accumulated through the site and were highly elevated with respect to EQS. Maxima of 3.9 μmol L^{-1} (Zn), 0.29 μmol L^{-1} (Cu) and 0.45 μmol L^{-1} (Pb) were recorded in the waters of Cholwell Brook, representing 55 x, 18 x and 12 x current long term EQS values for low alkalinity waters, respectively.

6.2 Characteristics of Tip Drainage and Tip Waste Mineralogy

Generally tip drainage was characterised by oxic waters, marking them apart from underground workings where reducing conditions often prevail. High

concentrations of dissolved Fe and As are often observed in adit discharges, but unusually in this study As concentrations were highest in the oxic drainage from the cinders waste tips, resulting in an estimated mean annual flux of 32000 mol y^{-1}. This was an order of magnitude higher than the predicted flux from the main adit discharge at the mine based on results from a previous study (Blanchdown Adit, 2570 mol y^{-1}).

Dissolved metal fluxes from mine wastes tips were estimates to exceed or be similar in magnitude to point discharges from adits. For example at Devon Great Consols, the predicted annual flux of dissolved metals from the final collection drain (FCD), which is thought to collect most of the tip drainage at the site, was compared with that from Blanchdown Adit and was found to be the same order of magnitude for Zn, Cd, Ni and Mn. Furthermore, dissolved Cu flux was much higher in the FCD (4660-75200 mol y^{-1}) than in the Blanchdown Adit discharge (999-5230 mol y^{-1}, Table 3.12).

The composition of mine waste varied between tips, but primary sulphide minerals (e.g. galena, chalcopyrite, and sphalerite) make up only a very small fraction (< 5%) of the total mineral assemblage from the surface of the tip (50 cm). Cu, As, Pb, Zn and Mn were associated with Fe-hydroxides (WAM, CIND) and Fe-As-Pb-S-O (WBN, WBS) secondary phases which were ubiquitous in most wastes, but appeared to be scarcer in wastes resulting from high temperature processing (furnace ash and cinders). The composite sample of waste removed from the south tips at Wheal Betsy (WBS) had a higher fraction of silts and clays (24.7 % < 63 μm) than other samples. Sorption to clay minerals was an important retention mechanism for contaminants, particularly Pb wastes from Wheal Betsy. The high fine fraction in WBS material also reduced permeability of the waste in the field, leading to a reduced flux of contamination from WBS waste tips compared with the more permeable north tips.

The textures and relative abundance of metal sulphide minerals suggests a higher proportion of arsenopyrite remains in all wastes. This may be a consequence of

mine closure before economic recovery of As-phases was completed. It could also indicate preferential weathering of other metal sulphides. Arsenopyrite appears less weathered than chalcopyrite, sphalerite and galena when the phases coexist in waste. This may be a consequence of galvanic armouring of arsenopyrite resulting in a higher resistance to dissolution. Galvanic effects have been shown to increase the dissolution of galena, sphalerite and chalcopyrite in a two phase system with pyrite (Abraitis *et al.*, 2004).

When ordered from highest to lowest, there was a strong relationship between total content and the released load indicating fractional release from the waste for Cu, Mn, Zn, Cd, Ni and Al, Table 5.9). However, this relationship broke down when the concentration of the metal of interest is low in the leachate, typically < 5 μmol L^{-1}. There was evidence to suggest that a selective adsorption of some metals retards mobility while increasing the mobility of others. This would account for the non-fractional behaviour observable at low concentrations. For example, the affinity of dissolved Cu was reduced for the WBS solid, in the presence of high concentrations of dissolved Pb.

6.3   Natural Attenuation Processes

Tip drainage from the cinders and WAM tips at DGC migrated approximately 400 m before reaching the River Tamar via a combination of surface drains and shallow groundwater transport. Dissolved concentrations and estimated annual fluxes of dissolved As entering the River Tamar via the final collection drain (0.226 μmol L^{-1} and 164 mol y^{-1}, respectively), were found to be much lower than cinders drain (294 μmol L^{-1} and 32000 mol y^{-1}, respectively). During transport, the waters from the individual tips at DGC became mixed, and waters emerging in the FCD were exposed to atmospheric oxygen (DO, $\bar{x} = 10.2$ mg L^{-1}) leading to the precipitation of $Fe(OH)_3$

phases. Sorption of dissolved anionic As species to these freshly precipitated mineral surfaces at low pH ($\bar{x}$ = pH 4.2, FCD) was predicted to be the major mechanism for natural attenuation of the metalloid. This retention effect was also observed within the WAM, WBN and WBS waste tip material itself. When examined under SEM/EDX, surface coatings on grains of waste were found to comprise As-rich Fe-hydroxy (WAM) and As- and Pb-rich Fe-hydroxysulphate phases. Attenuation of other dissolved metals, most notably Cu was also indicated by both field and SEM investigations. The composition of the waters in the final collection drain at DGC were therefore controlled by interaction with mineral surfaces and observed to be relatively stable between all surveys with respect to pH, Eh, DO and dissolved metals (Cu, Al, Zn, Mn, Ni, Cd all < 12.1 % RSD).

No such attenuation was observed at Wheal Betsy in migrating waters along a much shorter pathway (< 10 m) from source to the receiving watercourse, Cholwell Brook. This was good supporting evidence to suggest that proximity of the waste (weighted highly in the prioritisation model, Chapter 2), was a very important factor for determining the environmental impact of mine waste leachates to the receiving watercourse.

Sorption of dissolved metals, predicted to be in the dissolved cationic state (PHREEQC), occurred at low pH (min pH 2.3) even though the point of zero charge (PZC) for most of the minerals identified in the waste were much higher. Under these conditions, protonation of the mineral surfaces is favoured and the bond-strength of the cation to the mineral surface is low, increasing with increasing pH. At higher pH, higher retention of cationic species, such as dissolved Cu, was observed but was concurrent with lower retention of anionic As species. This explained why the cinders waste (CIND, Chapter 5) had the highest total extractable Cu content (50.8 mmol kg^{-1}), but released less into leachates with higher pH (pH 4.0-4.5, measured *in situ*) than the

WAM tip material (Cu content of 38.5 mmol kg^{-1}) with lower pH (pH 2.4-3.0, measured *in situ*). Conversely, all the waste materials studied had a comparable acid extractable As content (66.4-383 mmol kg^{-1}, Table 5.10), but only the cinders waste material released high concentrations of dissolved As. In all other leachates from WAM, WBN and WBS waste tips, in field and upflow column experiments, dissolved As was < 1.1 μmol L^{-1}, just above the freshwater EQS of 0.67 μmol L^{-1}.

6.4   The Application of Laboratory Leaching Experiments to Studies of Mine Waste

Dynamic up-flow percolation (column) experiments provided a good proxy for generating mine waste leachates under environmentally applicable conditions of high O$_2$ ingress and dynamic fluid flow. Despite the limited sample size, the dissolved concentrations of metals and As in column leachate fractions are largely consistent with the ranges observed in the field. Deviations occur because pH in the field is generally higher as a result of dilution with 'cleaner' drainage waters. Because tip drainage is largely oxic, pH appears to be the dominant control on metal and As mobility from mine wastes. A small change in pH can have a remarkable effect on the mobility of elements associated with clays and secondary Fe-hydroxy and Fe-hydroxsulphate phases. This was observed particularly for Pb, where a reduction in pH from field (pH 3.2-6.1) to laboratory conditions (pH 1.9-2.6) resulted in release of leachates with dissolved Pb up to a maximum of 81.2 μmol L^{-1}.

Field concentrations in waters issuing immediately from the mine wastes were dependent on the hydrological saturation state of the tip. The proportion of saturated tip waste depends on the height of the water table with a higher water table resulting in increased flux from the tips. Concentrations determined instantaneously following rainfall are also dependent on the state of the tip with respect to the 'first flush'. Based

on the column experiments, for most elements (Al, Cu, Zn, Mn, Cd, Ni) the difference between the saturated condition (i.e. chemical equilibrium between solid and liquid phase) and the dynamic equilibrium position is an order of magnitude (10x). The difference is also likely to be affected by flow rate. Faster flow rates result in a lower dynamic concentration. Column flow probably represents the upper end of this range due to enhanced compaction of the waste in the field.

Batch leaching experiments were a rapid means of assessing the leaching potential of mine waste. Equilibrium induced suppression of dissolution can underestimate the mobility of some elements compared to a dynamic system. Conversely, aggressive shaking can artificially enhance Fe and Al mobility by suspending fine particulate matter. Mobility of these elements is important in the suspended load because as Fe-oxides and clays both have capacity to transport other contaminant metals and arsenic as sorbed species in waters. Cationic exchange on clay minerals can be as important to Fe-oxide association in wastes with a high fine fraction. It is important to recognise the difference between true dissolved Fe and Al and the operationally defined dissolved fraction when interpreting elemental mobility.

Ionic strength and pH both exert control on the solubility of mine waste minerals. High ionic strength suppressed the concentration of dissolved elements, while pH dictates the affinity for the dissolved ions with the available mineral surfaces. Batch experiments using different chemical extractants showed that extractions did not necessarily target their intended fraction, e.g. acetic acid underestimated the amount of exchangeable Pb from Wheal Betsy wastes. pH was also generally higher in the batch experiments with MilliQ compared to column experiments. This was probably because the extractants can enforce a pH amendment on the waste, particularly with high L:S ratios. In tip porewaters L:S ratios are much lower and the system is dominated by the character of the solid phase.

Column experiments are a useful tool to elucidate the relative affinity of dissolved contaminants for the solid matrix. They also provide useful data for saturated concentrations likely to arise from 'first flush' events. However, they are labour intensive and still rely on the sample material being representative of that in the field. The results for the column experiments were highly reproducible which suggests they may be scaled down so that smaller amounts of material are required and experiments can reach completion (L:S>10) more quickly. Efficiency could also be improved by incorporating an automated method of sampling. Such method improvements would facilitate a higher throughput of samples. The degree to which the test may be scaled down, without compromising reproducibility, is a function of the particle size distribution of the mineral grains with coarser waste requiring a larger sample size.

Using a low ionic strength extractant (e.g. MilliQ) in batch experiments at a range of L:S ratios, preferably including L:S < 2:1 is still a useful tool to gauge the potential of a waste material to leach dissolved metals under oxic conditions. The use of extractants to target particular phases provides additional information on the behaviour of the samples with respect to changes in pH and ionic strength. However the results from phase-targeted extractions cannot be applied directly to the field to predict contaminant mobility because they do not replicate realistic field conditions.

6.5   Suitable Management Strategies

The findings from the studies of mine waste leaching behaviour and transport was consistent with the judgements applied to the prioritisation exercise in Chapter 2. Therefore the priority list offers a suitable starting point for further investigation in targeting high scoring waste tips in the Tamar catchment.

Enhancement of natural attenuation probably offers the most practicable and cost effective management option for metalliferous waste tips. In reactive catchments

with tips close to surface watercourses, stabilisation and reduction of tip permeability may offer the best solution to reducing fluxes. Disturbance of tip material is likely to result in an acute pollution event from suspension of particulate matter into stream waters. This was witnessed in the field and in the laboratory experiments where vigorous shaking of waste material enhanced the suspended load of fine particulates. The particulates are likely to contain Fe-oxides and clays which are important sorbents of ecotoxic metals. Transport of such particulate matter may cause the subsequent release of co-precipitated and adsorbed contaminant metals into waters.

Low permeability tips contribute less metal flux even if the metal content is high, because of the inhibited transport of percolating waters. Permeable coarse wastes contribute highly to overall fluxes and should be prioritised in mine water remediation schemes.

When mine waste is located far from a receiving watercourse the dividing area acts as a buffer, effectively filtering suspended solids and dissolved metal(loids) from discharge waters. For the buffer to work effectively, waters must remain oxic as development of reducing conditions will cause some secondary Fe-oxide phases to dissolved and release associated metals. This is particularly important in the case of As where speciation is dependent on redox condition and mobility of the reduced species (As(III)) is greater than As(V). Waters which discharge from underground workings or waters which migrate slowly in the subsurface tend to be rich in dissolved Fe due to isolation from the atmosphere. A rapid but tortuous pathway and an introduced source of dissolved Fe, perhaps from a nearby adit discharge are likely to enhance natural attenuation.

Although competitive sorption effects are small in magnitude compared to overall concentrations. They may prove to be an important consideration when implementing remedial measures. Sorption of one metal may cause the preferential

release of another with lower binding energy to mineral surfaces. For example Pb was highly abundant in the waste from Wheal Betsy but remained largely immobile under field conditions, but lower pH in laboratory experiments triggered release. Cu and Pb compete for binding sites on Fe-oxides (Baker, 1980), so in the presence of dissolved Pb, the natural attenuation of Cu is suppressed. Potentially, a release of dissolved Pb may be short lived in the environment but could result in a spike of the more mobile metal, here Cu, in downstream waters. pH exerted a very strong control on the mobility of all the studied elements. This was shown by differences in laboratory test results compared to field drainage. Higher mobility was observed for all cationic species as pH decreased, while anionic As was more mobile at higher pH.

Amendments applied to the waste or discharge waters must be carefully considered if they adjust the pH of the solid solution interface. At Devon Great Consols, the cinders tips had the largest copper content but the WAM tips release more dissolved Cu. This was attributed to the higher intrinsic buffering of the cinders waste which produces a higher pH in the waste porewaters (pH 4.0-4.5), compared to WAM waste (pH 2.4-3.7). In the cinders waste, As is released in very high concentrations in the field (294 μmol L^{-1}) where pH is highest (pH 5.0-5.4). In the laboratory experiments the pH of the cinders waste was lower and maximum As release was 10 x lower than observed in the field. Higher pH increases the cationic sorption capacity of the waste. Amending WAM tip waste with lime solution ($CaCO_3$ for example), may raise the pH and increase the retention of dissolved Cu to the solid phase. But the low pH is beneficial for the retention of anionic As species and therefore raising the pH could trigger release of As instead. Conversely reduced pH in the cinders waste would reduce the As flux but could result in a higher flux of Cu than currently observed from the WAM waste. Circumstances which could result in reduced pH might be the disturbance of the tip and inundation of O_2 to oxidise unweathered pyrites within the waste.

Overall, the waste tips at abandoned mines in the Tamar catchment have been shown to be major contributors to the pollutant flux of metals and metalloid entering watercourses. They are small by international standards, but contain high concentrations of metals and arsenic and are often in close proximity to watercourses subject to water quality regulations under the Water Framework Directive (2000/60/EC).

Management strategies should be implemented to reduce unauthorised use of the tips, to reduce human exposure to potentially harmful elements within the waste and to reduce the erosion of the tips. Measures could be taken to enhance the stability of the tips, thereby reducing the suspended load of contamination entering streams and reduce the exposure of fresh mineral surface to weathering.

The least invasive treatment would be to encourage natural accession of vegetation from bryophytes (nutrients from air, resistant to toxicity of waste) to nitrogen fixers (gorse and heather) to grasses and shrubs. Vegetation of the tips would increase stability, and reduce water movement and inhibit O_2 ingress, all favourable for the reduction of pollutant flux leaving the tips. Destructive or invasive measures should be avoided because disturbance of the tip material could increase the flux of metal and / or As contamination and would destroy the unique ecological and historical importance of the sites.

6.6   References

Abraitis, P. K., Pattrick, R. A. D., Kelsall, G. H. and Vaughan, D. J. (2004). Acid Leaching and dissolution of major sulphide ore minerals: processes and galvanic effects in complex systems. *Mineralogical Magazine.* **68** (2) pp343-51.

Baker, R. A., Ed. (1980). *Contaminants and Sediments Volume 2 Analysis, Chemistry Biology.* Ann Arbor, Michigan, Ann Arbor Science.

Klöppel, H., Fliedner, A. and Kördel, W. (1997). Behaviour and ecotoxicology of aluminium in soil and water - Review of the scientific literature. *Chemosphere.* **35** (1-2) pp353-63.

Mighanetara, K. (2009) *Impact of Metal Mining on the Water Quality of the Tamar Catchment* PhD Thesis Thesis.University of Plymouth.pp248

Rosseland, B. O., Blakar, I. A., Bulger, A., Kroglund, F., Kvellstad, A., Lydersen, E., Oughton, D. H., Salbu, B., Staurnes, M. and Vogt, R. (1992). The mixing zone

between limed and acidic river waters: complex aluminium chemistry and extreme toxicity for salmonids. *Environmental Pollution.* **78** (1-3) pp3-8.

~End of Chapter 6~

Final Appendix

Conference Papers

DYNAMIC UP-FLOW PERCOLATION TESTS - A MODEL FOR MINING WASTE LEACHATE GENERATION

ALISON TURNER[1], CHARLOTTE BRAUNGARDT[1], PAUL WORSFOLD[1], JOHN RIEUWERTS[1], BEN WILLIAMSON[2] and HUGH POTTER[3]

[1]School of Geography, Earth and Environmental Sciences, University of Plymouth, Plymouth, PL4 8AA, United Kingdom; E-mail: alison.turner@plymouth.ac.uk
[2]Camborne School of Mines, School of Geography, Archaeology & Earth Resources, University of Exeter, Penryn, Cornwall, TR10 9EZ, United Kingdom
[3]Environment Agency Science Department, Institute for Research on the Environment and Sustainability (IRES), University of Newcastle upon Tyne. NE1 7RU. United Kingdom

ABSTRACT

Column experiments, based on the European standard up-flow percolation test (TS 14405), were applied to waste rock from an abandoned Pb/Zn mine in southwest England. The aim was to investigate the range and magnitude of pollutants transported from mine waste tips to surface watercourses. The dynamic leaching test was chosen to mimic the transport of rainwater through mine spoil, thereby providing a laboratory proxy for field conditions. A range of metals (Cd, Cu, Mn, Pb, Zn) and major ions were determined in the column leachate, covering solid:liquid ratios of 0-10 L kg^{-1}. The highest concentrations of Zn (200 μmol L^{-1}), Cu (17.4 μmol L^{-1}) and Cd (0.70 μmol L^{-1}) in the leachate were observed at low L/S ratios. Leachate concentrations decreased exponentially for most elements, except Pb, which maintained high concentrations (up to 80 μmol L^{-1}) throughout the experiment. Batch extractions with L/S ratios of 2, 5 and 10 L kg^{-1} were applied to the same material. Concentrations in the supernatant were generally comparable to results from column experiments, but some differences at high L/S were attributed to the dynamic mode of leaching and the resulting higher adsorptive capacity of the solid phase in the column. Concentrations of Zn and Cd determined in shallow groundwater collected at the former mine site were of the same order of magnitude as concentrations obtained from the column experiments at high L/S ratios, showing that the column experiments provide a good approximation of field conditions. However, Pb and Cu concentrations, which showed close agreement between batch and column experiments, were much lower in the field (max. 3.0 μmol L^{-1} and 1.9 μmol L^{-1}, respectively), probably due to the prevailing higher pH and/or a higher L/S ratio. This discrepancy highlights the limitations of using laboratory experiments to predict pollutant sources at abandoned mine sites.

1. INTRODUCTION

In southwest England, the legacy of metal mines, abandoned before remediative action was required by law, affects the environmental quality of surrounding landscapes. In particular, the concentrations of metals (e.g. Cd, Cu, Pb,Zn) in some rivers and coastal waters and their sediments exceed limits set by the Environment Agency for England and Wales to meet the requirements of the European Water Framework Directive (WFD, 2000/60/EC; EA, 2008) and Probable Effect Levels in sediments (Langston *et al.*, 2003). Nine percent of rivers in southwest England have been categorised as 'at risk' or 'probably at risk' due to abandoned metal mine pollution (Jarvis *et al.*, 2008). Leachate and run-off from mining waste, collected in surface streams and outflows, have been reported to carry high concentrations of contaminants to watercourses of southwest England (e.g. Bowell and Bruce, 1995; Neal *et al.*, 2005; Mighanetara *et al.*, 2009) and elsewhere. However, metal fluxes from diffuse sources are difficult to determine accurately and expensive to investigate and hence remain largely unknown. The subtraction of point source fluxes from the total metal flux in a water course can provide a useful first estimate of diffuse inputs (Mayes *et al.*, 2008; Mighanetara *et al.*, 2008). However, this general approach does not provide detailed information on the dominant sources of contamination in a water course, as is required for river catchment assessment and management in the context of the WFD.

The aim of this study was to investigate diffuse metal fluxes emanating from a selection of mining-related sources in southwest England. In order to achieve this aim, controlled laboratory experiments were combined with field studies of run-off from mine spoil and shallow groundwater flow into surface water courses.

2. METHODS

Reagents and Apparatus

All aqueous solutions were prepared with MQ water (Millipore, R ≥18.2 MΩ cm^{-1}, reverse osmosis/ion exchange). Standard solutions and reagents were prepared in a Class 5 (BS EN 150 14644) laminar flow hood using trace metal clean techniques. Multi-element calibration standards were prepared as serial dilutions from standard solutions (1000 or

Abstracts of the International Mine Water Conference
Proceedings ISBN Number: 978-0-9802623-5-3
Produced by: Document Transformation Technologies cc

19th – 23rd October 2009
Pretoria, South Africa
Conference organised by: Cilla Taylor Conferences

858

10000 µg L^{-1}, Romil Pure Chemistry, Fisher and BDH) and acidified to <pH 2 with Q-HNO$_3$ (purification by sub-boiling distillation, Romil SPA). All equipment was immersed in detergent (Decon 90, 2% v/v, >24 h) and rinsed with MQ water before cleaning with analytical reagent grade acids. Polyethylene centrifuge tubes (50 mL) and high density polyethylene bottles (HDPE, Nalgene) used for sample collection and standard preparation were cleaned by immersion in a series of acids (HCl, 6 mol L^{-1}, ≥7 days, HNO$_3$, 2 mol L^{-1}, ≥7days). Perspex™ columns used in leach experiments were immersed in HNO$_3$ (pH 2, ≥7 days). Filtration units (polycarbonate, Nalgene) and other apparatus were immersed in HCl (2 mol L^{-1}, ≥3 days). All items were rinsed with MQ water after each of the cleaning steps, dried in a laminar flow hood and stored in plastic zip-lock bags.
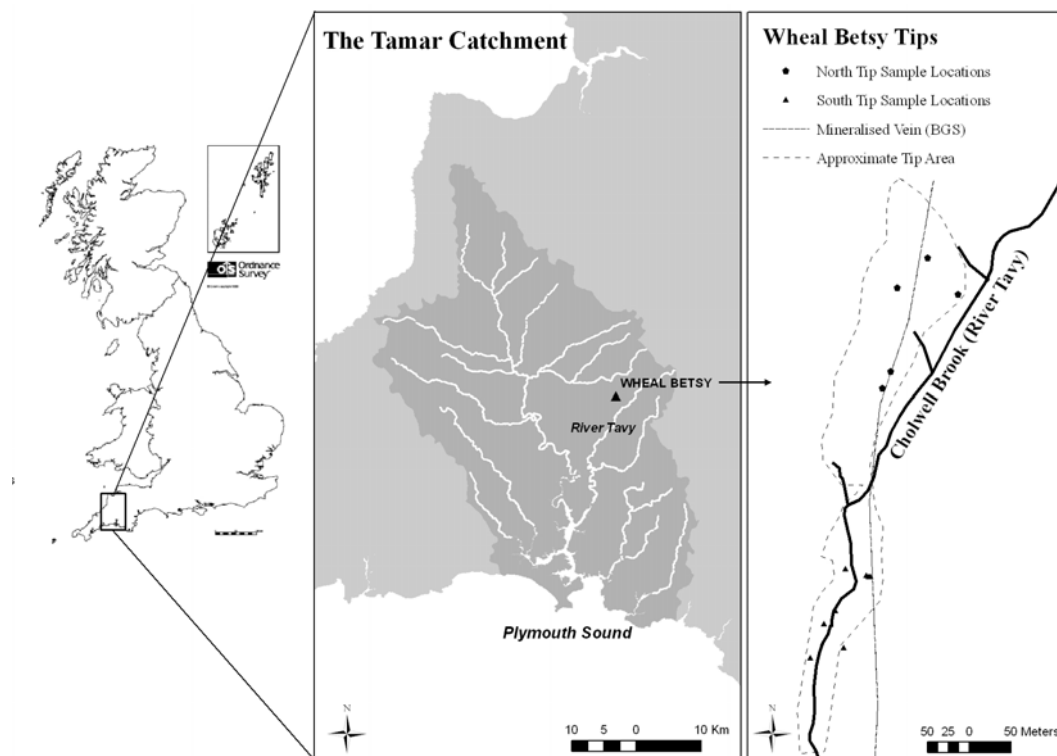
Site Description

Figure 1. Location of Wheal Betsy within the Tamar catchment, southwest England, showing major river courses (centre). Site plan (right) of tips in relation to Cholwell Brook (solid black line), showing sample locations of mine waste material (north tip: ●, south tip: ▲). © Crown Copyright/database right 2009. An Ordnance Survey/EDINA supplied service.

The metalliferous deposits of southwest England host two major types of economic mineralisation: Sn oxide (cassiterite), Cu, As and Zn sulphide mineralisation, largely in E-W trending lodes and N or NW trending lodes, known as crosscourses, comprising Pb, Ag and Zn veins. The abandoned Wheal Betsy, which is the subject of the current study, was worked for Pb, Ag and Zn between 1740 and 1877 (Dines, 1956). The bedrock consists of slates and thin beds of limestones and grits of the Carboniferous Culm Measures. The veins are dominated by quartz, siderite, galena and sphalerite, with minor presence of pyrite, arsenopyrite, some Cu and Ag ores and traces of cadmium bearing ores (Dines, 1956; Page, 2008). Underground workings followed the N-S trending lode from a depth of 65 to ca. 270 m and were serviced by several shafts, engines and adits. The underground workings were drained to ca 70 m by means of a connecting adit to Wheal Friendship, located to the south of the site (Richardson, 1995; Hamilton Jenkin, 2005; Dines, 1956). Today, the site features the remains of engine houses, adits and a number of waste heaps of diverse materials along the banks of Cholwell Brook, a small tributary of the River Tavy (Figure 1). The waste tips at the north of the site mainly consist of poorly sorted coarse to medium sand (60-80%), with some larger pebbles and cobbles of quartz and slate and with iron hardpan horizons. Material in the south tips is similar in composition, but more heterogeneous, containing more clay and fine sands (< 0.25 mm, 24% WBS and 14% WBN).

Sampling Protocol and Sample Treatment

Five composite samples of ca.1.5 kg were taken from both, the northern and southern tip areas using a stainless steel trowel (Figure 1, north tip: 10-50 cm depth, south tip: 10-40 cm depth) Surface crusts, root layers and large pebbles (>16 mm, Wentworth Scale) were omitted by hand sorting. The material was collected into zip lock bags and stored at 4°C. The individual mine waste samples were sieved (4 mm) and combined to form two composite samples representative of the north and south tip areas, respectively. The composite samples (<4 mm) in the columns constituted 39% and 53% by weight of the sample material for WBN and WBS, respectively. The composite samples were

homogenized by cone and quartering and recombining (5 repetitions), placed in an airtight HDPE container and stored at 4°C. To sample shallow groundwaters flowing through the northern mine spoil (WBN) and towards Cholwell Brook, five piezometers (50 mm diameter) were installed. A schematic of the installation is provided in Figure 2.
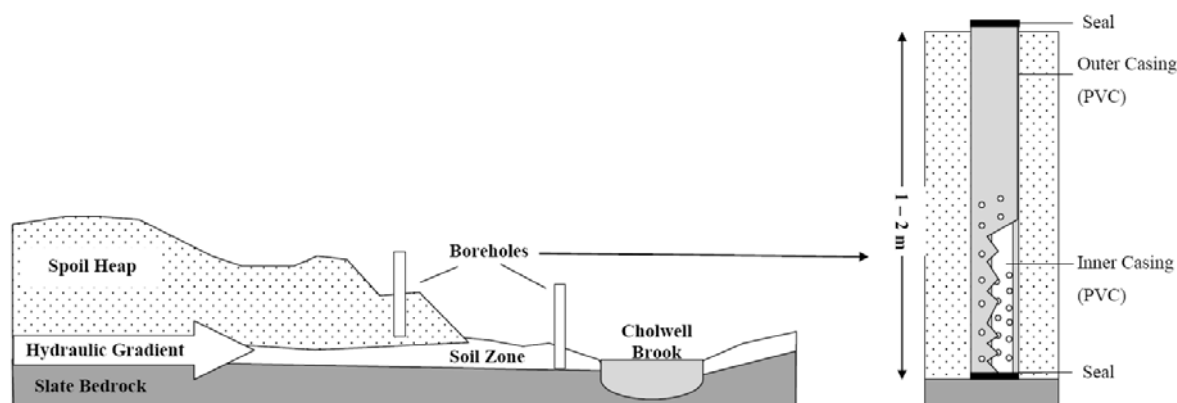

Figure 2. Cross-section schematic of borehole installation at Wheal Betsy (northern tips). On the right, the double-layer construction of the installed tubes is shown.

Double-layer tubes were installed into five boreholes (50 mm diameter) in order to intercept shallow groundwaters flowing from the northern mine spoil (WBN) towards Cholwell Brook (Figure 2). Boreholes were sampled via a Wattera™ bailer and purged to at least three borehole volumes prior to sample collection. Water samples were transferred to HDPE bottles after three rinses with sample water, and stored cool. Conductivity, pH and redox potential (Eh) were determined in situ using portable instruments (Hanna HI9635, MeterLab PHM201 and Hanna H9025 respectively). The pH meter was calibrated using standard solutions (pH 4 and 7, BDH), and the Eh measurements were made against ZoBell's solution (Nordstrom, 1977). In the laboratory, water samples were vacuum filtered (0.2 μm pore size, Whatmann Nuclepore). Samples for anion determination were stored cool (<3 days). Samples for metal determination were acidified (Q-HNO$_3$, pH 2).

Dynamic Up-Flow Column Experiments

Composite samples of mine spoil from the Wheal Betsy north (WBN) and south (WBS) tip areas were subjected in triplicate to up-flow column extraction procedures (standard European method (CEN/TS 14405, 2004). The leaching solution (aerated MQ water) was transported by a peristaltic pump at a constant flow rate (2.0 mL min-1) into the bottom of the column. The out flowing solution (leachate) was filtered in-line (filter holder 47 mm diameter, Swinnex) in two stages (0.45 μm and 0.2 μm, Whatman Nuclepore). The leachate was either directed through a flow chamber for in-line determination of Eh and pH, or was collected for chemical analysis (Figure 3).

The complete column flow circuit, including filter holders, was cleaned in-line by circulating Q-HNO3 followed by MQ water. The sample material was introduced to the column in 5cm layers, each reproducibly compacted with a 125g weight, dropped 50 times from a height of 20cm. The sample weight and the percent effective porosity of the column were determined gravimetrically. The columns were saturated with leaching solution (MQ water) and equilibrated at room temperature for 72 h. Subsequently, the MQ water was pumped continuously through the columns and leachate was sampled (ca. 30 mL) at L/S ratios from 0 to 10. Three aliquots (2 mL) of each sample were stored in glass HPLC vials and refrigerated pending quantification of anions. The remaining sample was stored in HDPE bottles and acidified (Q-HNO3, pH 2) for metal analysis. The leachate pH (Hanna HI9025, VWR electrode) and Eh (Hanna HI9025, redox-ORP electrode, VWR) were recorded at time intervals throughout the experiment. The cumulative leachate volume for all columns was >10 L kg-1.
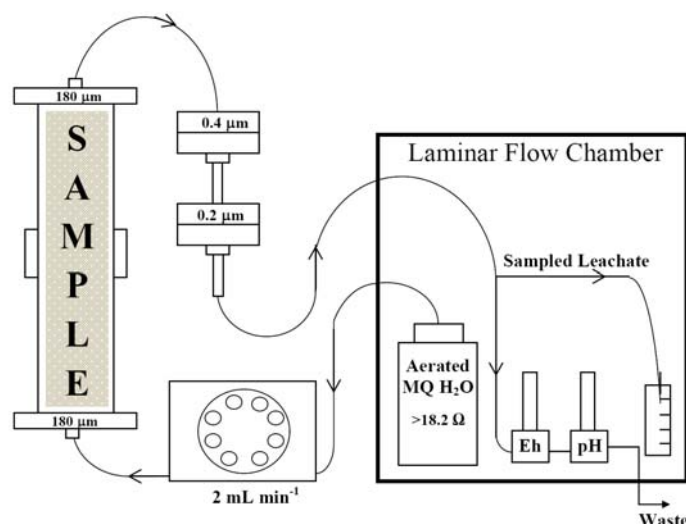
Figure 3. Schematic diagram of dynamic column experiment showing the complete flow circuit comprising leaching solution (aerated MQ water) supply, peristaltic pump, column packed with mine waste, double filtration and sample collection.

Batch Extractions

Composite Wheal Betsy north (WBN) and south (WBS) tip material was dried (40°C, 72 h). Sub-samples of homogenized material (4, 8 and 10 g) were accurately weighed into 50 mL centrifuge tubes. MQ water was added at L/S ratio's of 10, 5 and 2 respectively (in triplicate). Samples were laid horizontally and shaken for 16 h (orbital shaker), then immediately centrifuged (3000 rpm, 15 min). The supernatant was carefully removed via auto-pipette and acidified (Q-HNO_3, pH 2) for metal analysis.

Instrumentation and Analysis

Moisture content was determined in triplicate gravimetrically after drying (105°C) of sieved and homogenized samples (10 g). The organic matter content was determined gravimetrically as loss on ignition (450°C, 4h). Metal analysis in water samples and column leachate was carried out by ICP-OES (Varian 725-ES Inductively Coupled Plasma Optical Emission Spectrometer) and ICP-MS (VG Plasma Quad PQ2+ Turbo Inductively Coupled Plasma Mass Spectrometer) in an ISO9001:2000 accredited analytical research facility. Yttrium and indium (100 μg L^{-1}) were used as internal standards. Dissolved anions were determined by ion chromatography (Dionex DX-500 system, Dionex Ionpac AS9-HC column). Na and K analysis was performed by flame photometer (Corning 400). Analyses were verified against a certified reference material for trace elements (TMDA-64, National Water Research Institute, Canada) and the recovery was within 96 and 115% for all certified elements.

3. RESULTS AND DISCUSSION

Test Conditions

Up-flow percolation experiments were carried out at ambient tempreratures of 18.2-23°C, and the initial moisture content of the samples was 13.2-14.7%. The organic matter content (LOI) was 7.5% and 4.7% at WBN and WBS, respectively. Test conditions showed good reproducibility between the triplicate columns of the same waste material (Table 1). The minor variations in the dry mass (ca. 0.84 kg), saturated pore volume (ca. 0.084 L), linear velocity (32 cm h^{-1}) and flow rate (1.5 ± 0.2 ml min^{-1}) of the leachate arose from small differences in the packing of the columns. WBN and WBS material produced leachate of similar pH values (1.9-2.6), whereby a gradual decline in pH by ca.0.6 units was observed during the experiment. The redox potential in the leachate remained positive (715-800 mV) throughout the experiment, indicating that the columns were not oxygen limited.

Table 1. up-flow percolation test characteristics for each column: flow rate, moisture content, temperature, dry mass, saturated pore volume, linear velocity, initial l/s ratio, median ph and ph and eh ranges.

Tip Material:	Wheal Betsy North (WBN)			Wheal Betsy South (WBS)		
Column No.	1	2	3	4	5	6
Mean flow rate (mL min^{-1})	1.44	1.39	1.61	1.45	1.31	1.69
Dry mass of solid sample (kg)	0.866	0.833	0.810	0.848	0.842	0.850
Saturated pore volume (L)[1]	0.085	0.086	0.094	0.079	0.081	0.079
Linear Velocity (cm h^{-1})[2]	30.5	29.1	30.8	33.0	29.1	38.5
Initial L/S ratio (L kg^{-1})[3]	0.10	0.10	0.12	0.09	0.10	0.09
pH range	1.9-2.6	1.8-2.5	1.9-2.6	2.0-2.5	2.3-2.6	2.3-2.6
Median pH [4]	2.3			2.4		

[1] Water volume in saturated column, determined gravimetrically
[2] Determined from saturated pore volume per unit length of column (cm mL^{-1}) and the average flow rate (mL h^{-1})
[3] Initial L/S ratio calculated from saturated pore volume and dry sample mass
[4] Median pH determined from all three replicates at L/S ratio >0.2 L kg^{-1}.

Reproducibility of Dynamic Up-Flow Column Experiments

In Figures 4 and 5, the elemental concentrations in column leachate, normalised for dry mass, were plotted against the L/S ratio. The resulting release curves were highly reproducible for triplicate columns for all elements, as illustrated in Figure 4 for Zn leached from WBH tip material. In the following sections, triplicate column results were combined to produce a single data set for each sample.
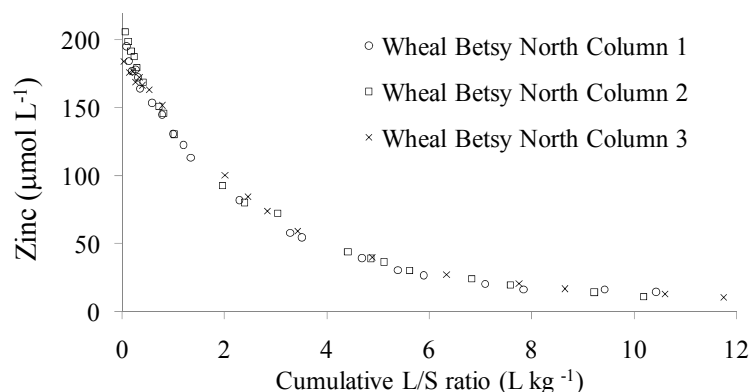

Figure 4. Concentration of dissolved Zn in leachate from replicate columns of WBN tip material versus cumulative liquid to solid (L/S) ratio. Concentrations were corrected for dry mass in the column. LODZn = 0.025 mol L-1.

Elemental Release Curves

The chloride release curve (Figure 5A) demonstrates the leaching behaviour of a highly soluble ion with low affinity for the column material. The shape of release curves reflects the release rate of an element under conditions of changing L/S ratios and is influenced by the solubility of the source mineral phase and the adsorption or complexation strength with the column matrix. The steep gradient of the Cl release curve at low L/S ratios can be seen as representative for the behaviour of the most mobile elements, which are rapidly removed from the tip material. Elemental concentration in leachate generated towards the end of the experiment (L/S ≤10) tended towards a steady state, termed here the *dynamic equilibrium* concentration. The dynamic equilibrium condition is reached when the rate of an element's release into pore waters is in equilibrium with the rate of its removal from the column by fluid transport. It represents the concentration of an element found in solution after the 'first flush' of the solid material with eluent.

In comparison to Cl, the release of Zn, Cd and Cu from the column (Figure 5A, B, D, E) occurred at a slower rate and exhibited exponential decrease with increasing L/S ratio. The shape of these curves indicates a release mechanism influenced by surface sorption/desorption processes for elements of lower mobility, relative to that of chloride. The maximum leachate concentrations recorded at low L/S (WBN: 200 μmol L^{-1} Zn, 0.7 μmol L^{-1} Cd, 17.4 μmol L^{-1} Cu; WBS: 13.8 μmol L^{-1} Zn, 0.17 μmol L^{-1} Cd, 0.71 μmol L^{-1} Cu) were an order of magnitude higher than the dynamic equilibrium concentrations, and provide an estimate of the peak release from the waste tip material after a cycle of drying and wetting. The Pb concentrations in the column leachate exhibited a small decrease (<15% of initial concentration) at low L/S ratios, before recovering to previous levels and remaining stable for the remainder of the experiment. This indicates that Pb release from the column is in dynamic equilibrium over the full range of L/S ratios

applied. As a result, Pb (35.3-77.9 μmol L^{-1}), along with SO$_4^{2-}$ (285-403 μmol L^{-1}), represent the dominant dissolved ions in the leachate at dynamic equilibrium.
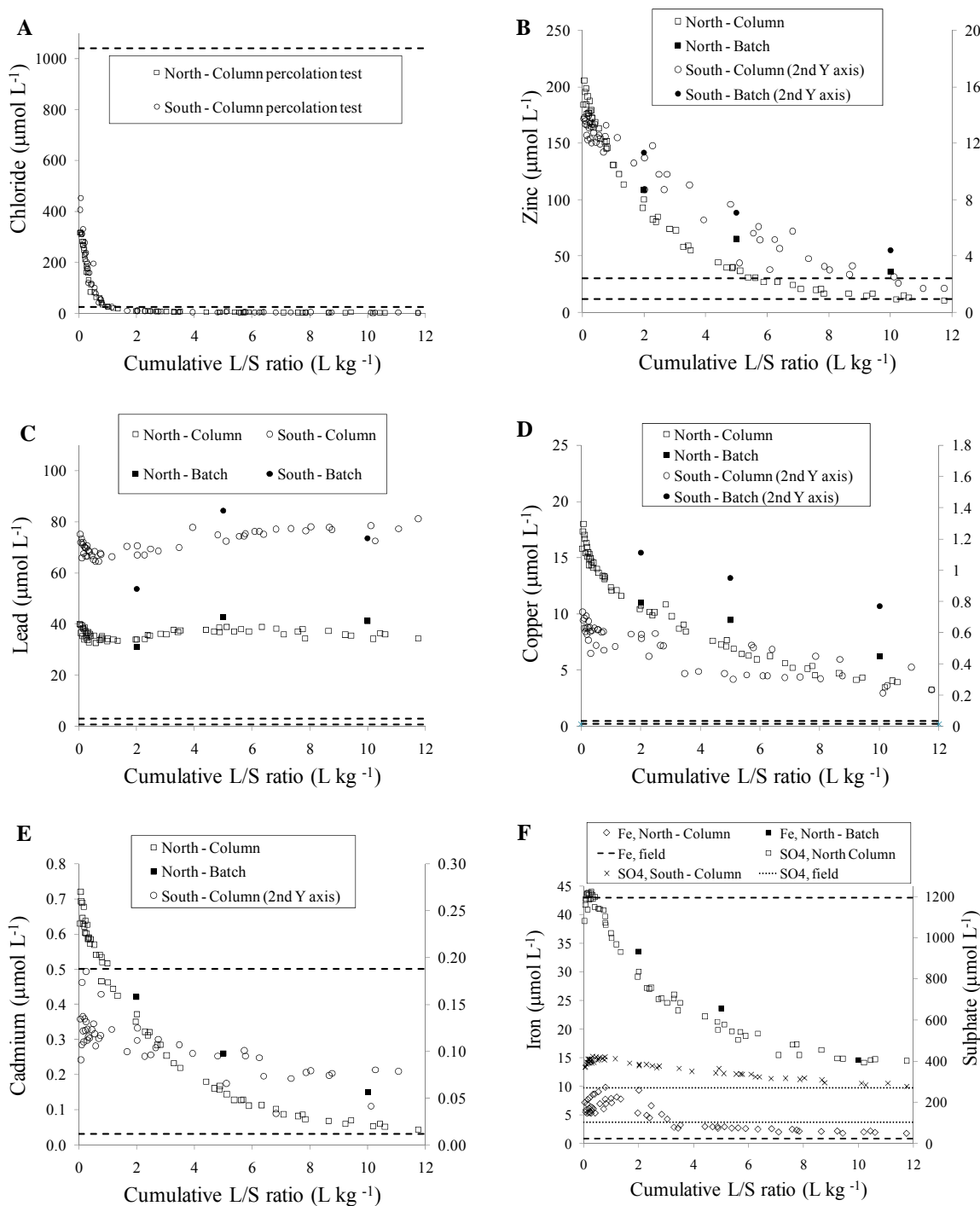

Figure 5. Dissolved concentrations of metals and chloride in column leachate and batch extractions with respect to L/S ratio (LOD, μmol L^{-1}): Zn (0.025), Cu (0.0036), Cd (0.003), Pb (0.003), Fe (0.32), Mn (0.05) SO$_4^{2-}$ (3.34) and Cl$^-$ (1.39). Dashed lines represent the range of concentrations determined in borehole samples at Wheal Betsy North (scale on left axis).

The iron release curve from Wheal Betsy north tips was characterised by an initial concentration increase (L/S <2) from 6.1 μmol L^{-1} Fe to a maximum of 9.2 μmol L^{-1} Fe (Figure 5F). After reaching the maximum, concentrations initially decreased steeply, then less so, reaching a dynamic equilibrium around 2 μmol L^{-1} Fe. The release curves for sulfate at WBN and WBS followed a similar trend. This behaviour indicates the interplay between mobilisation from the solid phase (dissolution of primary and secondary minerals and desorption) and loss from the dissolved phase due to the precipitation of secondary phases, such as amorphous iron hydroxides and iron hydroxysulphates, under changing conditions. It is likely that during the initial equilibration stage of the column, iron was mobilised into the pore water and reached a balance between the solid and dissolved phases. As the dynamic stage of the experiment commenced,

readily mobile Fe phases leached from the column at a rate that increased with the L/S ratio up to the point (at L/S >2) where the release curve followed an exponential decrease, as observed for Zn, Cd and Cu. Iron concentrations were below or very close to the LOD (0.32 μmol L^{-1}) in Wheal Betsy South leachate.

Based on the maximum observed concentrations in column leachate and assuming conservative transport, a dilution factor of 1000 would be required to reduce maximum Pb concentrations (WBS: 90 μmol L^{-1}, WBN: 39.7 μmol L^{-1}) below the current fresh water Environmental Quality Standard (EQS) (low alkalinity). Similarly, a dilution factor of 1000 (WBN) or 100 (WBS) would be necessary to reduce peak Zn concentrations (200 μmol L^{-1} and 13.8 μmol L^{-1}, resp.) and a dilution factor of 100 (WBN, WBS) would be necessary to reduce Cd concentrations (up to 0.7 μmol L^{-1}) in order to meet with EQS, and therefore WFD, requirements. Based on recent stream sampling and previous studies (Austin, 2005) Cholwell Brook enters the mine site with low background concentrations of contaminant metals but exceeds current freshwater EQSs for Zn, Cd, Pb and Cd upon leaving it. Given the size of the tips and their close proximity to Cholwell Brook, the tip drainage represents a significant source of contamination to the watercourse. The severity and downstream extent of the contamination depends on the magnitude of dilution and the mobility of individual metals. Therefore, accurate prediction of the impact of spoil heap drainage is limited by the availability of accurate hydrological data and knowledge of in-stream processes (i.e. dilution, element-specific sorption, complexation and precipitation).

Cumulative Element Loads

Cumulative contaminant loads (μmol kg^{-1} of dry mass) released during the experiment (Figure) were calculated by summing the product of the concentration of collected column fractions and the L/S ratio (up to L/S 10). Wheal Betsy south material leached predominantly Pb and Zn (730 μmol kg^{-1} and 59 μmol kg^{-1} respectively), while north tip material was characterised by a wider range of contaminants (including Zn at 518 μmol kg^{-1}) and a higher sulphate load (6.1 mmol kg^{-1}).
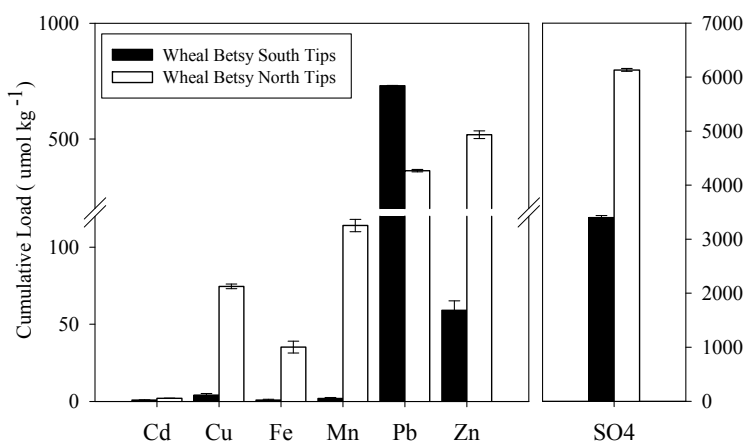

Figure 6. Cumulative metal and sulphate loads (μmol kg^{-1}) leached from Wheal Betsy north and south tip material during up-flow percolation tests. Error bars represent ±1 s.d (n=3).

The cumulative contaminant loads from the column experiments on WBN material are compared with results from batch extractions, performed on the same homogenised material at L/S ratios of 2, 5 and 10, in Figure 7. Batch and column tests showed closest agreement at L/S = 2, after which the column release curves diverged from the batch experimental results. Iron release was much lower in column experiments than in batch extractions (Figure 7E). This suggests that percolation as mode of leaching encourages the precipitation of iron oxides within the column matrix and as a consequence, through co-precipitation and/or adsorption, the mobility of other metals is also reduced. The ability of Fe and Mn hydroxides to adsorb metals has been shown to be particularly strong for Pb(II) and Cu(II), compared with Zn(II) and Cd(II) (Elliott et al., 1986; Han et al., 2006; Covelo et al., 2007; Dong et al., 2007). This may explain the lower release of Pb in the column experiment, compared with the batch experiments (Figure 7B). At high dissolved concentrations this adsorption effect can be masked, as was the case for Cu at WBN (Figure 7C), but becomes apparent at the lower concentrations released from WBS material (Figure 7F). Cadmium, released at lower concentrations than Cu at WBN (Figure 7D), did not exhibit the same behaviour, due to a lower affinity for Fe/Mn hydroxide binding sites.
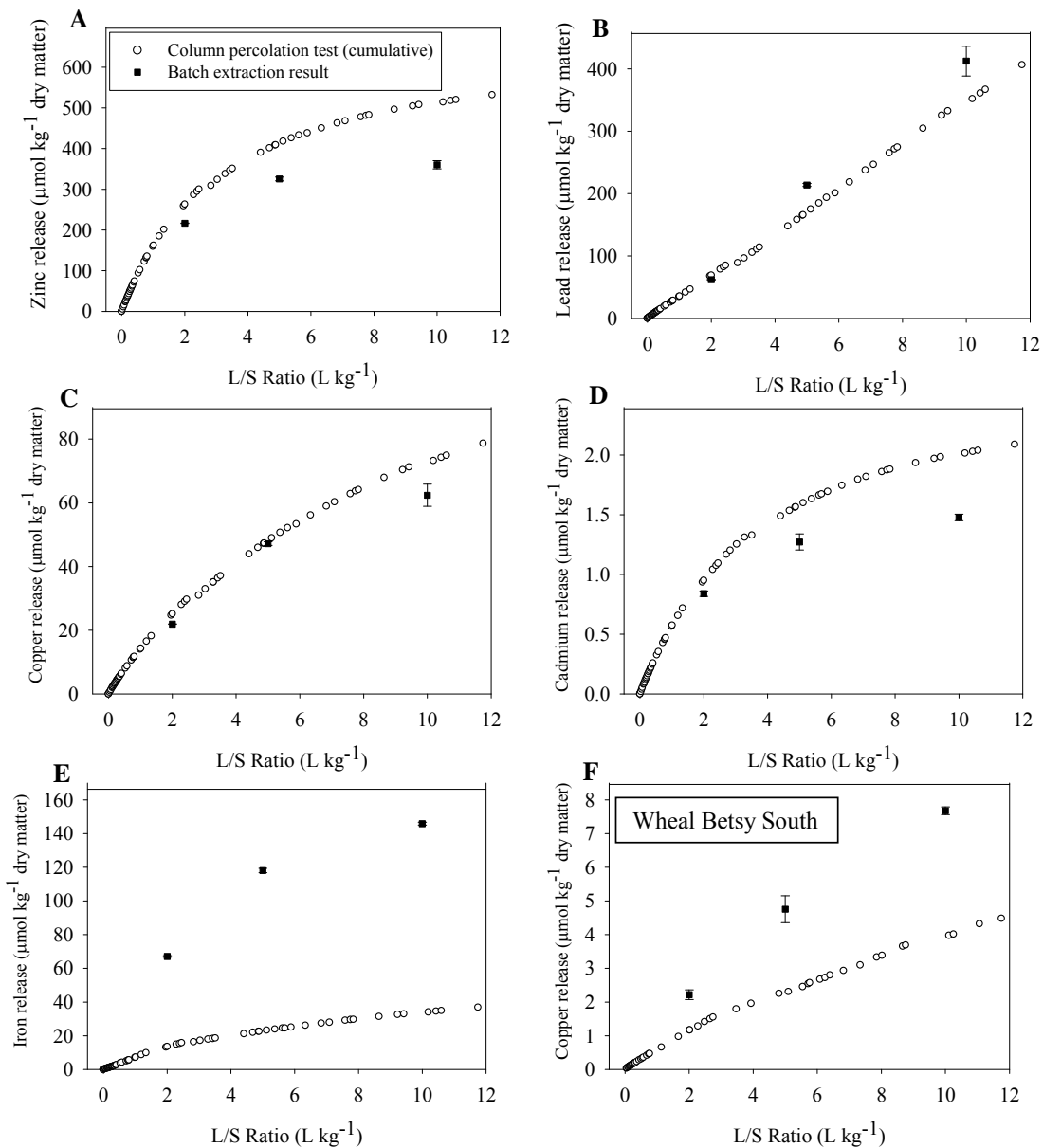
Figure 7. Metal, sulphate and chloride release from batch and column percolation tests for Wheal Betsy North material (μmol kg^{-1}) and Cu release from batch experiment for Wheal Betsy South material.
Error bars for batch extraction represent ± 1 s.d (n=3).

It has been shown that preferential adsorption can cause metals with the lowest affinity for the column matrix to largely remain in solution (Covelo *et al.*, 2007). This can also account for the number of moles of Zn, Cd and Cu released from the column being progressively higher with increasing L/S ratio than the metal release in the batch experiments. In the presence of high dissolved concentrations of metals with higher affinity for Fe/Mn hydroxide binding sites, Zn and Cd are more likely to remain in solution than Pb and Cu. Overall, the dynamic experiment appeared to encourage greater desorption than the static batch experiment, and this is consistent with previous studies. Several explanations have been given for this discrepancy, including the kinetics of adsorption (Allen *et al.*, 2002) and the effects of preferential flow within columns (Porro *et al.*, 2000). The dynamic leaching experiment creates a dissolved element concentration gradient within the column, with pristine leaching solution constantly supplied to one end. Therefore, it is unlikely that equilibrium conditions between the solid and the dissolved phases become established during a dynamic column experiment. However, in batch extractions metal mobilisation is constrained by this equilibrium (Plassard *et al.*, 2000).

Comparison with Natural Waters

The concentration ranges of Zn (12-30.4 μmol L^{-1}) and Cd (0.03-0.5 μmol L^{-1}) observed in the boreholes installed at Wheal Betsy were of the same order of magnitude as the respective dynamic equilibrium concentrations obtained in the column leach experiments (Figure 5). For these metals, the column leaching was a good proxy for the conditions of dynamic flow prevailing in mine spoil and below the water table, even though the composite samples used in the laboratory experiments cannot be fully representative of the waste tip material present in the field. Dissolved

concentrations of Pb (0.7-3.0 μmol L^{-1}) and Cu (0.2-1.9 μmol L^{-1}) in borehole samples were lower than in column leachate, but still exceeded freshwater EQSs by one order of magnitude. This discrepancy may be related to the higher pH values (pH 3.8-5.1) observed in the boreholes, compared with the column experiments (pH 1.8-2.6), influencing ion exchange and sorption of Pb and Cu onto Fe/Mn hydroxide phases. Ion exchange processes are pH dependant. According to results reported by Tan *et al.*, (2008) and Oh *et al.*, (2009), a shift from the pH range observed in column leachate to those determined in boreholes is likely to result in a markedly higher Pb sorption onto mineral surfaces. The redox potential (455-650 mV) varied between boreholes and surveys and was somewhat lower than values recorded during the column experiment (715-800 mV). The redox and pH sensitivity of Fe influences its distribution between the solid and dissolved phases, as well as that of associated metals, and can contribute to differences between field and laboratory data.

The L/S ratio of 10:1 in the column test was designed to elute all the easily mobilised metals from the spoil material. However, in the case of Pb and Cu, it appeared that the dynamic equilibrium position was not attained by the end of the column test and did not satisfactorily predict Pb and Cu mobility in the field. In shallow groundwater the L/S ratio is unknown, but over time is likely to be >>10. Therefore, it is plausible that the borehole concentrations represent the true dynamic equilibrium position for Pb and Cu, which was not approximated by the column test. However, not all spoil material in the field exists below the water table and is subject to cylic wet and dry conditions. The column experiments at low L/S ratio provide an important indicator of the maximum concentrations that could emanate from mine spoil following a heavy rainfall event.

A more detailed analysis of the field surveys is presented in the accompanying poster presentation: ' Braungardt *et al.*, Acid mine waters at Wheal Betsy, an abandoned Pb/Zn mine in southwest England'.

4. CONCLUSIONS

In cases where extensive field investigations are not viable, the up-flow percolation experiment provides a means of mimicking the conditions of dynamic flow through mine spoil. Results from column experiments and sampled boreholes were similar for some metals (Zn and Cd) and may provide a useful tool for prediction of leachate composition. The highest concentrations of Zn (200 μmol L^{-1}), Cu (17.4 μmol L^{-1}) and Cd (0.70 μmol L^{-1}) in the leachate were observed at low L/S ratios. Concentrations at dynamic equilibrium were one order of magnitude below the maxima, with the exception of Pb which remained high. Lowest observed leachate concentrations in the field and laboratory remained elevated by one order of magnitude, with respect to the EQSs. For all elements, the dynamic equilibrium concentration from column experiments was more closely matched to field conditions than results obtained from the batch extractions. The discrepancies between column and batch experiments was small enough to suggest that batch experiments could be useful for developing management strategies where it is necessary to survey large areas for contaminant mobility. The largest difference between laboratory and field experiments was observed for Pb and Cu concentrations, where mobility was much reduced in the borehole samples in comparison with the high loads recorded for both batch and column experiments. An explanation for this may be the higher pH measured in the borehole waters (pH 3.8-5.1) compared with the more acidic leachates derived in the laboratory. Alternatively, the borehole may represent the true dynamic equilibrium position for Pb at a higher L/S ratio. The differences observed between laboratory and field based assessment approaches, demonstrates the limitations of applying laboratory data to the field scale. It also highlights the necessity to consider the effect of different physico-chemical and hydrological situations on the contamination potential of mine spoil.

5. REFERENCES

Allen, H. E., Chen, Y.-T., Li, Y., Huang, C. P. and Sanders, P. F. (2002) "Soil Partition Coefficients for Cd by Column Desorption and Comparison to Batch Adsorption Measurements". *Environmental Science & Technology, **29** (8), 1887-1891.

Austin. S (2005) "Analysis of potentially toxic elements in the vicinity of Wheal Betsy, a former lead-silver mine." MSc Thesis. University of Plymouth.

Bowell, R. J. and Bruce, I. (1995) "Geochemistry of Iron Ochres and Mine Waters from Levant Mine, Cornwall." *Applied Geochemistry*, **10** (2), 237-250.

Covelo, E. F., Vega, F. A. and Andrade, M. L. (2007) "Competitive Sorption and Desorption of Heavy Metals by Individual Soil Components." *Journal of Hazardous Materials*, **140** (1-2), 308-315.

DD CEN/TS 14405:2004, Characterisation of Waste - Leaching Behaviour Test - up-Flow Percolation Test (under specified conditions). British Standards Institute.

Dines, H. G. (1956). *The Metalliferous Mining Region of South-West England*. British Geological Survey, HMSO, London.

Dong, D., Liu, L., Hua, X. and Lu, Y. (2007) "Comparison of Lead, Cadmium, Copper and Cobalt Adsorption onto Metal Oxides and Organic Materials in Natural Surface Coatings." *Microchemical Journal*, **85** (2) 270-275.

Elliott, H. A., Liberati, M. R. and Huang, C. P. (1986). "Effect of Iron Oxide Removal on Heavy Metal Sorption by Acid Subsoils." *Water, Air, & Soil Pollution*, 27 (3) 379-389.

Hamilton Jenkin, A. K. (2005). *Mines of Devon*. Cromwell Press, Trowbridge.

Han, R., Zou, W., Zhang, Z., Shi, J. and Yang, J. (2006) " Removal of Copper(II) and Lead(II) from Aqueous Solution by Manganese Oxide Coated Sand: I. Characterization and Kinetic Study". *Journal of Hazardous Materials*, **137** (1), 384-395.

Jarvis, A. P., Johnston, D., Mayes, W. H. and Potter, H. A. B. (2008) "Application of a New Methodology for Assessing the Priorities for Abandoned Mine Water Pollution Remediation at a National Scale: Results and Implications from a Study across England and Wales". Rapantova, N. and Hrkel, Z. (eds) *Conference Proceedings of the 10th International Mine Water Association Congress Karlovy Vary, Czech Republic*. 2-5 June 2008.

Langston, W. J., Chesman, B. S., Burt, G. R., Hawkins, S. J., Readman, J. and Worsfold, P. (2003) "Characterisation of the South West European Marine Sites: Plymouth Sound and Estuaries CSAC, SPA." *Journal of the Marine Biological Association of the United Kingdom, Occasional Publication No. 9.*

Mayes, W. M., Gozzard, E., Potter, H. A. B. and Jarvis, A. P. (2008). "Quantifying the Importance of Diffuse Minewater Pollution in a Historically Heavily Coal Mined Catchment". *Environmental Pollution*, **151** (1), 165-175.

Mighanetara, K., Braungardt, C. B., Rieuwerts, J. S. and Azizi, F. (2008) "Contaminant Fluxes from Point and Diffuse Sources from Abandoned Mines in the River Tamar Catchment, UK". *Journal of Geochemical Exploration*, **100**, 116-124.

Neal, C., Whitehead, P. G., Jeffery, H. and Neal, M. (2005). "The Water Quality of the River Carnon, West Cornwall, November 1992 to March 1994: The Impacts of Wheal Jane Discharges". *Science of The Total Environment*, **338** (1-2), 23-39.

Nordstrom, D. K. (1977). "Thermochemical Redox Equilibia of Zobell's Solution". *Geochimica et Cosmochimica Acta* , **41**, 1835-1841.

Oh, S., Kwak, M. Y. and Shin, W. S. (2009). "Competitive Sorption of Lead and Cadmium onto Sediments." *Chemical Engineering Journal*, **152** (2-3), 376-388.

Page, K. (2008). "County Geological Sites in West Devon and their Contribution to the Cornwall and West Devon Mining Landscape's World Heritage Site.", *Notes from the Devonshire Association Excursion*. University of Plymouth.

Plassard, F., Winiarski, T. and Petit-Ramel, M. (2000) "Retention and Distribution of Three Heavy Metals in a Carbonated Soil: Comparison between Batch and Unsaturated Column Studies." *Journal of Contaminant Hydrology*, **42** (2-4), 99-111.

Porro, I., Newman, M. E. and Dunnivant, F. M. (2000) "Comparison of Batch and Column Methods for Determining Strontium Distribution Coefficients for Unsaturated Transport in Basalt." *Environmental Science & Technology*, **34** (9), 1679-1686.

Richardson, P. H. G. (1995). *Mines of Dartmoor and the Tamar Valley after 1913*. Devon Books, Torquay.

Tan, X. L., Chang, P. P., Fan, Q. H., Zhou, X., Yu, S. M., Wu, W. S. and Wang, X. K. (2008). "Sorption of Pb(II) on Na-Rectorite: Effects of Ph, Ionic Strength, Temperature, Soil Humic Acid and Fulvic Acid." *Colloids and Surfaces A: Physicochemical and Engineering Aspects*, **328** (1-3), 8-14.

Risk-Based Prioritisation of Closed Mine Waste Facilities Using GIS

Alison J. M. Turner[1], Charlotte Braungardt[1], Hugh Potter[2]

[1]*School of Geography, Earth and Environmental Science, University of Plymouth, Drake Circus, Plymouth. PL4 8AA. U.K. alison.turner@plymouth.ac.uk*
[2]*Environment Agency, Tyneside House, Skinnerburn Road, Newcastle Business Park, Newcastle upon Tyne, NE4 7AR. U.K*

Abstract Recent EU legislation and relevant guidance documentation requires inventories of closed mine sites to be prepared and recommends a risk-based approach to the pre-screening of sites related to environmental and human health criteria. In this study, a geographical information system (GIS) was assembled to combine available data from five catchments in south west England, an area with a high density of abandoned metal mines. A series of risk factors was selected and risk classified according to their respective magnitude. Relative weightings for each risk factor were assigned within an analytical hierarchy procedure by applying expert knowledge and literature information. The model output provided a priority list for further investigation by the responsible statutory body. The GIS model is adaptable, in particular with respect to expert opinion and inclusion of additional risk factors and therefore showcases the application of ArcGIS software for processing readily obtainable data to produce rapid and flexible environmental risk assessments.

Key Words Mine waste, mining waste directive, risk assessment, GIS

Introduction

Directive 2006/21/EC on the Management of Waste from the Extractive Industries (Mining Waste Directive, MWD) requires all member states to produce an inventory of closed waste facilities by 01 May 2012. Furthermore, a pre-screening methodology has to be developed that identifies sites that pose a risk to human health or have the potential to cause negative environmental impacts (Stanley *et al.* 2010), whereby guidance documentation recommends the use of available data and a GIS system.

In England and Wales, the Environment Agency (EA) is responsible for the management of pollution resulting from historical metal mining. However, the spatial resolution of the EA's regular monitoring programme of watercourses is insufficient for the identification of individual pollution sources, which are often diffuse in nature and can be highly elevated in dissolved metals and metalloids compared to water quality standards. European member states are legally bound to meet such standards as part of European Water Framework Directive 2000/60/EC (WFD). This paper describes the design of a GIS based tool used to prioritize mine waste tips as potential pollutant sources in five river catchments of south west England. The work incorporates data on the location of abandoned mine sites collated by the EA into a GIS in a model that is based on three key attributes of mine waste tips. The methodology serves as a systematic and rapid screening tool. but it does not consider the concentrations of toxic metals and metalloids in the waste, since such information is only obtainable after site specific intrusive investigations.

Methods

The scope of the study was defined by the requirements of the EA and included the five management catchments shown in Figure 1. The input parameters of interest to this model were proximity of each waste tip to the nearest watercourse or body, the area occupied by the waste tip and the slope of the drainage pathway. The latter was defined for each waste tip from digital terrain model DTM (5 m resolution) using ArcHydro (Version 1.4) software. All other operations and output maps were created using ArcGIS (Version 9.3) in conjunction with XTools (Version 7.1).

Determination of Area and Proximity

Digitized hydrological information comprising catchment boundaries, a detailed river network (DRN), lakes and estuary outlines were provided by the EA. Catchment boundaries were extended by 50 m using the buffer tool, to prevent mine waste tips close to catchment boundaries being split between catchments. A database of mine features was provided by the EA as a polyline feature class, with unique identification (ID) codes. Polylines relating to areas of mine waste were selected using the select by attributes tool and saved to a new file. The new data set was divided into the five management catchments, shown in Figure 1, using the clip tool.

For each catchment, polyline features were converted to polygons using the convert polylines to single polygon tool (XTools). Polygons were sorted based on ID code and duplicate codes merged to construct individual polygons for each mine waste tip. The mine polygon files were inspected for errors caused by the conversion process, such
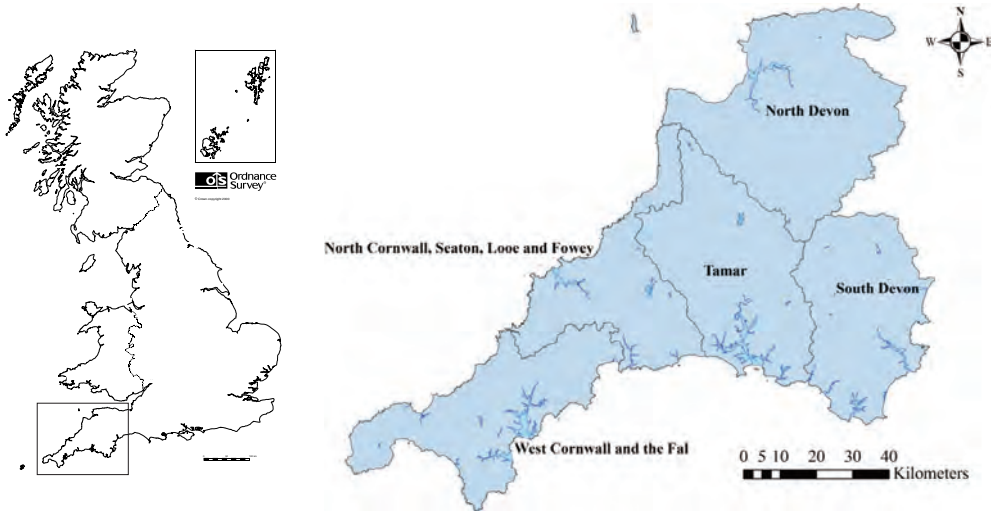
Figure 1 *Map showing the five management catchments subject to the model. Created in ArcMap, data supplied by the Environment Agency and used under license.*
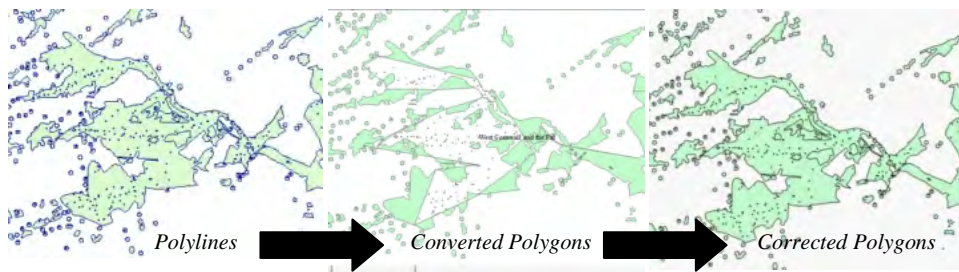

Polylines → *Converted Polygons* → *Corrected Polygons*

Figure 2 *Self intersection errors shown in polygon file (centre), caused by conversion process of polyline features (left) to polygon features. Corrected polygon features shown on right.*

as self intersections, and corrected as shown in Figure 2.

An additional field was added to the attribute table of each mine waste polygon file and was populated with the area of each polygon using the calculate geometry tool. Small areas of <1963 m² (for example the 25 m² default areas assigned to mine shafts by the EA in the original database) were re-

moved, leaving 1894 areas of waste. The remaining areas were statistically divided into six categories and assigned a risk score from 6 (largest), to 1 (smallest) (Table 1), which were, for each catchment, added to the attribute table in a new field.

The DRN polyline file provided accurate locations of rivers and streams, which were isolated for each management catchment by using the clip

Weighting	Nominal Risk Classification	Upper Threshold Areas (m²)					
		SD	ND	Tamar	NC	WC	Combined
6	Extreme	93185	16968	36781	176795	2510815	2510815
5	Very High	12601	10997	18048	12016	16920	15862
4	High	7266	5460	7534	6283	7778	7528
3	Moderate	5936	4571	4818	4356	5044	4951
2	Moderate -Low	3925	3519	3653	3519	3790	3747
1	Low	2986	3285	2778	2756	3019	2946
Number of waste tips > 1963 m²		130	23	309	184	1248	**1894 (Total)**

Table 1 *Table showing the upper threshold for area of mine waste in each risk category for each of the five catchments subject to model: South Devon (SD), North Devon (ND) Tamar, North Cornwall (NC) and West Corn (WC). Also show, are upper thresholds if data for all catchments is combined and classified (rightmost column).*

Table 2 Distance to nearest watercourse (stream/lake/estuary) and number of waste tips in each category for South Devon (SD), North Devon (ND) Tamar, North Cornwall (NC) and West Cornwall (WC).

Distance to Stream/River/Estuary	Risk Score	Risk Classification	Number of Waste Tips					
			SD	ND	TM	NC	WC	Combined
Direct contact (2 m buffer)	6	Extreme	31	8	89	38	173	339
2 - 50 m	5	Very High	27	5	59	23	133	247
50 - 100 m	4	High	30	2	43	26	107	208
100 - 250 m	3	Moderate	27	4	61	43	292	427
250- 500 m	2	Moderate - Low	1	4	48	43	311	407
> 500 m	1	Low	14	0	9	11	232	266

1894 (Total)

tool in conjunction with the catchment polygons (Figure 1). Estuarine areas were defined by modifying catchment polygons to include the estuaries of each river. The Union tool was used to create estuary polygons from the overlapping regions between the modified and original catchment polygons (Figure 3). A polygon file containing known lakes was provided ready to use by the EA. The proximity of each mine waste tip to the nearest watercourse (lake polygon, estuary polygon or river polyline) was determined using the select by location tool. Buffer distances and risk scores were assigned as defined in Table 2.

Determination of Drainage Pathways and Topographical Slope

The EA supplied catchment DTMs as individual raster tiles cataloged by UK Ordnance Survey grid squares. The tiles were combined into a single raster using the Mosaic tool in ArcCatalogue. Individual catchment DTMs were created using the mask tool and the management catchment polygons (buffered to 50 m). To determine surface water flow through the catchments, the DTMs were used to produce a series of hydrogrids in ArcHydro, using the Terrain Preprocessing (TP) tools in accordance with guidance documentation (Djorkic, 2008) as shown in Figure 3. The ArcHydro Watershed Processing toolbar was used to determine the catchment area of a given polygon (e.g. each mine waste tip). The application of the same tool to an inverted DTM allowed drainage areas to be determined (Figure 4).
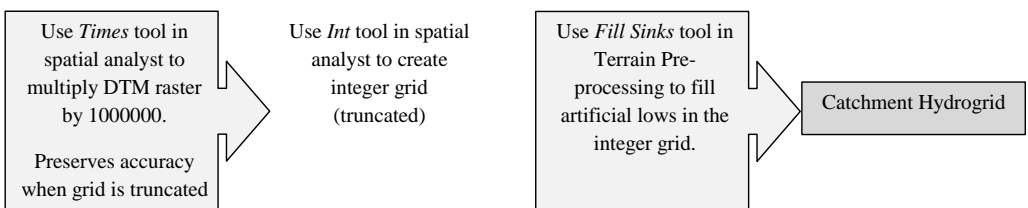
The slope (in degrees) for each of the drainage polygons was calculated using the slope tool in ArcHydro. Then steps shown in Figure 5 were followed resulting in the dissolved slope polygon file, indexed and joined to the drainage polygon file by utilizing their common HydroID field in the attribute table. The slope dataset was statistically divided into 6 equal groups, each of which was assigned a risk code (1—6).

Weighting of Input Parameters and Final Combination into Model

The weighting for each of the input parameters was determined using a pairwise comparison matrix first described by Saaty (1980) (Table 3). The matrix scores the relative importance of each input with respect to the other two. A score of one represents equal importance; a maximum score of 9 indicates much greater importance. The reciprocal score is awarded to the partner input for each comparison.

The weight of each layer (w) was calculated by dividing the sum of the row, M_i by the denominator of the matrix (Wang *et al.*, 2010):

$$w = M_i / \sum_{i=1}^{n} M_i$$

The resulting weightings were multiplied by 100 to avoid the use of decimals, which is favorable in ArcGIS. The weightings were added to the mine waste attribute table as new fields. The total
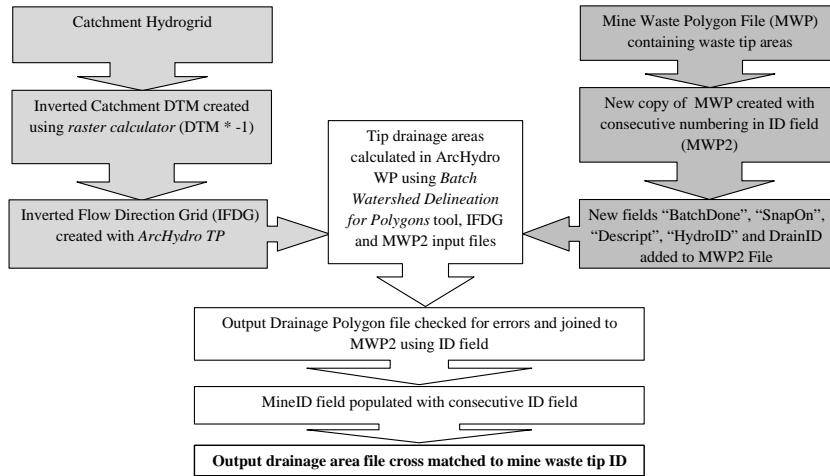

Figure 3 Pre-processing steps required to produce a hydrogrid from a catchment DTM.

Figure 4 Processes used to: invert the catchment hydrogrid (light grey boxes), sort and prepare mine waste polygon file (dark grey boxes), index drainage polygons to mine waste areas (white boxes). TP = Terrain Preprocessing and WP = Watershed Processing menus in ArcHydro.
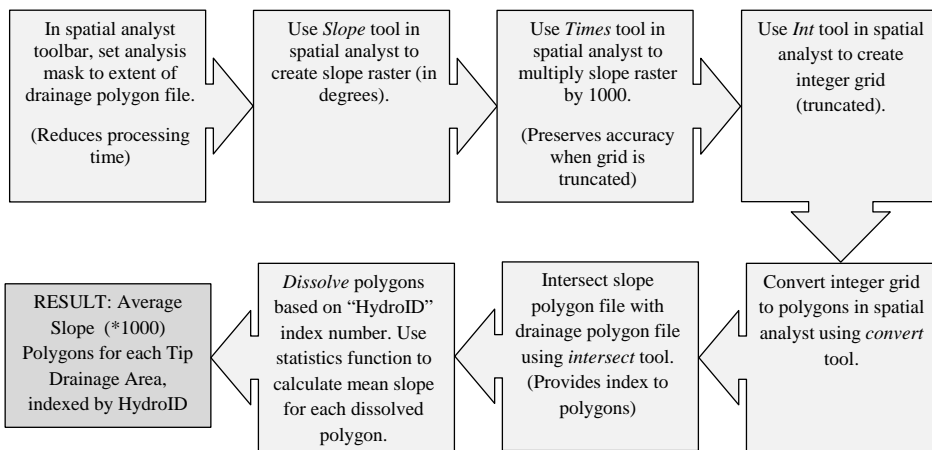

Figure 5 Process steps to produce average slope value (degrees x 1000), for each mine waste drainage polygon. The final slope field may be divided by 1000 to give result in degrees, if required.

Table 3 Pairwise comparison matrix used to calculate input weightings for proximity, area and slope.

	Proximity to Water Body	Area of Waste	Slope of Drainage Pathway	*Sum of row*	
Proximity to Watercourse	1	2	2	*5*	
Area of Waste	1/2	1	2	*3.5*	
Slope of Drainage Pathway	1/2	1/2	1	*2*	
Sum of Column	*2*	*3.5*	*5*	***10.5***	**Denominator of matrix**
Weighting	0.48	0.33	0.19	**1.0**	**Sum of weightings**

risk for each mine waste polygon was calculated from:

$$Combined\ Risk\ =\ \sum w_i.R_i$$

Where w is the weighting of each layer and R the risk score (1—6). The final total risk field may be sorted to give a prioritisation list for the catchment; a ranking may be added as a new field. The simplest way to populate this field is to export the layer to excel and add the priority number, then import back into ArcMap. The final attribute table for one of the catchments (North Devon) is shown in Figure 6.

Results and Discussion

The attributes of the nearest mine record (EA database of mine names, locations and available data) were joined by location to the results of the prioritisation exercise for each mine tip (Figure 8). The five waste tip/mine site combinations bearing the highest total risk for each of the five catchments are summarized in Table 4 and serve as an example of the output of such a prioritisation exercise, which may be subsequently explored further as site investigations.

Uncertainty in any GIS model similar to that presented here can arise from three areas, namely: errors in the input data sets, errors in the processing steps within the model, and incorrect assumptions made when designating the risk scores to attributes of an input. The first two may be minor if good quality data can be sourced and are processed by a knowledgeable GIS user. However it must be stressed that the time taken to construct the model is highly dependent on the quality of the input data and the amount of pre-processing required to remove errors. Expert judgment may be tested by testing the model's sensitivity to differences in relevant parameters, classifications and weightings.

This model considered three physical properties of the mine waste tips only. However a more complex model has been developed and run for the Tamar catchment (paper in preparation). This model followed the same principles outlined here but was extended to include additional input parameters, namely: bedrock geology, superficial geology, annual rainfall, rainfall intensity, vegetation cover and wind exposure. This flexibility, together with the power of GIS to consolidate many sources of information in an easy to access form

Table 4 *Results of prioritisation exercise showing nearest mine name to tips scored with highest total risk in each catchment. Likely contaminants identified in EA database shown in parenthesis.*

Priority	South Devon	North Devon	Tamar	North Cornwall	West Cornwall
1	Waterhill (Sn)	Fullabrook (Mn, Fe)	Harewood (Cu, As, Fe)	Esther (Sn)	Blue Hills (As, Cu, Fe)
2	Waterhill (Sn)	Ivy Tor (Cu, As, Fe, Bi, Ag)	Betsy (Pb, Ag, Zn, Cd, Fe)	West Caradon (Cu, As, Fe)	Friendly (Pb, Fe, Cu)
3	Hexworthy (Sn)	Bampfylde (Cu, Fe, Ag)	South Devon (Cu)	Penhale (Fe, Cu, Pb, Sb)	Ellen (Cu, Pb, Zn, Ag, Cd?)
4	Crownley Parks (Cu, Ag)	Steeperton (Sn)	Harewood (Cu, As, Fe)	Credis (Cu, Fe)	Carclaze (Zn, Pb, Cd?)
5	Great Eleanor (Sn)	Ramsley (Cu, As, Pb, Fe)	Hawkmoor (Cu, Fe, As)	Trehane (As, Pb, Ag, Cu, Fe, Cd?)	Geevor (Cu, Pb, Zn, As, Sb, Co, Mo, Fe, Ag, Hg, Bi, U, Rn?)

Figure 6 *Final attribute table for catchment prioritisation. Key to fields: Area = area of waste in m²; (Area/Prox/Slope)_Risk = risk score 1—6, (Area/Prox/Slope)_W = weighting attributed to each layer, Mean_Slope = average slope for drainage area in degrees x 1000; Total_Risk = result of Equation 2 for each object, Priority_N = priority number based on total risk score (and area when tied).*

are the main advantages of the GIS models presented here. This preliminary exercise not only directs regulators to sites of potential harm, but may be used to aid the design of site investigations. For example, the modeling of tip drainage pathways can assist in the accurate placing of boreholes and stream samplers to capture drainage waters.

Conclusions

The work presented here represents a principle rather than an absolute approach. The judgments made are flexible and any number of input parameters may be addressed depending on available data and the requirements of the user. The methodology presented here has already played a role delivering the EA's obligations under the WFD and, with some minor modifications, can meet the requirements of Article 20 of the MWD for pre-selection of potentially harmful abandoned mine sites.

References

Djorkic (2008). Comprehensive terrain preprocessing using Arc Hydro tools ESRI.

Saaty, T. L. (1980). The Analytic Hierarchy Process. New York, McGraw-Hill.

Wang, J., Chen, J., Ju, W. and Li, M. (2010). IA-SDSS: A GIS-based land use decision support system with consideration of carbon sequestration. Environmental Modelling & Software. 25 (4) pp539—53.